A flow cytometric approach to monitor the effects of gentle preservation techniques in the postharvest chain

vorgelegt von
Diplom-Ingenieurin
Antje Fröhling
aus Berlin

von der Fakultät III – Prozesswissenschaften
der Technischen Universität Berlin
zur Erlangung des akademischen Grades
Doktorin der Ingenieurwissenschaften
- Dr.-Ing. -
genehmigte Dissertation

Promotionsausschuss:
Vorsitzender: Prof. Dr. Dipl.-Ing. Frank-Jürgen Methner
1. Berichter: Prof. Dr. Dipl.-Ing. Dietrich Knorr
2. Berichter: Prof. Dr. Javier Raso-Pueyo
3. Berichter: Dr.-Ing. Oliver Schlüter

Tag der wissenschaftlichen Aussprache: 08.12.2010

Berlin 2011
D-83

For my parents

Zusammenfassung

Bakterielle Kontaminationen können bei der Gemüseproduktion zu hohen ökonomischen Verlusten führen und darüber hinaus auch ein potenzielles Gesundheitsrisiko für den Verbraucher darstellen. Übliche Wasch- und Reinigungsschritte reduzieren die Mikroorganismen aber nur um etwa 0,5-2 log Einheiten und konventionelle thermische Verfahren sind im Bereich leichtverderblicher Produkte wie bspw. frisches Obst und Gemüse in ihrer Anwendung limitiert, da bereits Temperaturen oberhalb von 45 °C zu unerwünschten Veränderungen der charakteristischen physiologischen Produkteigenschaften führen. Um die Qualität der Frischeprodukte zu erhalten und gleichzeitig die anhaftende mikrobielle Schadflora abzutöten, besteht daher ein besonderer Bedarf an innovativen, Produkt schonenden Behandlungsmethoden. Für eine Chargen gerechte Prozessauslegung muss einerseits der Kontaminationsgrad des Produktes frühzeitig erfasst und andererseits der Behandlungserfolg sichergestellt bzw. überwacht werden. Mit konventionellen sehr zeitintensiven mikrobiologischen Verfahren ist dies jedoch nicht möglich.

In dieser Studie wurde daher die Durchflusszytometrie im Hinblick auf eine schnelle Charakterisierung des Inaktivierungserfolges verschiedener Inaktivierungsverfahren (Thermische Behandlung, Behandlung mit Peressigsäure, Ozon und Atmosphärendruckplasma) untersucht. Hierzu wurden morphologische und physiologische Eigenschaften der Mikroorganismen (Größe, Oberflächenbeschaffenheit, Membranintegrität (Thiazole Orange & Propidiumjodid), Esteraseaktivität (Carboxfluoreszeindiazetat), Pumpenaktivität (Ausschluss von Carboxyfluoreszein) und Membranpotential (3,3'-Diethyloxacarbocyaninjodid)) durchflusszytometrisch bestimmt. Dabei mussten zuerst geeignete Färbeprotokolle für die verwendeten Farbstoffe entwickelt werden bzw. in der Literatur vorhandene Protokolle modifiziert werden. Insbesondere Gram-negative Bakterien erschweren z.B. die Aufnahme von Carboxyfluoreszeindiacetat zur Ermittlung der Esteraseaktivität aufgrund ihres Zellwandaufbaus. Durch Entwicklung eines Färbeprotokolls konnte eine geeignete Farbstoffkonzentration (0,83 mmol/l Carboxyfluoreszeindiacetat) und Färbezeit (45 min) bei 37 °C für die zuverlässige Bestimmung der Esteraseaktivität Gram-negativer Bakterien ermittelt und für die Überprüfung von Inaktivierungsverfahren verwendet werden. Es hat sich gezeigt, dass die verwendeten Bakterien (*E. coli, L. innocua, P. carotovorum*) nach den Behandlungsverfahren zwar ihre Kultivierbarkeit verlieren, jedoch teilweise noch physiologische Aktivitäten nachweisbar sind. Damit würde weiterhin die Möglichkeit eines Produktverderbs und Gefährdung der menschlichen Gesundheit bestehen. So konnte z.B. nach einer thermischen Behandlung von 70 °C für 10 min sowie nach einer Behandlung mit 0,25 % Peressigsäure für 2 min noch Esteraseaktivität in *E. coli* Zellen nachgewiesen werden. Ebenso zeigten *E. coli* Zellen nach einer zweiminütigen Plasmabehandlung bei 40 W noch Esteraseaktivität. Das Ausmaß der Schädigung der einzelnen Behandlungsverfahren ist dabei stark abhängig von den verwendeten Behandlungsparametern sowie von den behandelten Bakterien.

Diese Arbeit zeigt das Potenzial der Durchflusszytometrie einen Inaktivierungserfolg innerhalb kürzester Zeit zu ermitteln und gleichzeitig Aussagen über den jeweiligen verfahrensspezifischen Inaktivierungsmechanismus abzuleiten. Damit wird es ermöglicht, kritische Verfahrensparameter zu bestimmen.

Abstract

Microbial contamination of fruits and vegetables can lead to high economic losses as well as to foodborne diseases. Washing procedures, which are commonly applied, only reduce the microbial load by 0.5 to 2 log units. Conventional thermal inactivation processes cannot be applied to fresh fruit and vegetables because these products are physiologically active food systems and temperatures above 45 °C can result in unwanted deterioration. Since heat sensitivity of fruits and vegetables limits the application of thermal inactivation processes, new emerging inactivation technologies have to be established to fulfil the requirements of food safety without affecting the produce quality. On one hand an early detection of produce contamination is essential to enable a contamination-related process design and on the other hand the efficiency of inactivation treatments has to be ensured and monitored. Monitoring of inactivation effects is commonly performed using traditional cultivation methods which have the disadvantage of the length of time needed to obtain results.

In this study, the potential of flow cytometry in short-time monitoring of inactivation effects (thermal treatment, treatment with peracetic acid, ozone, and atmospheric pressure plasma) was investigated. For this purpose morphological and physiological properties of bacteria (size, granularity, membrane integrity (thiazole orange & propidium iodide), esterase activity (carboxyfluorescein diacetate), pump activity (carboxyfluorescein efflux), and membrane potential (3,3'-diethyloxacarbocyanine iodide)) were determined by flow cytometry. In the initial step appropriate staining procedures had to be developed. Especially, Gram-negative bacteria restrict the dye uptake due to their cell membrane constitution. This limits the determination of esterase activity of Gram-negative bacteria. In this study, an adequate dye concentration (0.83 mmol l^{-1} carboxyfluorescein diacetate) and incubation time (45 min) at 37 °C were defined which enables a reliable determination of esterase activity of Gram-negative bacteria. This developed staining procedure was successfully applied to monitor inactivation treatments. It was shown that the test bacteria (*E. coli, L. innocua, P. carotovorum*) lose their culturability due to the applied inactivation treatments but physiological activities were still detectable using flow cytometry. The remaining physiological activities may still result in product spoilage and also may cause human diseases. For example, *E. coli* cells still showed esterase activity after 10 min of thermal treatment at 70 °C and also after 2 min treatment with 0.25 % PAA at 10 °C. Esterase activity of *E. coli* cells was also detected after 2 min plasma treatment with an operating power of 40 W. The degree of bacterial damage due to the inactivation processes is highly dependent on treatment parameters as well as on treated bacteria.

This study clearly indicates the potential of flow cytometry to monitor the efficacy of inactivation processes within a short time. Additionally, important information regarding the inactivation mechanisms can be obtained by flow cytometric measurements and this enables the definition of critical process.

Acknowledgments

This dissertation is based on the experimental work at the Leibniz Institute for Agricultural Engineering Potsdam-Bornim (ATB) in collaboration with the Berlin University of Technology, Department of Food Process Engineering and Food Biotechnology from 2006 to 2010. Numerous people have given advice, encouragement and support to my work. My sincere gratitude goes to Prof. Dr. Dietrich Knorr for the interest in this work and for supporting and supervision of this dissertation. A very special thanks goes to Dr. Oliver Schlüter for giving me academic guidance and inspiration as well as support and very helpful discussions throughout the course of this work. I would like to acknowledge Prof. Dr. Javier Raso-Pueyo for coming to Berlin and taking his time to be a referee for my dissertation and Prof. Dr. Frank-Jürgen Methner for being the head of the commission.

This work was supported by the collaborative research project “Sensor-based technologies and integrated assessment models in food production chains - ProSenso.net2” (grant 0339992A) funded by the German Ministry of Education and Research (BMBF) and supported by Research Center Jülich (PtJ) and by the collaborative research project “Application of plasma technology for gentle preservation of perishables in the post-harvest chain (FriPlas)” funded by the Federal Institute of Food, Agriculture and Consumer Protection (BMELV) supported by the Federal Institute for Agriculture and Food (BLE) within the innovation program (FKZ 28-1-63.003-07).

I would like to express my gratitude to all present and former colleagues at the ATB for providing a very comfortable atmosphere. Special thanks to the colleagues from the Department for Horticultural Engineering for discussions concerning professional topics as well as private topics and for distraction during hard times. A particular thanks to Susanne Klocke for technical assistance, support and patience. Without her it would not have been possible to conduct all the experiments. I also would like to thank the colleagues from the molecular biology team for a very comfortable working atmosphere. Thank you to the diploma students Matthias, Manuela and Nadja as well as all the trainees for their support and activities. My present and former office mates Angelika, Ingo, Lena, Mario, Janina, and Julia I want to thank for encouraging me, support, and helpful discussions. I would also like to thank all PhD students for inspiring discussions, excursions, and nice atmosphere throughout the years.

Without the support and assistance of my family and friends this dissertation would not have been the same. A particular thanks to my family for believing in me and being proud of me. I would like to thank my friends for their patience during this dissertation and support during ups and downs in the last years. The encouragement of my family and friends highly contributed to the successful outcome of this work.

Index

List of Figures

List of Tables

List of Abbreviations

μ_m	Max. growth rate
1-f	Fraction of initial population in a minor population
2-NBDG	D-glucose analog 2-[*N*-(7-nitrobenz-2-oxa-1,3-diazol-4-yl) amino]-2-deoxy-d-glucose
a	Survivor count after heat treatment for t_1
A	Max. asymptote value
APGD	Atmospheric pressure glow discharges
APPJ	Atmospheric pressure plasma jet
ATP	Adenosine triphosphate
b	Survivor count after heat treatment for t_2
BOBO	2,2'-[1,3-propanediylbis[(dimethyliminio)-3,1-propanediyl-1(4H)-pyridinyl-4-ylidenemethy-lidyne]]bis[3-methyl]-tetraiodide
BOD	Biological oxygen demand
CAST	Council for Agricultural Sciene & Technology
CCCP	Carbonyl cyanide m-chlorophenylhydrazone
CD	Corona discharge
cF	Carboxyfluorescein
cFDA	Carboxyfluorescein diacetate
cFDA-AM	Carboxyfluorescein diacetate acetoxy methyl ester
CFU	Colony forming units
CMFDA	Chloromethylfluorescein diacetate
COD	Chemical oxygen demand
CTC	Chlorotetracycline
D	Decimal reduction time
DAPI	4'-6-Diamidino-2-phenylindole
DBD	Dielectric barrier discharge
DBP	Disinfection by-products
$DIBAC_4(3)$	Bis-(1,3-dibutylbarbituric acid) trimethine oxonol
$DIOC_2(3)$	3,3'-diethyloxocarbocyanine iodide
DMMP	Dimethyl-methyl phosphonate

DNA	Deoxyribonucleic acid
DSMZ	Deutsche Stammsammlung für Mikroorganismen und Zellkulturen
EB	Ethidium bromide
EDTA	Ethylenediaminetetraacetic acid
f	Fraction of initial population in a major population
F	Lethality value
FC	Faecal coliforms
FDA	U.S. Food and Drug Administration
FISH	Fluorescence *in situ* hybridisation
FL1	Photomultiplier tube with a bandpass filter of 525 nm
FL2	Photomultiplier tube with a bandpass filter of 575 nm
FL3	Photomultiplier tube with a shortpass filter of 620 nm
FL4	Photomultiplier tube with a longpass filter of 655 nm
FL5	Photomultiplier tube with a bandpass filter of 755 nm
FS	Forward scatter
GAP	Good Agricultural Practise
GHP	Good Hygiene Practise
GInaFiT	Geeraerd and Van Impe Inactivation Model Fitting Tool
GMP	Good Manufacturing Practise
GRAS	Generally recognised as safe
GTA	Glutardialdehyde
HAA	Haloacetic acids
HACCP	Hazard Analyses Critical Control Point
HSP	Heat Shock Protein
kmax	Specific inactivation rate
LPCP	Low pressure cold plasma
MAC	MacConckey agar
N	Number of colony forming units after treatment
n	Number of cell divisions
N_0	Inital number of colony forming units
$Na_2S_2O_3$	Sodium thiosulfate
N_{res}	Residual population density
OAUGDP	One atmosphere uniform glow discharge plasma

OD	Optical density
OD_{620}	Optical density measured at 620 nm
p	Weibull shape parameter
PAA	Peracetic acid
PBS	Phosphate buffered saline
PEF	Pulsed electric fields
PI	Propidium iodide
PMT	Photomultiplier tube
POPO	[4,4,8,8-tetramethyl-4,8- diazaundecamethylene)bis-4-(3-methyl-2,3-dihydrobenzo-1,3-oxazolyl)-2-methylidene]
R^2	Coefficient of determination
rf	Radio frequency
RMSE	Root mean square error
RNA	Ribonucleic acid
ROS	Reactive oxygen species
S_0	Electronic ground state
S_1	Lowest excited energy level
SCF	Scientific Committe on Food
SD	Standard deviation
SEM	Scanning electron microscopy
S_l	Shoulder length
S_n	Excited state
SS	Side scatter
ST-I	ST-I agar
SYBR Green I	N',N'-dimethyl-N-[4-[(E)-(3-methyl-1,3-benzothiazol-2-ylidene)methyl]-1-phenylquinolin-1-ium-2-yl]-N-propylpropane-1,3-diamine
t	Treatment time in min
t_d	Doubling time
T_1	Excited triplet state
TC	Total coliforms
TDT	Thermal death time
TE-buffer	Tris(hydroxymethyl)aminomethane/EDTA-buffer
TEM	Transmission electron microscopy

THB	Total heterotrophic bacteria
THM	Trihalomethanes
TO	Thiazole orange
TO-PRO	4-[3-(3-methyl-2(3H)-benzothiazolylidene)-1-propenyl]-1-[3-(trimethylammonio)propyl]-, diiodide
TOTO	1-1'-[1,3-propanediylbis[(dimethyliminio)-3,1-propanediyl]]bis[4-[(3-methyl-2(3H)-benzothiazolylidene)methyl]]-, tetraiodide
v	Rate of cell division
V_b	Breakdown voltage
z	Temperature needed to reduce D-value by ten-fold
δ	Weibull scale parameter
λ	Lag time

1. Introduction

With rising health consciousness and advice from the public health institutions to consume at least five portions of fruits and vegetables per day, the consumption of fruit and vegetables has increased in recent years (De Roever, 1998; Rediers *et al.*, 2009). Significant changes in lifestyles have lead to changes in consumption trends resulting in a higher demand for fresh-cut, minimally processed fruits and vegetables. In the United States 30 kg of ready-to-eat fruits and vegetables are consumed per person per year, while in Europe this figure stands at 1 to 12 kg per person per year (Abadias *et al.*, 2008). These minimally processed products are trimmed, peeled, sliced, chopped, shredded, cored, and washed before sale and have a shelf-life of days (FDA, 2008). An increased number of foodborne diseases are associated with these ready-to-eat products (Little & Gillespie, 2008; Doyle & Erickson, 2008) because they are consumed raw without further washing, cooking or preparation. 4.3 % of total foodborne disease outbreaks between 1992 and 1999 in Europe were due to fruits and vegetables (SCF, 2002), in the United states 12 % of foodborne diseases between1990 and 2003 were associated with fresh produce (Smith DeWaal *et al.*, 2006). Depending on the season and type of fresh produce the microbial load of fresh fruits and vegetables ranges between 2 and 9 log units per gram (Breidt Jr, 2006). The microbial load does not only consist of humanpathogenic bacteria, there are also phytopathogenic bacteria present on the fresh produce which result in postharvest losses or reduced consumer acceptance due to reduced shelf-life. Throughout the world, the estimated postharvest losses are 50 % of the harvested crops and most of these losses are due to rots caused by microorganisms (Wilson & Wisniewski, 1989).

Washing alone does only reduce the microbial load by ≤ 1 log unit (Beuchat, 1998). Thermal treatments are limited both by the requirements for the appropriate inactivation of pathogens which occurs at temperatures above 45 °C, and the negative produce quality incurred at these temperatures (Schlüter *et al.*, 2009). The disinfection of produce is therefore limited to non-thermal processes. Consequently, new emerging inactivation technologies have to be established to fulfil the requirements of food safety, whereas detailed knowledge about these inactivation methods is necessary to ensure efficacy of inactivation processes. In particular the safety assessment of the used substances, legal requirements, and the consumers' acceptance must be taken into account. The efficacy of available sanitising agents is variable and many are not able to ensure the elimination of pathogens (SCF, 2002). Chemical disinfection with chlorine leads to the formation of carcinogenic halogenated disinfection by-products (Ölmez & Kretzschmar, 2009) and the use of chlorine for ready-to-use vegetables is forbidden in some European countries including Germany, The Netherlands, Switzerland,

and Belgium (Rico *et al.*, 2007). In contrast, other chemical disinfection agents such as ozone and peracetic acid have the GRAS (generally recognised as safe) status but are forbidden for organic products in Europe (Ölmez & Kretzschmar, 2009). In recent years food microbiologists have increasingly focussed on bacterial inactivation by plasma treatment but the potential for food surface decontamination is not fully understood yet.

To obtain detailed knowledge about inactivation effects of new emerging technologies it is necessary to monitor these processes. Monitoring of inactivation effects is commonly performed using traditional cultivation methods. The main disadvantage of this method is the time needed to obtain results. Additionally, this method only detects culturable microorganisms however, the lack of culturability is not equivalent to cellular death because the bacteria can still be metabolically active (Bunthof & Abee, 2002). Thus, even after apparent inactivation, bacteria can be the cause of diseases or reduced shelf-life of produce. Because of this there is a growing demand for the application of alternative analysis methods to monitor inactivation treatments. Flow cytometric techniques are of special interest in food microbiology, because this technique enables a continuous detection of bacterial properties at a single cell level within a short time. Besides the detection of cell size; surface roughness and internal granularity; cell's nucleic acid content and sequence; physiological characteristics and specific antigens of single cells can be demonstrated by using appropriate fluorescent probes (Shapiro, 2000). Thus, non-culturable but metabolically active cells can be detected. The potential of flow cytometry to assess yeast cultures in food and beverage processing (e.g. bakery, wine industry, beer industry) is already shown (Herrero *et al.*, 2006). The application of flow cytometry for monitoring inactivation processes enables to ascertain important information about the inactivation mechanism of the treatment processes. Thereby, the obtained data can be used to define treatment parameters enabling the construction and optimisation of decontamination processes.

In this study, flow cytometry is used to investigate inactivation effects of thermal and non-thermal inactivation treatments and to prove the ability of flow cytometric techniques to monitor inactivation processes. Various bacteria associated with food contamination are selected in order to examine the inactivation effects on different types of microorganisms. *Listeria innocua* (Gram-positive) is chosen as indicator strain for the human pathogenic *Listeria monocytogenes* (Kamat & Nair, 1996), a non-pathogenic *Escherichia coli* (Gram-negative) strain is chosen as representative for faecal contamination, and the plant pathogenic strain *Pectobacterium carotovorum* (Gram-negative) is chosen as a spoilage bacterium. In a first step the growth curves of the selected bacteria are recorded (section 4.1) to evaluate the growth phase of the bacteria at the point of the inactivation treatments. Once the optimal harvest time of bacteria is determined, the culturability of the test organisms as

well as the total count (section 4.2) is investigated after thermal treatment and non-thermal treatments (ozone, peracetic acid, and atmospheric pressure plasma). Since the microbial contamination levels of foods is varied the inactivation effects of treatment processes on different bacterial counts is also evaluated. In order to establish an industrial application for an inactivation treatment it is necessary to model inactivation kinetics to achieve a reliable prediction of microbial inactivation. Therefore, the GInaFiT (Geeraerd and Van Impe Inactivation Model Fitting Tool), a freeware Add-in for Microsoft® Excel (Geeraerd *et al.,* 2005), is used to describe the obtained inactivation kinetics of thermal treatment, ozone treatment, peracetic acid treatment and atmospheric pressure plasma treatment.

Due to the fact that non-culturable but metabolically active bacteria are not detected by plate count methods the potential of flow cytometry to monitor inactivation processes is evaluated. Morphological and physiological parameters of bacteria cells such as membrane integrity, metabolic activity, pump activity, and membrane potential are investigated by means of the fluorescent dyes thiazole orange (TO), propidium iodide (PI), carboxyfluorescein diacetate (cFDA), and 3,3'-diethyloxacarbocyanine iodide ($DiOC_2(3)$). With these data important information regarding the inactivation mechanism are expected to be obtained. The ability of staining Gram-negative bacteria with fluorochromes such as cFDA is limited by the more complex membrane structure of these bacteria in comparison to Gram-positive bacteria. The outer membrane of Gram-negative bacteria often prevents the intrusion of hydrophobic macromolecules like cFDA. Therefore, the hydrophobic cFDA is not able to permeate efficiently into cells of Gram-negative bacteria (Novo *et al.*, 2000; Morono *et al.,* 2004). Other limiting factors for staining with cFDA are differences in dye uptake, the capacity for intracellular retention of cF, passive leakage, and the presence of active extrusion pumps (Nebe-von-Caron *et al.*, 2000). Thus, an appropriate staining protocol is necessary for viability testing of Gram-negative bacteria by means of cFDA and PI. Using the example of *Pectobacterium carotovorum* a staining protocol for Gram-negative bacteria with cFDA and PI is established (section 4.3). Subsequently, the developed staining protocol is applied to monitor the effects of heat treatment (section 4.4), ozone treatment (section 4.5), peracetic acid treatment (section 4.6), and atmospheric pressure plasma treatment (section 4.7) on metabolic activity of selected bacteria. Additionally, membrane integrity (TO/PI), pump activity (cF-Efflux), and membrane potential ($DiOC_2(3)$) is investigated after the inactivation processes (section 4.4-4.7). In order to evaluate critical treatment parameters as well as differences in inactivation effects on Gram-negative and Gram-positive bacteria the obtained kinetics are described using common mathematical models in a first approach.

2. Literature review

2.1. Bacteria associated with fresh produce

Fresh fruit and vegetables are naturally contaminated with microorganisms including humanpathogenic and phytopathogenic bacteria. The level of contamination depends on the season and on the type of fruit and vegetables and ranges between 3 and 7 log units per gram (Ölmez & Kretzschmar, 2009). The sources of microbial contamination are divers. Contamination of fresh produce can occur anywhere during production, from the farm to the consumer and relevant contamination sources are given in figure 2.1.

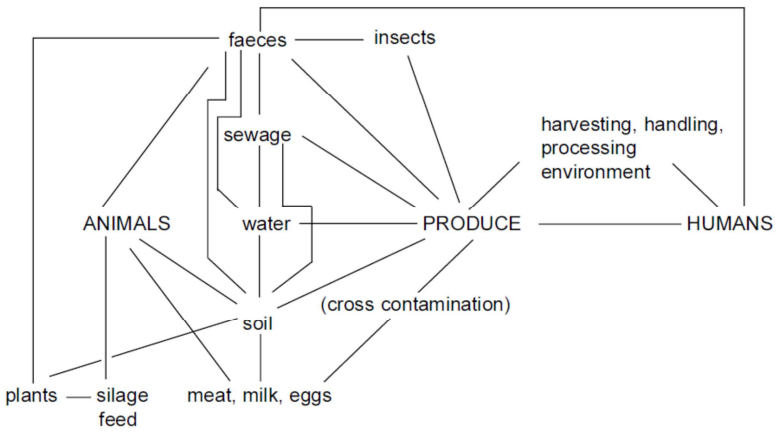

Figure 2.1: Sources of product contamination (Beuchat, 1996).

The fresh produce production chain can be divided into three stages: the growing stage, harvest and post harvest. At the growing stage possible source for produce contamination are seeds, soil, irrigation water, manure, humans, and animals. During harvest sources of contamination are faeces (animal), human handling, equipment and animals. At the post-harvest stage contamination of fresh produce is due to wash water, equipment, ice, vehicles, cross-contamination, improper storage, and improper handling (Everis, 2004).

2.1.1 Spoilage organisms associated with fresh produce

The indigenous micro flora of fruits and vegetables predominately consists of Gram-negative rods such as *Pseudomonas*, *Enterobacter*, or *Pectobacterium* (previously *Erwinia*) species, lactic acid bacteria, moulds and yeasts (Francis *et al.*, 1999; Everis, 2004). The spoilage of vegetables is predominately caused by pectolytic enzyme producing bacteria and the

spoilage of acidic fruits is caused by lactic acid bacteria, moulds, and yeasts (Liao, 2006).The most commonly isolated yeasts were *Cryptococcus, Rhodotorula*, and *Candida* and the most commonly isolated mould genera were *Aureobasidium, Fusarium, Mucor, Phoma, Rhizopus*, and *Penicillium.* There are still 5 to 7 log units per gram total count found on minimally processed vegetables (Francis *et al.*, 1999).

Soft rot is the main outcome of bacterial spoilage of vegetables and can be caused by divers groups of bacteria including *Pectobacterium, Pseudomonas, Xanthomonas, Clostridium, Bacillus*, and *Cytophaga* (Nguyenthe & Carlin, 1994). The latter species are generally considered to be secondary pathogens following the more aggressive *Pseudomonas* and *Pectobacterium* which together cause more than 90 % of soft rot of fresh produce (Liao, 2006). The main effects of contamination with soft rot bacteria are water soaking and disintegration of plant tissue due to the production of extracellular enzymes (e.g. pectinases, cellulases, proteases, phospholipases and xylanases) (Barras *et al.*, 1994).

The soft rot causing *Pseudomonas* group mainly consists of *Pseudomonas viridiflava* and five biovars of *Pseudomonas fluorescens* and is responsible for over 40 % of total bacterial rot. Over 30 % of total native bacteria on salad vegetables belong to the *Pseudomonas* group which are responsible for the decay of fresh produce stored at low temperatures due to their psychotrophic nature. The majority of vegetable spoilage is caused by the pectolytic *Pectobacterium* group which includes the species *Pectobacterium carotovorum* subsp. *carotovorum, Pectobacterium atrosepticum*, and *Pectobacterium chrysanthemi*. Diseases of crops grown in subtropical or tropical regions are mainly caused by *Pectobacterium chrysanthemi* whereas *Pectobacterium atrosepticum* occurs mainly in cooler regions and is associated with black leg of potatoes. *Pectobacterium carotovorum* has the broadest host range of the group and causes diseases in almost every vegetables species grown in temperate and subtropical regions (Liao, 2006).

Soft rot bacteria can have either an antagonistic or synergistic effect on human pathogens. Whether the effect is antagonistic or synergistic is dependent on the type of pathogens, type of fresh produce, and storage conditions. Wells and Butterfield (1999) reported that on rotted plant tissue more Salmonella can be detected than on healthy plant tissue. On potato or carrot slices the population of Salmonella increased 5- to 10-fold when the slices were co-inoculated with *Pectobacterium* or *Pseudomonas*. Similar results were obtained by Carlin *et al.* (1995) with *Listeria monocytogenes*. These results suggest that rotted plant tissue provides extra nutrients for the growth of human pathogens and may serve as reservoir. An antagonistic effect of rot pathogens was observed in various studies (Carlin *et al.*, 1996; Babic *et al.,* 1996; Liao & Sapers, 1999). In these studies the growth of *Listeria*

monocytogenes was reduced in the presence of diverse *Pseudomonas* strains. The inhibition effect was explained by the production of iron-chelating fluorescent siderophores or antimicrobials by *Pseudomonas* (Liao & Fett, 2001).

2.1.2 Humanpathogenic organisms associated with fresh produce

During the years 1990 to 2005 13 % of foodborne illnesses were caused by fresh produce in the United States and in Europe 4.3 % of outbreaks between 1992 and 1999 were associated with fruits and vegetables (SCF, 2002; Smith DeWaal & Bhuiya, 2007). The outbreaks were caused by a variety of microorganisms and the most common humanpathogenic organisms associated with fresh produce are listed in table 2.1 (Beuchat, 1996; Beuchat, 1998; De Roever, 1998; Francis *et al.*, 1999; SCF, 2002; Everis, 2004; Gorny, 2006; CAST, 2009).

Table 2.1: Humanpathogenic organisms associated with fresh produce

Bacteria	Viruses	Parasites
Listeria monocytogenes	Hepatitis A	*Cryptosporidium parvum*
Clostridium botulinum	Norovirus	*Giardia*
Shigella species	Enterovirus	*Cyclospora cayetanesis*
E. coli species		*Entamoeba histolytica*
Salmonella species		*Ascaris* species
Aeromonas species		
Staphylococcus aureus		
Bacillus cereus		
Vibrio species		
Yersinia enterocolitica		
Campylobacter species		

Contamination with parasites is linked to contaminated water or contaminated food handlers, contact with animal and human faeces, and sewage. The outbreaks caused by parasitic organisms are more associated with fruits than with vegetables. In the United States between 1990 and 2005 8 % of fruit outbreaks were associated with parasites compared with only 2 % of vegetables outbreaks (Figure 2.2). Protozoa such as *Cryptosporidium* and *Giardia* can survive in tap water, river water and cow manure for six month. Since those organisms are chlorine resistant, they are also able to survive in chlorine treated water. The illness after consumption of fruits and vegetables contaminated with parasites can last for days to several months. The symptoms of the illness induced by protozoa are chronic diarrhoea and vomiting with weight loss (Beuchat, 1998; Francis *et al.*, 1999; SCF, 2002; Everis, 2004).

Norovirus and Hepatitis A are the most common described viral contaminants of fruits and vegetables. In the United States between 1990 and 2005, 40 % of all outbreaks are caused by Norovirus (Figure 2.2). It is assumed that most cases of foodborne virus diseases are not identified because the specimens are not commonly examined for viruses. The symptoms of viral infection are nausea, diarrhoea, jaundice, vomiting and flu-like symptoms and the duration of illness is variable from 20 hours up to 3 month (SCF, 2002). The contamination sources of viruses are soil and water if contaminated sewage has been used and infected food handlers has also been identified as a contamination source.

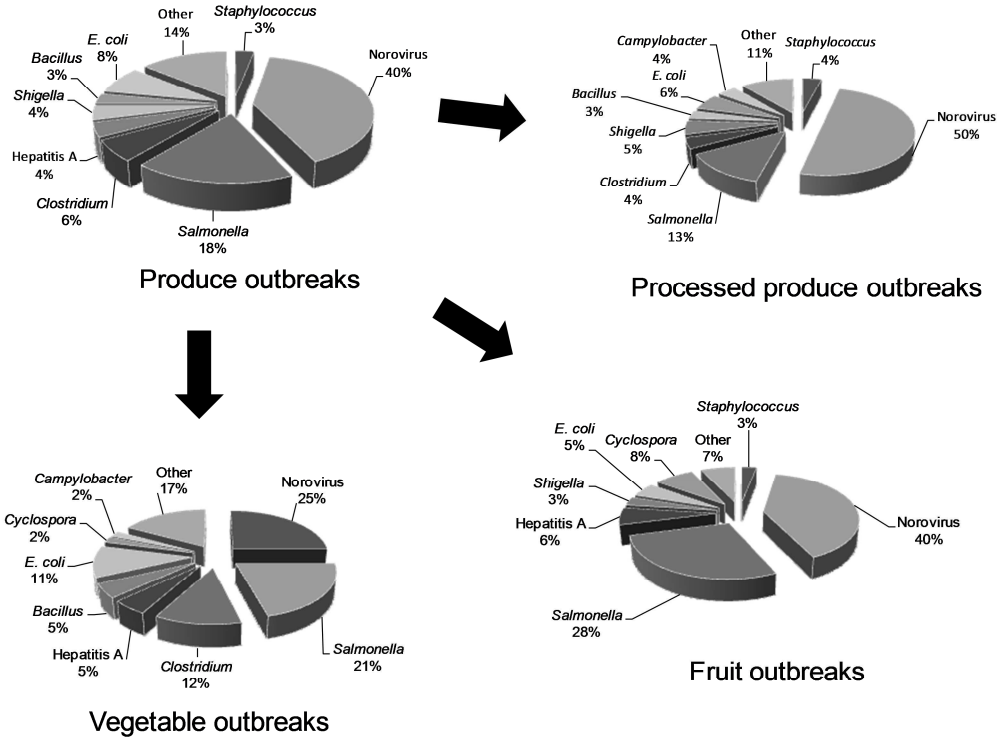

Figure 2.2: Most common causes of produce outbreaks in the USA between 1990 and 2005 (modified after Smith DeWaal & Bhuiya, 2007).

The microbial load of fresh produce with humanpathogenic bacteria are divers. Pathogens such as *Listeria monocytogenes*, *Clostridium botulinum*, and *Aeromonas* spp. are ubiquitous in the environment. *Escherichia coli, Salmonella* spp., *Yersinia enterocolitica* and *Campylobacter* spp. are associated with the intestinal tracts of animals and contamination with these bacteria is due to contact with faeces or contaminated soil and water (Francis *et al.*, 1999). The bacteria cause gastrointestinal diseases including diarrhoea, fever, vomiting, and abdominal cramps with a duration of 3 to 7 days (SCF, 2002). *Listeria monocytogenes* also grows at low temperatures and under low oxygen atmosphere which allows their

survival within ready-to-eat vegetables stored under modified atmosphere conditions. *Listeria monocytogenes* causes severe infections with a high mortality rate. Listerioses is often associated with Gastroenteritis and symptoms are likely to include fever, muscle ache and nausea. An infection with *Listeria* can lead to stillbirth and premature delivery and elderly people can develop meningitis or bacteraemia. Non-pathogenic *E. coli* species are part of the normal human and animal flora but a few pathogenic species are associated with diarrhoea. These species are able to produce toxins and have virulence factors such as adhesion and invasiveness. These enterovirulent *E. coli* species are designated according to their virulence properties, mechanism of pathogenicity, clinical syndromes and antigenic characteristics (Table 2.2). The most commonly recognised VTEC strain is *E. coli* O157. This strain was first identified in 1982 and has caused major outbreaks in Europe, North America and Japan (Beuchat, 1998; SCF, 2002).

Table 2.2: Divison of enterovirulent *E. coli*

Abbreviation	Description
AEEC	Attaching and Effecting *E. coli*
DAEC	Diffusely adherent *E. coli*
EAggEC	Enteroaggregative *E. coli*
EIEC	Enteroinvasive *E. coli*
EPEC	Enteropathogenic *E. coli*
ETEC	Enterotoxigenic *E. coli*
VTEC	Verocytotoxin-producing *E. coli*

2.1.3 Decontamination methods, guidelines, and regulations

2.1.3.1 Decontamination of fresh produce

To minimize the risk of foodborne diseases and to improve microbial quality decontamination of fresh produce is necessary. Washing of fruits and vegetables removes soil and dirt from the produce but only reduces microbial load by 1 or 2 log units (Sapers, 2001). But washing can also be a potential source for microbial contamination of produce.

A decontamination treatment has to be safe for humans and it is recommended that it results in the inactivation of at least 3 log units of enteric pathogens and 5 log units of total bacteria. The produce quality should not be affected by the treatments. Additionally, the survival of pathogens in treatment solutions should be prevented to avoid cross-contamination of produce or environment (Doyle & Erickson, 2008). An additional 10-fold to 100-fold reduction of bacterial load can be achieved using disinfectants, and some disinfectants are only suitable for equipments, others can be used in direct washing of products (Beuchat, 1998).

In the produce industry, chlorine (hypochlorite) is the most commonly used sanitizing agent. The effectiveness of chlorine is dependent on the amount of free available chlorine in the water, pH of the sample, the temperature, and the amount of organic matter. The type of organisms and the type of produce also influences the effectiveness of chlorine. The disadvantage of chlorine is the limited effectiveness against bacteria (1-2 log unit reduction) and lower effectiveness against protozoa (Everis, 2004; Doyle & Erickson, 2008). Additionally, the reactions between organic matter and chlorine lead to the formation of carcinogenic halogenated disinfection by-products (DBP), trihalomethanes (THMs), and haloacetic acids (HAAs). Chlorine also carries an environmental risk because it is associated with the production of high amounts of wastewater with high biological oxygen demand (Ölmez & Kretzschmar, 2009).

The problems associated with chlorine use lead to a high demand for alternative sanitizing agents in the fresh produce industry to enhance the microbial quality of convenience products. Therefore, the use of chemical agents such as chlorine dioxide, organic acids, hydrogen peroxide, peracetic (peroxyacetic) acid, and ozone are of interest to reduce microbial load of fresh produce (Beuchat, 1998; SCF, 2002; Ölmez & Kretzschmar, 2009).

Chlorine dioxide is more stable and has a higher oxidation power than chlorine. Additionally, it is not affected by pH and it does not react with organic matter in the same way as chlorine. Although it is less corrosive than chlorine and it does not form chloramines as hypochlorite, it is very unstable, explosive and has to be generated on-site. In the presence of iodine more iodinated DBP is formed by chlorine dioxide than by chlorine. It was shown that gaseous chlorine dioxide is more effective in microbial reduction on fresh produce than liquid chlorine dioxide but an adverse effect on sensory quality was observed. The lethal effect of hydrogen peroxide relies on its strong oxidizing power and the formation of cytotoxic agents such as hydroxyl radicals. The inhibitory effects are dependent on the pH, temperature and other environmental factors. Limitations of hydroxyl peroxide are its low antimicrobial efficacy and its long contact time. Moreover, it has a negative impact on overall produce quality and it is necessary to remove residual hydrogen peroxide after treatment.

Organic acids such as citric acid, lactic acid, acetic acid, succinic acid, malic acid, tartaric acid, benzoic acid or sorbic acid naturally occur on fruits and vegetables. The presence of organic acids reduces the pH of the produce and antimicrobial efficiency relies on this pH reduction. The antimicrobial efficiency varies among the types of organic acids; some are fungistatic while others prevent bacterial growth. Limitations of the organic acids are the long exposure times (between 5 and 15 min) and their negative effect on the sensory quality of the product. Therefore, their use is not of interest for the food industry (Beuchat, 1998;

Ölmez & Kretzschmar, 2009). Descriptions of peracetic acid and ozone as well as their antimicrobial effects are given in chapters 2.3 and 2.4, respectively.

Due to the fact that chemical disinfection methods lead to a formation of potential hazardous residuals on the product alternative inactivation treatments are of interest for the food industry. These alternative non-thermal processing methods are high hydrostatic pressure, irradiation, pulsed electric fields, ultrasound, UV light, and electrolysed water. High hydrostatic pressure leads to an inactivation of pathogens without appreciable heat generation. Additionally, the effects on the nutritional and sensory quality of treated products are minor and the shelf-life of products can be extended (Guan & Hoover, 2006). The use of irradiation to increase shelf-life and to reduce microbial contamination of fresh produce does not induce major damage on the physical and chemical properties of the product. Irradiation is effective against bacteria and protozoae but viruses are more resistant. The limitations of irradiation are the consumers' acceptance, costs and quality changes (Guan & Hoover, 2006). Pulsed electric field treatments are only applicable for the decontamination of liquid foods but it is effective against microorganisms without significant changes in the sensory quality of juices (Guan & Hoover, 2006). Ultrasound treatment is applicable to fruits, vegetables and juices and has the potential to inactivate microorganisms. However, use in combination with other preservation processes leads to a more effective inactivation of microorganisms. Another preservation treatment is the application of electrolysed water to reduce microbial load of fresh produce. Electrolysed water is effective against bacteria and fungi but the effects on produce quality have not been fully investigated (Guan & Hoover, 2006).

2.1.3.1 Guidelines and legislations

There are few guidelines available to enhance microbiological safety of fresh fruits and vegetables and the products thereof. The US Food and Drug Administration (FDA) published a guide to minimize microbial food safety hazards of fresh-cut fruits and vegetables. Therein, the FDA released recommendations regarding four areas of fresh-cut processing: a) personnel health and hygiene, b) training, c) building and equipment, and d) sanitation operations (FDA, 2008). The Codex Alimentarius Commission (1997) defined the good hygienic practice (GHP) in combination with a hazard analysis critical control point (HACCP) system as the basis of safe food production. Additionally, the Good Agricultural Practice (GAP) and Good Manufacturing Practice (GMP) are required tools for fruit and vegetable production. The identification of critical control points throughout the production of fruits and vegetables is considered to be problematic (Beuchat, 1996; SCF, 2002; Everis, 2004).

Beuchat (1996) described a model HACCP plan for fresh-cut produce developed by the International Fresh-Cut Association. Therein, critical control points within the production line of fresh-cut produce are identified and guidelines to achieve microbiological safety of fresh produce are given. A code of hygienic practice for fresh fruits and vegetables is published by the Codex Alimentarius Committee on Food Hygiene (2003). This code identifies environmental hygiene, hygienic production, handling, storage, transport, cleaning, maintenance, and sanitation as important the tasks for microbial safety. GAP and GMP should be applied to control microbial, chemical and physical hazards throughout the whole production line. In Europe, food hygiene is regulated by the Commission Regulation (EC) No. 852/2004 (European Commission, 2004). In this regulation rules for food business operators on the hygiene of foodstuffs are given. The rules are based on the following principles: i) the food business operator is primarily responsible for food safety; ii) food safety has to be ensured throughout the whole production chain; iii) the cold chain has to be maintained; iv) HACCP principles and GHP should be implemented; v) guides to good practice can be used as an instrument to aid food business operators at all levels of the food chain; vi) microbiological criteria and temperature control requirements have to be established; vii) imported foods are at least of an equivalent standard as food produced in the Community.

Microbiological criteria of food in Europe are regulated in the Commission Regulation (EC) No. 1441/2007 amending Regulation No. 2017/2005 on microbiological criteria for foodstuffs (European Commission, 2007). The microbiological criteria for fresh produce defined in this regulation are summarized in table 2.3.

Table 2.3: Microbiological criteria of fresh produce defined by the Commission Regulation (EC) No. 1441/2007 (European Commission, 2007)

Food	Microorganism	Sampling plan[1]		Limits[2]		Analytical reference method[3]	Stage of criterion
		n	c	m	M		
Ready-to-eat foods able to support growth of *L. monocytogenes* (for infants or medical purpose)[4]	*Listeria monocytogenes*	10	0	Absence in 25 g		EN/ISO 11290-1	Products placed on the market during their shelf-life
Ready-to-eat foods able to support growth of *L. monocytogenes* (not for infants or medical purpose)	*Listeria monocytogenes*	5	0	100 cfu g^{-1} [5]		EN/ISO 11290-2[6]	Products placed on the market during their shelf-life
		5	0	Absence in 25 g[7]		EN/ISO 11290-1	
Sprouted seed (ready-to-eat)[8]	*Salmonella*	5	0	Absence in 25 g		EN/ISO 6579	Products placed on the market during their shelf-life
Precut fruit and vegetable (ready-to-eat)	*Salmonella*	5	0	Absence in 25 g		EN/ISO 6579	Products placed on the market during their shelf-life
Unpasteurised fruit and vegetable juices (ready-to-eat)	*Salmonella*	5	0	Absence in 25 g		EN/ISO 6579	Products placed on the market during their shelf-life
Precut fruit and vegetable (ready-to-eat)	*E. coli*	5	2	100 cfu g^{-1}	1000 cfu g^{-1}	ISO 16649-1 or 2	Manufacturing process[9]
Unpasteurised fruit and vegetable juices (ready-to-eat)	*E. coli*	5	2	100 cfu g^{-1}	1000 cfu g^{-1}	ISO 16649-1 or 2	Manufacturing process[9]

[1] n = number of units comprising the sample; c = number of sample units given values between m and M
[2] m = criterion; M = warning value
[3] The most recent edition of the standard shall be used.
[4] Regular testing against criterion is not required for fresh, uncut and unprocessed vegetables and fruits, excluding sprouted seeds.
[5] This criterion shall apply if the manufacturer is able to demonstrate to the satisfaction of the competent authority, that the product will not exceed the limit of 100 cfu g^{-1} throughout the shelf-life. The operator may fix intermediate limits during the process that must be low enough to guarantee that the limit of 100 cfu g^{-1} is not exceeded at the end of shelf-life.
[6] 1 ml of inoculum is plated on a petri dish of 140 mm diameter or on three Petri dishes of 90 mm diameter.
[7] This criterion shall apply to products before they have left the immediate control of the producing food business operator, when he is not able to demonstrate to the satisfaction of the competent authority, that the product will not exceed the limit of 100 cfu g^{-1} throughout the shelf-life.
[8] Preliminary testing of the batch of seeds before starting the sprouting process or the sampling must be carried out at the stage where the highest probability of finding *Salmonella* is expected.
[9] Action in case of unsatisfactory results: improvements in production hygiene, selection of raw materials.

Across the worlds the regulation of substances used for the reduction of microbial load are inconsistent and uncertain (Gil *et al.*, 2009). An overview of legislations regarding alternative disinfectants is given in table 2.4 (Ölmez & Kretzschmar, 2009).

Food additives are regulated in the European Council directive 89/107/EEC. Legally food additives have to be safe and are not allowed to mislead the consumer. Processing aids are described in the Regulation (EC) No. 1333/2008 of the European Parliament and of the

Council of 16 December 2008 on food additives (European Commission, 2008). Therein, processing aids are defined as substances which i) are not consumed as foods itself; ii) are used in the processing of raw material, foods or ingredients to fulfil a technological purpose; iii) may result in the unintentional but technically unavoidable presence of residues in the final product, these residues do not have any healthy risk and no technological effect on the final product. It is important for the consumer acceptance whether the disinfectants used are classified as food additive or processing aids. Commonly consumers do not accept agricultural products labelled with the name of a chemical additive.

Table 2.4: Regulatory status of alternative disinfectants (used as processing aids) (Ölmez & Kretzschmar, 2009)

Regulation/Standard	Ascorbic acid (E 300)	Citric acid (E 330)	Ozone	Chlorine dioxide	Peroxyacetic acid	Hydrogen peroxide
Codex Alimentarius (1999) organically produced food; guidelines for the production, processing, labelling and marketing of organically produced foods (GL32 – 1999, Rev. 1-2001)	Allowed as additive	Allowed as additive	Not allowed	Not allowed	Not allowed	Not allowed
Council Regulation (ECC) No. 2092/91 and council regulation (EC) No. 834/2007 of 28 June 2007 on organic production and labeling of organic products and repealing Regulation (ECC) No. 2092/91	Allowed as additive	Allowed as additive and processing aid	Not allowed	Not allowed	Not allowed	Not allowed
IFOAM (International Federation of Organic Agriculture Movements) Basic Standard	Allowed as additive	Allowed as additive and processing aid	Not allowed	Not allowed	Not allowed	Not allowed
EU Food legislation-Regulation (EC) No. 178/2002 of the European Parliament and the Council of 28 January 2002 laying down the general principles and requirements of food law, establishing the European Food Safety Authority and laying down procedures in matters of food safety	Allowed	Allowed	*	*	*	*
FDA (U.S. Food and Drug Administration) (CFR Title 21)	Allowed	Allowed	Allowed	Allowed	Allowed	Not allowed

* Processing aids are not regulated, with that the mentioned processing aids can be used.

The regulations regarding processing aids need to be harmonised within the European Community and a global approach to processing aids in sanitizing wash water is necessary to minimize the risk of transmission of pathogens from water to produce (Gil *et al.*, 2009).

2.2 Heat

2.2.1 General principles of heat treatment

Heat treatment is the most commonly used treatment method in food processing (Moats, 1971; Earnshaw *et al.,* 1995; Rajkovic *et al.,* 2009). Depending on the applied time/temperature regime the microbial reduction from heat treatment can vary from limited microbial reduction to complete sterilisation of the product (Rajkovic *et al.*, 2009). The heating of products can be carried out by indirect and direct heating methods. Heat exchangers are used to apply the heat to food products. In direct heating processes the heat energy is passed directly to the food e.g. by steam injection or steam infusion. For food preservation three heating processes are used: blanching, pasteurisation, and sterilisation (Krämer, 1997; Zheleva & Kamburova, 2009).

Blanching is used for the preparation of fruits and vegetables for canning, freezing, or dehydration. During blanching processes enzymes (e.g. peroxydase, ascorbinase) or enzyme substrates are inactivated. This prevents undesirable changes of colour, vitamin content, and taste. Additionally, a reduction of volume is achieved by blanching resulting in an improved filling of cans; air and CO_2 are removed from intracellular spaces to prevent the occurrence of pseudo bomb gears. The bacterial count is reduced to approximately 1/50 to 1/100. Blanching temperatures are between 70 and 100 °C and the blanching time varies between 1 and 15 min (Tscheuschner, 2000). Immersion blanching in hot water is performed using temperatures between 75 and 95 °C resulting in a high loss of soluble nutrients. Steam blanching is performed at atmospheric or low pressure (150 kPa) with saturated steam and lower blanching losses can be achieved. Fruits and vegetables packaged in film bags were treated with microwave blanching achieving microbiological cleanliness with low losses of nutrient content (Zheleva & Kamburova, 2009).

Since the discoveries of Louis Pasteur in the1860s, mild-heat treatment, also known as pasteurization is widely used as food preservation method for products which are affected by excessive heat treatment (Moats, 1971). Pasteurisation processes are able to inactivate bacteria, viruses, protozoa, moulds, and yeast with often negligible changes in flavour and quality of the products. The number of viable pathogens is reduced to a level where a risk of disease is prevented as long as the product is consumed before the end of the expiration date and kept under optional refrigerated storage conditions. Heat-resistant spores are not inactivated by pasteurisation but enzymes present in the foods can be. The pH of food products highly influences the pasteurisation requirements. At a pH value below 4.5 pasteurisation targets are the inactivation of spoilage bacteria and enzymes whereas at pH values above 4.5 pathogenic bacteria need to be inactivated. Besides the most common

application of liquid milk pasteurisation other products such as wine, beer, and fruit juices are routinely pasteurized. Another application is the pasteurisation of egg products. Typical pasteurisation parameters are given in table 2.5 (Krämer, 1997; Zheleva & Kamburova, 2009).

Table 2.5: Pasteurisation conditions for food products

	Temperature	Time
Low temperature high time	65 °C	at least 30 min
Low temperature low time	71-75 °C	40 s-10 min
High temperature short time	85-90 °C	15-20 s

Sterilisation treatments are applied to inactivate and destroy all occurring bacteria including pathogens and heat-resistant spores (Tscheuschner, 2000; Zheleva & Kamburova, 2009). The temperatures needed to achieve a complete inactivation of endospores are between 115 and 135 °C and the sterilisation process is performed under pressure in an autoclave using steam or steam-heated water as heating medium. During sterilisation of food products a small number of spores may survive (Krämer, 1997). However, commercially sterility is achieved if twelve log decades of the target microorganism are reduced (Peleg, 2000).

Most published survivor curves of thermal treated microorganisms follow a first-order-reaction (Moats, 1971; Ramaswamy & Singh, 1997):

$$\frac{dN}{dt} = -kN \qquad \text{(eq. 2.1)}$$

Solving the equation 2.1 leads to the following first-order-reaction (Tscheuschner, 2000):

$$\frac{\lg N}{\lg N_0} = -0.4343kt \qquad \text{(eq. 2.2)}$$

In case of linear inactivation curves microbial destruction can be described with the decimal reduction time (D-value). The decimal reduction time is the heating time needed to reduce 90 % of the bacterial population at a given temperature. The D-value is calculated by the following equation:

$$D = \frac{t_2 - t_1}{\log(a) - \log(b)} \qquad \text{(eq. 2.3)}$$

The values a and b represents the survivor count after heat treatment for t_1 and t_2 min, respectively (Krämer, 1997; Ramaswamy & Singh, 1997).

The D-value is strongly dependent on the temperature. The higher the temperature the smaller is the D-value. The value used to describe the temperature which is needed to reduce the D-value by ten-fold is the z-value which is given in °C (equation 2.4;Tang *et al.*, 2000).

$$z = \frac{t_1 - t_2}{\log D_2 - \log D_1} \qquad \text{(eq. 2.4)}$$

Where D_1 is the D-value at temperature t_1 and D_2 is the D-value at temperature t_2. The z-values for vegetative bacteria, yeasts and moulds are between 4.4 and 6.6 °C. Endospores, *Clostridium* and *Bacillus* have z-values between 3 and 30 °C (Krämer, 1997).

Another value to describe the microbial reduction of heat treatments is the thermal death time (TDT). The TDT is the time needed to reduce all vegetative microorganisms at a given temperature. In contrast to the D-value the TDT is depending on the initial count and therefore represents a certain multiple of the D-value (Ramaswamy & Singh, 1997).

The lethality concept uses the lethality (F-value) to measure the lethality of a heat treatment or sterilisation process in order to compare relative sterilisation capacities of heat processes. The F-value is defined as the time in minutes which is needed to reduce a desired number of microorganisms at a specific temperature. It is an equivalent of heating for 1 min at a reference temperature of 121.1 °C. The F-value represents a certain multiple or fraction of the D-value depending on the type of microorganism (Ramaswamy & Singh, 1997).

However, the survival curves of heat-treated bacteria do not always follow a log-linear reaction (Figure 2.3; Moats, 1971). Non-log-linear curves can be observed after mild heat treatment (Geeraerd *et al.*, 2000). Therefore, the classical D-value concept is not applicable and mechanistic and empirical models are proposed (Couvert *et al.*, 2005).

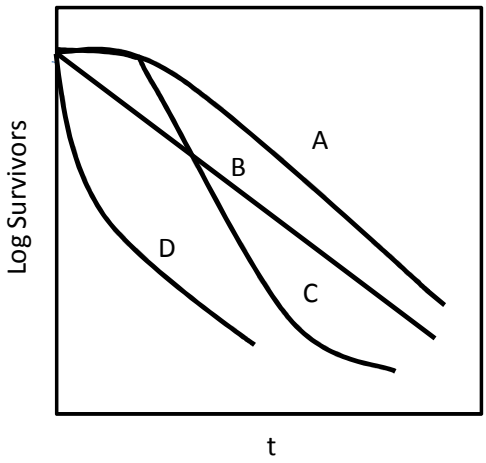

Figure 2.3: Types of survivor curves observed after heat treatment (Moats, 1971). A: convex survivor curve-initial lag in death rate followed by an approximately logarithmic death rate; B: logarithmic death rate; C: similar to curve A, but with tails; D: commonly observed with cells in logarithmic growth phase and considered to indicate a heterogeneous population.

2.2.2 Effects of heat treatment on microorganisms

Heat energy affects bacterial cells not at one specific target but rather affects the whole cells with their individual constituents, e.g. cell structure, molecules, and reactions within the cells. Heat resistance of bacterial cells may be due to the intrinsic stability of nucleic acids, ribosomes, enzymes, proteins inside the cells and within the cell membrane (Earnshaw *et al.*, 1995). Therefore, it is difficult to predict the event that causes injury or death of microorganisms (Propokov & Tanchev, 2007).

2.2.2.1 RNA and DNA damage

An early outcome of heat damage in a cell is the modification of RNA. Membrane damage induced by heat treatment leads to a depletion of Mg^{2+} within the cells. Mg^{2+} has a stabilising effect on ribosomes, e.g. 70S ribosomes, and a depletion of these ions produces 30S and 50S subunits preventing their biological activity. This may lead to an activation of ribonuclease and a further breakdown of the molecules (Earnshaw *et al.*, 1995). Ribosomal subunits are differentially affected by heat. 16S and 30S subunits are more rapidly degraded than the 23S and 50S subunits (Miller & Ordal, 1972). The higher heat stability of 50S subunits than of 30S subunits was also found by Mackey *et al.* (1991). Both subunits are more heat labile than the 70S particle. Nguyen *et al.* (2006) also identified an unfolding of the

30S subunit as well as an unfolding of essential proteins including subunits of RNA polymerase in *Campylobacter* cells during mild heat treatment resulting in cellular death. Heat resistance is achieved in the presence of high salt concentrations. Stephens & Jones (1993) proposed that the salt concentration lead to a dehydration of cells with resultant increase in internal solute concentration including Mg^{2+}. This leads to tighter coupled particles in the 30S subunit resulting in a higher temperature requirement for denaturation of the subunits. Tighter coupled particles also result in higher protein concentrations and therefore greater protein stability (Privalov & Khechinashvili, 1974; Anderson *et al.*, 1991).

2.2.2.2 Amino acids

Heat stress causes an accumulation of osmolytes in microorganisms. Amino acids and their derivates are known to be such osmolytes. These osmolytes are capable of stabilising proteins and protecting enzymes against heat inactivation (Santoro *et al.*, 1992). The role of osmolytes in protein stabilisation can be explained by two factors: i) exclusion of osmolytes, i.e. hydration of the folded protein domain increases the surface tension of water and opposes denaturation; ii) interaction of osmolytes with the unfolded protein (unfolded proteins are favoured for denaturation) (Taneja & Ahmad, 1994).

2.2.2.3 ATPase

The integrity of cytoplasmic and plasma membranes is damaged by heat treatment. Membrane-bound ATPase is associated with heat sensitivity of bacterial cells (Earnshaw *et al.*, 1995). ATPase is involved in ATP hydrolysis, active nutrient transport and maintaining the intracellular pH of the cells (Vallejo & Serrano, 1989). Due to sublethal injury the intracellular pH of *Saccharomyces cerevisiae* was lowered (Weitzel *et al.*, 1987). Increased ATPase activity in *Saccharomyces cerevisiae* was observed after exposure to lethal temperatures. This may be a possible mechanism to enable the restoration of intracellular pH. It was also shown that sublethal injury lead to a 50 % decrease in ATPase but the remaining ATPase was twice as active. ATPase seems to be essential for heat-resistance of bacteria (Earnshaw *et al.*, 1995).

2.2.2.4 Proteins and heat-shock proteins

Heat induces coagulation of proteins but water which is in close contact with proteins can influence the heat-resistance of the cells. Water can be attached at the surface of proteins or can be included in the tertiary structure of proteins. During heating vibration of water

molecules occurs and the S-S and hydrogen bonds of the surrounding proteins break. This breakage increases the mobility of peptide chains and in the presence of water new bonds are formed. In absence of water the dipoles of the protein chains interact, forming a strong heat-resistant complex (Earnshaw *et al.,* 1995). The pH-value also influences heat-based protein denaturation and a modification of food matrix pH can improve the efficacy of heating processes of foods with respect to bacteria inactivation (Condon *et al.*, 1992).

Microorganisms are able to adapt to sublethal conditions and this enables their survival in subsequent applications of more lethal temperatures. This effect may be attributed to heat-shock-proteins (HSP) which are normally present within the cells performing vital functions. Upon temperature increase HSP production is induced (Mackey & Derrick, 1986; Mackey & Derrick, 1987; Fedio & Jackson, 1989). It is supposed that HSP bind to polypeptides during sublethal heating to prevent misfolding and aggregation in proteins. They may also be involved in the recovery of heat denaturated proteins (Schlesinger, 1990). Some HSP of *E. coli* are also able to proteolyse irreversible damaged polypeptides, they take part in nucleic acid synthesis and cell division (Morris, 1993).

2.2.3 Application of heat inactivation processes

The heat resistance of *Salmonella typhimurium* was tested in the presence of tryptone soya broth, liquid whole egg, reconstituted dried milk, and minced beef at 54 and 60 °C (Mackey & Derrick, 1987). The heat resistance was similar in all tested model systems but 40 % reconstituted dried milk improved the heat resistance in comparison to 10 % reconstituted dried milk. A heat shock treatment (30 min at 48 °C) of the cells improved the thermotolerance of *Salmonella typhymurium.* The time needed to achieve the same degree of inactivation of *Salmonella* was twice as high in heat-shock treated cells than in untreated cells. The highest difference was observed for liquid whole egg heated at 54 °C. The authors suggested rapid heating of foodstuffs to lethal temperatures to avoid inducing thermotolerance during pasteurisation.

The control of postharvest diseases of strawberries was tested using hot water dips at 55 to 60 °C for 30 s. The decay incidence in terms of *Botrytis cinerea* was reduced from 28.5 % to 3.4 and 2.7 % at 55 and 60 °C, respectively. The significant reduction of natural fungal populations by hot water dips did not cause surface injuries, and did not affect weight loss or taste parameters in strawberries (Karabulut, Arslan, & Kuruoglu, 2004). The immersion of sweet cherries inoculated with *Penicillium expansum* spores and *Botrytis cinerea* spores in water at 55 °C for 30 s lead to a spore germination of 27 and 16 %, respectively. At 50 °C more than 80 % of the spores were able to germinate but at 60 °C no germination of the

spores occurred after 30 s. The mortality of spores was improved using heat treatment in combination with 10 % ethanol. The most effective treatment was the immersion of cherries in 10 % ethanol at 60 °C. The surface and stem colour of the cherries were not adversely affected by the treatment with hot water and ethanol (Karabulut, Arslan, Kuruoglu *et al.*, 2004). However, Wang (2000) treated strawberries with moist hot air and detected injuries of the fruits exposed to temperatures above 50 °C or after treatments at 45 °C for more than 60 min. The strawberries had lower titratable acidity, higher soluble content and higher levels of sugars after heat treatment than untreated fruits. Additionally, the fruits were less bright after treatment with moist hot air and they had a higher soluble solids/acid ratio. At temperatures ≤ 39 °C the quality attributes of treated strawberries were comparable to the attributes of untreated samples. Murine norovirus 1, *E. coli*, and *Bacillus fractilis* HSP-40-infecting phage B40-8 in raspberry puree were reduced by 1.86, 2.77 and 3.89 log units, respectively after mild heat treatment at 65 °C for 30 s. A reduction of 2.81, 3.44, and 3.61 log units was achieved after enhancing the temperature to 75 °C with a holding time of 15 s. Baert *et al.* (2008) suggested that for high initial contamination mild heat treatment is not suitable to reduce infectious norovirus particles. A combination of mild heat treatment with other preservation methods to improve microbial safety of foods seems to be an alternative to drastic heat treatments. Steenstrup (2002) showed a decreased heat resistance of *E. coli* O157:H7 in apple cider in the presence of sorbate, benzoate, and malic acid. At 47, 50 and 53 °C the D-value of *E. coli* decreased at the middle by a factor of 2 in the presence of the tested food additives.

Mild heat treatment induced by radio-frequency application followed by dipping in chlorinated ice water (100 ppm) reduced the initial microbial load of fresh cut carrots to approximately 1/3 within 2 min at 60 °C. The treatment was more effective than dipping in hot water or in chlorinated water (100 ppm). In contrast to hot water dipping and dipping into chlorinated water the colour and taste of the carrots was not affected by the RF thermal treatment (Orsat *et al.*, 2001).

Heat-shock is a high-temperature-short-time method which can be a useful process for quality preservation of fruits and vegetables. Usually, a washing step at temperatures between 45-70 °C is applied for less than 5 minutes. This method helps to prevent quality deterioration and to maintain the texture and quality of the products. The heat-shock method requires a combination with other sanitising methods (Rico *et al.*, 2007).

2.3 Peracetic acid

2.3.1 Theoretical basics of peracetic acid

Peracetic acid (PAA) is also known as peroxyacetic acid, acetyl hydroxide or ethaneperoxoic acid. The peroxide of acetic acid is a strong oxidant and disinfectant. The commercially available PAA is a quaternary equilibrium mixture that consists of acetic acid ($CH_3\ CO_2H$), hydrogen peroxide (H_2O_2), PAA (CH_3CO_3H) and water. The equilibrium is shown in the following equation (Wagner *et al.*, 2002; Gehr *et al.*, 2003; Kitis, 2004):

$$CH_3\ CO_2H + H_2O_2 \leftrightarrow CH_3CO_3H + H_2O$$

PAA is a colourless, clear liquid with an intense odour. Its acidic pH is less than 2 and it is soluble in water and polar organic solvents but only slightly soluble in aromatic solvents. In the presence of sulphuric acid as a catalyst, acetic acid or acetic anhydride reacts with hydrogen peroxide to PAA (Swern, 1949; Kitis, 2004).

PAA is unstable which is demonstrated by the 1 to 2 % loss of active ingredients per month in a 40 % PAA solution. Diluted PAA is more unstable in diluted solution and for stability the solutions should be stored at low temperatures in original containers. PAA is not affected by glass and most plastics, pure aluminium, stainless steel, tin-plated iron are resistant to it however, plain steel, copper, brass, bronze, and galvanised iron are susceptible to corrosion (Kitis, 2004).

PAA can be used over a wide temperature range (0 to 40 °C), it is not affected by protein residues, can be used with hard water, in cleaning-in-place processes and carbon dioxide saturated environments. Additionally, it is efficient over a wide range of pH (3.0 to 7.5) (Kunigk *et al.*, 2001). The decomposition products of PAA are water, oxygen, hydrogen peroxide, and acetic acid (Kitis, 2004; Wang *et al.*, 2006). There are three different decomposition reactions of PAA in aqueous solutions as described by Yuan *et al.* (1997a; 1997b):

i) Spontaneous decomposition:

$$2CH_3CO_3H \rightarrow 2CH_3CO_2H + O_2$$

ii) Hydrolysis:

$$CH_3CO_3H + H_2O \rightarrow CH_3CO_2H + H_2O_2$$

iii) Transition metal catalysed decomposition:

$$CH_3CO_3H + M \rightarrow O_2 + \text{Other decomposition products}$$

After reaction of PAA with organic material no or only small amounts of toxic or mutagenic by-products are formed (Liberti & Notarnicola, 1999; Mezzanotte *et al.*, 2003; Kitis, 2004; Koivunen & Heinonen-Tanski, 2005a; Wang *et al.*, 2006; Dell'Erba *et al.*, 2007). However, carboxylic acids were found in PPA treated river water and the formation of aldehydes was found after reaction of PAA with amino acids, phenols, and other aromatic substances from the wastewater (Kitis, 2004). Furthermore, PAA can cause skin and eye irritation and 524 mg m^{-3} after 1 h inhalation is the mean lethal concentration (LC_{50}). The tolerance for H_2O_2 presence in drinking water is 100 µg l^{-1} (Liberti & Notarnicola, 1999). These authors also described four major drawbacks of PAA disinfection: i) instability (metals are found in storage and dosing equipment, these metals can catalyse decomposition of PAA); ii) limited efficiency against viruses and parasites; iii) bacterial re-growth can be promoted by acetic acid; iv) influence of organic content and quality of treated product.

In the food processing industry (e.g. dairies, wineries, breweries, canneries, meat and poultry-processing plants, and beverage industry) PAA is used as disinfectant and for wastewater disinfection (Model, 1997; Orth, 1998; Kitis, 2004). PAA is used as disinfectant and decolouring agent in the pulp, textile, and paper industry (Koivunen & Heinonen-Tanski, 2005b; El Shafie *et al.*, 2009) as well as for the disinfection of ion exchangers and cooling towers and for pathogen reduction in sludge debulking, biosolids and for the reduction of solid odours (Kitis, 2004; Koivunen & Heinonen-Tanski, 2005b).

2.3.2 Inactivation mechanism of peracetic acid

PAA is a chemical disinfectant and therefore initially attacks microbial cell walls, membranes, enzymatic systems, and transport systems (Koivunen & Heinonen-Tanski, 2005a). The release of active oxygen by PAA leads to an oxidation of sulfhydryl (-SH) and sulphur (S-S) bonds in proteins as well as in enzymes. Additionally, other metabolites are oxidised and the bases of DNA molecules are affected. The action of PAA against Gram-negative cells is explained by the effect on outer membrane lipoproteins. The chemiosmotic function of the lipoprotein cytoplasmic membrane is disrupted by PAA and a transport of PAA occurs via dislocation or rupture of cell walls. The intracellular PAA can oxidise enzymes which results in affected biochemical pathways, the active transport across membranes is hindered and intracellular solute levels are impaired. PAA is able to inactivate bacterial catalase which serves to detoxify free hydroxyl radicals. Thus, free radicals can attack more efficiently and

lead to an inactivation of microbial cells (Leaper, 1984; Liberti & Notarnicola, 1999; Gehr *et al.*, 2003; Kitis, 2004; Koivunen & Heinonen-Tanski, 2005a). Protein destruction by PAA is an explanation for its activity against helminthes and nematodes (Liberti & Notarnicola, 1999). It is suggested that the inactivation of coliphages by PAA is due to changes or damage to their protein coat or attachment sites. These surface structures are needed for the infection of host cells (Koivunen & Heinonen-Tanski, 2005a). Spore inactivation by PAA induced by a degradation of spore coat followed by a damage of the inner membrane and the cell wall (Hilgren *et al.*, 2007).

The antimicrobial activity against microorganisms can be arranged as follows (Vandekinderen *et al.*, 2009; Figure 2.4):

Figure 2.4: Range of disinfection activity of PAA against microorganisms.

2.3.3 Application of peracetic acid for disinfection

2.3.3.1 Wastewater disinfection with peracetic acid

Since the 1980s the use of PAA as a disinfectant for wastewater and sewage effluent has been investigated (Kitis, 2004). Baldry *et al.* (1991) tested the activity of various concentrations PAA on the inactivation of sewage relevant bacteria, bacteriophages and viruses in absence and presence of organic matter. They showed that PAA is effective against the tested microorganisms and PAA is only little affected by the organic matter. Additionally, they still found viral inactivation one hour after PAA addition. A four log unit reduction was observed for total and faecal coliforms in settled sewage after 20 min contact time with PAA. However, PAA is less effective against poliovirus type 2 because less than 1 log unit reduction was achieved within 20 min (Morris, 1993).

PAA was described as a good alternative disinfectant to chlorine in wastewater treatment, especially if the wastewater contents easily oxidizable organic matter (Koivunen & Heinonen-Tanski, 2005a). Microbial culture was added to a synthetic wastewater-like test medium and subsequently treated with PAA in various concentrations for 10 min. A PAA concentration of 3 mg l^{-1} lead to a 2-3 log reduction of enteric bacteria, and 1-1.5 log units of coliphages MS2

were reduced by a PAA concentration of 7-15 mg l^{-1} in laboratory-scale experiments (Koivunen & Heinonen-Tanski, 2005a). The laboratory-scale experiments were verified by pilot-scale experiments. It was shown that the hygienic quality of primary, secondary, and tertiary effluents was improved by PAA treatment. A three log unit reduction of total coliforms and enterococci in secondary and tertiary effluents was achieved after 27 min with 2 to 7 mg l^{-1} PAA: In primary effluents a PAA concentration of 5 mg l^{-1} reduced total coliforms and enterococci by less than two log units. The increase of PAA concentrations to 10-15 mg l^{-1} lead to an increased reduction of 3-4 log units. Depending on the PAA dose and on the type of microorganism the microbial reduction occurred during the first 4-18 min treatment time (Koivunen & Heinonen-Tanski, 2005b).

Re-growth ability of *E. coli*, total coliforms (TC), faecal coliforms (FC), and total heterotrophic bacteria (THB) after PAA treatment was investigated by Mezzanotte *et al.* (2003) in a pilot scale study at a wastewater treatment plant. Bacterial count after PAA treatment with concentrations of 15 and 25 mg l^{-1} was performed using traditional culture methods and flow cytometry. They observed comparable disinfection efficiency for *E. coli*, TC and FC with an increase in disinfection with raising concentrations and contact time. In this process the contact time at lower doses had more effect on disinfection efficiency than at higher doses. THB are less affected by the test concentrations. Bacterial re-growth was not observed after quenching of the reaction with sodium thiosulfate and catalase. Flow cytometric analysis using SYBR Green I and propidium iodide showed a decrease of viable bacteria after treatment with 15 mg PAA l^{-1} for 12 min. Between 12 min and 36 min treatment time the percentage of viable bacteria only slightly decreased. Similar results were obtained by Antonelli *et al.* (2006) at PAA concentrations of 5 mg l^{-1} where no re-growth of coliform bacteria took place after 29 h. The authors concluded that bacterial damage induced by PAA is irreversible and attested both a bacteriostatic and bactericide effect of PAA. Flow cytometric analysis of PAA treated heterotrophic bacteria were also performed by Rossi *et al.* (2007) and Mezzanotte *et al.* (2007). In both studies the percentage of damaged cells was 5 % before and after PAA treatment and the percentage of viable cells only slightly decreased. Mezzanotte *et al.* (2007) suggested that the bacteria cells were disrupted by the PAA because the total bacterial count observed by flow cytometry decreased with increasing contact time and doses. Rossi *et al.* (2007) suggested that the bacteria cell were not able to repair the PAA induced damage.

The reduction of microbial load in various stages of wastewater treatment was investigated using 1.5 to 2 mg l^{-1} PAA with a contact time of 20 min. The faecal contamination was reduced by 97 %, thus the recommended limit by Italian law for discharge into surface water was reached. A rise in biological oxygen demand decreased the microbial reduction but a

rise in temperature increased the microbial reduction (Stampi, 2001). A PAA concentration of 0.6 to 1.6 mg l^{-1} was necessary to reach the target faecal coliform level in a wastewater treatment plant (Wagner *et al.*, 2002). The authors concluded that PAA may become a cost-effective alternative to UV radiation, chlorine or ozone for wastewater treatment in North America. In contrast, the same research group stated in 2003 that the PAA concentration needed to reduce the faecal coliform bacteria to the target level exceeded 6 mg l^{-1}. For the investigated wastewater treatment plant PAA was not suitable as disinfectant (Gehr *et al.*, 2003).

Biocide effects of PAA against total and faecal coliforms, *E. coli, Pseudomonas* sp., and *Salmonella* sp. Similar to the biocide effects of sodium hypochlorite were shown by Veschetti *et al.* (2003). The PAA related reduction of faecal *streptococci* and bacteriophages anti-*E. coli* was less than the reduction by sodium hypochlorite. In contrast to sodium hypochlorite treated sewage no significant variation in halogenated organic compound content was observed after PAA treatment.

2.3.3.2 Disinfection of food contact surfaces with peracetic acid

In food-processing and beverage industries PAA is indicated as ideal for cleaning-in-place disinfection (Kitis, 2004). The efficiency of PAA against bacteria in solution and adherent on stainless steel was tested by Kunigk & Almeida (2001). *E. coli* and *Staphylococcus aureus* in suspension were treated with 40 mg l^{-1} PAA at 25 °C. *Staphylococcus aureus* was more resistant against PAA than *E. coli* which is shown in a 6.2 log unit reduction after 10 min treatment time whereas *E. coli* was reduced by 8 log units after 4 min. The inactivation kinetics followed a first-order equation. The treatment time to reduce *Staphylococcus aureus* adherent on stainless steel by 6.5 log units was three times greater than of *Staphylococcus aureus* in suspension. The lower reduction was due to mechanical barriers such as surface irregularities and the external layer of PAA-destroyed cells. Similar results were obtained for *Listeria monocytogenes* in suspension and adherent on stainless steel. At PAA concentrations ≥ 5 ppm acomplete inactivation of *Listeria monocytogenes* in suspension was achieved after 5 min at 20 °C if bacterial concentration was ≤ 10^5 CFU ml^{-1}. Only a four log unit reduction was achieved after 10 min at bacterial concentrations of 10^8 CFU ml^{-1}. *Listeria monocytogenes* adherent on stainless steel or polytetrafluoroethylene was more resistant against PAA than in suspension. A total reduction of bacteria was not observed (Meylheuc *et al.*, 2006).

Rossini and Gaylarde (2000) compared the efficiency of hypochlorite and PAA against *E. coli, Pseudomonas fluorescens*, and *Staphylococcus aureus* isolated from chicken

carcasses and adherent on stainless steel. Although, hypochlorite showed a higher efficiency than PAA, the authors found an activity against *E. coli* and *P. fluorescens*. Both bacteria were reduced by more than 90 % at 250 mg l^{-1} PAA. In contrast, *S. aureus* was only reduced by 50 % at the same PAA concentration. The authors concluded that PAA cannot be recommended as a disinfectant for chicken process equipment. In contrast, Marques *et al* (2007) found a 5.26 log and 4.51 log unit reduction of *S. aureus* adherent onto glass surfaces and stainless steel, respectively after PAA treatment with a concentration of 0.3 %. A complete removal was not observed with the used concentration and the tolerable limit for food contact surfaces (2 CFU cm^{-2} (American Public Health Association) or 30 CFU cm^{-2} (World Health Organisation)) was not reached. The inactivation efficiency of bacteria adherent on food equipment by PAA is highly influenced by the food matrix. *L. monocytogenes* attached in salmon juices were totally reduced by PAA but in meat emulsions the reduction was only 1-2 log units (Gram *et al.*, 2007). The inactivation of *Staphylococcus* spp., *Listeria* spp., and *E. coli* by 0.05 to 0.4 % PAA in the presence of sterile skim milk, orange juice, liquid egg, and chocolate milk shake was tested by Briñez (2006). Orange juice had the lowest interference capacity and egg had the greatest interference capacity. However, in all cases a reduction by > 5 log units was achieved after 10 min and 0.1 % PAA. At low PAA concentrations *Staphylococcus* was more resistant than *Listeria* and *E. coli*. The influence of food residues on the inactivation of *Bacillus anthracis* spores was investigated by Hilgren *et al.* (2007). The spores were mixed with water, flour paste, whole milk, or egg yolk emulsion and dried on stainless steel. The inoculated stainless steel samples were covered with various concentrations of PAA for 10 min at 10, 20, and 30 °C. The minimum PAA concentration at 20 °C to achieve a 6 log unit reduction of spores without presence of food residues was 1.05 %. The presence of food residues had only minor effects on spore inactivation by PAA.

The efficiency of a combination of PAA and hydrogen peroxide against *Bacillus cereus* spores in suspension and on stainless steel and rubber discs was tested (Te Giffel *et al.*, 2010). The sporicidal effect of the disinfectant was less on stainless steel and rubber discs than in solutions containing 4 % milk. The sporicidal effect value in suspensions was between 1.2 log ml^{-1} and 1.8 log ml^{-1} after treatment with disinfectant concentrations of 0.5 and 0.7 % for 10 min at 50 °C, respectively. Experiments in milking installations showed similar sporicidal effect value of 0.4 log ml^{-1} as the surface experiments. Another use of peracetic acid in milk processing areas is the application spray equipment producing a constant fog of sanitizers. Using sanitizer solution containing 45 mg l^{-1} PAA reduced the number of total mesophilic aerobic bacteria by 0.55 log units m^{-3} (Salustiano *et al.*, 2004). The authors concluded that chemical sanitizers can control microbiological quality of air in

milk processing and therefore help to improve the microbiological safety in food processing. Drawbacks of fogging with chemical sanitizers in food processing areas are the potential development of bacterial resistance against the applied sanitizers (Bore, 2005). The authors recommend the alternation of disinfectants to overcome the problems of resistance.

2.3.3.3 Disinfection of food and model systems with peracetic acid

Oh *et al.* (2005) used aerosolized PAA to inactivate *Bacillus cereus, Listeria innocua, Staphylococcus aureus*, and *Salmonella typhimurium* inoculated on tryptic soy agar petri dishes. The inoculated petri dishes were placed at different locations in a semi-trailer cabinet and exposed to aerosolized PAA (1800 ppm) and hydrogen peroxide (8800 ppm) for 1 h. A 3.09, 7.69, 6.93, and 8.18 log unit reduction per plate was achieved for *Bacillus cereus, L. innocua, S. aureus*, and *S. typhimurium,* respectively. No significant differences in inactivation of *L. innocua, S. aureus*, and *S. typhimurium* according to their location in the cabinet were observed. These results indicate the potential of aerosolized PAA for commercial application of produce decontamination.

Gram *et al* (2007) showed that PAA is less effective against bacteria in meat emulsions. These results are in agreement with results from Gill & Badoni (2004). Chilled beef from two slaughtering plants was treated with 0.02 % peroxyacetic acid. Only small effects on aerobics, coliforms, and *E. coli* were observed after treatment.

Contamination of fresh produce can be caused by contaminated process water. Therefore, the decontamination of process water is an important task during food processing. Effective disinfectants to reduce fungal and yeast load in processing water to improve product quality and extend shelf-life of the products are of growing interest. Hilgren (2000) compared the efficiency of peroxyacetic acid (80 ppm) and a mixture of peroxyacetic and octanoid acid (64 ppm) to inactivate *Candida parapsilosis*, *Rhodotorula* species, *Cryptococus* species, *Zygosaccharomyces baili*, *Aspergillus* species, *Penicillium* species, and *Cladosporium* species. The mixture of peroxyacetic and octanoid acid was more effective than peroxyacetic acid alone. Lower number of yeasts and moulds in processing water as well as on potatoes were detected after treatment with peroxyacetic/octanoid acid mixture. PAA was also applied to reduce brown rot and soft rot on stone fruits (Mari *et al*., 2004). A significant reduction of naturally present *Monilinia laxa* on stone fruits was achieved after dipping the stone fruits in 125 mg l^{-1} PAA solution for 1 min. *Rhizopus stolonifer* was inoculated on wounded stone fruits and significantly reduced after dipping in 250 mg l^{-1} PAA solution for 1 min. These results imply that PAA is a useful tool to prevent the spread of diseases throughout processing and marketing.

The efficiency of PAA against bacteria on fresh fruits and vegetables as well as on fresh-cut fruits and vegetables was examined in various studies (Beuchat *et al.*, 2004; Wang *et al.*, 2006; Kim *et al.*, 2006; Yuk *et al.,* 2006; Ruiz-Cruz *et al.,* 2007; Vandekinderen *et al.*, 2009; Alvaro *et al.,* 2009). Cantaloupe inoculated with *E. coli* O157:H7 was treated with a peroxyacetic acid-based sanitizer Tsunami 100 (80 mg l^{-1}) and a reduction in viable count of 0.77 log units was achieved after one min treatment (Wang *et al.,* 2006). A one minute treatment with 40 µg ml^{-1} of a peroxyacetic acid-based Tsunami 200 reduced *Enterobacter sakazakii* by ≥ 4 log units on apples (Kim *et al.*, 2006). On fresh-cut apples 1.2 log unit reduction of *E. coli* O157:H7 occurred after one min treatment with Tsunami 100 (80 mg l^{-1}) (Wang *et al.*, 2006). *Salmonella* was inoculated on artificially wounded bell pepper or cucumber, smooth surfaces of bell pepper or cucumber and on stem scar tissue of bell pepper. Afterwards, the bell pepper and cucumbers were washed with a PAA solution (75 ppm). *Salmonella* was reduced by 1 log unit on wounded bell peppers, > 2 log units on stem scar tissue, and no *Salmonella* were detected on smooth surfaces of bell pepper and cucumber. *Salmonella* on wounded cucumber was reduced by 2 log units (Yuk *et al.*, 2006). Similar results were obtained by Alvaro *et al.* (2009). The shelf-life of bell pepper, cucumber, and tomatoes was improved using PAA and the taste characteristics were not affected (Alvaro *et al.*, 2009). More than 3.7 log units *Enterobacter sakazakii* were reduced on tomatoes after treatment with 40 µg ml^{-1} Tsunami for 5 min (Kim *et al.*, 2006). The same disinfectant concentration leads to an inactivation of ≥ 5.31 log units of *Enterobacter sakazakii* inoculated on lettuce after 5 min treatment (Kim *et al.*, 2006). Beuchat *et al.* (2004) tested the efficiency of the peroxyacetic acid-based sanitizer Tsunami 100 (80 mg ml^{-1}) against *Listeria monocytogenes* inoculated on iceberg lettuce pieces, shredded iceberg lettuce, and Romaine lettuce pieces. The order of reduction of *Listeria monocytogenes* in different types of lettuces was given as follows: shredded iceberg lettuce > iceberg pieces > Romaine pieces. The dependence of PAA disinfection efficiency on the type of fresh produce was also shown by Vandekinderen *et al.* (2009). The highest reduction of natural flora by PAA was found in carrots and white cabbage (0.5-3.5 log units), followed by iceberg lettuce (0.4-2.4 log units). On fresh-cut leek the reduction of natural flora was lowest after PAA treatment (0.4-1.4 log units). All vegetables were acceptable for consumption after PAA treatment. The inactivation of *E. coli* O157:H7, *Salmonella*, and *Listeria monocytogenes* inoculated on fresh-cut carrots by washing with 40 ppm PAA was investigated by Ruiz-Cruz *et al.* (2007). The inoculated fresh-cut carrots were washed with PAA in tap water and processing water. 2.1 log units of *Salmonella* were inactivated under process water conditions. *E. coli* O157:H7 and *Listeria monocytogenes* were only reduced by 1.24 log units and 0.83 log units, respectively, both under process water conditions and tap water conditions.

2.4. Ozone

2.4.1 Theoretical basics of ozone

The triatomic molecule Ozone (O_3) is an allotropic modification of oxygen (Kim, Yousef, & Dave, 1999). The molecular structure of ozone is a resonance hybrid of the four canonical forms with delocalized bonding (Figure 2.5) with an angle of 116.8° between the 2 O-O bonds and a bond length of 1.278 anstrons (Guzel-Seydim *et al.*, 2004; Mahapatra *et al.*, 2005).

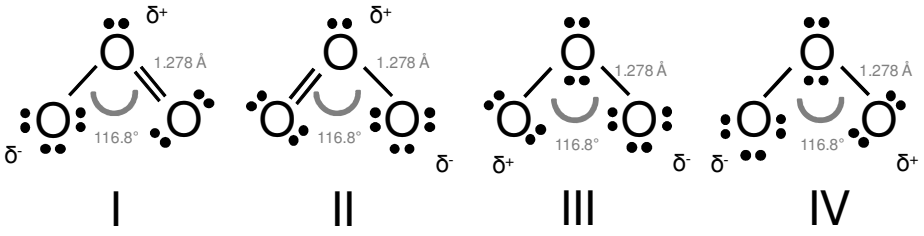

Figure 2.5: Resonance structures of ozone molecules (Trambarulo *et al.*, 1953).

The relative molecular mass of ozone is 48 g mol^{-1}; the melting point is -192.5 °C and the boiling temperature is -119.5 °C. In the gaseous state ozone is light blue to nearly colourless and in both liquid and solid state it is opaque blue-black. Ozone has a characteristic pungent odour which can be described as similar to fresh air after a thunderstorm (Graham, 1997; Kim *et al.*, 2003; Guzel-Seydim *et al.*, 2004; Mahapatra *et al.*, 2005). The detectable odour level is 0.01-0.05 ppm (Mahapatra *et al.*, 2005). With an oxidizing potential of 2.07 V, ozone is the fifth in thermodynamic oxidation potential behind fluorine, chlorine trifluoride, atomic oxygen, and hydroxyl free radical (Graham, 1997). This oxidising potential makes ozone the strongest disinfection agent available for the contact with foods (Mahapatra *et al.*, 2005) and water and wastewater treatment (Graham, 1997). The density of gaseous ozone is 2.14 g l^{-1} at 0 °C and 101.3 kPa which is greater than the density of air under similar conditions (Kim *et al.*, 2003).

The solubility of ozone in water is dependent on several parameters. Ozone and water form a true physical solution. The solubility of ozone in liquids follows Henry's law which states that the amount of gas in a solution is linearly proportional to the partial pressure of the gas at given temperatures. The temperature of the water highly influences the solubility of ozone. The solubility rate of ozone ranges between 0.31 and 1.13 dependent on the temperature with higher solubility at lower temperatures. Bubble size also influences the ozone solubility. Smaller bubble sizes increases solubility due to larger surface area of contact. Optimal

bubble size for ideal dissolution of ozone in water is 1 to 3 mm in diameter. Another influence parameter is the pH of the water. An increased rate of decomposition of molecular ozone into hydroxyl radicals was observed at increased pH of the liquid. The presence of minerals or organic matter may also catalyse the decomposition of ozone. As a consequence, high purity of water increases the solubility of ozone. The half-life of ozone in gaseous state is 12 h at room temperature and in pure, clean water (pH 7-8) the half-life is 20-30 min (Khadre *et al.*, 2001; Kim *et al.*, 2003). The decomposition of ozone in solution is a stepwise fashion accompanied by the production of free radicals such as hydroperoxyl ($^{\bullet}HO$), hydroxyl ($^{\bullet}OH$), and superoxide ($^{\bullet}O_2^-$) (Figure 2.6). These free radicals have a great oxidising power and the reactivity of ozone is attributed to these radicals.

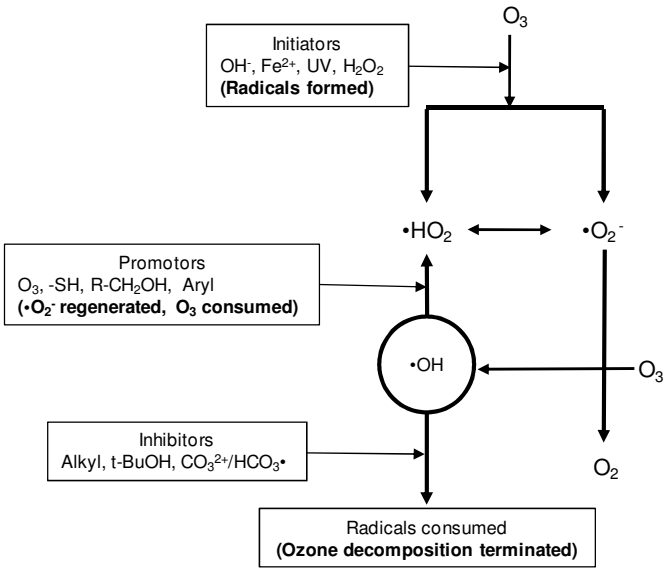

Figure 2.6: Ozone decomposition reactions (modified after Khadre *et al.*, 2001).

The reaction of organic and inorganic compounds in water with ozone occurs in two ways:

i) Direct reaction of organic compound (M) with molecular ozone:

$$O_3 + M \rightarrow M_{ox}$$

ii) Decomposition of ozone in water into a radical (e.g. OH) which reacts with the organic matter (M):

$$O_3 \xrightarrow{OH^-} OH \xrightarrow{M} M_{ox}$$

The reactions of ozone are selective and limited to unsaturated aromatic and aliphatic compounds. These compounds are oxidised to double-bonds through cycle-addition. Sulphydryl groups are also oxidised by ozone. A breakage of glycosidic bonds and a formation of aliphatic acids and aldehydes occur upon reaction of ozone with polysaccharides which is a slow reaction. Hydroxy-hydroperoxides are formed by the reaction of ozone with primary and secondary aliphatic alcohols. The reaction of ozone with glucosamines is very fast but glucose and N-acetyl glucosamine are relatively resistant to degradation. Ozone also attacks the nitrogen atom of the R group of amino acids and proteins. A slow reaction of ozone with saturated fatty acids has been detected but unsaturated fatty acids are oxidized and cycle-addition products are formed. Additionally, ozone rapidly reacts with nucleobases such as thymine, guanine, and uracil resulting in a release of carbohydrates and phosphate ions (Khadre *et al.*, 2001).

Ozone is a toxic gas at high concentrations. Headaches, dry throats, irritation of the respiratory tract, and smarting eyes are symptoms after exposure to 0.1 to 1.0 ppm ozone. Exposure to 1.0 to 100 ppm ozone can cause asthma-like symptoms. Therefore, the ozone concentration has to be monitored at the working place. The exposure limit to ozone under normal working conditions is 0.1 ppm for 8 hours per day and 40 hours per week. The limit for short-time exposure to ozone is 0.3 ppm for less than 15 min and not more than 4 times a day. Between the short-time exposures to ozone has to be a time range of 1 hour (Guzel-Seydim *et al.*, 2004; Mahapatra *et al.*, 2005; Pascual *et al.*, 2007; Goncalves, 2009). Most materials are resistant against ozone at concentrations between 1 and 3 ppm but an increased corrosion potential of stainless steel was observed above 1 ppm ozone (Ölmez & Akbas, 2009).

Only a small concentration of ozone naturally occurs at the Earth's surface (Kim *et al.*, 2003). Ozone is formed by the action of UV solar radiation (<240 nm) on molecular oxygen in the stratosphere (15-35 km altitude). A small proportion is transported to the troposphere (<15 km altitude) and about 10 % of the atmospheric ozone is present in the troposphere. For industrial scale ozone can be produced by three different methods: electrical discharge, electrochemical, and UV radiation.

In the UV generation method oxygen is exposed to UV light (140-190 nm). The UV light splits the oxygen into oxygen atoms and the oxygen atoms combine with other oxygen molecules to ozone molecules (Figure 2.7). To produce ozone by electrochemical method an electrical current is applied between an anode and cathode in an electrolyte solution. Ozone and oxygen are produced at the anode.

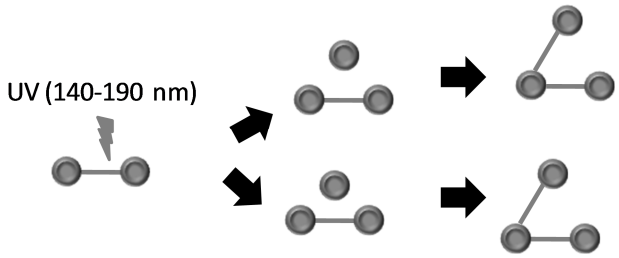

Figure 2.7: Ozone generation by the UV method.

The most commonly used ozone generation method is the electrical discharge (Figure 2.8).

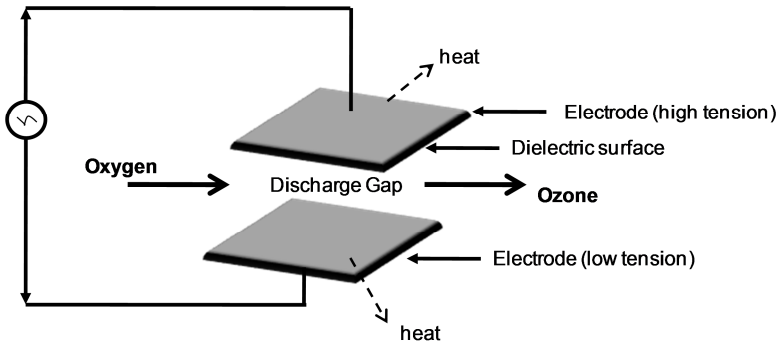

Figure 2.8: Ozone generation by the electrical discharge method (modified after Kim *et al.* (1999) and Karaca & Velioglu (2007)).

Properly dried air or O_2 is passed through a space between two high-voltage electrodes. These electrodes are separated by a dielectric material, i.e. glass. Upon supply of voltage to the electrodes a corona discharge is formed between them and the O_2 is converted to ozone. The oxygen molecule is split to oxygen atoms and these atoms react with oxygen molecules to form ozone. Between 1 and 3 % ozone is generated with the ozone generator using dried air. 3 to 6 % ozone is produced using high purity oxygen as feed gas (Kim, Yousef, & Dave, 1999; Guzel-Seydim *et al.*, 2004; Mahapatra *et al.*, 2005; Karaca & Velioglu, 2007; Goncalves, 2009).

The effects of ozone have been known for more than hundred years. A brief overview is given in table 2.6. Ozonation has been adopted for water treatment and disinfection in France, Germany, the Netherlands, Austria, Switzerland and many other countries (Graham, 1997). Over the world more than 3000 ozone-based water treatment are installed (Mahapatra *et al.*, 2005).

Table 2.6: History of ozone application (adopted from Graham, 1997; Goncalves, 2009)

Year	Application	Country
1857	Design of an ozone generator by Siemens	Germany
1888	U.S. patent for an apparatus to produce ozone for deodorizing sewer gases was issued by Fewson	USA
1902	First full-scale-ozone generating plant for water treatment was built by Siemens and Halske	Germany
1906	Ozone used to provide safe drinking water in Nice	France
1910	First use of ozone in a German meat packing plant	Germany
1918	Ozone used to sanitise swimming pools	USA
1936	Ozone used to treat shellfish	France
1942	Ozone used in egg storage rooms and cheese storage facilities	USA
1972	Ozone used to purify process water	Germany
1977	Ozone used to reduce *Salmonella* in egg shells	Russia
1982	Ozone declared GRAS (Generally Recognized as Safe) for bottled water-Reaffirmed GRAS in 1995	USA
1997	Expert Panel convened by EPRI declared ozone GRAS in food processing	USA
2000	Food Additive Petition filed with the FDA, August 15, 2000	USA
2001	FDA recognizes ozone as a secondary direct food additive to kill foodborne pathogens	USA
2001	Food Safety and Inspection Service (FSIS) declares acceptable in poultry and meat products	USA

2.4.2 Inactivation mechanism of ozone

The efficiency of ozone is dependent on target microorganism, initial inoculum level, and physiological state of the treated bacteria, ozone delivery method, and type of food (Ölmez & Akbas, 2009). Ozone inactivation of microorganisms is a complex process. Ozone attacks various cell membrane and wall constituents (e.g. unsaturated fats) and cell content constituents (e.g. enzymes, proteins, and nucleic acids). The microorganisms are inactivated by cell wall disruption or disintegration leading to leakage of the cell contents (Kim, Yousef, & Dave, 1999; Khadre *et al.*, 2001; Kim *et al.*, 2003; Guzel-Seydim *et al.*, 2004; Mahapatra *et al.*, 2005; Pascual *et al.*, 2007). This action of ozone implies that the microorganisms cannot be resistant against ozone inactivation (Pascual *et al.*, 2007). Khadre *et al.* (2001) summarised the mechanism of microbial action of ozone described in the literature. The cell envelope of microorganisms seems to be the primary target of ozone attack. Ozone affects the cell envelope by oxidising cellular compounds such as polyunsaturated fatty acids, membrane-bound enzymes, glucoproteins, and glycolipids. This may lead to leakage of cellular compounds and cell lyses. The oxidation of the double-bonds of unsaturated fats and the oxidation of sulfhydryl groups of enzymes lead to a disruption of the cellular activity and cell permeability followed by rapid cell death. The spore coat is the primary protector barrier against ozone activity. Spores are rapidly inactivated by ozone in the absence of spore coat protein in comparison to intact spores.

The greater resistance of Gram-positive bacteria against ozone compared to Gram-negative bacteria can be explained by the greater amount of peptidoglycans in the cell wall of Gram-

positive bacteria. It was shown that N-acetyl glucosamine which is present in peptidoglycan is resistant against the action of ozone. Inactivation of enzymes by ozone is due to the oxidation of the sulfhydryl groups in cysteine residues. In contrast to chlorine which selectively destroys certain enzymes, ozone acts as a general protoplasmic oxidant. Ozone generally destroys the dehydrogenating enzyme system of bacterial cells, whereas the cytoplasmic â-galactosidase activity decreased to a greater degree than periplasmic alkaline phosphatase in *E. coli* cells. Nucleic acids are modified by ozone *in vitro,* and thymine is more sensitive to ozone than cytosine and uracil. It was shown that ozone opened the circular plasmid DNA and reduced its transforming ability. Additionally, single- and double-strand breaks are produced in plasmid DNA and the transcription activity decreased. Bacteriophages were inactivated by attacking the capsid protein with liberation and inactivation of the nucleic acids. An alteration of polypeptide chains in virus protein coat was observed after ozone treatment. The resistance of microorganisms against ozone can be arranged as follows (Kim, Yousef, & Dave, 1999; Khadre *et al.*, 2001; Figure 2.9):

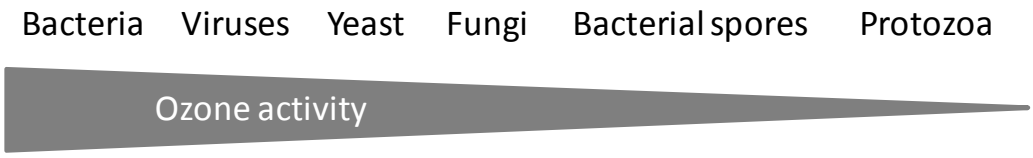

Figure 2.9: Range of disinfection activity of ozone against microorganisms.

2.4.3 Application of ozone

In the food industry ozone applications are related to decontamination of product surfaces, food plant equipment, reuse of waste water, and lowering biological oxygen demand (BOD) and chemical oxygen demand (COD) of food plant waste (Guzel-Seydim *et al.*, 2004). Inactivation of contaminated microflora on meat, poultry, eggs, fish, fruits, vegetables, and dry food by ozone was met with mixed success (Kim, Yousef, & Dave, 1999).

2.4.3.1 Ozone in non-food application

Dental medicine uses ozone to reduce oral microorganisms. The antimicrobial effect of ozonated water against *Enterococus faecalis* and *Streptococcus mutans* infections in bovine dentin has been evaluated (Nagayoshi, Fukuizumi *et al.*, 2004). A significant decrease in bacteria viability was observed after irradiation (30 ml min^{-1}) with ozonated water (4 mg l^{-1}) for 10 min. A combination of irrigation with ozonated water and sonication had the same

antimicrobial effect as 2.5 % sodium hypochloride which is the major used endodontic irradiant. Similar results were obtained with *Streptococcus mutans* in experimental dental plaque. After exposure to ozonated water (4 mg l^{-1}) for 10 s the number of viable bacteria remarkably decreased in experimental and human dental plaque *in vitro* (Nagayoshi, Kitamura *et al.*, 2004). No antimicrobial effect of gaseous ozone and ozonated water against *Enterococcus faecalis* in human root canals were found by Estrela *et al.* (2007). Ozone saturated PBS solution was used to inactivate microbial load of toothbrushes. The microbial load of toothbrushes was between 10^2 and 10^7 CFU and after 30 min of ozone exposure a complete decontamination was detected while short time periods were inefficient (Bezirtzoglou *et al.*, 2008).

Ozone disinfection of wastewater is highly influenced by the organic matter (Janex *et al.*, 2000). Swine wastewater can act as reservoir of antibiotic-resistant bacteria and to prevent the spread of these bacteria effective disinfection methods are needed. Ozone reduced the bacterial load of swine lagoon by 3.3 to 3.9 log units at a concentration of 100 mg l^{-1}. A chlorine concentration of 30 mg l^{-1} reduced the bacterial load only by 2.2 to 3.4 log units (Macauley *et al.*, 2006). Ozone treatment of a pilot wastewater treatment plant reduced the number of faecal coilforms, total coliforms, and *E. coli* by > 4 log units at concentrations of 3.6 mg l^{-1}, 4.8 mg l^{-1}, 5.3 mg l^{-1} and contact times of 12.8 min, 12.8 min and 6.4 min, respectively (Mezzanotte *et al.*, 2007). Microorganisms are often occluded in wastewater particles and are associated with health risks of post-infected effluents. Therefore, the ability of ozone to penetrated particles was evaluated. Significant transport of ozone within particles greater than 6 µm require large initial ozone concentrations and a complete inactivation of all particle sizes was not possible. The reduction of health risks associated with wastewater particles requires particle removal and particle inactivation (Dietrich *et al.*, 2007).

2.4.3.2 Ozone in food application

The ability of ozone to decontaminate equipment surfaces was evaluated in various studies (Greene *et al.*, 1993; Moore *et al.*, 2000; Khadre *et al.*, 2001; Li & Wang, 2003; Fielding *et al.*, 2007; Naitou & Takahara, 2008). Biofilms in the food industry are difficult to destroy and may influence the microbiological quality of the food. Ozonated water (0.5 ppm) reduced > 99 % of *Pseudomonas fluorescens* and *Alicaligenes faecalis* in milk films on stainless steel after 10 min immersion (Greene *et al.*, 1993). Different food relevant bacteria were incubated (4 h) on stainless steel and exposed to gaseous ozone (2 ppm, 4 h). Depending on the type of microorganism the reduction of bacteria was between 7.56 and 2.41 log. Gram-negative bacteria were more sensitive than Gram-positive bacteria and the tested yeast strain was

more sensitive than bacteria. The reduction of biofilms by gaseous ozone was only between 5.64 and 1.65 log units and between 5.66 and 0.37 log units in the presence of milk and meat broth, respectively. These results indicate the influence of organic matter on ozone activity and imply that ozone is an effective disinfectant after adequate cleaning (Moore *et al.*, 2000). Ozonated water reduced biofilms of beer lines containing *Enterobacter* and yeast by 3 log units indicating its potential as disinfection agent for commercial beer lines (Fielding *et al.*, 2007). In Japan, ozone is used for sterilisation of food packaging films. It was shown that ozonated water with concentrations of 10 to 30 ppm reduced all microorganisms in tank, cup, and film. The inactivation is strongly dependent on the ozone concentrations (Naitou & Takahara, 2008).

The sensitivity of *Escherichia coli*, *Bacillus cereus*, and *Bacillus megaterium* to ozone was evaluated in the presence and absence of organic matter. Lethal threshold concentrations were 0.12 mg l^{-1}, 0.19 mg l^{-1}, and 0.19 mg l^{-1} for 5 min treatment of *E. coli, Bacillus cereus*, and *Bacillus megaterium*, respectively. The lethal threshold level for *Bacillus cereus* and *Bacillus megaterium* spores was 2.29 mg l^{-1} for a 5 min treatment. Low concentrations of ozone were ineffective in microbial reduction in the presence of organic matter (Broadwater *et al.*, 1973). The influence of organic matter on ozone activity was also observed by Restaino *et al.* (1995). Food-related bacteria were inactivated in the presence and absence of soluble starch and bovine serum albumin by ozonated water. The presence of soluble starch did not affect the activity of ozone but the inactivation of bacteria was significantly reduced in the presence of bovine serum albumin. Similar results were obtained for *E. coli, Staphylococcus aureus,* and *Bacillus stearothermophilus* spores treated with 0.4 ppm ozone for 10 min. Soluble starch had no protective effect compared to the buffer control. The protective effect was enhanced in the presence of locust bean gum and the highest protective effect was achieved in the presence of caseinate and whipping cream (Guzel-Seydim *et al.*, 2004).

Rheological characteristics and colour of ozonated hydrocolloid dispersions were significantly different from untreated hydrocolloid dispersions and no recovery of the structure was observed after 24 h storage. These results indicate that attention should be given before addition of these hydrocolloids to food formulations which are subsequently ozonated in food preservation methods (Tiwari, Muthukumarappan, O'Donnell *et al.*, 2008).

Pathogens on beef carcass surfaces were not significantly reduced in comparison to washing. The bacterial load of carcass surface was 10^6 to 10^7 CFU and aqueous ozone with a concentration of 95 mg l^{-1} was sprayed on the inoculated surface after a washing step. The applied ozone treatment did not improve the reduction of pathogens on beef carcass

surfaces (Castillo *et al.*, 2003). Ozone suppresses the smell characteristics of fresh fish and bivalve molluscs but should not be used to mask low quality (Goncalves, 2009). The shelf-life of vacuum-packaged mussels was extended after ozonation (1 mg l^{-1}, 90 min) from 9 to 12 days. The bacterial population was reduced by 0.3 to 2.5 log units depending on the type of microorganism. The chemical indicators for spoilage were lower of ozonated samples than of untreated samples after 12 days of storage. Total volatile basic nitrogen value was relative low during 6 days of storage and then increased (Manousaridis *et al.*, 2005).

In fruit and vegetable processing ozone is used in gaseous state and dissolved in water to improve food safety (Xu, 1999). Karaca & Velioglu (2007) gave an overview of ozone treatment studies for microbial inactivation in fruits. Since the approval of ozone as a direct food additive the application of ozone in liquid food processing has been triggered. Ozone is mainly applied in the liquid food industry in bubble columns. Among others, orange juice, apple cider, strawberry juice, and blackberry juice were treated with gaseous ozone to improve the quality (Cullen *et al.*, 2009). No significant changes in pH, °Brix, titratable acidity, cloud value, and non-enzymatic browning were found after ozonation (0.6-10.0 % w/w, 0-10 min; 0-0.25 l min^{-1} flow rate) of orange juice. The colour values were significantly affected by ozone concentration, flow rate, and treatment time (Tiwari, Muthukumarappan, Donnell *et al.*, 2008). The influence of orange juice organic matter on antimicrobial activity against *E. coli* was investigated by Patil *et al.* (2009). Model orange juice, fresh unfiltered juice, juice without pulp, and filtered juice was inoculated with 10^6 CFU ml^{-1} *E. coli* strains and treated with 75-78 µg ml^{-1} ozone for 0-18 min. A total reduction of *E. coli* was achieved after 60 s in model orange juice and after 6 min in juice with low pulp content. High pulp content increased the needed time to achieve a total reduction of *E. coli* to 15 to 18 min. A 5 log unit reduction of *E. coli* O157:H7 and *Salmonella* in orange juice and apple cider containing dimethyl dicarbonate or hydrogen peroxide was achieved after 90 min ozone treatment with 0.9 g h^{-1}. More than 5 log unit reduction was achieved after combination of antimicrobials with ozone treatment followed by refrigerated storage. This implies that ozone treatment is an alternative to thermal pasteurisation (Williams *et al.*, 2005). The anthocyanin and ascorbic acid content in strawberry juice was significantly reduced upon 10 min ozone treatment at an ozone concentration of 7.8 % w/w. Additionally, the juice was lighter after ozone treatment which is expressed in an increased L^* value and decreased a^* and b^* values (Tiwari *et al.*, 2009).

Gaseous ozone was applied to different fruits and vegetables. Whole black peppercorns were immersed in water and sparged with gaseous ozone (6.7 mg l^{-1}) for 10 min. The microbial population of peppercorn was reduced by 3-4 log units. The microbial population of ground black pepper was reduced by 3-6 log units after treatment with gaseous ozone and

various moisture levels for 6 h. Oxidation of certain volatile oil constituents occurred in ground black pepper but no significant effect on volatile oil constituents were observed in whole black peppercorns (Zhao & Cranston, 1995). The storage life of broccoli and seedless cucumber was enhanced by cold storage at 3 °C in the presence of 0.04 µl l^{-1} ozone. Minimal response to ozone was observed for mushrooms stored at 4 °C and cucumber stored at 10 °C. Ozone was able to reduce the ethylene level to a non-detectable level in apple and pear storage without affecting fruit quality. The application of ozone in storage rooms may enable the storage of ethylene-sensitive fruits and vegetables together with ethylene-producing fruits and vegetables (Skog & Chu, 2001). The daily growth rate of fungi on carrots was reduced by 50 % at an ozone concentration of 60 µl l^{-1}. With increased ozone concentration the respiration rate, electrolyte leakage, and colour difference increased. The ozone-treated carrots were less intense in colour than untreated carrots (Liew & Prange, 1994). No damage or off-flavour in whole or sliced tomato was found after ozone treatment but microbial load was substantially reduced. However, higher sugar and organic acid content was found after treatment with 0.5 µl l^{-1} ozone for 30 min every 3 h for 15 days at 5 °C. The tissue of whole tomatoes appears to be firmer in the presence of ozone, the tissue of sliced tomatoes was not affected but a reduced aroma was observed. The respiratory rate of tomatoes was initially stimulated and after 2 days the metabolic activity decreased (Aguayo *et al.*, 2006). Ten mg l^{-1} gaseous ozone applied for 5 to 15 min was effective against *Salmonella enteritidis* inoculated on sweet cherries (Das *et al.*, 2006). A novel ozone-generation system consisting of a pair of electrodes with an adjustable gap inside a package was used to inactivate *E. coli* O157:H7 on fresh package spinach. The novel system was capable to reduce 3-5 log units per leaf after 24 h of storage. The initial ozone concentration after 5 min treatment was 1.6 and 4.3 mg l^{-1} for air and oxygen gas, respectively and was not detectable after 24 h. Further studies are needed to evaluate quality changes of the packaged product (Klockow & Keener, 2009). Red pepper could be detoxified of aflatoxin B_1 by ozone treatment. 80 and 93 % aflatoxin B_1 was reduced in flaked and chopped red peppers by 60 min treatment with ozone concentrations of 33 mg l^{-1} and 66 mg l^{-1}, respectively (Inan *et al.*, 2007). Ozone was effective in reduction of vegetative bacteria on dried figs. *E. coli* and *Bacillus cereus* were inactivated by 3.5 log units after 6 h ozone treatment (1 ppm) and *Bacillus cereus* spores were inactivated by 2 log units after 360 min ozone treatment (1 ppm). No significant changes were observed between sweetness, rancidity, flavour, appearance and overall palatability of ozonated and untreated fruits (Akbas & Ozdemir, 2008). *E. coli* and *Staphylococcus aureus* on date fruits were inactivated after exposure to 5 ppm gaseous ozone for 60 min (Najafi & Khodaparast, 2009). Gaseous ozone (10 ppb, 30 min) was also effective against microbial population of cantaloupe melon. Mesophilic, psychotrophic bacteria, moulds and coliforms were reduced by 1.1, 1.3, 1.5, and

1.3 log units, respectively. A reduction of 3.8, 5.1, 2.2, and 2.3 log units, respectively, was achieved using gaseous ozone in combination with hot water (75 °C, 1 min). No damage was observed in fruits after treatment and initial texture and aroma was maintained (Selma, Ibñez *et al.*, 2008). *Salmonella* was reduced by 4.2 and 2.8 log units on physiologically mature non-ripe and ripe melons, respectively, after ozone treatment (10 ppb, 30 min under vacuum). The microbial load of fresh-cut cantaloupe in terms of total coliforms, *Pseudomonas fluourescens*, yeast, and lactic acid bacteria was reduced after treatment with gaseous ozone (5000 and 20 ppb, 30 min). Maximal reduction was achieved at Ct-value (concentration x exposure time) of 600,000 ppm min with maintenance of an acceptable visual quality, aroma, and firmness during 7-day storage at 5 °C (Selma, Ibáñez *et al.*, 2008). The postharvest quality of strawberries was evaluated after gaseous ozone treatment. The ozone concentration was 0.35 ppm, and the strawberries were stored for 3 days at 2 °C, following 4-days storage at 20 °C. The ozone treatment was ineffective against fungal decay and significant differences in sugar and ascorbic acid content was found. The vitamin C content of ozonated fruits was three times higher than that of control fruits but a 40 % reduced emission of volatile esters was observed after ozone treatment (Perez *et al.*, 1999). A reversible loss of fruit aroma in strawberries was observed after storage in ozone-enriched atmosphere (1.5 µl l^{-1}) for 3 days at 2 °C. The storage in ozone-enriched atmosphere reduced decay incidence, weight loss, and fruit softening (Nadas *et al.*, 2003).

Using ozonated water to reduce *E. coli* O157:H7 and *Salmonella* on raspberries and strawberries indicates the potential of ozone to decontaminate small fruits. A treatment with ozone concentrations of 8.9 mg l^{-1} for 64 min at 20 °C reduced 4.8 and 4.4 log units of *E. coli* and *Salmonella* on raspberries, respectively. The reduction at 4 °C was 5.6 and 4.5 log units for *E. coli* and *Salmonella*, respectively. The reduction of *E. coli* and *Salmonella* on strawberries at 4 and 20 °C was lower than on raspberries. 2.9 and 2.6 log units of *E. coli* were reduced at 20 °C and 4 °C, respectively, at ozone concentrations of 8.9 mg l^{-1} for 64 min. *Salmonella* was only reduced by 3.3 and 2.4 log units at 20 and 4 °C, respectively (Bialka & Demirci, 2007). Ozonated water reduced brown rot on fruit and gray mould on table grapes, where the inoculums were on the surface of fruits but did not reduce decay when pathogens had been inoculated into wounds. The fruits quality was affected at ozone concentrations needed to reduce surface-borne decays (Smilanick *et al.*, 2002). Five ppm ozonated water treatment for 5 min was not able to inactivate or remove surface microorganisms from strawberries and cucumbers. Fungal populations of strawberries were reduced by 0.9 log units, a 0.4 log reduction of aerobic mesophilic bacteria was achieved and coliforms were reduced below the detection limit. On cucumbers, the ozone treatment reduced fungal population by 0.8 log units, 0.7 log units of aerobic mesophilic bacteria were

reduced and 1.5 log units of coliforms were inactivated (Koseki *et al.*, 2004). Ozone treated (1 mg l^{-1}) packaged fresh-cut green asparagus was stored at 3 °C for 25 days under modified atmosphere. Enzyme activities including phenylalanine ammonia lyase, superoxide dismutase, ascorbate peroxidise, and glutathione reductase were inhibited by ozone treatment (An *et al.*, 2007). Enhanced sensory quality of fresh-cut celery was observed after ozone treatment. The vitamin C and total sugar content of ozone-treated celery was not significant different when compared to the content of untreated celery. The respiration rate and polyphenoloxidase acitivity was inhibited after ozone treatment. Additionally, the microbial population was lowered to 1.69 log CFU g^{-1} at an ozone concentration of 0.18 ppm for 5 min (Zhang *et al.,* 2005). Maintenance of typical cilantro aroma and overall quality was observed in ozone-treated fresh-cut cilantro after storage at 0 °C for 14 days packaged in polyethylene bags (Wang *et al.*, 2004). Ozone concentrations between 0.3 and 3.95 mg l^{-1} for 20 s to 30 min were used to reduce natural microbial load of pre-cut green peppers. The maximum reduction of 0.72 log units is considered to be too small for commercial application (Ketteringham *et al.*, 2006). The physiological activity of carrots was not affected by an ozone treatment for 2 min using an ozone concentration of 4 ppm. At the chosen treatment conditions soft-rot causing *Pectobacterium carotovorum* was effectively inactivated on carrots (Hassenberg *et al.*, 2008). Mesophilic count and psychotrophic bacteria decreased by 1.4 and 1.8 log units, respectively, after bubbling of 1.3 mM ozone for 3 min in a mixture of shredded lettuce and water (Kim, Yousef, & Chism, 1999). Lettuce washed in ozonated water (5 ppm) for 10 min showed a reduction of 1.5 log CFU g^{-1} viable aerobe bacteria. It was confirmed that ozonated water reduces aerobic bacteria, coliforms, yeasts, and moulds on the surface of lettuce. Residual microorganisms were either inside the cellular tissue or occur as biofilms on the surface. Spores were not reduced by the applied ozone treatment. Damage to lettuce structure was not observed after ozone treatment (Koseki *et al.,* 2001). Best sensory and microbiological quality was maintained in shredded iceberg lettuce treated with chlorine, but ozone (1 mg l^{-1}) was less effective in prolonging product shelf-life (Baur *et al.*, 2004). No significant changes in moisture content and texture of fresh-cut iceberg lettuce were observed after dipping in ozonated water (4 ppm). Colour, β-carotene, and vitamin C values did not significantly change until day 8 of storage. The mesophilic and psychotrophic bacteria population was reduced by 1.7 and 1.5 log units, respectively (Akbas & Ölmez, 2007). *Shigella sonnei* in water could be reduced by 3.7 and 5.6 log units after treatment with 1.6 and 2.2 ppm ozonated water, respectively, for 1 min. On shredded lettuce, *Shigella sonnei* was reduced by 1.8 log units after ozone treatment (5 ppm) for 5 min (Selma *et al.*, 2007). Ölmez & Akbas (2009) evaluated optimal processing conditions for green leaf lettuce. The authors suggested that the application of 2 ppm ozonated water for 2 min is optimal to reduce microbial load and maintain sensory quality of green leaf lettuce during cold storage.

2.5 Plasma

2.5.1 Theoretical basics

Plasma is an ionized gas and has been defined as the fourth state of matter since more than 90 % of the universe exists as plasma (e.g. sun). Plasma can be generated under high pressure (thermal plasma) or atmospheric and low-pressure (non-thermal plasma). Thermal plasmas are characterised by an almost thermodynamic equilibrium between the electrons and the heavy species resulting in high gas temperatures (5000 to 20000 K). Examples of thermal plasmas are inductively coupled plasma system, a plasma-cutting torch, and the sun. The electron temperature of non-thermal plasmas is much higher than the gas temperature. Therefore, these plasmas are defined as non-equilibrium plasmas. Fluorescent light, neon signs, arc, and radio frequency inductively coupled plasma discharges are examples for non-equilibrium plasmas (Fridman *et al.*, 2005; Keener, 2008; Moreau *et al.*, 2008). Equilibrium plasma (thermal plasma) is not applicable to heat-sensitive materials due to the high gas temperature and non-equilibrium plasmas (non-thermal plasma) are preferred. Low pressure plasma can be generated by direct current discharges, radio frequency discharges (e.g. capacitively coupled discharges, inductively coupled discharges), and microwave discharges (Schmidt, 2010). Low-pressure plasmas generate high concentrations of reactive species and gas temperatures are below 150 °C. Low pressure plasmas have found wide applications in material processing but have several drawbacks: i) vacuum systems are expensive and require maintenance, ii) load locks and robotic assemblies are needed to shuttle materials in and out of vacuum, iii) the size of the treated object is limited by the vacuum chamber (Schütze *et al.*, 1998). Since a vacuum will support liquid to gaseous phase changes in high-moisture food products the most applicable non-equilibrium plasma system to food processing is atmospheric-pressure plasma where no extreme conditions are required and low temperatures occur (Moreau *et al.*, 2008). Atmospheric-pressure plasma is commonly generated by corona discharge (CD; negative and positive corona), dielectric barrier discharge (DBD), or plasma jet (APPJ) (Keener, 2008; figure 2.10). Atmospheric pressure plasmas can also be generated by radio frequency plasma torches, gliding arcs, micro-discharges, and some kinds of microwave discharges (Schmidt, 2010).

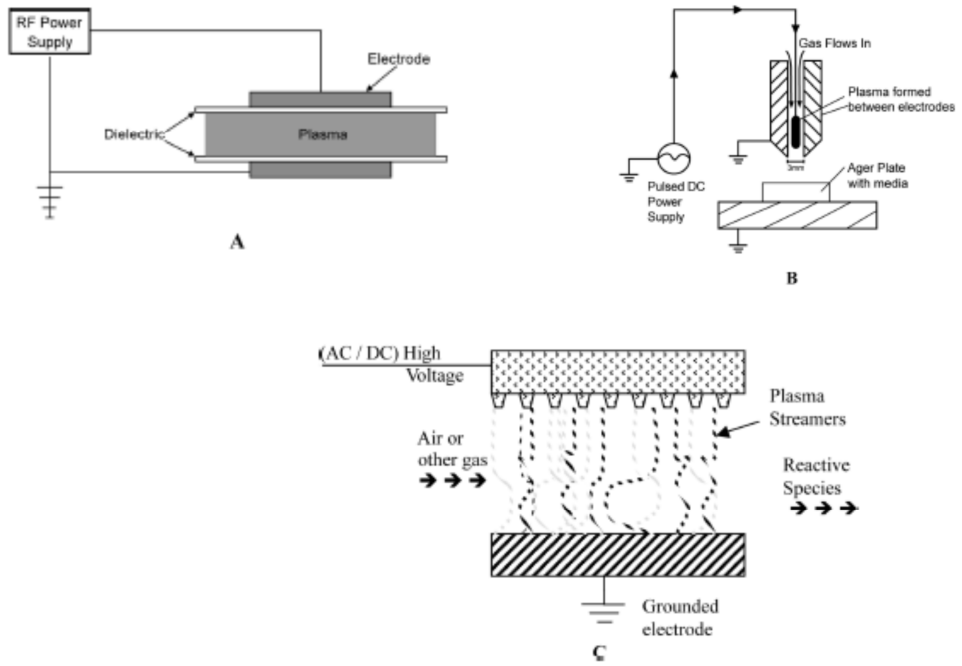

Figure 2.10: Atmospheric pressure plasma generation systems: A) dielectric barrier discharge, B) plasma jet, C) corona discharge (Keener, 2008).

The DBD system consists of two electrodes that can be arranged in a horizontal or cylindrical configuration. The electrodes are covered with dielectric plates and are separated by a small gap which is filled with a gas at atmospheric pressure. A high voltage is applied to the electrodes and the gas between the electrodes is ionised when the applied voltage exceeds the ionisation energy of the gas. Electrons are created during the ionising process. These electrons react with gas molecules and ions, metastable states of chemistry species, UV, and heat is formed. Very high voltages are needed to produce corona discharge. In this system, gas flows through two plates. One plate is grounded and a high current is applied to the other plate (Keener, 2008). For the treatment of non-uniformly shaped products (e.g. fresh cut lettuce) the application of APPJ offers advantages due to various options regarding design and construction of plasma jets. The APPJ source consists of a centre electrode and a grounded outer electrode. The gas flows between the electrodes, is ionized and ejected from the source. The generated plasma contains chemical species, charged species, radicals, heat, and UV in different concentrations. The concentrations of the reagents are dependent on the process parameters and the gas used (Weltmann *et al.*, 2008). The plasma characteristics of the different plasma systems in comparison to low pressure discharges are given in table 2.7.

Table 2.7: Plasma characteristics of different plasma generation systems (adopted from Schütze *et al.*, 1998)

Source	Breakdown voltage V_b [kV]	Plasma density [cm^{-3}]	Electron temperature [eV]	Gas temperature [°C]	Density [cm^{-3}]		
					O^+, O_2^{+*}, O^-	O	O_3
Low pressure discharge	0.2-0.8	10^{8}-10^{13}	1-5	<150	10^{10}	10^{14}	<10^{10}
Corona discharge	10-50	10^{9}-10^{13}	~5	50-400	10^{10}	10^{12}	10^{18}
Dielectric barrier discharge	5-25	10^{12}-10^{15}	1-10	50-400	10^{10}	10^{12}	10^{18}
Plasma jet	0.05-0.2	10^{11}-10^{12}	1-2	25-200	10^{12}	10^{16}	10^{16}

The advantages of low pressure discharges are the low breakdown voltage V_b (the breakdown voltage of the gas must be exceeded to ignite a plasma), the stable operating window between spark ignition and arcing, an electron temperature of dissociating molecules (1-5 eV), but a low temperature, high concentrations of ions and radicals, and a uniform glow over a large gas volume. The atmospheric pressure plasma jet exhibits the greatest similarity to a low pressure glow discharge taking all the properties of plasma into account (Schütze *et al.*, 1998).

The presence of free radicals, UV emitting species, and charged particles is associated with the antimicrobial effect of the plasma (Laroussi, 2002; Moisan *et al.*, 2002). The capability of non-thermal atmospheric plasmas to inactivate vegetative cells, including Gram-negative and Gram-positive bacteria, yeast and fungi, biofilm formers, endospores, and biomolecules such as proteins was shown in various studies (Laroussi, 2005; Vleugels *et al.*, 2005; Brandenburg *et al.*, 2007; Deng, Shi *et al.*, 2007). However, the emitted reagents do not only react with bacteria, but they may also react with food components such as water, lipids, proteins, and carbohydrates (Keener, 2008). Sterilisation can be achieved in the plasma discharge itself or in its afterglow. The afterglow contains relatively few charged particles e.g. neutral atoms, radicals, and molecules which can exist in an excited state (Moisan *et al.*, 2002).

2.5.2 Inactivation mechanism of plasma

In various studies the antimicrobial activity of non-thermal plasma against gram-negative and gram-positive bacteria, yeast and fungi, biofilm formers, endospores, and biomolecules such as proteins was shown (Kelly-Wintenberg *et al.*, 1999; Montie *et al.*, 2000; Laroussi, 2005; Vleugels *et al.*, 2005; Brandenburg *et al.*, 2007; Deng, Shi *et al.*, 2007). Although several reviews focus on the inactivation mechanisms of plasma (Moisan *et al.*, 2001; Boudam *et al.*,

2006; Gaunt *et al.*, 2006; Moreau *et al.*, 2008), the inactivation mechanism is up to now not fully understood. Moisan *et al.* (2002) stated that three basic mechanisms are involved in low pressure plasma inactivation of spores resulting in a three-phase inactivation curve: i) Destruction by UV irradiation of genetic material which is a statistical process requiring a sufficient number of lesions of the DNA strands ii) Erosion of the microorganisms atom by atom, through intrinsic photodesorption by UV irradiation, breaking the chemical bonds in microorganisms and formation of volatile compounds from intrinsic atoms of microorganisms. These volatile by-products are small molecules such as CO and CH_x, and iii) Erosion of the microorganisms, atom by atom, through etching to form volatile compounds as a result of slow combustion using oxygen atoms or radicals emanating from the plasma. Formed volatile products are, for example, CO_2 and H_2O. The elimination rate of microorganisms is increased in some cases if etching is activated by UV protons (Figure 2.11).

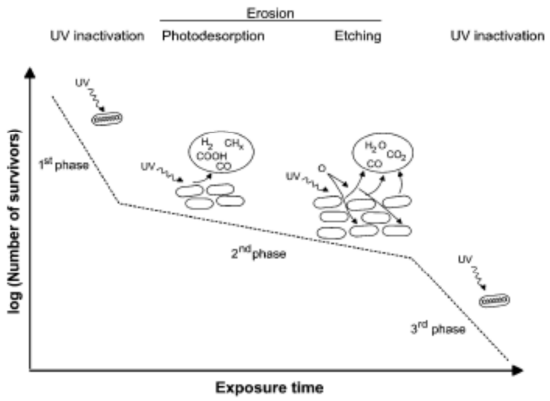

Figure 2.11: Illustration of a three-phase spore survival cure after plasma treatment (Moisan *et al.*, 2002).

Laroussi (2002) summarised that the inactivation kinetics obtained from atmospheric-pressure plasma treatments show different shapes depending on the type of microorganisms, support material, and method of exposure. Single-phase, double-phase, and multi-phase survivor curves were obtained (Figure 2.12).

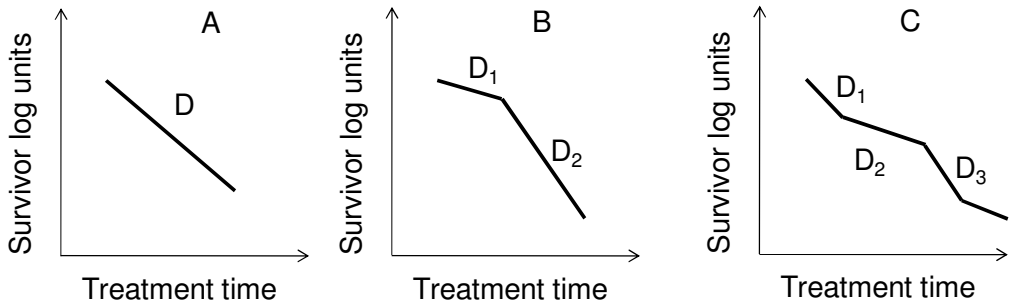

Figure 2.12: Survivor curves of bacteria after atmospheric pressure plasma treatment. A) Single-phase survivor curve; B) Two-phase survivor curve, and C) Multi-phase survivor curve (modified after Laroussi (2002)).

Although three-phase survivor curves were reported in low-pressure plasma studies the explanation of the inactivation mechanism cannot be transferred to atmospheric-pressure plasma studies (Laroussi, 2002). The role of UV inactivation at atmospheric pressure plasma is controversy discussed in the literature. Most of the researches claim that UV plays a minor role in the inactivation of microorganisms at atmospheric pressure and the inactivation process is controlled by chemically reactive species. However, it was shown that in some cases UV photons can play a role in the inactivation process of microorganisms at atmospheric pressure (Boudam *et al.*, 2006). Moreau *et al.* (2008) compared plasma inactivation effects to the effects of micro pulses. Similar to the effects of micro pulses the cell membrane of microorganisms is perforated after plasma treatment. Besides the perforation of the cell membrane the inactivation effect of plasma is induced by the bombardment of the cell membrane by radicals (OH or NO). These radicals are absorbed into the bacteria surface and volatile components are formed (etching). Two mechanisms of plasma inactivation described by Gaunt *et al.* (2006) are the electrostatic disruption of cell membranes and lethal oxidation of cellular components. During electrostatic disruption, the total electric force exceeds the total tensile force of the membrane. The electric force is caused by an accumulation of surface charge which is greater where some surface irregularities give regions of higher local curvature as is shown in Gram-negative bacteria. A lower accumulated charge is required for lyses of Gram-negative bacteria than for Gram-positive bacteria, because they have a thinner murein layer (~ 2 nm *vs* ~ 15-18 nm) which confers the tensile strength of the membrane. A reaction of reactive oxygen species (ROS) with cellular macromolecules was found after bacterial exposure to plasma. The ROS react with membrane lipids resulting in the formation of unsaturated fatty acid peroxides, amino acids are oxidised (e.g. formation of 2-oxohistidine) as well as nucleic acids (e.g. formation of 8-hydroxy-2 deoxyguanosine). The membrane lipids seem to be the most vulnerable macromolecules in the cells, probably due to their location near to the cell surface. An

alteration of membrane lipids results in a leakage of macromolecules. Gram-negative bacteria are more sensitive to one atmosphere uniform glow discharge plasma (OAUGDP) exposure than Gram-positive bacteria. It is suggested that the thick polysaccharide layer on the outside of Gram-positive bacteria cells is resistant to chemical changes but a diffusion of ROS in the cytoplasmic membrane is possible (Montie *et al.*, 2000). The different types of inactivation mechanisms can be explained by differences in the plasma sources, types of microorganisms, and the supporting medium (Laroussi, 2002).

2.5.3 Inactivation of bacteria by plasma

2.5.3.1 Low pressure plasma

There are two sterilisation systems using low-pressure plasmas commercially available: the Steerad®-100S (Advanced Sterilisation Products, Johnson and Johnseon, Irvine, California) and the Plazlyte™ sterilisation system (AbTox Inc., Mundelein, Illinois) (Lerouge *et al.*, 2001). However, the plasma of these commercial systems has no bactericidal action. It serves as a detoxifying agent by removing noxious residues and limiting the oxidation effect of the highly reactive chemical elements injected in the form of vapours as the sterilising agent (Moreau *et al.*, 2000). Moreau *et al.* (2000) investigated the bactericidal effects of flowing afterglow on *Bacillus subtilis* spores. Within 40 min and in pressures between 1 and 7 Torr a total inactivation of 10^6 spores was achieved using a gas mixture of 2 % O_2/98 % N_2. The gas temperatures in the afterglow did not exceed 50 °C and thus is a possible alternative sterilisation method for heat sensitive materials. Microwave-induced argon plasma reduced *E. coli* cells after 30 min plasma treatment at low pressures. With increasing applied microwave power density the reduction of *E. coli* increased and temperatures were at the highest 58 °C. The inactivation effect of the plasma was higher at the centre and less effective at two opposite edges of the bio-indicator holder (Purevdorj *et al.*, 2002). Bacterial spore inactivation is dependent on the process conditions. For instance, a 30 min to one hour treatment of spores in flowing afterglow is needed to reduce 6 units of spores whereas in the discharge the same reduction is achieved after one second. It was shown that plasma is capable to affect pyrogens as well as proteins and prions (Rossi *et al.,* 2006). Sporicidal effect of low pressure plasma was observed in various studies indicating the potential of low pressure plasma as alternative sterilisation method for heat-sensitive materials (e.g. Lerouge, Wertheimer *et al.*, 2000; Lerouge, Fozza *et al.,* 2000; Lassen *et al.*, 2005; Messerer *et al.*, 2005; Nagatsu *et al.*, 2005). The drawbacks of low pressure plasma limit its application for food disinfection and sterilisation. Therefore, the bactericidal activity of atmospheric pressure plasma is of growing interest.

2.5.3.2 Atmospheric pressure plasma

During recent years, the number of publications dealing with the antimicrobial effects of atmospheric pressure plasma has increased. In these studies the antimicrobial effect was investigated using different plasma sources, different working gases, and different types of microorganisms. Examples of applications to inactivate bacteria with different plasma sources are described below.

Corona discharge

Corona plasma can be used for the surface decontamination. The application of corona discharges to reduce dimethyl-methyl phosphonate (DMMP), a stimulant for the chemical agent Sarin, resulted in a greater than four log destruction of DMMP on aluminium surface after 10 min (Moeller *et al.,* 2002). A pulsed-water corona discharge was used to inactivate *E. coli, Bacillus subtilis*, and *Bacillus subtilis* spores in water. Eight corona discharges were needed to reduce *E. coli* by three orders of magnitude. The corresponding energy was 10 J cm^{-3}. 30 discharges with a corresponding energy of 40 J cm^{-3} were needed to reduce vegetative *Bacillus subtilis* by three orders of magnitude but no effect was observed on *Bacillus subtilis* spores (Abou-Ghazala *et al.,* 2002). Negligible effects on the spores of *Bacillus subtilis* by corona treatment were already found by Sigmond *et al.* (1999). Pulsed corona discharges seem to be a promising tool for water purification and may play a major role in the water treatment industry in the future (Malik *et al*., 2001). Corona discharge was efficient against *E. coli* on a semiliquid cultivating media covered with a protective gel layer (protective exposition) or uncovered (direct exposition). At discharge current of 0.05 mA no cultivated colonies on agar surface were detected after 240 s corona treatment for protected and unprotected bacteria. In case of protective exposition the inactivation followed a linear inactivation kinetic. Using direct exposure an exponential inactivation kinetic was observed (Kríha, 2007).

Dielectric barrier discharge

Different surfaces were treated with DBD to evaluate the antimicrobial activity of the plasma against different bacteria. Among others, treated surfaces were plastic bags, polypropylene, agar, PET, suspensions, filter, and glass inoculated with *E. coli, Staphylococcus aureus, Bacillus subtilis, Streptococcus, Clostridium botulinum, Listeria monocytogenes, Pseudomonas aeruginosa,* spores, yeast, fungi and others. The inactivation effect of the tested DBD systems against the different bacteria was strongly dependent on the treatment conditions i.e. working gas, type of microorganisms, and treated surface (Kelly-Wintenberg *et*

al., 1998; Gadri *et al.,* 2000; Heise *et al.*, 2004; Laroussi, 2005; Kayes *et al.*, 2007; Sun *et al.*, 2007; Fridman *et al.*, 2007; Tanino *et al.*, 2007; Muranyi *et al.*, 2008; Shi *et al.*, 2008).

A DBD plasma jet is a plasma jet coupled with a DBD plasma system. The effective area of a DBD plasma jet with argon as working gas exceeded the plasma treatment area inducing an inactivation of *E. coli* and *Bacillus subtilis* on agar by plasma afterglow. While *E. coli* inoculated on filter paper was inactivated by 7 log units within 5 s, only 1 log unit of *Bacillus subtilis* was inactivated under the same conditions and a 2 log unit reduction was achieved after 60 s. The addition of oxygen and hydrogen peroxide vapour increased the inactivation of *Bacillus subtilis* to 6 log units after 30s with oxygen addition and after 20 s with hydrogen peroxide vapour addition. This indicates the dependence of antimicrobial effects on treatment conditions (Deng *et al.*, 2008). The treatment of an *E. coli* and *Staphylococcus aureus* suspension with a DBD plasma jet (working gas: argon) resulted in a 5.36 and 5.38 log unit reduction with treatment times of 60 s and 90 s, respectively. SEM images of treated bacteria indicated that the major role is played by reactive species in bacterial inactivation and heat, electric field, and UV photons had minor effects (Xu *et al.*, 2009).

Plasma Jet

Flexible plasma sources working under atmospheric pressure are of growing interest for biomedical applications. Therefore, the use of plasma jets for microbial inactivation treatments is under intensive investigation. An rf-driven atmospheric pressure plasma jet (working gas: mixture of He-O_2-H_2O) was used to inactivate *Bacillus subtilis* spores inoculated on glass surfaces. The spores were reduced by 7 log units within 30 s. However, sample temperatures of 175 °C were measured which is not suitable for heat-sensitive materials (Herrmann *et al.*, 1999). Brandenburg *et al.* (2007) used an rf-driven atmospheric plasma jet to inactivate *E. coli* and *Bacillus atrophaeus* spores on polyethylene strips. After 2 min treatment *E. coli* was reduced by 3.8 log units and the spores were reduced by 4.3 log units after 7 min treatment. The surface temperatures were between 80 and 90 °C. The plasma needle used to inactivate *E. coli* on agar and *Streptococcus mutans* in biofilms is a miniaturised rf-driven APPJ with a potential application in dentistry. After 10 s treatment *E. coli* was reduced by 4 to 5 log units and no re-growth of *Streptococcus mutans* was observed after 1 min treatment in absence of sucrose. In the presence of sucrose the bacteria growth was only reduced (Sladek *et al.,* 2007). Inactivation of *Bacillus subtilis* spores on filter papers by helium plasma was dependent on initial count of the spores. An initial concentration of 10^6 spores was reduced by three log units within 200 s. 360 s were needed to reduce the spores by three log units at an initial count of 10^9 spores. The sporulation

temperature also influences the inactivation by the plasma. Higher sporulation temperatures resulted in increased resistance against plasma (Deng *et al.*, 2005). The influence of initial microbial load on plasma inactivation capacities was also shown by Yu *et al.* (2006). The higher the microbial load of *E. coli* on filter papers the less was the inactivation of the used plasma jet (working gas: helium). At microbial loads of 10^{11} CFU only 1 log unit reduction was achieved after 1 min of treatment whereas a 7 log unit reduction of *E. coli* was achieved after 2.5 min when the initial concentration was 10^7 CFU The influence of the working gas on antimicrobial activity was investigated by Laroussi *et al.* (2006). The inactivation of *E. coli* was enhanced by addition of oxygen to the processing gas helium. Similar results were obtained by Uhm & Lim (2007). *Bacillus atrophaeus* spores were inactivated by 5 log units within 40 s using an argon-oxygen mixture as processing gas. Only 1 log unit inactivation was achieved after 3 min using a mixture of helium and oxygen as processing gas. The treated surface also influences the antimicrobial activity of plasma. The highest inactivation of *E. coli* and *Micrococcus luteus* by using a plasma jet (working gas: argon) was observed in suspension, followed by the inactivation on agar and on filter papers (Yu, 2007). The antimicrobial efficiency of APPJ against yeast was investigated by Kolb *et al.* (2008). With the working gas air and gas temperatures of 45 °C no growth of *Candida kefyr* on agar was observed after 90 s of treatment. Kim *et al.* (2009) reported that the addition of a ground ring electrode to a microplasma jet resulted in an enhanced discharge current, intensity of reactive radicals, and sterilisation effects. In contrast, the antimicrobial efficiency of APPJ was not significantly changed after addition of a grounded ring electrode to the plasma nozzle. However, the impedance matching of the system was more stable and less sensitive to spray capacitances (Ehlbeck *et al.*, 2008).

2.5.4 Plasma effects on contaminated food matrices

Low operating temperatures and the antimicrobial effects enable the application of non-thermal plasma for food surface decontamination. Up to now, inactivation of food-related microorganisms by plasma treatment was commonly conducted using model systems. An overview of microbial inactivation of model systems using non-thermal plasma published during the last three years is given by Wan *et al.* (2009). Furthermore, in recent years the number of studies dealing with the inactivation of microorganisms inoculated on food surface increased. Selected works are presented in table 2.8.

Montenegro (2002) used a pulsed non-thermal plasma system to inactivate *E. coli* O157:H7 in apple juice. He reduced the viable count of *E. coli* in the apple juice up to 7 log units after plasma treatment at < 100 Hz and 4000 pulses of 9000 V and showed the potential of

non-thermal plasma as a food decontamination technique. The influence of plasma on juice quality such as colour, taste or ingredients was not investigated.

Another possible application of non-thermal plasma is the decontamination of nuts or seeds. A 5-log reduction of *E. coli* inoculated on almonds was found after 30 s non-thermal plasma treatment at 30 kV and 2000 Hz (Deng, Ruan *et al.*, 2007). Basaran *et al.* (2008) treated various nut samples inoculated with *Aspergillus parasiticus* and tested the anti-fungal efficiency of low pressure cold plasma (LPCP). They used air gases and sulfur hexafluoride (SF_6) and found that SF_6 plasma application (5-log reduction) was more effective than air gas plasma treatment (1-log reduction). In contrast, the efficiency of air gas plasma against aflatoxin was greater than the efficiency of SF_6 plasma. Selcuk *et al.* (2008) treated seeds inoculated with *Aspergillus* spp. and *Penicillium* spp. were treated with LPCP using air gases and SF_6. The fungal attachment was reduced to below 1 % by the treatment while the germination quality of the seeds was preserved.

The potential of non-thermal plasma treatment to decontaminate fruits and vegetables is investigated in various studies. Critzer *et al.* (2007) used a one atmosphere uniform glow discharge plasma (OAUGDP) to inactivate *E. coli* on mangos and *E. coli* O157:H7, *Salmonella, L. monocytogenes* on apples, cantaloupe and lettuce, respectively. They showed the capability of this process to reduce microbial contamination on produce surfaces. Perni, Shama *et al.* (2008) and Perni, Liu *et al.* (2008) used cold atmospheric plasma pen to inactivate *Saccharomyces cerevisiae, Pantoea agglomerans*, and *Gluconacetobacter liquefaciens* inoculated on pericaps of mango and melon. Additionally, cut melon and mango pieces inoculated with *E. coli, S. cerevisiae, G. liquefaciens,* and *L. monocytogenes* were treated with the cold plasma. Comparable to Critzer *et al.* (2007), a decontamination of the fruit pericaps was detected whereas the efficiency on cut fruit surfaces was reduced. This reduction of efficiency was explained by a migration of the microorganisms into the fruit pieces. The potential of non-thermal plasma to reduce pathogens of fresh produce was also shown by Niemira & Sites (2008) who treated inoculated apples with cold plasma and reduced the microbial load by approximately 3 log after 3 min plasma treatment with a gliding arc. However, the food quality must not be reduced by the decontamination treatment. Therefore, the influence of atmospheric pressure glow discharges (APGD) on the quality of bell pepper was examined by Vleugels *et al.* (2005). Additionally, they investigated the inactivation of *Pantoea agglomerans* on a synthetic membrane to determine the maximum inactivation efficiency and minimal food damage. They found no unacceptable discolouring of the bell peppers after APGD treatment but an effective inactivation of *P. agglomerans* on the model system at the tested treatment conditions. The inactivation of *P. agglomerans* inoculated on bell pepper was not subject of this study.

Another possible application of non-thermal plasma is the treatment of packaged products. Schwabedissen *et al.* (2007) described the different application fields of the *PlasmaLabel™*, e.g. fresh food conservation or packaged goods. Packaged spinach was also treated with an atmospheric, non-equilibrium plasma system (Klockow & Keener, 2008). They detected a discolouration and wilting of spinach leaves after plasma treatment but at the same time a reduction of the microbial load.

Table 2.8: Literature overview (Plasma and Food Matrices)

Food matrix	Pathogen	Food quality evaluated	Plasma source	Reference
Apple juice	*E. coli* O157:H7	-	Pulsed non-thermal plasma system	Montenegro, 2002
Bell pepper	*Pantoea agglomerans*	colour	He-O_2 APGD[a]	Vleugels *et al.*, 2005
Apple	*E. coli* O157:H7,	-	OAUGDP[b]	Critzer *et al.*, 2007
Cantaloupe Lettuce	*Salmonella, L. monocytogenes*			
Almond	*E. coli*	-	Non-thermal plasma	Deng, Ruan *et al.*, 2007
Packaged goods	*B. subtilis*	colour	PlasmaLabel™ surface DBD[c]	Schwabedissen *et al.*, 2007
Nuts	*Aspergillus parasiticus*	organoleptic tests	LPCP[d]	Basaran *et al.*, 2008
Packaged spinach	*E. coli* O157:H7	colour	Atmospheric non-equilibrium plasma	Klockow & Keener, 2008
Apple	*E. coli* O157:H7	colour sensory damage	Gliding arc	Niemira & Sites, 2008
Mango Melon	*E. coli,S. cerevisiae, Pantoea agglomerans, Gluconacetobacter liquefaciens*	-	Cold atmospheric plasma pen	Perni, Liu *et al.*, 2008
Mango Melon	*E. coli, S. cerevisiae, Gluconacetobacter liquefaciens, L. monocytogenes*	-	Cold atmospheric plasma pen	Perni, Shama *et al.*, 2008
Seeds	*Aspergillus* spp., *Penicillum* spp.	-	LPCP[d]	Selcuk *et al.*, 2008
Sliced cheese Sliced ham	*L. monocytogenes*	-	Atmospheric pressure plasma	Song *et al.*, 2009
Lamb's lettuce	-	surface morphology secondary metabolites	RF-glow discharge	Grzegorzewski *et al.*, 2010

[a]APGD, atmospheric pressure glow discharge
[b]OAUGDP, one atmosphere uniform glow discharge plasma
[c]DBD, dielectric barrier discharge
[d]LPCP, low pressure cold plasma

These studies indicates the potential of non-thermal plasma treatment for food decontamination, however further studies including the determination of inactivation efficiency of this process on microorganisms inoculated on food surfaces are essential as well as the determination of the influences on food quality.

2.6 Flow Cytometry

2.6.1 Definition and history of flow cytometry

Flow cytometry is a process in which characteristics of single cells are measured in a fluid stream. Up to 10^4 cells s^{-1} can be analysed with modern flow cytometers. In modern clinical haematology laboratories, flow cytometers perform counts of red cells, white cells, and platelets in blood as well as counts of leukocytes. Today, more than 10,000 fluorescence flow cytometers are in clinical and other laboratory use throughout the world (Shapiro, 2003). A detailed history of flow cytometer development is given by Shapiro (Shapiro, 2003). In the following review some key points of flow cytometer development are described. As early as in the 1930's automated flow analysis of single cells was reported. Moldavan (1934) used a brightfield photoelectric method for counting cells, e.g. blood cells, flowing through a capillary tube located on a microscope stage but this design was limited in sensitivity. Similar methods were used in a patent by Kielland in 1945 (Kielland, 1945), by Beirne and Hutcheon for particle counts of 50-700 µm in diameter (Beirne & Hutcheon, 1957), and by Cornwall and Davidson for trypan blue-stained cells (Cornwall & Davison, 1960). The first working flow cytometer was described by Gucker and co-workers (1947). During World War II the aim of the work, which was sponsored by the US Army, was the rapid identification of airborne bacteria and spores used as biological warfare agents. The basics of hydrodynamic focussing, the technique all flow cytometer instruments make use of today, were established by Crossland-Taylor in 1953 (Crossland-Taylor, 1953). The development of a flow instrument for electrical measurement of cell volume by Wallace Coulter in the mid 1950's was the beginning of modern flow-system instrument development (Coulter, 1956). In the 1960's a dark-field photoelectric method for counting blood cells was described by Frommer (1962). The blood cells pass through a flow channel and are monitored by a low power microscope objective. In 1965 the first 'true' flow cytometer was described by Kamentsky and co-workers (1965). A flow-system was used to measure UV absorption and visible light scatter from cells flowing through a narrow channel using a microscope photometer. As a result, a device for physically separating cells was developed and for the first time absorption, light scatter, and fluorescence measurements on single cell level was possible. In the same year, the first flow sorter was described by Fulwyler (1965). With this instrument, biological cells were separated according to their cell volume. The measurement of cells stained with fluorescent dyes was reported by Van Dilla and co-workers in 1967 (Van Dilla *et al.*, 1967) using the flow chamber design of Crossland-Taylor. Further developments resulted in flow instruments for two-fluorescence measurements and measurements of cell volumes using electronic sensors. Two of early commercial instruments were outgrowths of Kametsky's spectrophotometers. The 'Cytograph' and 'Cytofluorograph' used an argon laser and helium

neon laser as excitation sources, respectively. In the early 1970's the use of multiparameter flow automation had its beginnings in cytochemistry. A system was developed to perform differential leucocyte counts using absorption and light scattering characteristics of cytochemical enzyme markers to classify leucocytes into groups of lymphocytes, monocytes, neutrophils, basophils, and eosinophils. The application of flow cytometry in microbiology was limited due to the small size and low concentrations of cellular constituents of bacteria cells which was under the detection limit of early flow cytometers. Flow cytometry was not successfully applied to microbiology before the improvements in optics technology and the development of better fluorescent dyes in the late 1970's (Steinkamp, 1984; Davey & Kell, 1996; Shapiro, 2003).

2.6.2 Principles of flow cytometry

The technology of current flow cytometers is substantially similar to 30 years ago. The technology used consists of fluidics, light sources, optics, detectors, and a computer for data analysis. Additionally, flow cytometer can be equipped with a cell-sorting device (Steen, 2000).

2.6.2.1 Fluidics

In the flow cell particles are delivered in single file to pass a focussed light beam. This is achieved by hydrodynamic focusing in a core stream encased within a sheath stream resulting in a laminar flow, a necessary factor for optimal measurements in flow cytometers. The sample is injected in a flowing stream of sheath fluid (water or saline) and a coaxial flow is created that moves from a larger to a smaller orifice. Thereby, a parabolic velocity profile with a maximum at the centre is created (Figure 2.13).

Due to the hydrodynamic focussing effect the cells remain in the centre of the core fluid and a small differential pressure between sheath fluid and sample (sample is 1-2 PSI above the sheath) forces the cells in single file through the core to the point of detection (Robinson, 2004).

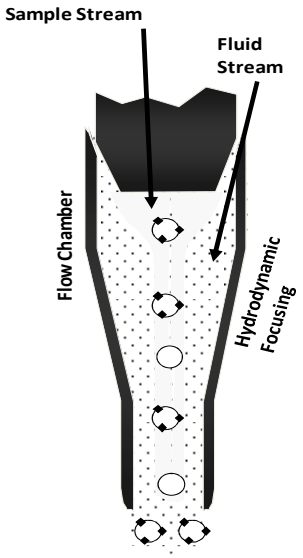

Figure 2.13: Basic structure of a typical flow cell.

2.6.2.2 Light sources

The light sources usually used in flow cytometers are lasers or arc lamps. The sensitivity and efficiency of flow cytometers are defined by the light source. Laser is the preferred light source because its light is monochromatic, coherent, polarised, and can be focused to a spot size (Steinkamp, 1984). The most commonly used laser in flow cytometers is the air-cooled argon ion laser with an emission wavelength of 488 nm. As a second source a diode laser emitting at a wavelength of 635 nm is used (Shapiro, 2003). The laser beam produces light scatter and fluorescence upon illumination of particles.

2.6.2.3 Optics

The optical system of a flow cytometer has two functions. Firstly, the incident light is focused on the crossing particles. Secondly, the optical system recovers the scattered light and fluorescence emitted by the particles and directs them to the appropriate detectors (Alvarez-Barrientos *et al.*, 2000). The optical system of the flow cytometer used in this study is shown in figure 2.14.

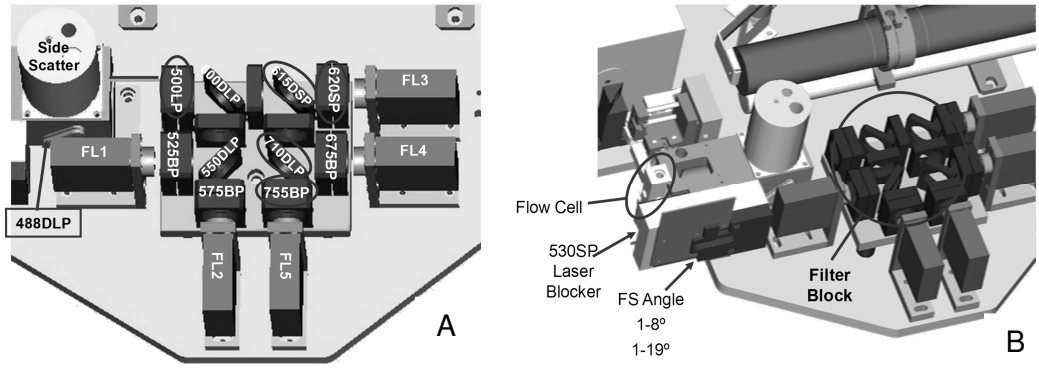

Figure 2.14: Optical system of the Cytomics FC 500. A) Design-layout of the flow cytometer. B) Optical layout of the flow cytometer (Beckman Coulter).

Light scatter

The scattered light of particles is detected in two directions. The light scattered in small angles relative to the incident beam is called the forward scattered light and the scattered light detected in an angle of 90° to the incident beam is called the side scattered light. The forward scatter light provides information about cell sizes (Vesey *et al.,* 1994). However, forward scatter light is also dependent on the refractive index difference between particles and medium and therefore an accurate measurement of cell size is not possible although good estimation of microbial cell size is possible (Davey & Kell, 1996; Shapiro, 2003). Side scattered light correlates with cell refractibility and thus, provides information about the surface structure and internal structure of the cells (Vesey *et al.*, 1994; Shapiro, 2003). Higher levels of cytoplasmic granularity result in higher intensity in side scatter signals (Davey & Kell, 1996).

Fluorescence

Besides the detection of morphological cell parameters by flow cytometry additional information can be achieved by the measurement of fluorescence properties. Fluorescence measured in flow cytometers can either be autofluorescence of the cells or fluorescence from fluorophores added to the cells. Those extrinsic probes can be related to some cellular components or properties (Haugland, 1994). Fluorescence is the emission of remaining excitation energy as photons (Shapiro, 2003). The absorption of UV, visible, or infrared light by a molecule brings the molecule into an excited state. The reduction of the excited molecule to a non-excited state is illustrated in the Jablonski diagram (Figure 2.15).

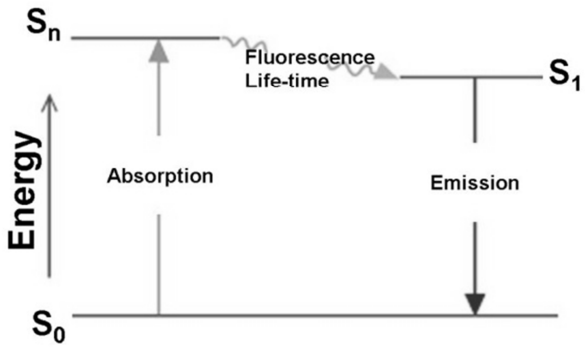

Figure 2.15: Jablonski diagram of electronic energy levels, states, and transitions.

Absorption of energy involves the transition from the electronic ground state S_0 to the excited state S_n. The conversion from the S_n state to the S_1 (lowest excited energy level) is called internal conversion and vibrational relaxation. This change in energy level is not accompanied by the emission of photons. The transition of the first electronic excited state S_1 to the electronic ground state S_0 can be reached by several ways: i) surplus energy is converted into heat during transition from S_1 to S_0; ii) energy transition may take place to a vibrational level of the first excited triplet state T_1 (intersystem crossing). Transition from the T_1 state to the S_0 state occurs by the emission of phosphorescence. Phosphorescence is less likely to occur than fluorescence; iii) the energy difference between the S_1 and S_0 state is lost by the emission of fluorescence. Thereby, the energy content of the emitted photons is lower than the energy content of the originally absorbed photons. Thus, the fluorescence emission will occur at longer wavelengths than the excitation wavelengths. The difference between the excitation and the emission wavelength is known as Stokes shift. The fluorescence intensity is proportional to the amount of light absorbed and is determined by the specific quantum efficiency of the corresponding fluorophore (Shapiro, 2003).

Each fluorophore has a characteristic excitation and emission wavelength. Therefore, the number of fluorescent dyes and probes used in flow cytometry is relatively low. These limitations are due to the excitation sources used in the flow cytometer. The dyes used need to have an appreciable absorption at the emission wavelength of the used light sources (Haugland, 1994).

2.6.2.4 Detectors

The detectors of the flow cytometer transform the incoming scatter light and fluorescence signals into electronic pulses and the magnitude of these pulses are distributed into channels. This allows the plotting of the number of cells against the channel number in histograms (Alvarez-Barrientos *et al.*, 2000). Photomultiplier tubes (PMT) and photodiodes are the commonly used detectors in flow cytometers. Both detectors take photons in and put electrons out but photodiodes put only seven electrons out for every ten photons, whereas PMT put 10^7 electrons out for each incoming photon. Usually, the forward scattered light is detected by photodiodes and the side scattered and fluorescence light is detected in PMT because the forward scattered light consists of more photons than the side scattered light (Shapiro, 2003).

2.6.2.5 Data analysis

A huge amount of information is produced by multiparameter data acquisition. This information are analysed by the data analysis system. The data analysis of flow cytometry includes all operations used to derive information about biological cell characteristics from measured physical characteristics (Shapiro, 2003). Particular subpopulations can be independently studied with analytical software, statistical analysis can be performed and data can be represented in different ways such as monoparametric and diparametric histograms and three-dimensional graphs. Besides the growing market of commercial analysis software for flow cytometers free software is also available (Alvarez-Barrientos *et al.*, 2000).

2.6.2.6 Sorting

Cell sorting by flow cytometry allows the isolation of target cells and separation of these cells from the original sample for further analysis. The technique is based on the identification of cells by the measured signals, the identification of its physical position and the placement of a charge to the stream at exactly the right time for physical collection of the sorted cell in a vessel (Robinson, 2004).

2.6.3 Flow cytometry in microbiology

Since the development of appropriate fluorescent dyes and improvement of optic technology, flow cytometric techniques penetrated the world of microbiology and the number of publications dealing with flow cytometry in microbiology has significantly increased (Fouchet *et al.*, 1993). The importance of single-cell analysis was described by Davey & Kell (1996).

The heterogeneity of microbial populations including axenic laboratory cultures is far greater than normally assumed. This implies the need for quantitative analysis of microbial performance. There are three principle sources of microbial heterogeneity: i) genotypic through mutations; ii) phenotypic via progression through the cell cycle; and iii) phenotypic due to changes in the exact local environment. Another task for the use of flow cytometry in microbiology is the determination of cell viability. Cellular viability can be classified in four categories: i) proliferating or reproductively viable cells; ii) vital cells; iii) intact cells; and iv) dead cells. Reproductively viable cells are able to grow under laboratory conditions and are the primary measurement of cell viability. However, long lag phases and sensitivity on growth conditions make it difficult to detect stressed, injured, or other so-called viable-but non-culturable (VBNC) bacteria (Joux & Lebaron, 2000; Hewitt & Nebe-von-Caron, 2004). In vital cells metabolic activity or cellular response to extracellular conditions can be demonstrated. Selective permeability or cell membrane integrity is detectable in intact cells and dead cells are particles with genetic information but without intact cell membrane (Nebe-von-Caron & Badley, 1995). A classification of physiological cell states is also given by Bunthof (2002) (Figure 2.16).

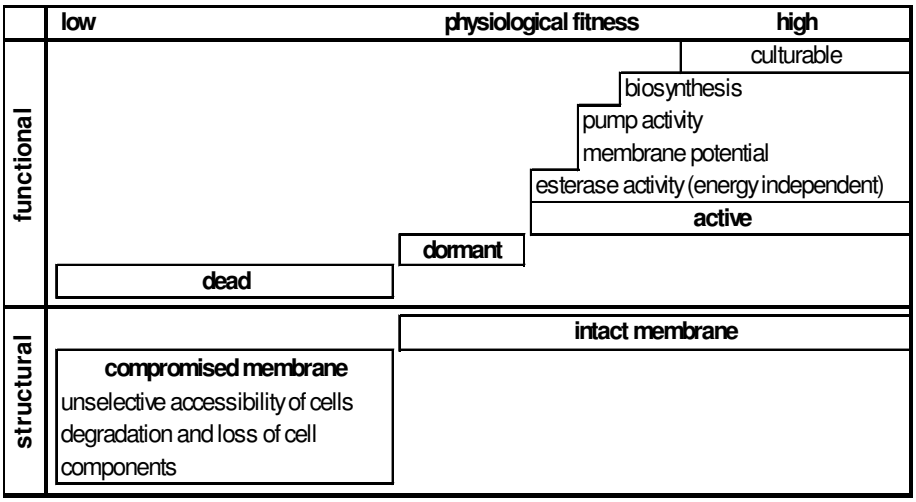

Figure 2.16: Physiological cell states (Bunthof, 2002).

Reproductive growth is the highest level of physiological fitness and metabolic activity can be detected at different levels. These cells are called active. Dormant, injured, or starved cells may in time reverse to an active state but their physiological fitness is reduced. The three cell categories have an intact cell membrane in common. Dead cells have no functional properties and a compromised cell membrane which results in a loss of cell components.

Fluorescent dye technology offers probes for a variety of cellular functions (Joux & Lebaron, 2000). The use of fluorescent dye mixtures enables the classification into three types of

viable cells: metabolically active, intact, or permeabilised cells (Hewitt & Nebe-von-Caron, 2004). The types of fluorescent dyes primary used in flow cytometry are: i) fluorescent immunoconjugates and probes for fluorescence *in situ* hybridisation; ii) nucleic acid strains; and iii) physiological probes to measure ions, membrane potential, enzymatic activity, viability, organelles, phagocytosis, cell development, and other cell properties (Haugland, 1994). The different cellular target sites for physiological and taxonomic fluorescent dyes are illustrated in figure 2.17 and further explained below with special focus on the fluorescent dyes used in this study.

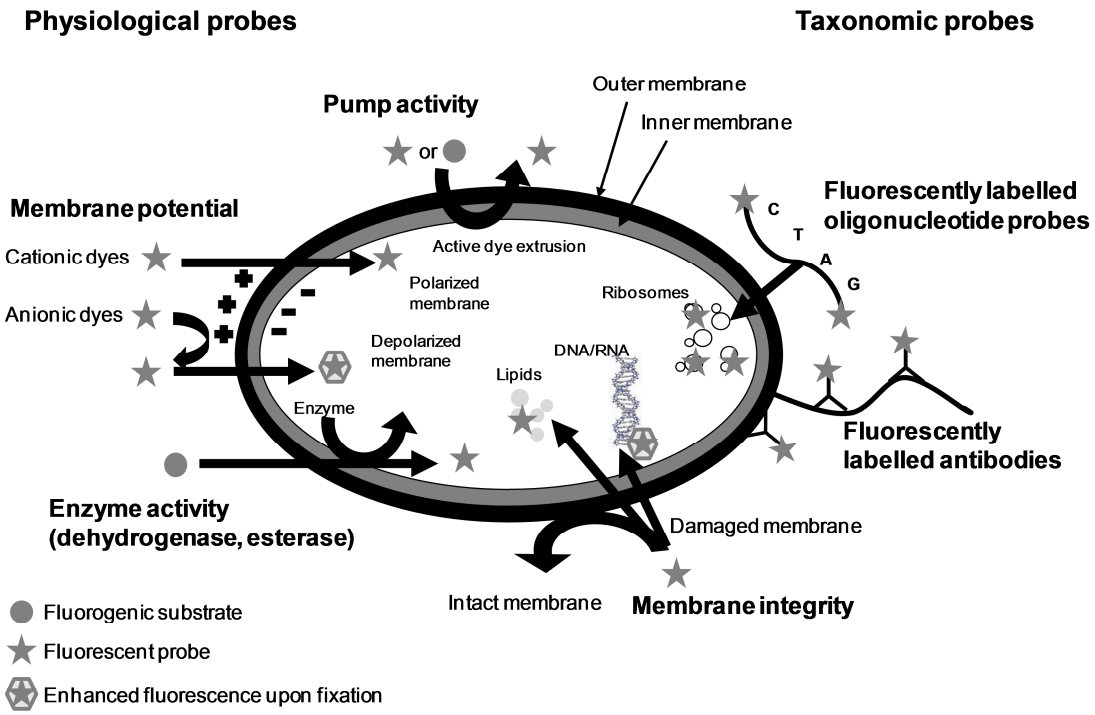

Figure 2.17: Cellular target sites for fluorescent dyes used for flow cytometry measurements in microbiology (modified after Joux & Lebaron (2000) and Ben-Amor (2004)).

Fluorescently labelled oligonucleotide probes and antibodies

The automated and specific detection of pathogens is an important task in food microbiology. The use of fluorescently labelled oligonucleotide probes and antibodies in flow cytometry allows the specific and automated identification of microorganisms in pure culture and also in environmental samples (Amann *et al.*, 1990; Wallner *et al.*, 1993; Vesey *et al.*, 1994; Davey, 2002; Tang *et al.*, 2005). Antibodies recognise and bind to specific surface epitopes and single-strand nucleic acid probes hybridise specifically to complementary strands of target DNA or RNA (Wallner *et al.*, 1993). The 16S rRNA is the common target for determinative

hybridisation probes (Amann *et al.,* 1990).The use of direct or indirect fluorescence in situ hybridisation (FISH) in flow cytometry is increasing and the most common dyes for preparing fluorescent immunoconjugates are fluorescein and its derivates (Haugland, 1994). It was shown that fluorescently labelled oligonucleotides specific for 16S rRNA can be used to monitor growth of bacteria in pure or mixed populations, sewage, lake water, and activated sludge. Quantitative and qualitative detection of specific microorganisms is possible using rRNA targeted fluorescent probes in combination with ethidium bromide. Fluorescent antibodies are also able to detect bacteria in water, sewage, and soil (Thomas *et al*., 1997). Monoclonal antibodies were successfully used to detect *E. coli* O157:H7 by flow cytometry and the authors in this study concluded that it may be a useful method to detect pathogen *E. coli* in food ingredients (Kusunoki *et al*., 1998). Iannelli *et al.* (1998) successfully used flow cytometry to detect antibodies against *Brucella abortus* and *Staphylococcus aureus* in milk samples of different origins. The combination of fluorescent antibodies with fluorescent dyes allows specific detection of bacteria as well as the determination of cell viability. Rodriguez & Thornton (2008) identified and quantified viable *Saccharomyces cerevisiae* and *Oenococcus oeni* in Chardonnay fermentations using fluorescent antibodies and fluorescent dyes in combination. Polyclonal antibodies were successfully applied to detect spores of *Clostridium tyrobutyricum* in milk by flow cytometry (Lavilla *et al.,* 2010).

Membrane integrity

Membrane integrity of cells is used as an indicator of cell damage or cell death. Measurement of membrane integrity of bacteria cells is complicated by their complex membrane structure. Gram-negative bacteria have an outer membrane, a rigid petidoglycan layer and the plasma membrane. Gram-positive bacteria do not have an outer membrane. Membrane-impermeant nucleic acid dyes are often used for membrane integrity measurements. Uptake of these dyes is associated with irreversible loss of membrane integrity. Upon uptake the dyes bind to nucleic acids and the fluorescence is enhanced (Ueckert *et al*., 1995; Davey *et al*., 1999; Joux & Lebaron, 2000). Propidium iodide, TOTO/BOBO/POPO/YOYO dimer family based on benzothiazolium-4-pyridinium and benzoxazolium-4-pyridinium, TO-PRO series, and SYTOX are the used impermeant nucleic acid dyes for measurement of membrane integrity (Petit *et al*., 1993; Davey & Kell, 1996; Schumann *et al*., 2003). Direct count of bacteria can be achieved using membrane-permeant dyes (Nebe-von-Caron *et al*., 2000) such as thiazole orange (TO), ethidium bromide (EB), DAPI, SYTO series, Hoechst dyes, and acridine orange (Nebe-von Caron *et al.,* 1998; Veal *et al*., 2000). However, DNA-specific Hoechst dyes and DAPI require UV excitation and therefore, they are not appropriate for flow cytometer applications (Winson & Davey, 2000).

Propidium iodide (PI) is an intercalating nucleic acid dye. Upon uptake the dye intercalates between base pairs of double-stranded DNA and RNA and has no sequence preference. It binds with a stoichiometry of one dye molecule per 4-5 base pairs of DNA (Petit *et al.*, 1993; Bunthof, 2002). PI is excluded from intact cells by its additional charge (Shapiro, 2003; Figure 2.18).

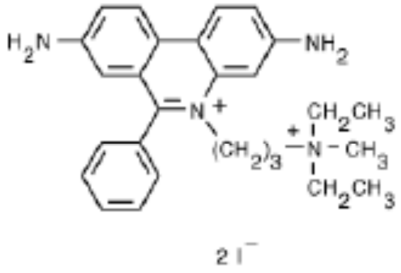

Figure 2.18: Chemical structure of propidium iodide.

The molecular weight of PI is 668 and its fluorescence intensity increases 20-30-fold upon binding to nucleic acids. The excitation wavelength is 536 nm and maximum emission is at 620 nm. The maximum molar extinction coefficient is 6400 cm^{-1} M^{-1} and at 488 nm the molar emission coefficient is 4000 cm^{-1} M^{-1} (Haugland, 1994; Joux & Lebaron, 2000). The large Stokes shift makes PI a useful probe for simultaneous detection with other probes for bacterial viability evaluation (Bunthof, 2002).

Thiazole orange (TO) was originally synthesized as a stain for blood reticulocyte analysis (Lee *et al.*, 1986). The extinction maximum of TO is 509 nm and the maximum emission wavelength is 525 nm. The maximum molar extinction coefficient is 54000 cm^{-1} M^{-1} and at 488 nm the molar emission coefficient is reduced to 34000 cm^{-1} M^{-1} (Haugland, 1994). The chemical structure of TO is shown in figure 2.19. TO binds as monomer and dimer to DNA and the quantum yield increases 50-2000 fold upon binding to nucleic acids, depending on sequence, structure, and temperature. TO binds to double-stranded DNA, single stranded polypurines and single-stranded polypyrimidines with decreasing affinity. Monomer TO stacks between DNA bases and dimer TO binds with single-stranded polypyrimidines (Nygren *et al.*, 1998). TO binds both to DNA and RNA with higher fluorescence intensity of the TO-DNA complex (Berdalet & Dortch, 1991).

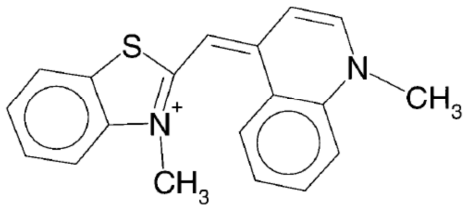

Figure 2.19: Chemical structure of thiazole orange.

Membrane potential

Normally, electric potential differences exist across cell membranes. These differences are due to concentration gradients of Na^+, K^+, and Cl^- ions across the cell membrane and also due to operation of electronic pumps. The potential difference across the cytoplasmic membrane of bacteria is between -100 and -200 mV with interior negative (Shapiro, 1994). The membrane potential is an essential part of bacterial physiology. It is involved in the generation of ATP, bacterial autolysis, glucose transport, chemotaxis, and survival at low pH. Depolarisation of cells is the reduction of membrane potential to zero due to destruction of the cell membrane integrity by physical agents or due to elimination of proton gradients across the membrane by proton ionophores such as carbonyl cyanide m-chlorophenylhydrazone (CCCP) (Novo *et al.,* 1999). Potential-sensitive dyes used for membrane potential measurements are merocyanines, cyanines, and oxonols. Fluorescent dyes can also be divided into slow response and fast response. Slow response dyes respond to changes in membrane potential in seconds and fast response dyes respond in microseconds. Cyanine and oxonol dyes can work by both mechanisms (Waggoner, 1979).

Oxonol dyes are anionic lipophilic dyes which concentrate within cells with reduced membrane potential and bind to lipid-rich components. Bis-(1,3-dibutylbarbituric acid)trimethine oxonol ($DiBAC_4(3)$) was used to measure depolarised Gram-negative and Gram-positive bacteria in combination with a EDTA pretreatment. Uptake of oxonols is more related to membrane integrity rather than membrane depolarisation (Joux & Lebaron, 2000). Cationic lipophilic cyanine dyes freely diffuse into cell with a negative interior membrane potential gradient and cells are equilibrated with the dyes. Depolarisation (decrease of membrane potential) of the cells leads to a release of the dye and hyperpolarisation (increase in membrane potential) leads to an additional uptake of dyes (Shapiro, 1994; Novo *et al*., 2000).

Novo *et al*. (1999) tested different cyanine dyes ($DiYC_{n+1}(2m+1)$) for accurate measurement of membrane potential and developed a radiometric technique for membrane potential

estimation. Diethyloxacarbocyanine iodide ($DiOC_2(3)$; Figure 2.20) was found to be the best dye for accurate and precise estimation of membrane potential by radiometric technique. At an excitation wavelength of 488 nm $DiOC_2(3)$ emits at 530 nm and a second peak occurs at < 600 nm when $DiOC_2(3)$ is used in high concentrations. The authors added $DiOC_2(3)$ in high concentrations (30 µM) to bacteria suspensions and the emitted green fluorescence was independent of membrane potential but the emitted red fluorescence significantly changed with changes in membrane potential. The ratio of red to green fluorescence provides a measure of membrane potential that is largely independent of cell size. A calibration with valinomycin showed that the developed method was accurate over a membrane potential range from -50 mV and -120 mV (Novo *et al.*, 1999).

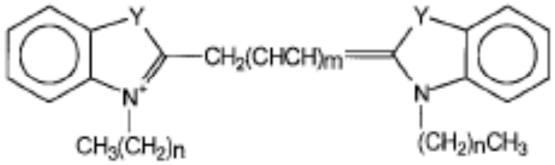

Figure 2.20: Structure of cyanine dyes with the formula $DiYC_{n+1}(2m+1)$.

Enzyme activity

Enzyme activity is another essential factor in cellular viability and thus, esterase activity is often monitored using flow cytometry. Polar, membrane permeable fluorescent dyes are esterified with non-fluorescent permeable acetyl or acetoxymethyl esters resulting in lipohilic, uncharged and non-fluorescent fluorogenic substrates. Inside vital cells the substrate is cleaved by non-specific enzymes to a fluorescent product and is retained within intact cells. The most commonly used fluorogenic substrates are fluorescein derivatives because they have high extinction coefficients, a high quantum yield, and can be excited at 488 nm. Fluorescein diacetate is cleaved by esterases releasing fluorescein which only gives weak signals because it is poorly retained within the cells. Hydrophobic fluorescein diacetate derivatives such as carboxyfluorescein diacetate (cFDA), chloromethylfluorescein diacetate (CMFDA), and carboxyfluorescein diacetate acetoxy methyl ester (cFDA-AM) are cleaved into hydrophilic products which are retained more efficiently in the cells. The most widely applied fluorescein diacetate derivatives in flow cytometry is cFDA (Ueckert *et al.*, 1995; Veal *et al.*, 2000; Joux & Lebaron, 2000). The poor dye uptake, low labelling efficiency of some species, and active extrusion limits the application of fluorogenic esterase substrates. Furthermore, Gram-negative bacteria are generally impermeable to lipophilic probes due to

their additional outer membrane and permeabilisation is required (Bunthof *et al.*, 1999; Bunthof *et al.*, 2000). In various studies cFDA (Figure 2.21) is used in combination with membrane-impermeant dyes to evaluate bacterial viability (e.g. Breeuwer *et al.*, 1994; Breeuwer *et al.*, 1995; Breeuwer *et al.*, 1996; Bunthof *et al.*, 2000; Bunthof *et al.*, 2001; Budde & Rasch, 2001; Bunthof & Abee, 2002; Ben- Amor *et al.*, 2002; Da Silveira *et al.*, 2002; Hoefel *et al.*, 2003; Hoefel *et al.*, 2005; Ananta *et al.*, 2005; Chitarra *et al.*, 2006; Da Silveira & Abee, 2009).

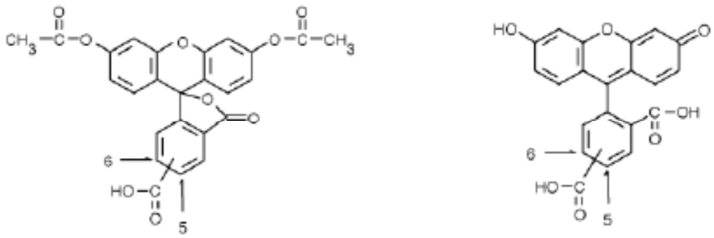

Figure 2.21: Chemical structures of 5(6)-carboxyfluorescein diacetate (left) and 5(6)-carboxyfluorescein (right).

The non-fluorescent cFDA is hydrolysed to carboxyfluorescein (cF). The molecular weight of cFDA is 460 and that of cF is 376. Carboxyfluorescein has four protolytic groups: cation, neutral, monoanion, dianion, and trianion. The groups have different fluorescence intensities with the highest fluorescence intensity of the trianion. The maximum excitation of cF is at a wavelength of 492 nm and at 516 nm cF has its maximum emission. The quantum yield in 0.1 NaOH is 0.92 and the maximum excitation coefficient is 78000 cm^{-1} M^{-1} (Bunthof, 2002).

2.6.4 Monitoring of inactivation treatments by flow cytometry

Flow cytometry is used in various studies to monitor bacterial inactivation. Cellular injuries of spray-dried *Lactobacillus rhamnosus* GG was investigated using cFDA and PI in combination. The bacterial membrane was identified as the main site of injury during spry drying. A good correlation between CFU and cF-stained cells indicate that cells capable of retaining cF inside the cells after spray-drying are also culturable (Ananta, 2005).

$DiBAC_4(3)$, SYTOX Green, redox dye CTC, and the Baclite viability test kit have been used to investigate the effects of antibiotics against *Pseudomonas aeruginosa, E. coli,* and *Staphylococcus aureus*. In comparison to plate count methods the number of nonviable bacteria was overestimated by $DiBAC_4(4)$ and SYTOX Green. Several subpopulations were detected using CTC. The population heterogeneity was suggested to be antibiotic-induced.

Two viable populations and one dead population were observed with the Baclite viability test kit (Suller & Lloyd, 1999). The antimicrobial activity of vanillin against *E. coli, Lactobacillus plantarum*, and *Listeria innocua* was observed using propidium iodide. Although the PI uptake increased upon exposure to vanillin, a significant proportion of cells remained unstained (Fitzgerald, 2004). *Lactobacillus* species were exposed to several bacteriocins and the antimicrobial effect was investigated using cFDA. A rapid leakage of cF was observed after exposure to pediocin but bacteria were detected as CFU when plated on rich medium. This suggested that the cells were able to repair after exposure to pediocin (Budde & Rasch, 2001).

Ethanol-adapted and non-adapted *Oenococcus oeni* cells were stained with cFDA and PI in combination. A positive effect of ethanol was shown by the fact that the cells were only stained with cF and retained their membrane integrity. The use of cFDA and PI in combination led to a population stained both with cF and PI indicating damaged cells. The application of this staining method allows the characterisation of different levels of ethanol damage in bacterial populations (Da Silveira *et al.*, 2002). Subpopulations of *Oeneocossus oeni* cells were found after exposure to 12 % ethanol using cFDA-staining. One of the subpopulations was able to extrude cF and the other populations remained cF-stained. Ethanol-adaption of the cells was found after growing of the cells in 8 % ethanol before exposure to 12 % ethanol. This treatment resulted in robust cells which were able to extrude cF (Da Silveira & Abee, 2009).

Efflux pump activity and viability of *E. coli* cells after UVA irradiation was observed using ethidium bromide, SYTO 9 and propidium iodide. During the first two hours of irradiation the cells stayed intact and the measured functions were active. With increasing irradiation time the efflux pump activity decreased but membrane permeability only slightly increased. After 50 h treatment almost all cells appeared intact (Berney *et al.*, 2007). Solar disinfection efficiency against *E. coli* was tested using ethidium bromide/SYTO 9 (efflux pump activity), $DiBAC_4(3)$ (membrane potential), LIVE/DEAD BacLight™ (membrane integrity), and 2-NBDG (glucose uptake activity). Using these dyes could allow a typical inactivation pattern to be observed. Shortly after the start of exposure efflux pump activity stopped, followed by the loss of membrane potential and reduced glucose uptake ability and finally, the cells were permeabilised (Berney *et al.*, 2007).

Membrane permeabilisation of *Lactobacillus* species after treatment with pulsed electric fields (PEF) was demonstrated using propidium iodide (Wouters *et al.*, 2001). Propidium iodide was also used to investigate membrane permeabilisation of *E. coli, L. innocua*, and *Saccharomyces cerevisiae* after PEF treatment. Membrane permeabilisation was influenced

by electric field strength and pulse duration. *S. cerevisae* was the most sensitive, followed by *E. coli* and *L. innocua* (Aronsson *et al.*, 2005). The enumeration of actively respiring *E. coli, L. monocytogenes*, and *Bacillus cereus* cells after PEF treatment were performed using CTC and 4,6-diamidino-2-phylindole. This staining showed a good correlation with the plate count method. Sublethally injured cells were not detected (Yaqub *et al.,* 2004).

High pressure induced damage was investigated by flow cytometry in various studies. Sublethally injured *Lactobacillus rhamnosus* GG cells were detected after high pressure treatment using cFDA and PI. The loss of culturability did not correlate with the absence of esterase activity. The comparison of high pressure treatment with heat treatment demonstrated the different pathways of inactivation mechanisms. Thermal-induced death was achieved with or without membrane degradation and high pressure induced cell death is due to irreversible damage of the membrane-bound transport systems (Ananta *et al.*, 2004; Ananta & Knorr, 2009). Brul *et al.* (2000) concluded that the primary high pressure inactivation step in the treatment of yeasts involves a perturbation of membranes after application of propidium iodide to treated cells. The cell morphology of *L. monocytogenes* was measured by light scattering in flow cytometry and it was shown that the morphology was not affected by high hydrostatic pressure. Esterase activity measured with cFDA was dramatically lowered after high pressure treatment. Membrane integrity measured with PI was preserved and membrane potential measured by oxonol uptake was reduced (Ritz *et al.*, 2001; Ritz *et al.*, 2002). Mathys *et al.* (2007) used SYTO 16 and propidium iodide to monitor effects of high pressure on *Bacillus licheniformis* spores. A three step model of inactivation was suggested. Follwing germination hydrolysis of the spore cortex occurs and finally the spore's inner membrane is physically compromised. The effects of high pressure induced ice I to ice III phase transitions on *L. innocua* were monitored by flow cytometry using cFDA and PI. In comparison to liquid or frozen *L. innocua* a complete inactivation due to cell rupture was observed for cells subjected to ice I to ice III transitions (Luscher *et al.*, 2004). Similar results were obtained by Shen *et al.* (2009). A significant population of *Bacillus subtilis* was stained with propidium iodide after high pressure induced ice I to ice III transition. The remaining population was severely stressed and ghost cells were found. However, impaired esterase activity did not indicate the absence of viability.

3. Material and Methods

3.1. Storage and cultivation of bacteria

Listeria innocua, *Escherichia coli*, and *Pectobacterium carotovorum* spp. *carotovorum* were provided by the German Collection of Microorganisms and Cell Cultures in Braunschweig. The optimal cultivation temperature and cultivation medium for the bacteria are summarized in table 3.1. The selected bacteria were stored as glass bead cultures at -80 °C for long-term maintenance. To reactivate the bacteria one glass bead was given to 5 ml filtrated nutrient broth (Roth, Germany) and incubated for 24 h without shaking at their optimal growth temperature (pre-culture). Afterwards, optical density (OD) of the bacteria suspension was measured at 620 nm (OD_{620}) in the range of 0.01 and 1 in a spectral photometer Unicam UV1-100 (Nicolet Instruments GmbH, Germany) and 100 ml nutrient broth was inoculated with bacteria suspension at a calculated OD_{620} of 0.07 ml^{-1} (Figure 3.1). *L. innocua, P. carotovorum,* and *E. coli* were harvested after 18 h of incubation at their optimal cultivation temperature (Table 3.1). To avoid the measurement of particles as unstained bacteria in flow cytometric analyses nutrient broth was filtered with a 0.2 µm membrane filter.

Table 3.1: Summary of the selected bacteria with their collection number, cultivation temperature, and growth medium for reactivation

	Collection number[a]	Growth medium[b] reactivation	Optimal cultivation temperature [°C]
L. innocua	DSM 20649	NB	37
E. coli	DSM 1116	NB	37
P. carotovorum	DSM 30168	NB	30

[a]DSM, Deutsche Stammsammlung für Mikroorganismen (German Collection of Microorganisms and Cell Cultures, Germany)
[b]NB, nutrient broth (Roth, Germany)

All bacteria (100 ml in each case) were harvested by centrifugation at 3220 x *g* for 15 min at 4 °C. The bacteria pellet was suspended in 50 mM phosphate buffered saline and the optical density was adjusted as required for the experiments (see sections 3.3.2.1, 3.3.2.3, and 3.3.3). The phosphate buffered saline (PBS) was prepared of 137 mM NaCl, 2.7 mM KCl, 40.6 mM Na_2HPO_4, and 7.1 mM KH_2PO_4. The pH was adjusted to 7.0 with HCl and finally filtered with a 0.2 µm membrane filter. All reagents were provided by Roth, Germany.

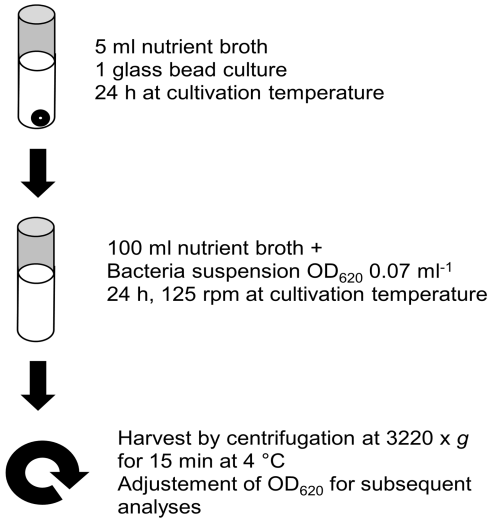

Figure 3.1: Scheme of bacterial cultivation and harvest.

3.2 Growth curves

The growth behaviour of *L. innocua*, *E. coli*, and *P. carotovorum* was recorded to obtain bacteria from the stationary growth phase for inactivation treatments. 200 ml filtrated nutrient broth was inoculated with bacteria suspension (pre-culture) at a calculated OD_{620} of 0.07 ml^{-1}. For each growth curve two samples were inoculated at the same time. The optical density of the bacteria suspensions, the number of colony forming units (CFU) ml^{-1}, the cell number and cell size as well as the membrane integrity of the cells was measured at their optimal growth temperature (Table 3.1) every one to three hours over a time range of 57-63 h.

The dilution series with deionized water were performed in duplicate using Rotilabo®-microtest plates (96er U-profile, Roth, Germany). 100 µl of each dilution was spread on the cultivation medium. The number of colony forming units (CFU ml^{-1}) was obtained after growth for 48 h (*L. innocua, P. carotovorum*) or 24 h (*E. coli*) at optimal growth temperature to determine the viable cell count.

A Multisizer™ 3 Coulter Counter® (Beckman Coulter, Germany) was used to measure the cell number and cell size during bacteria growth. Each sample was measured in triplicate. The measurement parameters of the Multisizer are listed in section 3.4

The membrane integrity was measured in a flow cytometer (Cytomics FC 500, Beckman Coulter, Germany) using thiazole orange (Sigma-Aldrich, Germany) and propidium iodide (Sigma-Aldrich, Germany). Therefore, the sampled bacteria suspension was diluted in 50 mM phosphate buffered saline (pH 7.0) to obtain a cell concentration of ~10^6 cells ml^{-1}

and 0.42 µM thiazole orange (TO) and 30 µM propidium iodide (PI) was added. The dyes were allowed to penetrate the bacteria for 10 min at room temperature in the dark before flow cytometric measurements. The measurement parameters of the flow cytometer are listed in section 3.3.6.

3.3 Flow cytometric measurements

3.3.1 Flow cytometer and settings

All experiments were performed using a Cytomics FC 500 flow cytometer (Beckman Coulter, Germany) equipped with a 20 mW argon ion laser emitting at a wavelength of 488 nm. The field stop was either set on 1-19° (growth curves, plasma treatment) or 1-8° (growth curve, heat, PAA, ozone treatment). The discriminator to reduce background noise was either set on the forward scatter (FS=0; growth curves, plasma treatment) or side scatter (SS=2; growth curve, heat, PAA, ozone treatment). The fluorescence of thiazole orange, carboxyfluorescein, and green $DiOC_2(3)$ was collected in the FL1 photomultiplier with a band pass filter of 525 nm and the fluorescence of propidium iodide and red $DiOC_2(3)$ was recorded in the FL3 photomultiplier with a short pass filter of 620 nm (Figure 3.2).

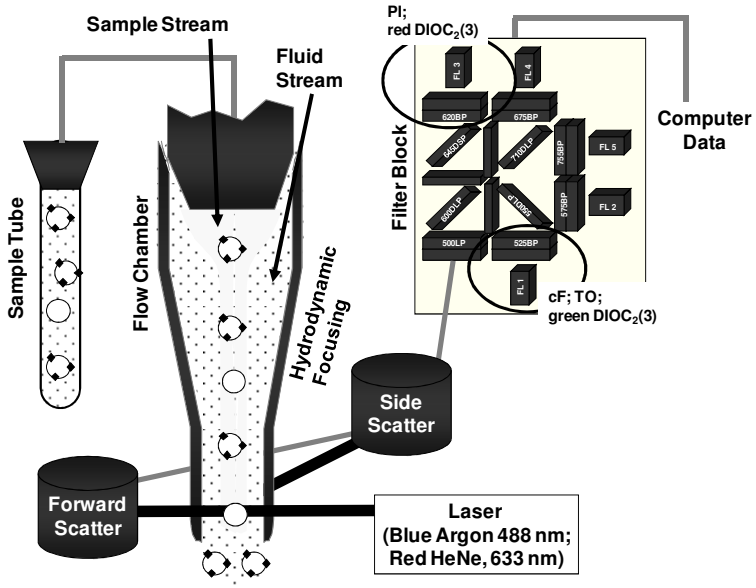

Figure 3.2: Principle of Cytomics FC500.

Fluorescence compensation was performed to correct the overlap of one dye's emission into another dye's detector. The flow cytometer settings for the different experiments are given in tables 3.2 to 3.9. The parameters were collected as logarithmic signals and the obtained data

was analysed using CXP Analysis software (Beckman Coulter, Germany) and (OriginPro 7.5, OriginLab Corporation). 10,000 events were measured at a flow rate of approximately 300 events s^{-1}.

Table 3.2: Flow cytometer settings for measurements of membrane integrity (TO+PI) during growth curves of *E. coli*, and *P. carotovorum*. The field stop was set to 1-19° and the discriminator was FS=0

Detector	Voltage [V]	Gain	Compensation				
			FL1	FL2	FL3	FL4	FL5
FS	896	2					
SS	75	5					
FL1	714	1	-	0	30	0	0
FL2	337	1	0	-	4.8	0	0
FL3	550	1	25.5	0	-	0	0
FL4	450	1	0	0	6.4	-	0
FL5	577	1	0	0	8.7	0	-

Table 3.3: Flow cytometer settings for measurements of membrane integrity (TO+PI) during growth curves of *L. innocua* The field stop was set to 1-8° and the discriminator was SS=2

Detector	Voltage [V]	Gain	Compensation				
			FL1	FL2	FL3	FL4	FL5
FS	600	10					
SS	800	10					
FL1	714	1	-	0	30	0	0
FL2	337	1	0	-	4.8	0	0
FL3	630	1	25.5	0	-	0	0
FL4	450	1	0	0	6.4	-	0
FL5	577	1	0	0	8.7	0	-

Table 3.4: Flow cytometer settings for measurements of esterase activity and membrane integrity (cF+PI) during the development of a staining protocol for *P. carotovorum*. The field stop was set to 1-19° and the discriminator was FS=0

Detector	Voltage [V]	Gain	Compensation				
			FL1	FL2	FL3	FL4	FL5
FS	600	2					
SS	56	5					
FL1	473	1	-	0	30	0	0
FL2	364	1	1.9	-	4.8	0	0
FL3	530	1	30.3	0	-	0	0
FL4	363	1	1.4	0	6.4	-	0
FL5	481	1	1.5	0	8.7	0	-

Table 3.5: Flow cytometer settings for measurements of esterase activity and membrane integrity (cF+PI) after plasma treatment. The field stop was set to 1-19° and the discriminator was FS=0

Detector	Voltage [V]	Gain	Compensation				
			FL1	FL2	FL3	FL4	FL5
FS	600	2					
SS	800	5					
FL1	532	1	-	0	30	0	0
FL2	364	1	1.9	-	4.8	0	0
FL3	630	1	30.3	0	-	0	0
FL4	363	1	1.4	0	6.4	-	0
FL5	481	1	1.5	0	8.7	0	-

Table 3.6: Flow cytometer settings for measurements of membrane integrity (TO+PI) after plasma treatment. The field stop was set to 1-19° and the discriminator was FS=0

Detector	Voltage [V]	Gain	Compensation				
			FL1	FL2	FL3	FL4	FL5
FS	600	2					
SS	800	5					
FL1	714	1	-	0	30	0	0
FL2	337	1	0	-	4.8	0	0
FL3	630	1	25.5	0	-	0	0
FL4	430	1	0	0	6.4	-	0
FL5	577	1	0	0	8.7	0	-

Table 3.7: Flow cytometer settings for measurements of esterase activity and membrane integrity (cF+PI) after heat, PAA, and ozone treatment. The field stop was set to 1-8° and the discriminator was SS=2

Detector	Voltage [V]	Gain	Compensation				
			FL1	FL2	FL3	FL4	FL5
FS	600	10					
SS	800	10					
FL1	532	1	-	0	30	0	0
FL2	364	1	1.9	-	4.8	0	0
FL3	630	1	30.3	0	-	0	0
FL4	363	1	1.4	0	6.4	-	0
FL5	481	1	1.5	0	8.7	0	-

Table 3.8: Flow cytometer settings for measurements of membrane integrity (TO+PI) after heat, PAA, and ozone treatment. The field stop was set to 1-8° and the discriminator was SS=2

Detector	Voltage [V]	Gain	Compensation				
			FL1	FL2	FL3	FL4	FL5
FS	600	10					
SS	800	10					
FL1	714	1	-	0	30	0	0
FL2	337	1	0	-	4.8	0	0
FL3	630	1	25.5	0	-	0	0
FL4	450	1	0	0	6.4	-	0
FL5	577	1	0	0	8.7	0	-

Table 3.9: Flow cytometer settings for measurements of membrane potential ($DIOC_2(3)$) after heat, PAA, and ozone treatment. The field stop was set to 1-8° and the discriminator was SS=2

Detector	Voltage [V]	Gain	Compensation				
			FL1	FL2	FL3	FL4	FL5
FS	600	10					
SS	800	10					
FL1	350	1	-	0	0	0	0
FL2	316	1	0	-	0	0	0
FL3	550	1	0	0	-	3.6	0
FL4	420	1	0	0	51.5	-	0
FL5	325	1	0	0	0	0	-

3.3.2 Development of a cFDA- staining procedure for Gram-negative bacteria

P. carotovorum was chosen as test organism to develop an appropriate staining protocol for the measurement of esterase activity of Gram-negative bacteria. *P. carotovorum* was stored as a glass bead culture at -80 °C for long-term maintenance or on nutrient agar tubes at 4 °C for short-time maintenance.

One-stage cultivation

For the reactivation of bacteria stored on nutrient agar 100 ml nutrient broth was inoculated with bacteria from one agar tube and incubated at 30 °C for 24 h (mid-stationary growth phase) without shaking. One-stage cultivation was only applied for the first experiments with reagents to alternate the cell membrane. For all further experiments two-stage-cultivation was applied.

Two-stage-cultivation

The two-stage cultivation of *P. carotovorum* was performed as described in section 3.1 (see also Figure 3.1).

To investigate the adaptability of the developed staining method to other Gram-negative bacteria, *E. coli* was chosen as additional target organism.

3.3.2.1 Photometric determination of cell densities

The optimal cell density was determined for staining procedures. Therefore, the optical density (OD) was measured at 620 nm in the range of 0.01 and 1 in a spectral photometer Unicam UV1-100 (Nicolet Instruments GmbH, Germany) to calculate the required amount of

PBS for suspension of the pellet. Optical densities of 0.1, 0.5, 1.0, 2.5, 5.0, 7.5, and 10 were adjusted and tested for staining.

3.3.2.2 Alteration of cell membrane permeability

To improve the permeability of the cell membrane of Gram-negative cells to cFDA, EDTA respectively TRIS/EDTA-buffer (TE-buffer) and glutardialdehyde (GTA) in varying concentrations were used in several studies (Diaper & Edwards, 1994; Hoefel *et al.*, 2003; Morono *et al.*, 2004; Ananta *et al.*, 2005; Miyanaga *et al.*, 2007). According to these studies, TE-buffer and GTA-buffer were tested for their ability to improve cFDA uptake of *P. carotovorum* cells. The applied concentrations and incubation times are given in table 3.10. GTA-buffer or TE-buffer were prepared and, after harvesting the selected bacteria, were suspended in these buffer dilutions with an OD_{620} of 0.1 or 5.0.

Table 3.10: Staining parameters of *P. carotovorum*

Growth condition	Optical density at 620 nm	Dye concentration [mM]	Staining time [min]	Reagents to improve cell membrane permeability	
				GTA-buffer [mM]	TE-buffer [mM]
One-stage cultivation (24 h, 30 °C, 0 rpm)	0.1; 5	0.05	30; 60	94; 71; 47; 24	TRIS: 10 EDTA: 0.5
	5	0.05	10	n.a.	n.a.
Two-stage cultivation (24 h, 30 °C, 125 rpm)	0.1	0.05	15; 30; 45; 60	94; 71; 47; 24	n.a.
	0.5; 1; 2.5; 5; 7.5; 10	0.05; 0.83	15; 30; 45; 60	n.a.	n.a.

n.a., not analysed

3.3.2.3 cFDA staining

5(6)-carboxyfluorescein diacetate mixed isomers (cFDA) was provided by Sigma-Aldrich, Germany. cFDA was resolved in 50 mM PBS (pH 7.0) to obtain stock solutions with concentrations of 0.1 mM and 5 mM. Final concentrations for cFDA staining were 0.05 mM either in TE-buffer, GTA-buffer, or PBS and 0.83 mM in PBS (1 ml in each case). The incubation times were set to 15, 30, 45, and 60 min at a temperature of 37 °C. The temperature was chosen according to the optimum temperature of enzymes and was therefore not changed during experiments. After incubation the reaction mixture was centrifuged at 4000 x *g* for 6 min at 4 °C to remove surplus cFDA. The cell pellet was resuspended in 50 mM PBS to a cell concentration of approximately 10^6 cells ml^{-1}.

3.3.3 Esterase activity of Gram-positive bacteria

The bacteria suspension was centrifuged (4000 x *g* for 6 min at 4 °C (plasma treatment, 1 ml in each case) or 12000 x *g* for 10 min at 4 °C (heat and ozone treatment, 10 ml in each case) after inactivation treatments. The centrifugation parameters were changed to 12000 x *g* and 10 min to improve the recovery rate of *L. innocua* within the sample. The pelleted material was resuspended in PBS (50 mM, pH 7) to obtain a calculated OD_{620} of approximately 10 for staining procedure. 50 µM cFDA was added to the bacterial suspension in the sample tubes and allowed to penetrate into the cells for 15 min in a water bath set to 37 °C. Afterwards, surplus cFDA was removed by centrifugation for 6 min at 4000 x *g* and 4 °C (heat and ozone treatment) or 12000 x *g* for 10 min at 4 °C (plasma treatment). The pelleted material was re-suspended in PBS and diluted in PBS to obtain a cell concentration of approximately 10^6 cells ml^{-1}.

3.3.4 cF-efflux

The cF-efflux as an additional viability marker of bacteria was measured upon energising of cF-labelled cells (1 ml in each case). Therefore, 20 mM D-glucose was added to the cF-labelled bacteria and the sample was incubated in a water bath at 37 °C for 60 min before flow cytometric measurements. The loss of cF-fluorescence intensity is related to pump activity.

3.3.5 Membrane integrity

To investigate membrane integrity of bacteria cells 30 µM propidium iodide was added to cFDA treated cells and allowed to penetrate into permeablised cells for 10 min at 4 °C in the dark before flow cytometric measurements.

Thiazole orange (TO) and Propidium iodide (PI) were used to distinguish between RNA and DNA in bacteria cells as well as to indicate compromised cell membranes and DNA damage. Therefore, 0.42 µM TO and 30 µM PI were added to a bacteria suspension containing ~10^6 cells ml^{-1} and incubated for 10 min at room temperature in the dark before flow cytometric measurements. Due to the fact that the TO-RNA-complex shows lower fluorescence intensities than the TO-DNA-complex the mean value of TO-fluorescence intensity was used to distinguish between RNA and DNA staining.

3.3.6 Membrane Potential

3,3'-diethyloxacarbocyanine iodide ($DiOC_2(3)$) was applied to measure the membrane potential of bacteria cells. The staining procedure used was modified after Novo *et al.* (1999). $DiOC_2(3)$ was provided by Sigma-Aldrich, Germany. For staining with $DiOC_2(3)$ the bacteria suspension was diluted in PBS containing 20 mM D-glucose to achieve a cell concentration of ~10^6 cells ml^{-1}. 30 µM $DiOC_2(3)$ was added and incubated for 15 min in the dark at room temperature. Afterwards the suspension was centrifuged at 4000 x *g* and 4 °C for 6 min (Gram-negative bacteria) or 12000 x *g* for 10 min at 4 °C (Gram-positive bacteria). The pelleted material was resuspended in PBS to a cell density of ~10^6 cells per ml and immediately measured in the flow cytometer.

Cells were completely depolarised with carbonyl cyanide m-chlorophenylhydrazone (CCCP) to set the parameters of the flow cytometer. Therefore, 15 µM CCCP was added to prepared bacteria solution and allowed to depolarize the bacteria for 15 min. Afterwards, 30 µM $DiOC_2(3)$ was added and the depolarised bacteria were stained as described above and measured in the flow cytometer. The settings of the FL1 (green $DiOC_2(3)$-fluorescence intensity) and FL3 (red $DiOC_2(3)$-fluorescence intensity) photomultiplier were chosen so that the mean fluorescence of green and red $DiOC_2(3)$ was detected in the same channel. The ratio of mean red to mean green $DiOC_2(3)$- fluorescence channel value was calculated to investigate changes in the membrane potential. Due to the chosen cytometer settings the red/green $DiOC_2(3)$-fluorescence ratio of depolarized cells was ≤ 1. It was assumed that the red/green ratio of untreated cells represent the membrane potential of intact cells. A reduction of the red/green ratio stands for the loss of cell membrane potential.

3.4 Total cell count and viable cell count

The total cell count of the bacterial suspensions after treatment was determined using the Multisizer™ 3 Coulter Counter® (Beckman Coulter, Germany) with a 30 µM aperture in triplicate. Additionally, the cell volume of each measured cell was recorded. Therefore the bacteria suspension was diluted with the electrolyte solution IsoFlow Sheath Fluid (Beckman Coulter, Germany) to obtain a measurement concentration between 1 and 10 %. The measurement volume was 50 µl and the cell size and cell number was recorded between 0.426 and 18 µm (corresponding volume: 0.0405 and 3054 $µm^3$). The region of interest for analyses of cell volume and cell number was between 0.103 $µm^3$ and 9.937 $µm^3$. The electrolyte solution was measured without bacteria suspension and the obtained particle number and size distribution was set as background level to minimize the noise level. The measurement settings of the apparatus are given in table 3.11.

Table 3.11: Measurement settings of the Multisizer™ 3 Coulter Counter®

	Settings
Aperture current	-400 µA
Gain	4
Sizing threshold	0.506 µm^3
Minimal pulse width	4.0 µs
Maximum pulse width	5000 µs
Noise level	0.506 µm^3 (3.1 % of aperture diameter)
Waste tank vacuum	6 "Hg
Waste tank vacuum tolerance	±0.2 "Hg
Metering pump vacuum	6 "Hg
Metering pump minimum flow	2.6 µl/s
Metering pump maximum flow	4.67 µl/s

The viable cell count of bacteria after inactivation treatments was determined by traditional culture methods in duplicate. Therefore, the samples were serially diluted in Rotilabo®-microtest plates (96er U-profile, Roth, Germany) using 0.05 M PBS (pH 7) as dilution solution. 100 µl of each dilution was spread on the cultivation medium. The number of colony forming units (CFU ml^{-1}) was obtained after growth for 48 h (*L. innocua, P. carotovorum*) or 24 h (*E. coli*) at the optimal cultivation temperature to determine the viable cell count. The optimal cultivation temperature and the cultivation medium for the plate count analyses are summarized in table 3.12. The detection limit of plate count analyses was 10 CFU ml^{-1} for thermal, peracetic acid, and ozone treatment and 100 CFU cm^{-2} for plasma treatment analysis. If no growth occurred on the agar plates at least one colony forming unit was assumed to be present in the samples. This assumption was confirmed by plating 1 ml of undiluted sample on nutrient agar whereas at the highest one CFU cm-^{2} or one CFU ml^{-1} was detected. The bacteria counts are presented as averages with standard deviation of six values (three independent experiments analysed in duplicate).

Table 3.12: Optimal cultivation temperature and growth medium for plate count analyses of selected bacteria

	Growth medium[a] plate count	Optimal cultivation temperature [°C]
L. innocua	ST-I	37
E. coli	ST-I	37
P. carotovorum	MAC	30

[a] ST-I, Standard-I agar (Roth, Germany);
MAC, MacConkey agar (Roth, Germany)

3.5 Inactivation treatments

3.5.1 Thermal treatment

Cell suspensions containing approximately 10^7 CFU ml^{-1} (*L. innocua, E. coli* or *P. carotovorum*) were treated for 0, 1, 3, 5, and 10 min at 50 and 90°C in a water bath. The treatment volume was 10 ml whereas 0.2 ml bacteria suspension (containing ~10^9 cell ml^{-1}) was added to 9.8 ml temperate PBS. The influence of cell concentration on inactivation effects was investigated at 70 °C with cell concentrations of 10^7, 10^5, and 10^3 cells ml^{-1}. Immediately after the defined treatment period the samples were cooled to room temperature in an ice bath and analyses were performed. Each treatment was performed in triplicate. The temperature of the samples was recorded during treatment using thermocouples Typ T. The schema of thermal treatment is given in figure 3.3.

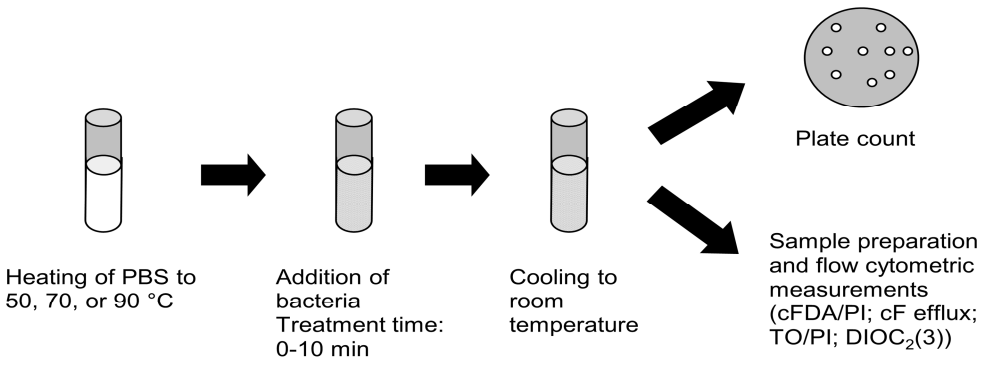

Figure 3.3: Procedure of thermal treatment and subsequent analyses.

3.5.2 Inactivation with peracetic acid

The inactivation efficiency of peracetic acid was tested against *E: coli* at various concentrations, temperatures, and treatment times. Wofasteril® E400 (Kesla, Germany) was used as peracetic acid solution (PAA). Immediately before the treatments the tested concentrations of PAA (0.25 and 0.5 %) were prepared using potable water and the treatment temperatures of 0, 10, and 20 °C were either adjusted in ice bath or water bath. The treatment volume was 10 ml whereas 0.2 ml *E. coli* solution was added to 9.8 ml temperate PAA solution. The initial count of *E. coli* in the solution was set to approximately 10^7 cfu ml^{-1}. The treatment times were 0.25, 0.5, 0.75, 1, 1.5, and 2 min. To stop the reaction after the defined treatment times the solution was added to 30 ml 50 mM PBS containing 0.6 M sodium thiosulfate ($Na_2S_2O_3$) and mixed for 10 s. As a control 0.2 ml *E. coli* solution

was added to 9.8 ml temperate potable water. Each treatment was performed in triplicate. After treatment the samples were centrifuged at 3220 x *g* for 15 min at 4 °C and afterwards the pelleted material was resuspended in 10 ml 50 mM PBS for analyses of inactivation effects. It was also tested, whether $Na_2S_2O_3$ also lead to an inactivation of *E. coli*. For that, 10 ml *E. coli* solution was added to 30 ml PBS buffer containing 0.6 M $Na_2S_2O_3$. With 0.2 log cycles inactivation a minor effect of $Na_2S_2O_3$ on *E. coli* was detected by plate count method. These results were also confirmed by flow cytometry. The temperature of the samples was recorded during treatment using thermocouples Typ T. The scheme of the peracetic acid treatment is given in figure 3.4.

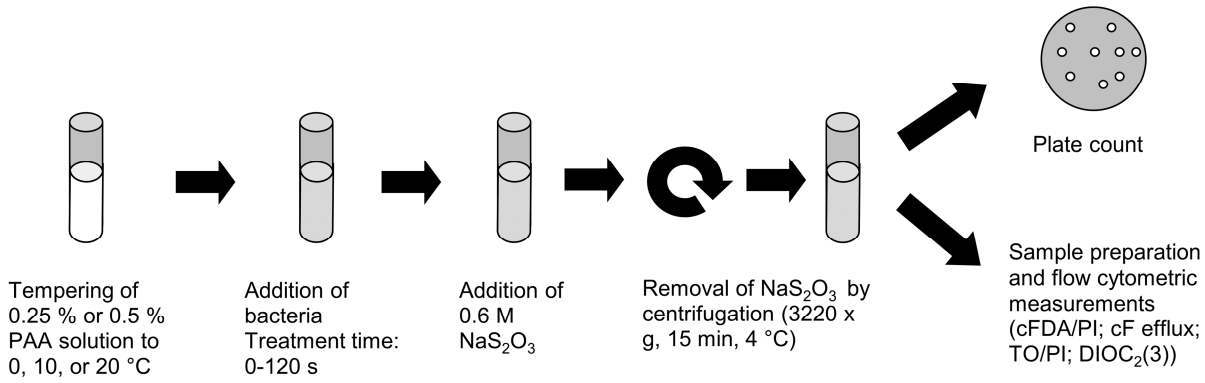

Figure 3.4: Procedure of PAA treatment and analyses.

3.5.3 Treatment with ozonated water

3.5.3.1 Ozone generator

A Bewazon 1 (BWT Wassertechnik GmbH, Germany) ozone generator was used to generate ozonated water (Figure 3.5). Ambient air is injected into the generator and dried to 1 % relative humidity. Subsequently, ozone is generated from the dried air between two electrodes via dielectric discharges. The generated ozone is injected into potable water by the use of low pressure. The ozone generates 1 g h^{-1} ozone and the water flow rate is between 1.5 and 2 m^3 h^{-1}.

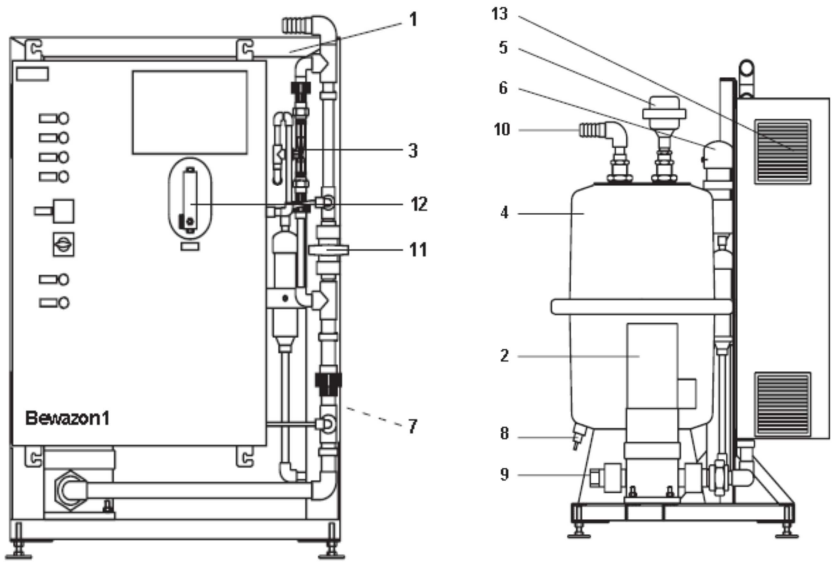

1. Rack; 2. Booster pump; 3. Injector; 4. Tank; 5. Vent valve; 6. Annihilation of residual ozone; 7. Water reservoir; 8. Drain valve; 9. Water entrance; 10. Water outlet; 11. Bypass valve; 12. Gas flow meter; 13. Air filter

Figure 3.5: Experimental set-up of the ozone generator Bewazon 1.

3.5.3.2 Determination of ozone concentration

The ozone concentration in mg l^{-1} was measured in the spectrophotometer DR2800 (Hach Lange, Germany) using the LCK310 Chlorine/Ozone cuvette test (Hach Lange, Germany) with a measuring range of 0.05-2.0 mg l^{-1} ozone. Three drops of potassium iodide solution (Hach Lange, Germany) was added to the cuvettes immediately before the ozonated water was added. The cuvette was closed and inverted a few times. After 2 min the ozone concentration was measured at 510 nm.

3.5.3.3 Procedure of ozone treatment

Ozonated water was generated with ozone concentrations of 0.7 mg l^{-1}, 1.7 ± 0.1 mg l^{-1}, 2.8 ± 0.1 mg l^{-1}, 3.8 ± 0.4 mg l^{-1}. 9.8 ml ozonated water was transferred into sample tubes and 0.2 ml bacteria suspension (cell concentration: ~10^9 CFU ml^{-1}) was added to achieve an initial cell concentration of ~10^7 CFU ml^{-1}. The treatment time was set to 0.17, 0.5, 1, 1.5 and 2 min. To stop the reaction the sample tubes were intensively shaken for approximately 30 s. As a control 0.2 ml bacteria solution was added to 9.8 ml potable water. The influence of cell concentration on inactivation effects was investigated at 2.8 ± 0.1 mg l^{-1} with cell concentrations of 10^7, 10^5, and 10^3 cells ml^{-1}. Each treatment was performed in triplicate.

To prove an inappropriate removal of residual ozone and to avoid false positive inactivation of bacteria $Na_2S_2O_3$ was used to stop the reaction. Exemplary, the bacteria were treated with ozonated water (3.8 mg l^{-1} O_3) as described above and the reaction was stopped with $Na_2S_2O_3$. After the defined treatment time 44.1 mM $Na_2S_2O_3$ was added to the sample tubes and the tubes were shaken for 2-3 s to allow a homogenous distribution of $Na_2S_2O_3$ within the sample. An inactivation effect of $Na_2S_2O_3$ was excluded in preliminary experiments. After treatment the samples were centrifuged at 3220 x *g* for 15 min at 4 °C and afterwards the pelleted material was resuspended in 0.05 M PBS for analyses of inactivation effects. The treatment procedure is given in figure 3.6.

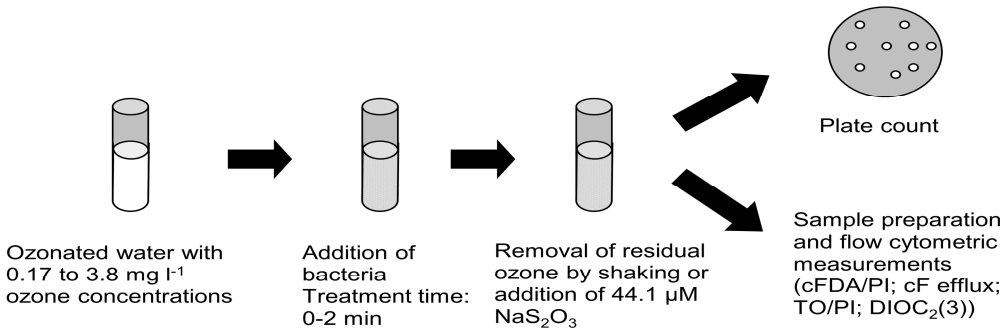

Figure 3.6: Scheme of ozone treatment and analyses.

3.5.4 Atmospheric pressure plasma treatment

3.5.4.1 Sample preparation before plasma treatment

Bacteria were harvested by centrifugation at 3220 x *g* for 15 min at 4 °C. The pelleted material was resuspended to an OD_{620} of 10 in 0.05 M phosphate buffered saline (PBS, pH 7.0), and stored at 4 °C for 3 h before plasma treatment. Gelrite® (Roth, Germany) was chosen as model system. Gelrite® is a polysaccharide gel that is used as an agar substitute. The polysaccharide gel is stable at high temperatures, and prevents migration of organisms within the gel. Nevertheless, the gel structure effectively supports growth of microorganisms. The gel was prepared with 1 % calcium chloride in petri dishes and stored at room temperature before use. Plates (A = 1 cm², thickness 3 - 4 mm) were cut out and each platelet was inoculated with 25 µl bacteria suspension, and dried at room temperature under aseptic conditions for 30 minutes in petri dishes. The initial bacterial concentration of each gel plates was ~10^8 CFU cm^{-2}.

3.5.4.2 Plasma source and plasma treatment

The plasma was generated in argon gas at atmospheric pressure and was driven by a radio frequency of 27.12 MHz. The plasma jet consists of a ceramic nozzle with a needle electrode inside, a grounded ring electrode at the nozzle outlet, an rf- generator, and a gas supply system (Figure 3.7). Argon flows through the nozzle with a gas flow of 20 standard litre min^{-1} (slm). The rf-voltage is coupled with the needle electrode. The plasma is generated at the tip of this electrode and expands into the air outside the nozzle. Depending on the gas flow rate and the applied power the plasma has a length of up to 30 mm and a diameter of about 8 mm.

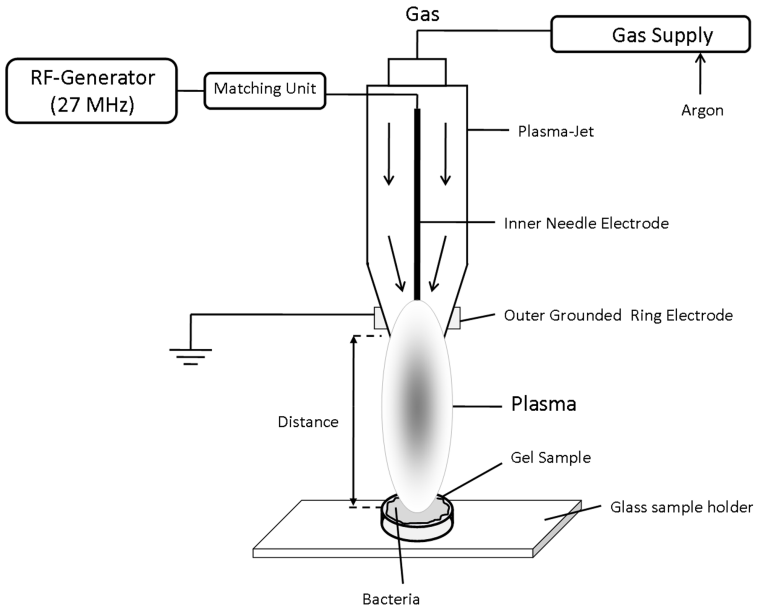

Figure 3.7: Experimental set-up of the used atmospheric pressure plasma jet.

For plasma treatment the gel samples were placed in the centre of a glass sample holder. The operating power of the plasma jet was set to 10, 20, and 40 W. The distance between the nozzle and the sample was 10 mm so that the plasma covered the inoculated region completely. Treatment times ranged between 0.25 and 5 min. The temperature of the samples during plasma treatment was recorded using a thermography camera (SC500, Flir Systems GmbH, Germany). The distribution of reactive species was previously determined for a similar APPJ using Optical Emission Spectroscopy (Brandenburg *et al.*, 2007).

Inoculated control gel samples were handled as described but without plasma treatment. Each treatment was performed in triplicate.

3.5.4.3 Sample analysis procedure

Treated and untreated gel samples were transferred into sample tubes, and stored over night at 4 °C before analysis. Effects of overnight storage on the obtained results were excluded in preliminary tests. To re-suspend the bacteria five sterile glass spheres and 1 ml sterile PBS (50 mM, pH 7) were added to each sample tube and agitated for 5 min at 750 rpm and 37 °C. The obtained bacteria suspension was transferred to sample tubes (1.5 ml) for plate count analysis and flow cytometric sample preparation.

Figure 3.8 shows the complete experimental procedure.

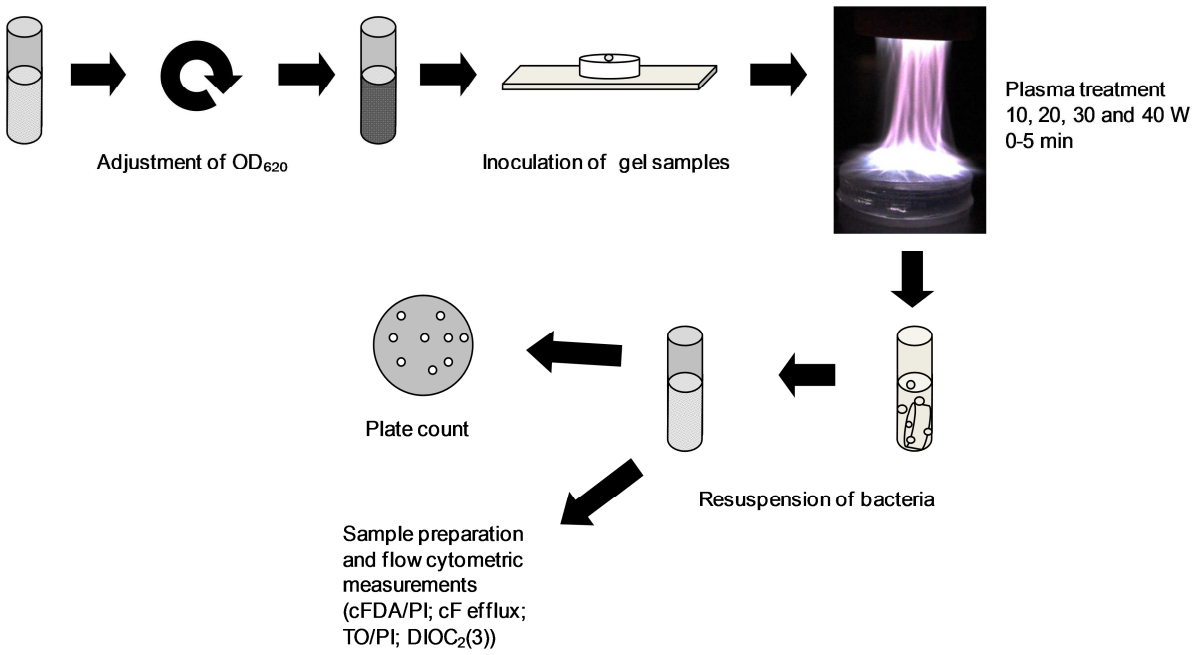

Figure 3.8: Flow chart of plasma treatment and analyses.

3.6 Mathematical modelling

3.6.1 Modelling of growth curves

The growth curves were fitted with DMFit v2.0 software (Baranyi and Le Marc, United Kingdom) based on the model of (Baranyi & Roberts, 1994). From these derived data the doubling time t_d,

$$t_d = \frac{ln2}{\mu_{max}} \qquad \text{(eq. 3.1)}$$

with the growth rate μ_{max} obtained from the Baranyi model, the rate of cell division v,

$$v = \frac{1}{t_d} \quad \text{(eq. 3.2)}$$

And the number of cell divisions n

$$n = \frac{N - N_0}{log2} \quad \text{(eq. 3.3)}$$

with N the number of colony forming units after treatment and N_0 the initial number of colony forming units was calculated.

3.6.2 Modelling of inactivation kinetics

To obtain an inactivation kinetic for each treatment parameter, the average of six values of colony forming units were calculated. The inactivation kinetics obtained were modelled with GInaFiT (Geeraerd and Van Impe Inactivation Model Fitting Tool), a freeware Add-inn for Microsoft® Excel. This tool enables the testing of nine different types of microbial survival models and five statistical measures support the choice of the best fit. The models used were described as follows (Geeraerd *et al.*, 2005):

Log-linear regression:

$$logN = logN_0 - \frac{k_{max} t}{ln10} \quad \text{(eq. 3.4)}$$

Where N represents the number of colony forming units after treatment, N_0 the initial number of colony forming units and k_{max} is the first order inactivation constant.

Log-linear regression with shoulder and tail:

$$logN = log\left[\left(10^{logN_0} - 10^{logN_{res}}\right) \times e^{-k_{max}t} \times \left(\frac{e^{k_{max}S_l}}{1+(e^{k_{max}S_l}-1)\times e^{k_{max}t}}\right) + 10^{N_{res}}\right] \quad \text{(eq. 3.5)}$$

Where N_{res} is the residual population density, k_{max} is the specific inactivation rate and S_l represents the shoulder length. Reduced models (models with tail or shoulder) can be derived by setting N_{res} and S_l equal to zero.

Weibull model:

$$logN = logN_0 - \left(\frac{t}{\delta}\right)^p \quad \text{(eq. 3.6)}$$

Where δ is the scale parameter and p is the shape parameter. In the case of p=0 the scale parameter can be denoted as the time for the first decimal reduction. Convex curves are obtained if p>1 and concave curves are obtained if p<1.

If the concave, convex, or linear curve is followed by a tailing effect, the curve can be described by the following equation:

$$logN = log\left[\left(10^{logN_0} - 10^{logN_{res}}\right) \times 10^{-\left(\frac{t}{\delta}\right)^p} + 10^{logN_{res}}\right] \quad \text{(eq. 3.7)}$$

Biphasic models:

$$logN = logN_0 + log\left(f \times e^{-k_{max1}t} + (1-f) \times e^{-k_{max2}t}\right) \quad \text{(eq. 3.8)}$$

Where k_{max1} and k_{max2} are the specific inactivation rates of two populations, *f* is the fraction of the initial population in a major population and (1-*f*) is the fraction of the initial population in a minor population. A shoulder formation followed by a biphasic pattern can be described as follows:

$$logN = logN_0 + \log\left(\left(f \times e^{-k_{max1}t} + (1-f) \times e^{-k_{max2}t}\right) \times \frac{e^{k_{max1}S_l}}{1+(e^{k_{max1}S_l}-1)\times e^{-k_{max1}t}}\right) \quad \text{(eq. 3.9)}$$

According to Ratkowsky (2004) the root mean square error (RMSE) value was chosen as indicator for the goodness-of-fit of the tested models.

3.6.3 Modelling of flow cytometric data

The GInaFiT tool was also applied to the obtained flow cytometric data. For this purpose, the logarithm of the obtained percentages of PI-stained, TO-stained and cF-stained was calculated and used for modelling. All models described in section 3.6.2 were tested for best fit taking into account the RMSE value. Additionally, different growth models were used to model increasing curves. These data were fitted with Origin® 7.5 software (OriginPro 7.5 SR6 v7:5885(B885), OriginLab Corporation, USA). The models used were described as follows:

Linear growth:

$$logN = A + kt \quad \text{(eq. 3.10)}$$

Where A is the maximum asymptote value and k is the maximum growth rate.

Sigmoidal growth curves:

Non-linear increase of flow cytometric data were either modelled with the Gompertz model (equation 3.11) or a logistic model (equation 3.12).

$$logN = A \times e^{e^{(-k(t-\lambda))}} \quad \text{(eq. 3.11)}$$

$$logN = \frac{A_1 - A_2}{1 + (\frac{t}{\lambda})^k} + A_2 \quad \text{(eq. 3.12)}$$

Where A_1 is the minimum asymptote value and A_2 is the maximum asymptote value, *k* represents the maximum growth rate and λ is the lag time.

3.7 Data illustration

The correlation of data obtained from density plots of CXP analysis software and the distribution of fluorescence presented in the following results is given in figure 3.9. The density plot is gated into four regions. The regions represent cells with different physiological properties. The average of the percentage values obtained from three density plots was calculated and illustrated as kinetics in diagrams where the x-coordinate displays the treatment time and the y-coordinate the percentage of stained cells. The standard deviation of all experiments is given in the annex. Statistical analyses to evaluate significant difference between the data were performed using Origin® 7.5 software. One-Way-ANOVA with Tukey test and a significance level of 0.05 were used.

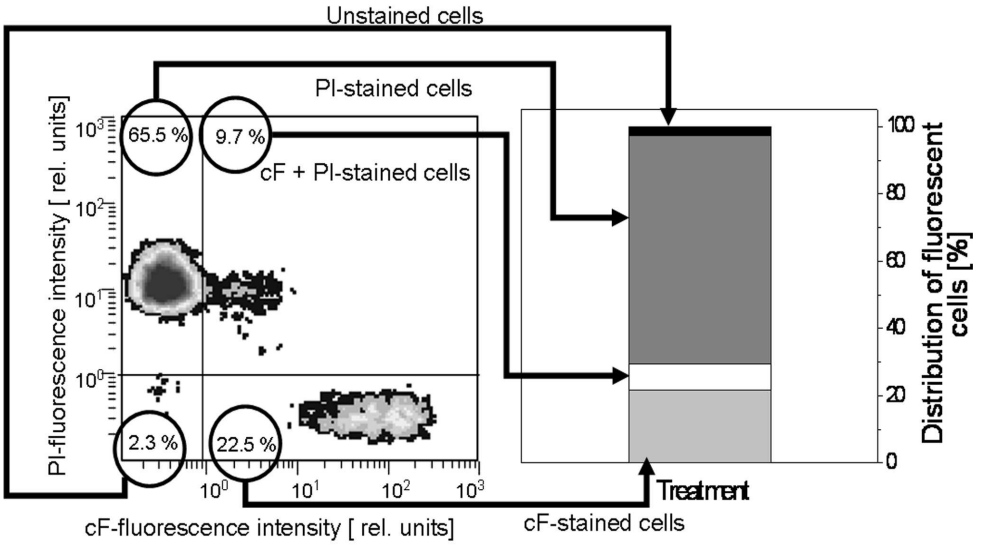

Figure 3.9: Illustration of cF- and PI-fluorescence in a density plot and the transcription of fluorescence distribution into bar charts. Black bars representing unstained cells; dark grey bars indicating permeabilised cells; white bars representing slightly permeabilised cells with esterase activity and light grey bars indicating intact cells with esterase activity.

4. Results and Discussion

4.1 Growth curves

Growth conditions greatly influence the growth of bacteria. Therefore, the growth of each test bacterium was monitored to determine the growth phase of bacteria at the harvest point. The viable and total cell counts obtained over a time period of up to 63 hours are given in figure 4.1.

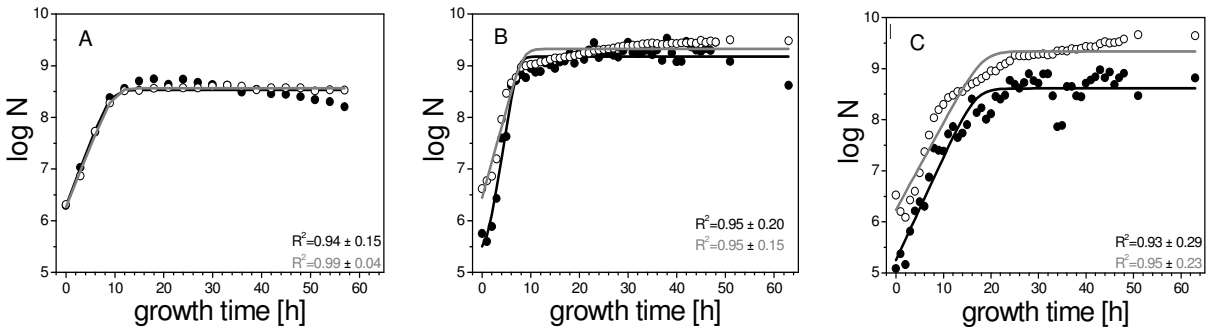

Figure 4.1: Growth curves of test bacteria in nutrient broth and with shaking at 125 rpm. Total count (open circles) and viable cell count (circles) of *Listeria innocua* DMS 20649 (A) at 37 °C, *E. coli* DSM 1116 (B) at 37 °C, and *Pectobacterium carotovorum* sp. *carotovorum* DSM 30168 (C) at 30 °C fitted with DMFit (black line: viable count fit; grey line: total count fit). The goodness of fit expressed as R^2 is given in the figure.

The stationary phase of *E. coli* was reached after 10 h (Figure 4.1 B); 18 h were needed to achieve the stationary phase of *P. carotovorum* (Figure 4.1 C) and 12 h for *L. innocua* (Figure 4.1 A). The growth of the test organisms could be modelled by the DMFit software based on the model of (Baranyi & Roberts, 1994) with an $R^2 > 0.93$ for all curves. A good correlation was found between viable cell count measured by plate count methods and total cell count measured by Coulter Counter. The best correlation with an R^2 of 0.96 was achieved for *E. coli* followed by *P. carotovorum* and *L. innocua* with an R^2 of 0.94. Discrepancies between viable and total count of all bacteria can be explained by the measurement of viable as well as non-viable cells by Coulter Counter (Smither, 1975) while by plate count methods only viable cells were detected.

Table 4.1: Growth parameters of test organisms derived from the Baranyi model using DMFit software

	E. coli		*P. carotovorum*		*L. innocua*	
	Plate count	**Coulter Counter**	**Plate count**	**Coulter Counter**	**Plate count**	**Coulter Counter**
N_0 [log CFU ml^{-1}]	5.50	6.45	5.25	6.23	6.29	6.27
N [log number ml^{-1}]	9.18	9.33	8.61	9.34	8.53	8.56
μ_{max} [h^{-1}]	1.30	0.79	0.46	0.39	0.56	0.54
t_d [h]	0.53	0.88	1.49	1.76	1.23	1.29
v [h^{-1}]	1.88	1.14	0.67	0.57	0.81	0.78
n	12.21	9.57	11.16	10.31	7.44	7.63

The maximum growth rate μ_m of *L. innocua* was 0.56 h^{-1}. The highest maximum growth rate was observed for *E. coli* and the lowest maximum growth rate was observed for *P. carotovorum*. Equally, the doubling time t_d and the rate of cell division v indicate that growth of *E. coli* is the fastest, followed by the growth *L. innocua*. *P. carotovorum* growth was the slowest. In contrast, the number of cell divisions was higher for *P. carotovorum* than for *L. innocua* (Table 4.1). The mean cell volume of bacteria ranges between 0.6 μm^3 and 1.7 μm^3 and changes during growth (Figure 4.2).

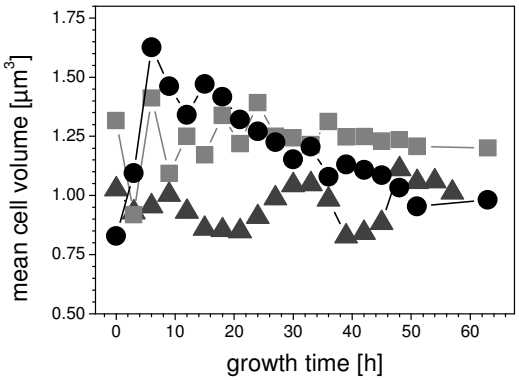

Figure 4.2: Mean cell volume of *L. innocua* DSM 20649 (triangles), *E. coli* DSM 1116 (squares), and *P. carotovorum sp. carotovorum* DSM 30168 (circles) during growth.

During the first growth hours cell volume increased. This can be explained by the cell division and the measurement of cells during division. The cell volume of *P. carotovorum* showed the greatest increase whereas the *L. innocua* showed the smallest increase. The cell volume of *E. coli* and *P. carotovorum* was 1.34 μm^3 and 1.42 μm^3, respectively and after 18 h growth time the cell volume of *L. innocua* was 0 0.85 μm^3. An increase of *E. coli* cell volume during exponential growth was also observed by Smither (1975).

Membrane integrity of the bacteria changed during growth and is different for the selected bacteria species (Figure 4.3). During exponential growth of bacteria the percentage of TO-stained cells increased for all tested bacteria indicating intact cells and remained almost constant during stationary phase. The percentage of TO-stained of *L. innocua* cells decreased after growth of >40 h indication the end of stationary growth phase. A permeabilisation of bacteria cells did not occur during growth because PI-fluorescence could not be detected.

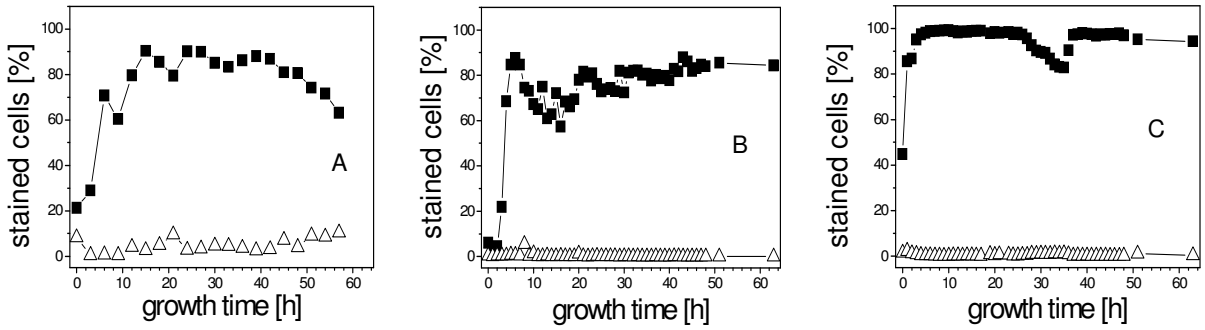

Figure 4.3: Membrane integrity of test organisms during growth indicated by TO (squares) and PI (open triangles)-stained bacteria. A) *L. innocua* cells; B) *E. coli* cells; C) *P. carotovorum* cells.

According to the growth curves, all test bacteria were in the stationary phase at the point of harvest.

4.2 Treatment related inactivation kinetics and modelling

4.2.1 Heat treatment

The impact of heat treatment on the selected test bacteria was evaluated since thermal treatment is commonly applied in food industry. The results obtained should allow a comparison with the effects of alternative treatment methods. The efficiency of heat treatment at different temperature levels was tested for *E. coli*, *L. innocua*, and *P. carotovorum* at initial counts of 5.5 ± 0.1*10^7 CFU ml^{-1}, 6.1 ± 0.7 *10^7 CFU ml^{-1} and 1.7 ± 0.3*10^7 CFU ml^{-1}, respectively.

At 50 °C the number of colony forming units remained constant for *E. coli* and *L. innocua* within 10 min treatment time whereas the number of colony forming units of *P. carotovorum* was reduced by 3 log units after one min treatment (Figure 4.4). An additional reduction of 1 log unit was achieved within the next two treatment minutes. The reduction of *E. coli* was similar for both higher treatment temperatures at 70 °C and 90 °C. After one minute of

treatment a 3 log reduction was achieved. A 3 log reduction with tailing was also achieved for *L. innocua* after one minute at 70 °C. At 90 °C *L. innocua* was reduced below the detection limit after one minute of treatment. The higher sensitivity of *P. carotovorum* was also shown at 70 °C and 90 °C with a five log reduction at 70 °C after one treatment minute and a reduction below the detection limit was observed after one minute at 90 °C.

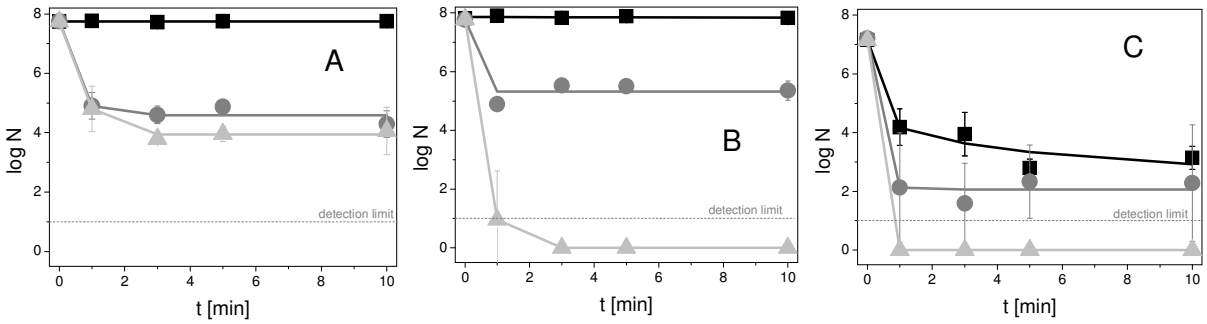

Figure 4.4: Inactivation kinetics of *E. coli* (A); *L. innocua* (B) and *P. carotovorum* (C) after heat treatment at 50 °C (squares), 70 °C (circles), and 90 °C (triangles). The lines represent the inactivation obtained from the applied models from the GInaFit tool.

All models available in GInaFiT tool were applied to the experimental data and the goodness-of-fit of the models was compared using the RMSE. The statistical measures and parameters of the best fitted model for thermal inactivation of the test bacteria are given in table 4.2.

The inactivation kinetics of *L. innocua* and *E. coli* at 50 °C can be described with the traditional log-linear model but the calculated inactivation rate was 0.01 min^{-1} and 0.00 min^{-1}, respectively. Thus, the inactivation at 50 °C is negligible. In contrast, the inactivation of *P. carotovorum* at 50 °C cannot be described with the log-linear model. The inactivation kinetic showed an upward concave shape and could be described with the Weibull model. The upward concavity shape of the curve implies that the treated bacteria population is heterogeneous and consists of two subpopulations with different heat sensitivity. The more heat sensitive population is inactivated at a high rate. The higher resistant population remained unaffected or minor effects occurred (Peleg, 2000). At 70 °C all tested bacteria showed tailing after a log-linear inactivation. The same phenomenon was observed at 90 °C for *E. coli* cells. At the same temperature *L. innocua* and *P. carotovorum* were inactivated below the detection limit after 1 min treatment time. The log-linear model with tailing was the best fitted model for both kinetics but the residual population was zero. As a consequence, no real tailing occurred at 90 °C for *L. innocua* and *P. carotovorum*.

Table 4.2: Statistical measures and parameter values obtained from GInaFit Version 1.5 for experimental data of thermal inactivated *E. coli*, *L. innocua*, and *P. carotovorum*

Treatment	Model type	RMSE	Log N_0 [CFU ml^{-1}]	K_{max} [1 min^{-1}]	Log N_{res} [CFU ml^{-1}]	δ [min]	P [-]
E. coli							
50 °C	Log-linear regression	0.02	7.74	0.00			
70 °C	Log-linear + tail	0.29	7.75	7.21	4.59		
90 °C	Log-linear + tail	0.13	7.74	6.91	3.94		
L. innocua							
50 °C	Log-linear regression	0.04	7.86	0.01			
70 °C	Log-linear + tail	0.36	7.76	25.44	5.32		
90 °C	Log-linear + tail	0.00	7.78	15.83	0.00		
P. carotovorum							
50 °C	Weibull	0.48	7.15			0.01	0.15
70 °C	Log-linear + tail	0.42	7.21	13.70	2.06		
90 °C	Log-linear + tail	0.00	7.15	24.84	0.00		

The inactivation within the first treatment minute seems to be linear but due to the limited data an appropriate application of the log-linear model is not possible. The different shapes of survivor curves after thermal treatment were already described by Moats (1971) and the tailing effect was explained by Cerf (1977). According to the mechanistic theory the subpopulation which is responsible for the tailing is very resistant to heat, inaccessible to the heat, adapted to the heat or genetically more resistant. Moreover, tailing can be the result of experimental artefacts such as heterogeneity of treatment, clumping or false enumeration of survivors. Although the inactivation curves showed similar shapes for all tested bacteria the heat sensitivity is different. *E. coli* showed the lowest inactivation rate at all tested temperatures. At 70 °C the inactivation rate is highest for *L. innocua* and at 90 °C the highest inactivation rate was observed for *P. carotovorum*. The different thermal tolerance of the microorganisms depends on the growth conditions and cell structure. *E. coli* (Gram-negative) was more heat resistant in comparison to *Lactobacillus planatarum* (Gram-positive) (Lee & Kaletunc, 2002). In this study, a higher heat resistance of the Gram-negative *E. coli* in comparison to the Gram-positive *L. innocua* was also observed. In contrast, the Gram-negative *P. carotovorum* is more sensitive than *L. innocua*. A possible explanation could be the growth phase of both bacteria. *L. innocua* and *E. coli* were treated after growth to the mid-stationary phase and *P. carotovorum* was treated after growth to the beginning of stationary growth phase. Bacteria from the stationary growth phase show a higher resistant against inactivation treatment than bacteria from the exponential growth phase (Benito *et al.*, 1999; Pagan & Mackey, 2000; Manas & Mackey, 2004).

Table 4.3: Total cell count after thermal treatment at different temperature levels

	50 °C Log cell count ml^{-1}	70 °C Log cell count ml^{-1}	90 °C Log cell count ml^{-1}
E. coli			
0 min	7.76^{a}	8.07^{a}	7.76^{a}
1 min	7.73^{a}	7.15^{a}	7.62^{b}
3 min	7.74^{a}	7.68^{a}	7.59^{b,c}
5 min	7.75^{a}	7.66^{a}	7.58^{b,c}
10 min	7.73^{a}	7.66^{a}	7.54^{c}
L. innocua			
0 min	7.91^{a}	7.83^{a}	7.80^{a}
1 min	7.91^{a}	7.79^{b}	7.69^{b,c}
3 min	7.91^{a}	7.76^{b,c}	7.69^{b,c}
5 min	7.90^{a}	7.76^{c,d}	7.70^{b}
10 min	7.85^{b}	7.73^{d}	7.64^{c}
P. carotovorum			
0 min	7.60^{a}	7.70^{a}	7.60^{a}
1 min	7.58^{a}	7.70^{a}	7.63^{a}
3 min	7.64^{a}	7.70^{a}	7.63^{a}
5 min	7.63^{a}	7.69^{a}	7.62^{a}
10 min	7.65^{a}	7.69^{a}	7.66^{a}

$^{a-d}$, Different letters within the columns indicate significant differences at a significance level of 0.05

The total count of *E. coli* before treatment at 50 °C, 70 °C, and 90 °C was not significantly different from the plate count at a significance level of 0.05. In contrast, the total count of *P. carotovorum* before thermal treatment was significant different from plate count. For *L. innocua* a significant difference between total count and plate count was observed for samples before thermal treatment at 50 °C and 90 °C whereas no significant difference was observed for total count and plate count before treatment at 70 °C. The observed total count was higher than the observed plate count for all bacteria and treatment parameters. This can be explained by the measurement method. With the Coulter Counter all bacteria within the samples are measured while only viable bacteria that are cultivable were detected by the plate count method (Smither, 1975). The total count of *P. carotovorum* remained constant during thermal treatment at all tested temperatures without significant changes within the temperatures. Similar results were obtained for *E. coli* but at 90 °C significant differences in cell count were detected during treatment. The total count decreased with increasing treatment time. Significant changes in total count were also observed for *L. innocua* after thermal treatment. At 50 °C the total count decreased after 10 min and at 70 °C and 90 °C the changes in terms of a significant decrease of total count already occurred after one minute of treatment (Table 4.3). The reduction of total count at higher temperatures may be explained by a total disruption of the cells due to the thermal treatment. A reliable determination of cell count was already observed by Swanton *et al.* (1962). The authors showed that electronic characteristics are different for different bacteria and also for

untreated and treated bacteria. This may be the explanation for the changes in total counts of *E. coli*, *L. innocua*, and *P. carotovroum.*

The influence of initial bacterial count on inactivation effects of heat treatment was tested as an example. The initial concentration of bacterial suspensions was set to 10^7, 10^5, and 10^3 CFU ml^{-1} and the suspensions were treated with 70 °C (Figure 4.5).

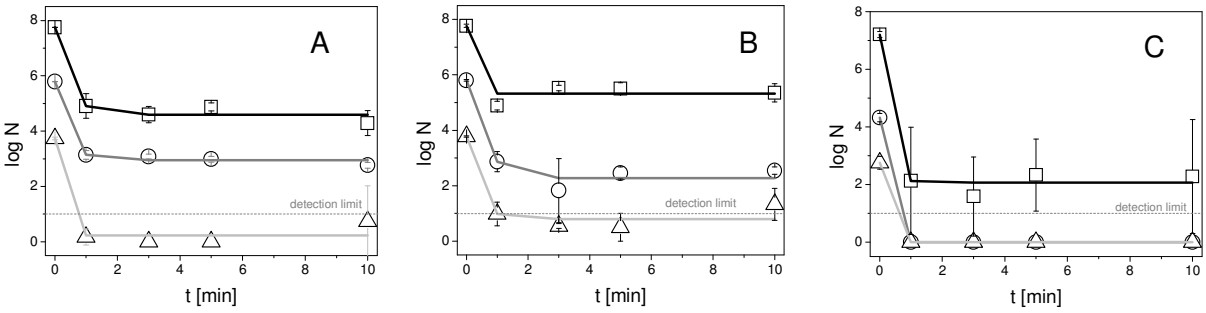

Figure 4.5: Inactivation kinetics of *E. coli* (A), *L. innocua* (B), and *P. carotovorum* (C) at 70 °C with different initial counts (open squares: 10^7 CFU ml^{-1}; open circles: 10^5 CFU ml^{-1}; open triangles: 10^3 CFU ml^{-1}). The lines represent the modelled inactivation obtained from the GInaFit Version 1.5.

At an initial concentration of 10^3 CFU ml^{-1} *E. coli* is reduced to the detection limit (3.57 log unit reduction) after 0.5 min heat treatment time (Figure 4.5). A 2.85 log unit reduction was achieved for an initial count of 10^7 CFU ml^{-1} and an initial concentration of 10^5 CFU ml^{-1} led to a 2.65 log unit reduction after the same treatment time. With decreasing initial count of *P. carotovorum* the degree of reduction was curtailed. The highest reduction of *L. innocua* after 0.17 min was observed at an initial concentration of 10^5 CFU ml^{-1} and the lowest reduction was found at an initial concentration of 10^3 CFU ml^{-1}. All models available in the GInaFiT tool were applied to the experimental data and the goodness-of-fit of the models was compared using the RMSE. The statistical measures and parameters of the best fitted model for inactivation by heat are given in table 4.4.

The shapes of survival curves of bacteria after heat inactivation at 70 °C were the same for all tested bacterial concentrations. The inactivation rate of *E. coli* at a cell concentration of 10^7 CFU ml^{-1} was higher than the inactivation rate at a cell concentration of 10^5 CFU ml^{-1} but lower than at a cell concentration of 10^3 CFU ml^{-1}. The same results were obtained for *L. innocua* but in contrast, the inactivation rate was higher at a cell concentration of 10^3 CFU ml^{-1} than at a cell concentration of 10^5 CFU ml^{-1}. For *P. carotovorum* with cell concentrations of 10^5 CFU ml^{-1} and 10^3 CFU ml^{-1} the inactivation rates were higher than at the cell concentration of 10^7 CFU ml^{-1}. The tailing at lower cell concentrations observed by the applied model cannot be assumed to be real tailing because the residual population is zero

and below the detection limit. This could lead to an overestimation of the inactivation rate. *L. innocua* seems to be more heat resistant than *E. coli* and *P. carotovorum* at lower cell concentrations. A higher reduction of pathogens was found after high pressure inactivation if the initial count was < 10^5 CFU ml^{-1} (Vachon *et al.*, 2002).

Table 4.4: Statistical measures and parameter values obtained from GInaFit Version 1.5 for experimental data of thermal inactivated *E. coli*, *L. innocua*, and *P. carotovorum* at 70 °C and different initial count

Treatment	Model type	RMSE	Log N_0 [CFU ml^{-1}]	k_{max} [1 min^{-1}]	Log N_{res} [CFU ml^{-1}]
E. coli					
10^7 CFU ml^{-1}	Log-linear + tail	0.29	7.75	7.21	4.59
10^5 CFU ml^{-1}	Log-linear + tail	0.16	5.79	7.12	2.95
10^3 CFU ml^{-1}	Log-linear + tail	0.43	3.74	24.56	0.23
L. innocua					
10^7 CFU ml^{-1}	Log-linear + tail	0.36	7.76	25.44	5.32
10^5 CFU ml^{-1}	Log-linear + tail	0.39	5.8	7.05	2.28
10^3 CFU ml^{-1}	Log-linear + tail	0.47	3.78	7.47	0.79
P. carotovorum					
10^7 CFU ml^{-1}	Log-linear + tail	0.42	7.21	13.70	2.06
10^5 CFU ml^{-1}	Log-linear + tail	0.00	4.32	18.53	0.00
10^3 CFU ml^{-1}	Log-linear + tail	0.00	2.75	14.48	0.00

The comparison of total count and viable count before thermal treatment showed no significant differences for *E. coli* at an initial count of 10^7 CFU ml^{-1} and 10^5 CFU ml^{-1} as well as for *L. innocua* at an initial count of 10^7 CFU ml^{-1}. But for *P. carotovorum* the total count was significant higher than the viable count for all tested initial counts. Significant higher counts were also observed for *L. innocua* at initial counts of 10^5 and 10^3 CFU ml^{-1} and initial counts of 10^3 CFU ml^{-1} for *E. coli*. The greatest discrepancies were found at initial counts of 10^3 CFU ml^{-1}. Thereby, the total count was at least 1 log unit higher than the viable count for all tested bacteria. An overestimation of low bacteria numbers were also observed by Drake (1973). A reliable determination of total cell count was only achieved at cell counts ≥ 10^5. No significant changes in total count of *L. innocua*, *E. coli* and *P. carotovorum* were observed within ten minutes of treatment at 70 °C with the exception of *L. innocua* at an initial count of 10^7 CFU ml^{-1}. The total count of *L. innocua* decreased with increasing treatment time (Table 4.5).

Table 4.5: Total count after thermal treatment at 70 °C and different initial counts

	70 °C 7 Log cell count ml^{-1}	70 °C 5 Log cell count ml^{-1}	70 °C 3 Log cell count ml^{-1}
E. coli			
0 min	8.07^{a}	5.81^{a}	5.01^{a}
1 min	7.15^{a}	5.80^{a}	4.94^{a}
3 min	7.68^{a}	5.77^{a}	4.97^{a}
5 min	7.66^{a}	5.80^{a}	4.96^{a}
10 min	7.66^{a}	5.80^{a}	4.93^{a}
L. innocua			
0 min	7.83^{a}	5.95^{a}	4.94^{a}
1 min	7.79^{b}	5.89^{a}	4.88^{a}
3 min	7.76^{b,c}	5.90^{a}	5.02^{a}
5 min	7.76^{c,d}	5.89^{a}	4.87^{a}
10 min	7.73^{d}	5.88^{a}	4.76^{a}
P. carotovorum			
0 min	7.70^{a}	5.89^{a}	5.18^{a}
1 min	7.70^{a}	5.82^{a}	4.99^{a}
3 min	7.70^{a}	5.73^{a}	5.11^{a}
5 min	7.69^{a}	5.82^{a}	4.99^{a}
10 min	7.69^{a}	5.82^{a}	5.12^{a}

$^{a-c}$, Different letters within the columns indicate significant differences at a significance level of 0.05

4.2.2 Peracetic acid treatment

Thermal treatment of fresh fruits and vegetables is not possible due to the heat sensitivity of the products. Therefore, alternative non-thermal inactivation processes are required and detailed knowledge about the impact of these treatments is essential to implement those processes into the production chain. Therefore, the efficiency of the chemical disinfectant PAA was tested against selected bacteria. In preliminary experiments it was observed that *E. coli* had the highest resistance against PAA in comparison to *L. innocua* and *P. carotovorum*. *E. coli* can be used as indicator for faecal contamination and is also relevant in other primary production processes such as milk production. Therefore, the efficiency of 0.25 % and 0.5 % PAA was tested initially against *E. coli* at 0 °C, 10 °C, and 20 °C. The concentrations of PAA were chosen according to the recommendations of the producer of Wofasteril® E400. Different temperatures were tested because of the different temperature conditions during food processing. The initial count of *E. coli* for PAA treatment was 5.4 ± 0.8 *10^{7} CFU ml^{-1}. The obtained inactivation with the corresponding models obtained from GInaFit Version 1.5 tool are given in figure 4.6.

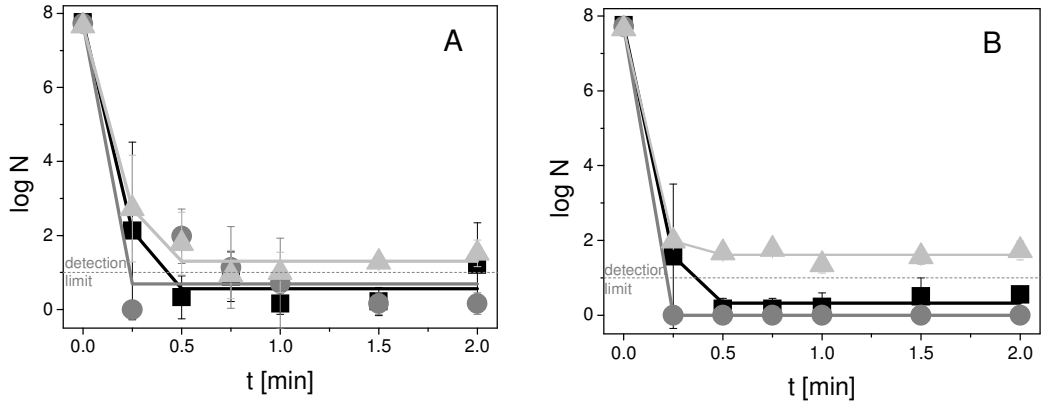

Figure 4.6: Inactivation kinetics of *E. coli* after 0.25 % (A) and 0.5 % (B) PAA treatment at different temperature levels (squares: 0 °C; circles: 10 °C; triangles: 20 °C). The lines represent the inactivation obtained from the applied models from the GInaFit tool.

At 0°C *E. coli* was inactivated by 5.6 log and 6.2 log units using 0.25 % and 0.5 % PAA, respectively after 0.25 min. An increased temperature of 10 °C led to a 7.7 log unit inactivation of *E. coli* for both concentrations after 0.25 min. At 20 °C the inactivation after 0.25 min treatment time was only 4.9 and 5.7 log cycles for 0.25 % and 0.5 % PAA; respectively. Tailing could be observed for all tested concentrations and temperatures. Tailing was also found for *P. aeruginosa* after 50 to 200 mmol l^{-1} PAA treatment (Lambert, 1999). Kunigk & Almeida (2001) found an 8 log unit inactivation of *E. coli* in suspension at 25 °C after 3.1 min and 4 min for 60 mg l^{-1} PAA and 40 mg l^{-1} PAA, respectively with curves showing first-order reaction kinetics. According to the authors the inactivation curve of *S. aureus* after 40 mg l^{-1} PAA treatment also followed first-order-kinetics.

Table 4.6: Statistical measures and parameter values obtained from GInaFit Version 1.5 for experimental data of PAA inactivated *E. coli*

Treatment	Model type	RMSE	Log N_0 [CFU ml^{-1}]	K_{max} [1 min^{-1}]	Log N_{res} [CFU ml^{-1}]
0.25 %					
0 °C	Log-linear + tail	0.46	7.76	51.95	0.56
10 °C	Log-linear + tail	0.85	7.72	118.61	0.69
20 °C	Log-linear + tail	0.35	7.66	45.56	1.31
0.5 %					
0 °C	Log-linear + tail	0.19	7.76	57.14	0.32
10 °C	Log-linear + tail	0.00	7.72	105.12	0.00
20 °C	Log-linear + tail	0.17	7.66	54.52	1.62

All models available in GInaFiT tool were applied to the experimental data and the goodness-of-fit of the models was compared using the RMSE. The statistical measures and parameters of the best fitted model for PAA inactivation of *E. coli* are given in table 4.6. The best fitted model for all inactivation kinetics was the log-linear model followed by tailing. However, at a PAA concentrations of 0.5 % and a treatment temperature of 10 °C the residual population

was zero and therefore, no real tailing can be assumed. The highest inactivation rates were observed at 10 °C and at 20 °C the lowest inactivation rates for both tested PAA concentrations were observed. This is in contrast to other studies showing increased disinfectant efficiency with increasing temperatures (Stampi, 2001; Hilgren *et al.*, 2007). The higher PAA concentration led to higher inactivation rates with the exception of 10 °C. At 10 °C and a PAA concentration of 0.5 % the applied model is not appropriate because the residual population is zero and therefore, the calculated inactivation rate may be underestimated by the model. The reduced inactivation at 20 °C can be explained by the decomposition of PAA at higher temperatures. Decreasing stability of PAA with increasing temperatures was observed by (Kunigk *et al.*, 2001).

The total count and viable count of *E. coli* before PAA treatment at different temperature levels differed significantly at 0 °C but no significant differences were obtained at 10 °C and 20 °C. Thereby, the viable count was slightly lower than the total count at 20 °C but at 10 °C and 0 °C the viable count was higher than the total count. This implies that *E. coli* cells have different electronic characteristics at lower temperatures.

Table 4.7: Total cell count of *E. coli* after PAA treatment at different concentrations and temperature levels

	0 °C Log cell count ml^{-1}	10 °C Log cell count ml^{-1}	20 °C Log cell count ml^{-1}
0.25 % PAA			
0 min	7.70^{a}	7.70^{a}	7.68^{a}
0.25 min	7.53^{b}	7.55^{b}	7.45^{b}
0.5 min	7.59^{b}	7.56^{b}	7.54^{a}
0.75 min	7.57^{b}	7.56^{b}	7.55^{a}
1 min	7.55^{b}	7.57^{b}	7.52^{a}
1.5 min	7.55^{b}	7.59^{b}	7.56^{a}
2 min	7.54^{b}	7.60^{b}	7.50^{a}
0.5 % PAA			
0 min	7.70^{a}	7.70^{a}	7.68^{a}
0.25 min	7.61^{b}	7.61^{b}	7.59^{b}
0.5 min	7.60^{b}	7.60^{b}	7.61^{a,b}
0.75 min	7.59^{b}	7.59^{b}	7.59^{a,b}
1 min	7.59^{b}	7.59^{b}	7.57^{b}
1.5 min	7.59^{b}	7.59^{b}	7.58^{b}
2 min	7.59^{b}	7.58^{b}	7.58^{b}

^{a,b}, Different letters within the columns indicate significant differences at a significance level of 0.05

The total count decreased after PAA treatment and significant changes could be observed for all tested concentrations and temperature levels with an exception of PAA treatment at 20 °C (Table 4.7). The differences in total count before and after PAA treatment can be due to changes in electronic characteristics induced by the temperatures and by PAA. Changes in electronic characteristics after treatment of bacteria were also observed by Swanton *et al.*

(1962). Another explanation is a disruption of cells due to PAA treatment resulting in reduced total count.

4.2.3 Ozone treatment

The influence of initial bacterial count on the efficiency of ozone was tested at an ozone concentration of 2.8 mg l^{-1}. In these experiments, the residual ozone was removed by shaking. All bacteria were instantaneously inactivated below the detection limit at all tested cell concentrations (Figure 4.7).

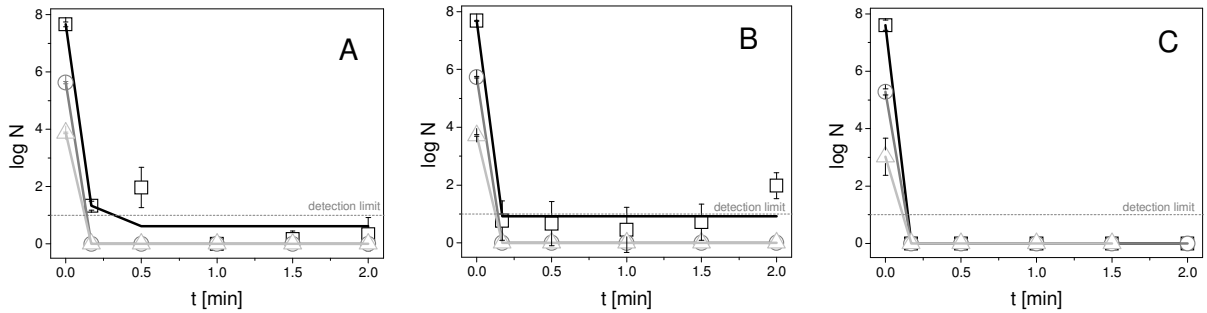

Figure 4.7: Inactivation kinetics of *E. coli* (A), *L. innocua* (B), and *P. carotovorum* (C) at 2.8 mg l^{-1} with different initial counts (open squares: 10^7 CFU ml^{-1}; open circles: 10^5 CFU ml^{-1}; open triangles: 10^3 CFU ml^{-1}). The lines represent the modelled inactivation obtained from the GInaFit Version 1.5.

All models available in the GInaFiT tool were applied to the experimental data and the goodness-of-fit of the models was compared using the RMSE. The statistical measures and parameters of the best fitted model for inactivation by ozone are given in table 4.8.

Table 4.8: Statistical measures and parameter values obtained from GInaFit Version 1.5 for experimental data of ozone inactivated *E. coli*, *L. innocua*, and *P. carotovorum* at 2.8 mg l^{-1} and different initial count

Treatment	Model type	RMSE	Log N_0 [CFU ml^{-1}]	k_{max} [1 min^{-1}]	Log N_{res} [CFU ml^{-1}]
E. coli					
10^7 CFU ml^{-1}	Log-linear + tail	0.91	7.67	87.10	0.62
10^5 CFU ml^{-1}	Log-linear + tail	0.00	5.63	119.64	0.00
10^3 CFU ml^{-1}	Log-linear + tail	0.00	3.88	102.38	0.00
L. innocua					
10^7 CFU ml^{-1}	Log-linear + tail	0.70	7.68	172.33	0.92
10^5 CFU ml^{-1}	Log-linear + tail	0.00	5.73	125.86	0.00
10^3 CFU ml^{-1}	Log-linear + tail	0.00	3.72	96.16	0.00
P. carotovorum					
10^7 CFU ml^{-1}	Log-linear + tail	0.00	7.60	151.28	0.00
10^5 CFU ml^{-1}	Log-linear + tail	0.00	5.28	114.43	0.00
10^3 CFU ml^{-1}	Log-linear + tail	0.00	3.02	82.97	0.00

All survivor curves could be described with the log linear regression model with tailing. However, at concentrations ≤ 10^5 CFU ml^{-1} the residual population was zero and a real tailing could not be assumed. The inactivation rates for *E. coli* were higher at cell concentrations ≤ 10^5 CFU ml^{-1} than at a cell concentration of 10^7 CFU ml^{-1}. In contrast, the inactivation rates of *L. innocua* and *P. carotovorum* decreased with decreasing cell concentration and *L. innocua* was more sensitive to ozone than *P. carotovorum* and *E. coli*. This is in contrast to the inactivation by heat treatment where *L. innocua* seems to be more resistant at lower cell concentrations. Kim (2000) tested the effectiveness of ozone against different cell concentrations of *Leuconostoc mesentreriodes* and observed a lower inactivation at higher cell concentrations. The author concluded that the effectiveness of ozone varies with inoculum size and the ratio between amount of cells and ozone concentrations need to be considered for effective ozone inactivation.

Table 4.9: Total count after ozone treatment at 2.8 mg l^{-1} and different initial counts

	2.8 mg l^{-1} 7 Log cell count ml^{-1}	2.8 mg l^{-1} 5 Log cell count ml^{-1}	2.8 mg l^{-1} 3 Log cell count ml^{-1}
E. coli			
0 min	7.65^{a}	5.83^{a}	6.09^{a}
0.17 min	7.66^{a}	6.55^{b}	7.07^{b}
0.5 min	7.56^{a}	6.54^{b}	7.02^{b}
1 min	7.51^{a}	6.53^{b}	7.05^{b}
1.5 min	7.58^{a}	6.54^{b}	7.02^{b}
2 min	7.52^{a}	6.52^{b}	7.05^{b}
L. innocua			
0 min	7.54^{a}	$5.71^{a,c}$	$6.20^{a,b}$
0.17 min	7.15^{b}	7.76^{b}	$6.31^{a,b}$
0.5 min	$7.25^{b,c}$	6.77^{c}	6.33^{a}
1 min	$7.24^{b,c}$	6.82^{c}	5.99^{b}
1.5 min	7.33^{c}	6.75^{c}	$6.09^{a,b}$
2 min	7.33^{c}	6.80^{c}	6.32^{a}
P. carotovorum			
0 min	$8.22^{a,c}$	6.19^{a}	5.83^{a}
0.17 min	8.12^{b}	6.90^{b}	$7.05^{b,d}$
0.5 min	$8.15^{b,c}$	6.96^{b}	$6.98^{b,c,d,e}$
1 min	$8.13^{b,c}$	6.92^{b}	$6.91^{c,d,e}$
1.5 min	$8.12^{b,c}$	6.79^{c}	$6.96^{d,e}$
2 min	8.17^{c}	6.80^{c}	6.90^{e}

$^{a-e}$, Different letters within the columns indicate significant differences at a significance level of 0.05

Similar to the measurements before heat treatment, the viable count of all tested bacteria was significantly lower than the total count at a cell concentration of 10^3 CFU ml^{-1}. This supports the assumption that a reliable cell count can only be achieved at cell concentrations of ≥ 10^5. Otherwise, the cell concentration may be overestimated using the applied measurement method. In contrast to the heat treatment, the total count increased during ozone treatment at lower cell concentrations (Table 4.9). At higher concentrations no

significant differences were observed for *E. coli* and the total count of *L. innocua* and *P. carotovorum* significantly decreased during ozone treatment. This implies that a cell rupture at lower cell concentrations did not lead to a decreased total count. However, a more feasible explanation is an overestimation of total count due to artefact measurements at lower cell concentrations which is already apparent in at untreated suspensions with lower cell concentrations.

The efficiency of ozone to inactivate *E. coli, L. innocua*, and *P. carotovorum* in pure suspensions was tested using different concentrations of ozone. The initial bacteria concentration was set to 4.7 ± 1.1*10^7 CFU ml^{-1}, 4.9 ± 1*10^7 CFU ml^{-1}, and 3.7 ± 3.1*10^7 CFU ml^{-1} for *E. coli, L. innocua,* and *P. carotovorum*, respectively. The temperature of the ozonated water during treatment was approximately 12 °C. All tested bacteria were inactivated by ozone at low concentrations. *E. coli*, *L. innocua*, and *P. carotovorum* was already reduced by 5.52 log units, 7.48 log units, and 6.57 log units, respectively, after 0.17 min treatment with an ozone concentration of 1.7 mg l^{-1}. An increased treatment time did not further enhance the inactivation but an increased ozone concentration up to 3.8 mg l^{-1} led to a reduction of bacteria to the detection limit after a treatment time of 0.17 min (Figure 4.8). Lower ozone concentrations of 0.7 mg l^{-1} led to an inactivation of *P. carotovorum* by 4.55 log units after 0.17 min treatment and after 2 min 6.57 log units were inactivated. Instantaneous killing of bacteria was also observed by Restaino (1995) and Kim & Yousef (2000).

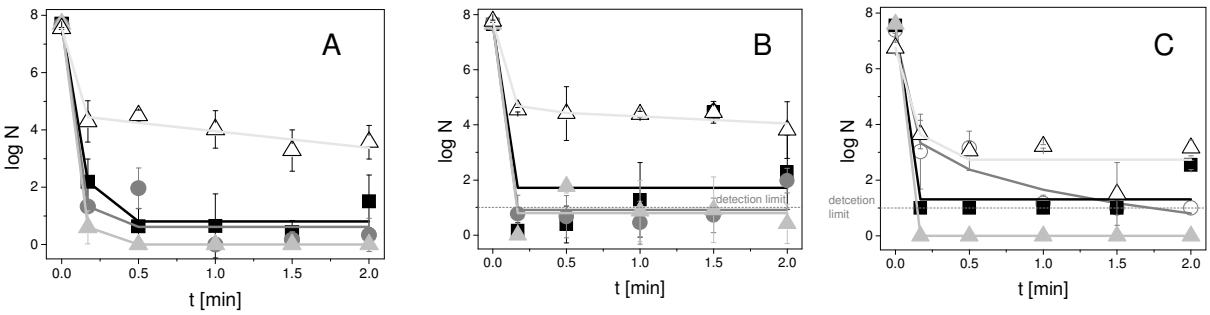

Figure 4.8: Inactivation kinetics of *E. coli* (A); *L. innocua* (B) and *P. carotovorum* (C) after ozone treatment at various concentrations: 0.7 mg l^{-1} (open circles), 1.7 mg l^{-1} (squares), 2.8 mg l^{-1} (circles), 3.8 mg l^{-1} (triangles), and 3.8 mg l^{-1} with sodium thiosulfate (open triangles) ozone treatment. The lines represent the inactivation obtained from the applied models from the GInaFit tool.

In order to make sure that the reaction of ozone with bacteria is stopped after the defined treatment times the ability of $Na_2S_2O_3$ to stop the reaction was compared to the routinely applied degassing of ozone by shaking for 30 s. A negative effect of $Na_2S_2O_3$ on the bacteria was excluded in preliminary experiments. $Na_2S_2O_3$ has been used in various inactivation

studies as neutralising agent (Kim *et al.*, 1999; Kemp & Schneider, 2000; Mezzanotte *et al.*, 2003; Abadias *et al.*, 2008). In comparison to degassing of ozone as a method of stopping the reaction the inactivation of *E. coli, L. innocua*, and *P. carotovorum* at 3.8 mg l^{-1} was reduced after treatment with $Na_2S_2O_3$.

All models available in GInaFiT tool were applied to the experimental data and the goodness-of-fit of the models was compared using the RMSE. The statistical measures and parameters of the best fitted model for inactivation by ozone are given in table 4.10. Similar to the inactivation by PAA, the inactivation of *E. coli* by ozone followed a log-linear regression with tailing. The inactivation rates of the ozone treatments at all concentrations were lower than the inactivation rate of the PAA treatment at 10 °C and both tested PAA concentrations. The residual *E. coli* population after ozone treatment was higher than after PAA treatment. The residual *E. coli* population after ozone treatment with 3.8 mg l^{-1} ozone was zero and therefore the applied log-linear model with tailing is not suitable for describing the observed inactivation. Similar results were obtained for *P. carotovorum* at 2.8 mg l^{-1}. Due to the limited data an application of a log-linear is not possible for both bacteria. The inactivation of *L. innocua* also followed a log-linear regression with tailing and the inactivation rates were higher than the inactivation rates of *E. coli* and *P. carotovorum* with the exception for ozone concentration of 1.7 mg l^{-1}. The inactivation of *P. carotovorum* showed a log-linear regression with tailing at ozone concentrations of 1.7 mg l^{-1} and 2.8 mg l^{-1}. In contrast, an upward concave shape was observed for *P. carotovorum* after ozone treatment at a concentration of 0.7 mg l^{-1}. Thus, *L. innocua* seems to be more sensitive against ozone than *P. carotovorum* and *E. coli*. A higher resistance of Gram-negative bacteria against ozone in comparison to Gram-positive bacteria has also been described in other studies (Restaino *et al.*, 1995; Kim *et al.*, 1999; Pascual *et al.*, 2007).

The comparison of ozone inactivation stopped by shaking and ozone inactivation stopped by $Na_2S_2O_3$ indicated that shaking did not efficiently remove the ozone and consequently an ongoing effect of the applied ozone is assumed. Both experimental procedures showed the instantaneously inactivation effect of ozone. However, a longer treatment time in the experimental set with ozone removal by $Na_2S_2O_3$ did not reach the same reduction level as experiments with ozone removal by shaking. This implies that reactive ozone species which possibly penetrated the bacteria cells were effectively quenched by the $Na_2S_2O_3$ whereas these species were not destroyed by the shaking.

Table 4.10: Statistical measures and parameter values obtained from GInaFit Version 1.5 for experimental data of ozone inactivated *E. coli, L. innocua,* and *P. carotovorum*

Treatment	Model type	RMSE	Log N_0 [CFU ml^{-1}]	K_{max} [1 min^{-1}]	Log N_{res} [CFU ml^{-1}]	δ [min]	p [-]	f [-]	K_{max1} [1 min^{-1}]	K_{max2} [1 min^{-1}]
E. coli										
1.7 mg l^{-1}	Log-linear + tail	0.48	7.71	74.99	0.80					
2.8 mg l^{-1}	Log-linear + tail	0.91	7.67	87.10	0.62					
3.8 mg l^{-1}	Log-linear + tail	0.00	7.71	97.94	0.00					
3.8 mg l^{-1} + $Na_2S_20_3$	biphasic	0.37	7.54					0.99	60.43	1.33
L. innocua										
1.7 mg l^{-1}	Log-linear + tail	2.02	7.64	162.97	1.73					
2.8 mg l^{-1}	Log-linear + tail	0.70	7.68	172.33	0.92					
3.8 mg l^{-1}	Log-linear + tail	0.76	7.65	182.19	0.79					
3.8 mg l^{-1} + $Na_2S_20_3$	biphasic	0.28	7.72					0.99	48.06	0.60
P. carotovorum										
0.7 mg l^{-1}	Weibull	0.59	7.17			0.00	0.21			
1.7 mg l^{-1}	Log-linear + tail	0.80	7.55	168.76	1.31					
2.8 mg l^{-1}	Log-linear + tail	0.00	7.60	151.28	0.00					
3.8 mg l^{-1} + $Na_2S_20_3$	Log-linear + tail	0.82	6.74	42.86	2.73					

However, the inactivation of *E. coli, L. innocua* and *P. carotovorum* at an ozone concentration of 3.8 mg l^{-1} was reduced after stopping the reduction with $Na_2S_2O_3$ instead of ozone removal by shaking. Additionally, the shape of the survival curves is different for *E. coli* and *L. inncoua*. The inactivation kinetics of both bacteria could be described using a biphasic model. The inactivation rate of the first phase is higher than the inactivation rate of the second phase. In contrast to the experiments without $Na_2S_2O_3$ to stop the reaction, the inactivation rates of *L. innocua* were lower than the inactivation rates of *E. coli*. The inactivation of *P. carotovorum* by ozone using $Na_2S_2O_3$ as a neutraliser can be described with the log-linear model with tailing. The inactivation rate of *P. carotovorum* was reduced during this experiment and was lower than the inactivation rates of *E. coli* and *L. innocua.* This is in contrast to the assumption that Gram-negative bacteria are more resistant against ozone than Gram-positive bacteria. Broadwater *et al.* (1973) also found no differences in ozone resistance of bacteria as a result of different membrane structures. The higher resistance of *P. carotovorum* against ozone may be related to the presence of $Na_2S_2O_3$. *P. carotovorum* strains are able to produce H_2S from sodium thiosulfate (Dickey, 1979; Fassihiani & Nedaeinia, 2008). The presence of $Na_2S_2O_3$ may support bacterial growth due to enhanced availability of nutrients and may enable growth of stressed bacteria. It seems that the ability to utilize sodium thiosulfate is reduced in *L. innocua* and *E. coli* cells as they are not able to produce H_2S (Pine *et al.*, 1987; Holt *et al.*, 2000) which could be the explanation for a reduced resistance against ozone when compared to *P. carotovorum*. A tailing of survivor curves after ozone treatment with subsequent addition of $Na_2S_2O_3$ was also found by Kim

(2000). They related the tailing to bacterial clumps in the suspension which protect bacteria against ozone.

Table 4.11: Total cell count after ozone treatment at different concentrations

	0.7 mg l^{-1} Log cell count ml^{-1}	1.7 mg l^{-1} Log cell count ml^{-1}	2.8 mg l^{-1} Log cell count ml^{-1}	3.8 mg l^{-1} Log cell count ml^{-1}	3.8 mg l^{-1} + $Na_2S_2O_3$ Log cell count ml^{-1}
E. coli					
0 min	n.a.$^{+}$	8.07^{a}	7.65^{a}	8.07^{a}	7.70^{a}
0.17 min	n.a.$^{+}$	7.90^{b}	7.66^{a}	7.85^{b}	7.57^{b,c}
0.5 min	n.a.$^{+}$	7.84^{b}	7.56^{a}	7.71^{c}	7.61^{b}
1 min	n.a.$^{+}$	7.86^{b}	7.51^{a}	7.76^{b,c}	7.56^{b,c}
1.5 min	n.a.$^{+}$	7.82^{b}	7.58^{a}	7.80^{b,c}	7.53^{c,d}
2 min	n.a.$^{+}$	7.92^{b}	7.52^{a}	7.80^{b,c}	7.51^{d}
L. innocua					
0 min	n.a.$^{+}$	7.82^{a}	7.54^{a}	7.80^{a}	7.84^{a}
0.17 min	n.a.$^{+}$	7.17^{b}	7.15^{b}	7.32^{b}	7.74^{b}
0.5 min	n.a.$^{+}$	7.32^{c,d}	7.25^{b,c}	7.41^{b,d}	7.72^{b}
1 min	n.a.$^{+}$	7.27^{b,c,d}	7.24^{b,c}	7.57^{c,d}	7.75^{b}
1.5 min	n.a.$^{+}$	7.38^{d}	7.33^{c}	7.60^{c}	7.72^{b}
2 min	n.a.$^{+}$	7.37^{c,d}	7.33^{c}	7.49^{d}	7.72^{b}
P. carotovorum					
0 min	8.25^{a}	8.36^{a}	8.22^{a,c}	n.a.$^{+}$	7.46^{a}
0.17 min	7.98^{b}	8.14^{b}	8.12^{b}	n.a.$^{+}$	7.27^{b}
0.5 min	8.07^{b}	8.15^{b}	8.15^{b,c}	n.a.$^{+}$	7.30^{b}
1 min	8.13^{b}	8.10^{b}	8.13^{b,c}	n.a.$^{+}$	7.29^{b}
1.5 min	8.01^{b}	8.14^{b}	8.12^{b,c}	n.a.$^{+}$	7.24^{b}
2 min	8.17^{b}	8.19^{b}	8.17^{c}	n.a.$^{+}$	7.28^{b}

$^{a-d}$, Different letters within the columns indicate significant differences at a significance level of 0.05
*n.a., not analysed

As shown for thermal treatment and PAA treatment, the total count of bacteria was also significantly reduced after ozone treatment at different concentrations (Table 4.11). For all treated bacteria the total count was significantly different from the viable count and in most cases the total count was higher. The reduction of total count after ozone treatment can be explained by changes in electronic characteristics of the bacteria after treatment. Additionally, a disruption of cells and cell lyses may be the result of treatment with ozone and therefore a lower total count was observed.

4.2.4 Plasma treatment

The heating effects due to plasma application were determined by thermography images of the sample surface. Temperature measurements at 20 W showed that the average temperature slightly increased to approximately 27 °C, whereas the average temperature on the gel surface remained constant during plasma treatment with 10 W operating power

(Figure 4.9). At 40 W an increase of the average temperature on the surface of the gel plates from room temperature to 47 °C within 130 s was determined.

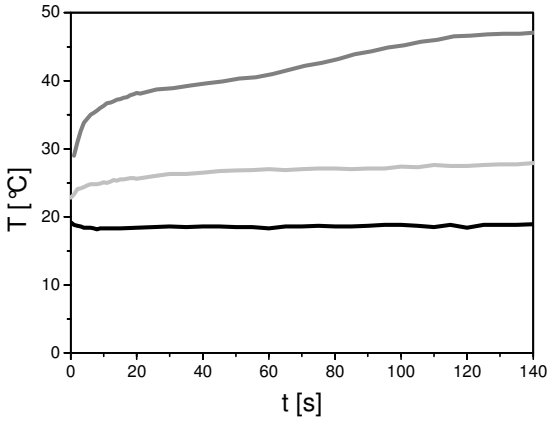

Figure 4.9: Development of sample surface temperature due to plasma treatment at different power levels. Black line: 10 W; light grey line: 20 W, and grey line: 40 W.

Inactivation of *E. coli*, *L. innocua,* and *P. carotovorum* due to plasma treatment at different power levels with an rf-driven APPJ is shown in figure 4.8. The initial count of *E. coli* and *L. innocua* before the treatments were 1.05± 2.73*10^8 CFU cm^{-2} and 1.34 ± 0.3*10^8 CFU cm^{-2}, respectively. The initial count of *P. carotovorum* was set to 3.41 ± 0.3*10^7 CFU cm^{-2}. Less than one log unit reduction of *E. coli* and *L. innocua* (Figure 4.10 A,B) was determined at plasma power of 10 W and 4 min treatment time, but *P. carotovorum* could be reduced by 1.86 log applying the same parameters (Figure 4.10 C). Increasing the operating power of the plasma jet to 20 W led to one log reduction of *E. coli* and *L. innocua* after 1 min. A three log unit reduction was obtained after 3 min and an inactivation by six log units after 4 min treatment time. The required treatment time to achieve an inactivation of colony forming units by more than 6 log units was reduced from 4 min at 20 W to 1.5 min using 40 W. The higher sensitivity of *P. carotovorum* against plasma in comparison to *E. coli* and *L. innocua* was also shown at 20 W with a six log unit reduction already after 2.5 min and at 40 W after 0.75 min.

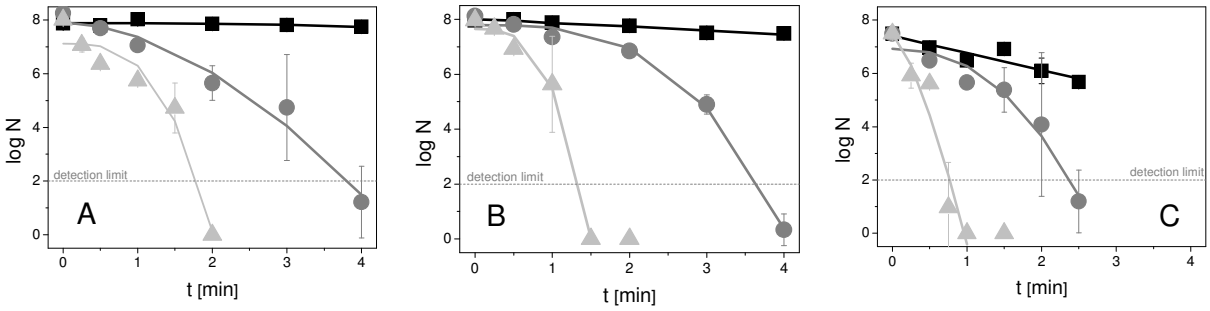

Figure 4.10: Inactivation kinetics of *E. coli* (A), *L. innocua* (B), and *P. carotovorum* (C) cells after plasma treatment at 10 W (squares), 20 W (circles), and 40 W (triangles). The lines represent the modelled inactivation obtained from the GInaFit Version 1.5.

All models available in the GInaFiT tool were applied to the experimental data and the goodness-of-fit of the models was compared using the RMSE. The statistical measures and parameters of the best fitted model for inactivation by plasma are given in table 4.12. The GInaFiT tool was successfully applied to microbial inactivation of bacteria and yeast by gliding arc discharges (Kamgang, 2007; Kamgang-Youbi *et al.*, 2007; Kamgang-Youbi *et al.*, 2009).

Table 4.12: Statistical measures and parameter values obtained from GInaFit Version 1.5 for experimental data of plasma inactivated *E. coli*, *L. innocua*, and *P. carotovorum*

Treatment	Model type	RMSE	Log N_0 [CFU ml^{-1}]	δ [min]	p [-]
E. coli					
10 W	Weibull	0.10	7.89	2.88	7.75
20 W	Weibull	0.55	7.92	1.4	1.78
40 W	Weibull	0.77	7.12	1.06	3.08
L. innocua					
10 W	Weibull	0.07	8.00	7.29	1.53
20 W	Weibull	0.29	7.80	2.11	3.13
40 W	Weibull	0.42	7.65	3.11	0.78
P. carotovorum					
10 W	Weibull	0.34	7.42	1.54	0.98
20 W	Weibull	0.59	6.92	1.20	2.33
40 W	Weibull	1.25	7.48	1.38	0.22

Modelling of microorganism inactivation is used to adapt inactivation technologies to practical applications. The classical description of inactivation with the Bigelow model of first-order kinetics is not applicable to non-linear inactivation curves. In recent years many alternative models were published with the Weibull model as the predominant model (Marks, 2008). Yu *et al.* (2006) used the Baranyi model to describe inactivation kinetics of *E. coli* after treatment with a cold atmospheric plasma pen and stated that the model fits the data well. It was stated that the Baranyi model is an appropriate model to describe non-thermal plasma inactivation

kinetics of *B. subtilis* spores and can be used as a base to identify physiological and biological mechanisms (Perni *et al.*, 2006). Perni *et al.* (2006) also noted that the fit of the Baranyi and Weibull models were in some cases better than a polynomial model when the inactivation curves were biphasic. They proposed the application of the Weibull model to the description of non-thermal plasma inactivation, whereas an empirical model seemed to better describe the obtained triphasic inactivation curves.

In this study, the inactivation kinetics of all tested bacteria obtained by atmospheric pressure plasma treatment could be described with the Weibull model. A downward concavity was observed for *E. coli* at 10-40 W, for *L. innocua* at 10 and 20 W, and for *P. carotovorum* at 20 W. An upward concavity was found for *L. innocua* at 40 W and for *P. carotovorum* at 10 and 40 W. An upward concavity implies that the remaining cells are able to adapt to the applied stress and downward concavity implies that the remaining cells became increasingly damaged (van Boekel, 2002). The scale parameter from the Weibull model has a probabilistic interpretation and represents the time of the first decimal reduction (Virto *et al.*, 2006). With increasing plasma operating power the scale parameter of *E. coli* decreased whereas the scale parameter of *P. carotovorum* and *L. innocua* was highest at 20 W and lowest at 40 W. However, the scale parameter of the tested bacteria indicated that *L. innocua* is more resistant against atmospheric pressure plasma than *E. coli* and *P. carotovorum*. Montie *et al.* (2000) stated that the inactivation rate is dependent on the type of microorganism and the surface on which they were treated. Biphasic survival curves were obtained for various types of microorganisms including Gram-negative and Gram-positive bacteria, yeasts, and bacterial endospores on glass, agar, and polypropylene after treatment with a One Atmosphere Uniform Glow Discharge Plasma (OAUGDP) (Kelly-Wintenberg *et al.*, 1998; Kelly-Wintenberg *et al.*, 1999) and for *E. coli* on polypropylene samples under direct OAUGPD exposure (Montie *et al.*, 2000) with slower inactivation rates at the beginning of the treatment followed by a rapid inactivation phase. Kelly-Wintenberg *et al.* (1999) hypothesized that during the first inactivation segment active species diffuse through the cell surface and generate alterations followed by irreversible damage and lyses of cells during the second inactivation segment due to high concentrations of active species. The differences between Gram-positive and Gram-negative bacteria can be explained by the cell structure. Three-phasic inactivation curves were reported for low-pressure plasma treatment with the shortest D-value during the first phase, followed by a second phase with the slowest inactivation rate and a third phase with similar D-values to the first phase. The inactivation during the first phase can be mainly attributed to UV irradiation. In the second phase a slow erosion process by active species resulted in the slowest kinetic and during the last phase UV affects the genetic material (Moisan *et al.*, 2001). In contrast to these results, UV plays a

minor role at atmospheric-pressure plasma treatment (Laroussi, 2002). For high pressure cold plasma treatments three inactivation mechanisms are proposed: i) lipid peroxidation by hydroxyl radicals; ii) protein oxidation, and iii) DNA oxidation by oxygen radicals (Montie *et al.*, 2000).

Table 4.13: Total count of bacteria after plasma treatment at different operating powers

Treatment time [min]	*E. coli* Log cell count ml^{-1}			*L. innocua* Log cell count ml^{-1}			*P. carotovorum* Log cell count ml^{-1}		
	10 W	20 W	40 W	10 W	20 W	40 W	10 W	20 W	40 W
0	8.54^{a}	8.62^{a}	8.54^{a}	8.47^{a}	8.37^{a}	8.47^{a}	8.50^{a}	8.40^{a}	8.50^{a}
0.25	n.a.	n.a.	8.47^{a}	n.a.	n.a	8.10^{b}	n.a.	n.a	8.15^{b}
0.5	n.a.	8.41^{b}	8.12^{b}	n.a.	8.33^{a}	7.90^{c}	8.30^{b}	8.18^{b}	8.11^{b}
0.75	n.a.	n.a.	n.a.	n.a.	n.a	n.a	n.a.	n.a	8.22^{c}
1	8.47^{a,b}	8.46^{c}	7.87^{c}	8.17^{b}	8.20^{b}	7.67^{d}	8.33^{c}	8.11^{c}	7.85^{d}
1.5	n.a.	n.a.	7.61^{d}	n.a.	n.a	7.27^{e}	8.39^{d}	8.00^{d}	7.80^{d}
2	8.47^{a,b}	8.26^{d}	6.88^{e}	8.34^{c}	7.44^{c}	6.61^{f}	8.34^{c}	8.31^{e}	n.a
2.5	n.a.	n.a.	n.a.	n.a.	n.a.	n.a.	8.35^{c}	7.96^{d}	n.a
3	8.44^{b,c}	8.04^{e}	n.a.	8.21^{b}	7.69^{d}	n.a.	n.a.	n.a	n.a
4	8.37^{c}	8.06^{e}	n.a.	8.20^{b}	7.50^{e}	n.a.	n.a.	n.a	n.a

n.a., not analysed
$^{a-f}$, Different letters within the columns indicate significant differences at a significance level of 0.05

Before plasma treatment the total count of all bacteria was significantly higher than the viable count of bacteria at a significance level of 0.05. This implies that the re-suspension of bacteria lead to an amount of gel pieces in the suspension that are measured in the same size range as bacteria by the Coulter Counter and may lead to an overestimation of total bacteria count. During plasma treatment the total count of all bacteria significantly decreased with increasing treatment time at all operating powers (Table 4.13). This leads to the assumption that an erosion of bacteria occurred during plasma treatment. An inactivation of bacteria due to erosion has previously been suggested for low-pressure plasma treated spores (Moisan *et al.,* 2002).

4.3 Development of a staining protocol for cFDA

Conventional microbiological plate count methods for pathogenic bacteria detection are often time-consuming and expensive, limiting the possibility of integration in the postharvest production chain. Furthermore, bacteria in food samples may exist in a viable-but-not-culturable (VBNC) state (Ben-Amor *et al.*, 2002) hardly detectable by conventional culture-based methods. However, bacteria in a VBNC state may be able to cause plant diseases or foodborne diseases (Oliver, 2005). Thus, it is crucial to determine the physiological state of bacteria in foods using fast detection methods. Flow cytometry is a potential tool for microbial

characterisation and conceivably, flow cytometry techniques can be implemented into the production chain to monitor inactivation processes. In this context, carboxyfluorescein diacetate (cFDA) and propidium iodide (PI) are frequently used dyes for viability testing of bacteria. (Ben-Amor *et al.*, 2002; Ben-Amor, 2004; Hoefel *et al.*, 2005; Chitarra *et al.*, 2006; Uyttendaele *et al.,* 2008). The potential for staining Gram-negative bacteria with fluorochromes such as cFDA is limited by the more complex membrane structure of these bacteria in comparison to Gram-positive bacteria. The outer membrane of Gram-negative bacteria often prevents the intrusion of hydrophobic macromolecules like cFDA. Therefore, the hydrophobic cFDA is not able to permeate efficiently into cells of Gram-negative bacteria (Shapiro, 2000; Morono *et al.*, 2004). Other limiting factors for staining with cFDA are differences in dye uptake, the capacity for intracellular retention of cF, passive leakage, and the presence of active extrusion pumps (Nebe-von-Caron *et al.*, 2000). Chelating reagents such as EDTA can be used to improve the membrane permeability to cFDA. The aim of this study was to develop a benchmark measurement protocol for viability testing of Gram-negative bacteria by flow cytometry using phytopathogenic *P. carotovorum*.

4.3.1 Alteration of cell membrane permeability

Bacterial suspensions with a calculated OD_{620} of 5.0 were prepared with PBS (untreated sample), TE-buffer (10 mmol l^{-1} TRIS, 0.5 mmol l^{-1} EDTA) or GTA-buffer (94 mmol l^{-1} GTA) to improve cFDA uptake of *P. carotovorum* cells (Figure 4.11).

After 15 min incubation time of 0.05 mmol l^{-1} cFDA and 10 min incubation of 0.03 mmol l^{-1} PI 44.7 % *P. carotovorum* cells in PBS remained unstained. Using TE-buffer instead of PBS reduced the percentage of unstained cells to 33.8 % whereas the percentage of PI-stained cells (cells with permeabilised cell membrane) increased to 18.5 %. In contrast to TE-buffer, 77.7 % unstained cells using GTA-buffer were detected after one-stage cultivation. The percentage of PI-stained cells was higher than the percentage of PI-stained cells of untreated samples but lower than in TE-buffer.

After changing the growth conditions, the percentage of unstained cells was reduced to 15.4% using GTA-buffer but 37.3 % of the cells were highly permeabilised. Neither the reduction of GTA concentration nor the reduction of EDTA concentration improved the cFDA uptake by *P. carotovorum* cells (data not shown).

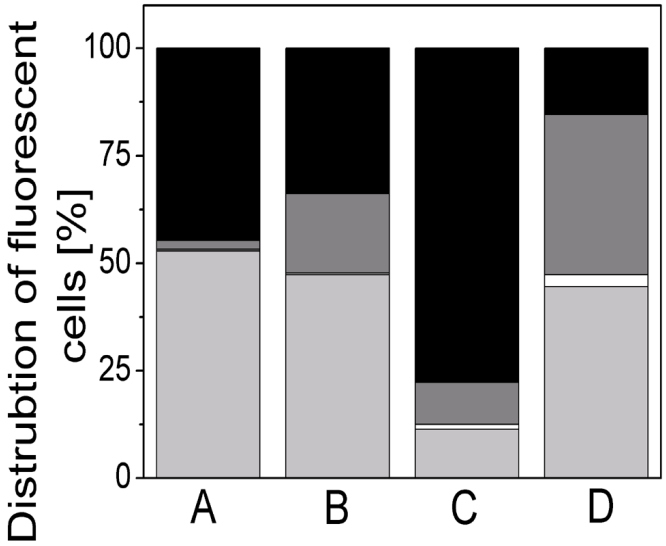

Figure 4.11: Effect of TE-buffer (10 mmol l^{-1} TRIS / 0.5 mmol l^{-1} EDTA) and GTA-buffer (94 mmol l^{-1}) on stainability and viability of *P. carotovorum* in suspension with OD_{620}=5.0 in comparison to untreated cells. Cells were incubated with 0.05 mmol l^{-1} cFDA for 15 min at 37 °C and 0.03 mmol l^{-1} PI was allowed to penetrate permeabilised cells for 10 min in an ice bath. A) Untreated sample, B) TE-buffer, C) GTA-buffer after one-stage-cultivation, D) GTA-buffer after two-stage cultivation. Black bars: cells without fluorescence; dark gray bars: PI-fluorescence; white bars: cF+PI-fluorescence; light gray bars: cF-fluorescence.

Variation of the bacterial optical density in combination with GTA-buffer or TE-buffer also did not increase the cFDA uptake ability of *P. carotovorum*, whereas best staining results were obtained using higher optical densities (Figure 4.12). EDTA permeabilises the outer membrane of Gram-negative bacteria by chelating divalent cations from their binding sites in lipopolysaccharides but leakage of cF was not prevented. Due to the cross-linking of GTA with free amino groups in bacteria cells, the bacteria become more hydrophobic and leakage of cF was prevented (Miyanaga *et al.*, 2007). Although permeability of Gram-negative cell membrane could be increased with TE-buffer and GTA-buffer, the number of dead and damaged cells was increased and consequently, monitoring of inactivation processes was not possible. The high concentration of GTA seems to be toxic to bacteria (Vives-Rego *et al.*, 2000). Monitoring of inactivation processes was not possible, even though the percentage of PI-stained cells slightly decreased with declining GTA concentrations. GTA-induced cell death could not be discriminated from cell death induced by inactivation processes. The disadvantages such as decreasing scatter properties, impossibility of verifying physiological properties and lower fluorescence outweigh the advantages of fixation or permeabilisation of bacteria (Breeuwer *et al.*, 1995).

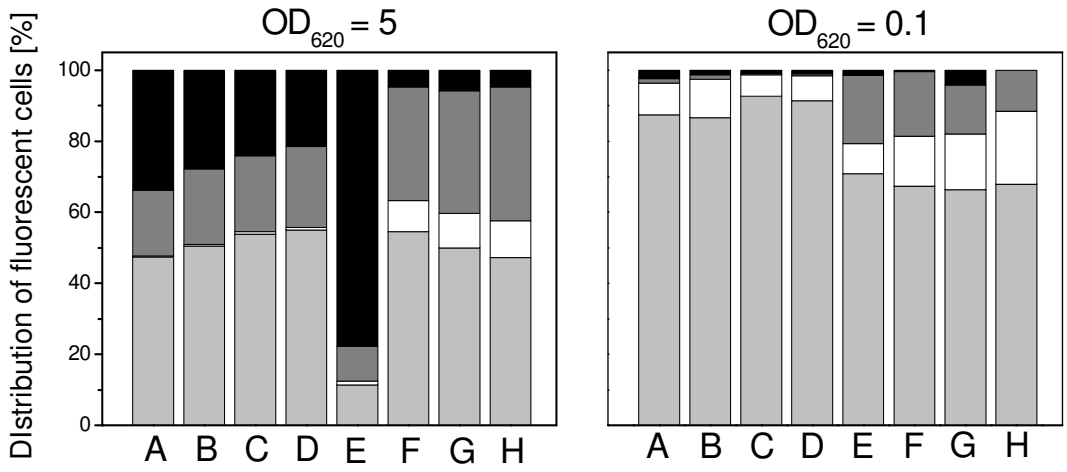

Figure 4.12: Effects of optical density and incubation time on stainability of TE or GTA treated *P. carotovorum* cells. A) TE-buffer, 15 min incubation; B) TE-buffer, 30 min incubation; C) TE-buffer, 45 min incubation; D) TE-buffer, 60 min incubation; E) GTA-buffer, 15 min incubation; F) GTA-buffer, 30 min incubation; G) GTA-buffer, 45 min incubation; H) GTA-buffer, 60 min incubation. Black bars: cells without fluorescence; dark gray bars: PI-fluorescence; white bars: cF+PI-fluorescence; light gray bars: cF-fluorescence.

4.3.2. Optical density, dye concentration, and dye incubation

The influence of bacterial optical densities on cFDA uptake was determined before using GTA-buffer and TE-buffer. Here, different optical densities in combination with different dye concentrations and incubation times were tested for cFDA staining since previous investigations of buffers did not allow the monitoring of process-induced effects on membrane integrity. *P. carotovorum* suspensions were incubated with 0.05 mmol l^{-1} (Figure 4.13) or 0.83 mmol l^{-1} (Figure 4.14) cFDA for 15, 30, 45, or 60 min. The optical densities of the bacterial suspensions were adjusted to 0.5, 1, 2.5, 5.0, 7.5, or 10.

Optical densities below 5.0 led to an increased percentage of unstained cells. In comparison to 85.5 % unstained cells at 0.05 mmol l^{-1} cFDA, the percentage of unstained cells at 0.83 mmol l^{-1} cFDA was 66.1 % at an optical density of 0.5 (45 min incubation time). At optical densities above 5.0 the percentage of cF-stained cells increased with increasing incubation time for both cFDA concentrations. However, incubation times above 45 min impaired the staining results because of the further increase in the percentage of unstained cells. In addition, the percentage of permeabilized cells increased at 0.83 mmol l^{-1} cFDA concentration. The percentage of cF-stained cells at 0.83 mmol l^{-1} cFDA for optical densities above 5.0 was around 95 % for incubation times of 15, 30, and 45 min.

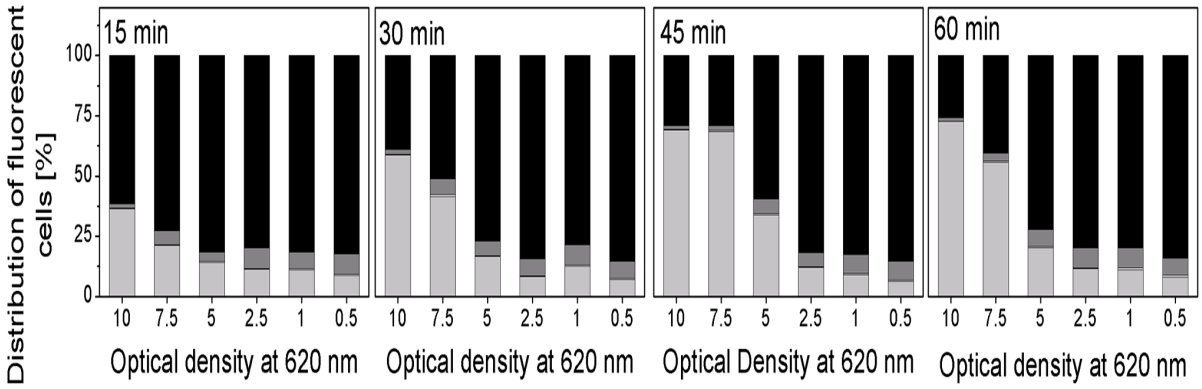

Figure 4.13: Influence of optical density and dye incubation time on stainability of *P. carotovorum*. Cells were incubated with 0.05 mmol l^{-1} cFDA for 15 min, 30 min, 45 min, and 60 min at 37 °C. 0.03 mmol l^{-1} PI was allowed to penetrate permeabilised cells for 10 min in an ice bath. Black bars indicating cells without fluorescence, dark gray bars indicating PI-fluorescence (permeabilised cells), white bars indicating cF+PI-fluorescence (permeabilised cells with esterase activity), light gray bars indicating cF-fluorescence (intact cells with esterase activity). Black bars: cells without fluorescence; dark gray bars: PI-fluorescence; white bars: cF+PI-fluorescence; light gray bars: cF-fluorescence.

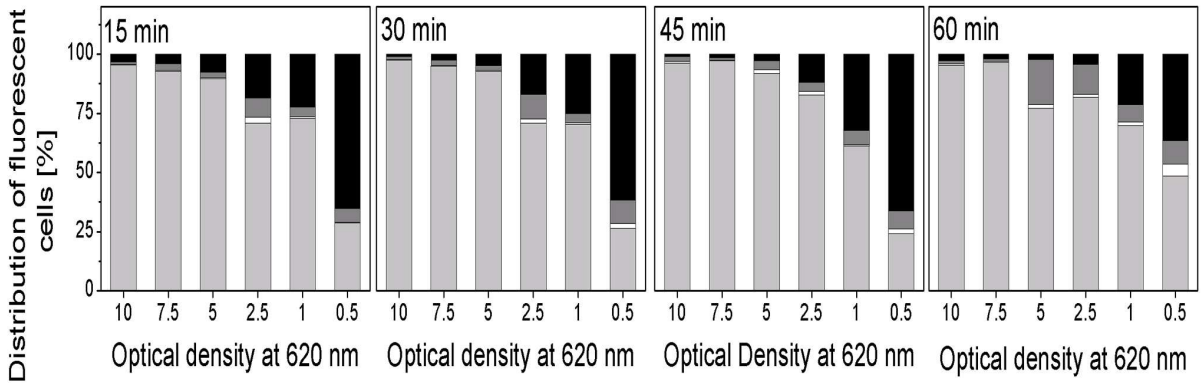

Figure 4.14: Influence of optical density and dye incubation time on stainability of *P. carotovorum*. Cells were incubated with 0.83 mmol l^{-1} cFDA for 15 min, 30 min, 45 min, and 60 min at 37 °C. 0.03 mmol l^{-1} PI was allowed to penetrate permeabilised cells for 10 min in an ice bath. Black bars indicating cells without fluorescence, dark gray bars indicating PI-fluorescence (permeabilised cells), white bars indicating cF+PI-fluorescence (permeabilised cells with esterase activity), light gray bars indicating cF-fluorescence (intact cells with esterase activity). Black bars: cells without fluorescence; dark gray bars: PI-fluorescence; white bars: cF+PI-fluorescence; light gray bars: cF-fluorescence.

It is apparent from the density plot (Figure 4.15) the fluorescence intensity was more homogeneous after 45 min at 37 °C. Below an optical density of 5.0 the influence of the incubation time on stainability is negligible in the case of the application of 0.05 mmol l^{-1} cFDA.

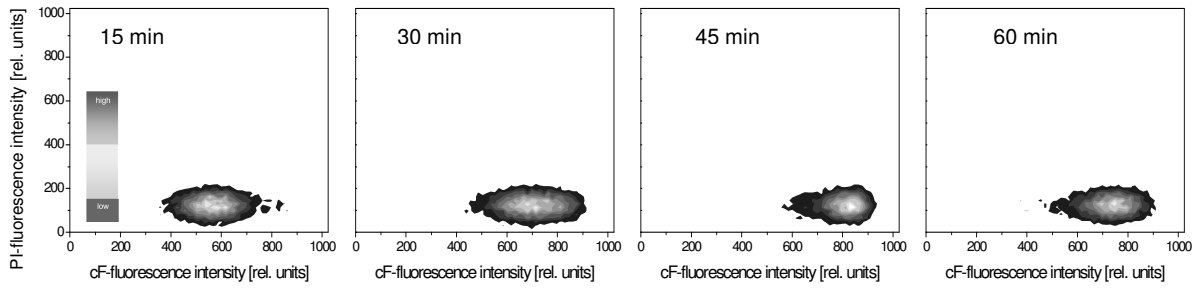

Figure 4.15: Density plots of cF-stained *P. carotovorum* cells after different dye incubation times.

Additional experiments to investigate the cellular retention of accumulated cF in *P. carotovorum* cells were performed using 0.83 mmol l^{-1} cFDA at an incubation temperature of 37 °C for 45 min. Flow cytometric measurements showed that the percentage of unstained cells increased from 1.6 % to 14.3 % after a storage time of 40 min before measurement in comparison to the measurement immediately after the staining procedure (Figure 4.16).

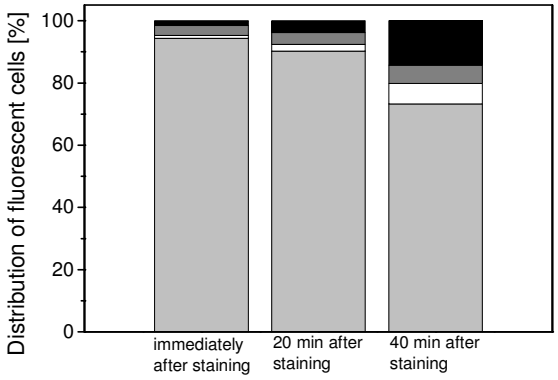

Figure 4.16: Time-dependent cellular retention of accumulated cF in *P. carotovorum* cells. Black bars: cells without fluorescence; dark gray bars: PI-fluorescence; white bars: cF+PI-fluorescence; light gray bars: cF-fluorescence.

As reagent-assisted permeability did not improve cFDA staining of *P. carotovorum*, the influence of optical density, dye concentration, and dye incubation time on stainability was investigated. It was shown that besides the optical density of the bacteria suspension, the dye concentration has an important influence on stainability of *P. carotovorum*. Increased cF-staining of viable *P. carotovorum* cells is caused by higher optical densities and higher dye concentrations. Furthermore, the incubation time of cFDA affects the staining results. With increasing incubation time the percentage of cF-stained cells increased, but above 45 min a

decrease in cF-stained cells was observed. At higher cFDA concentrations the percentage of permeabilised and damaged cells increased. This suggests that high cFDA concentrations in combination with incubation times above 45 min at 37 °C negatively affect the viability of *P. carotovorum* cells. Another explanation of the decreased cF-staining at incubation times > 45 min is the passive or active extrusion of the dye or fluorescent quenching caused by the high intracellular cF concentrations (Breeuwer *et al.*, 1995). Breeuwer *et al.* (1995) suggested that the uptake of cFDA by *Saccharomyces cerevisiae* is a slow passive diffusion process and the transport rate was not saturated at high cFDA concentrations. Hence, higher dye concentrations lead to an enhanced uptake rate through the cell envelope. Assuming comparable transport mechanisms in *P. carotovorum* cells, the more homogenous cF-staining after 45 min can be explained by a slow uptake rate of cFDA. From these experiments the staining parameters for viability testing of *P. carotovorum* with cFDA and PI are set to 0.83 mmol l^{-1} cFDA with an incubation time of 45 min at 37 °C. The optical density of the bacteria suspension had to be adjusted to a value above 5.0 to achieve the best staining results. After dye incubation, the residual cFDA had to be removed by centrifugation before 0.03 mmol l^{-1} PI is added to the sample. PI was allowed to penetrate permeabilised cells for 10 min in an ice bath before flow cytometric measurements.

The investigation of the ability of *P. carotovorum* cells to retain accumulated cF inside the cells reveals that with increased post-staining time the percentage of cF-stained cells decreased. The reduced percentage of cF-stained cells can be explained by passive leakage of cF out of the cells or by active extrusion pumps (Nebe-von-Caron *et al.*, 2000). However, active extrusion is an energy-dependent step, and as, in this study, the cells were not energised by addition of glucose this indicates that the reduced cF-staining is due to passive extrusion. To avoid a reduction of cF-staining the samples should be measured immediately after staining.

4.4. Monitoring of heat treatment by flow cytometry

4.4.1. Morphological changes of heat-treated cells

Morphological characteristics of bacteria before and after heat treatment were observed using the forward scatter and side scatter measurements by flow cytometry. The forward scatter measurements relate to the cell size but are also affected by cell structure or chemical composition (Julia *et al.*, 2000). The side scatter measurements relate to cell granularity and can be seen as a function of the distribution of mass within the cells (e.g. cell walls, nucleotides, ribosomes, cell appendages) which is heterogeneous (Koch *et al.*, 1996).

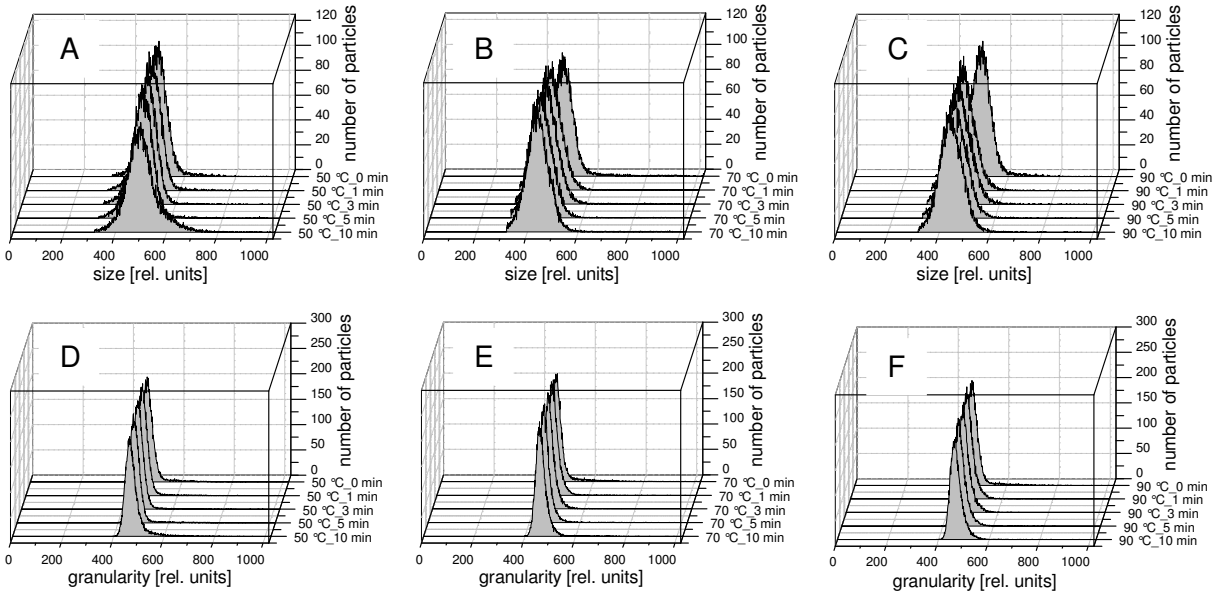

Figure 4.17: Size (A-C) and granularity (D-F) changes of *E. coli* cells after heat treatment at temperatures of 50 °C (A,D), 70 °C (B,E), and 90 °C (C,F).

The size of *E. coli* measured as forward scatter intensity did not change during treatment at 50 °C but at 70 °C and 90 °C the intensity decreased. This implies that the cell size decreased due to the heat treatment. A reduction of cell size was also observed for *Staphylococcus epidermidis* after heat treatment at 60 °C using different light intensities (Broadwater *et al.*, 1973). Generally, it is considered that dead cells have lower forward scatter intensities than viable cells (Shapiro, 2003). The cell granularity of *E. coli* measured as side scatter intensity did not change during heat treatment (Figure 4.17) which implies that the distribution of mass within the cells did not change due to the heat treatment.

The size of *L. innocua* (Figure 4.18) did not change during heat treatment but the forward scatter intensities were lower than the forward scatter intensities of *E. coli*. This implies that *L. innocua* is smaller than *E. coli*. Similar to *E. coli,* the granularity of *L. innocua* did not change during heat treatment. The side scatter intensity of *L. innocua* was at the same level as the scatter intensity of *E. coli*. *P. carotovorum* cells (Figure 4.19) showed the same forward scatter intensity as *E. coli* and the side scatter intensity of *P. carotovorum* is similar to the side scatter intensity of *L. innocua* and *E. coli*. This implies that the size of *E. coli* and *P. carotovorum* is in the same range. Similar to *L. innocua*, the forward scatter intensity and side scatter intensity did not change during heat treatment.

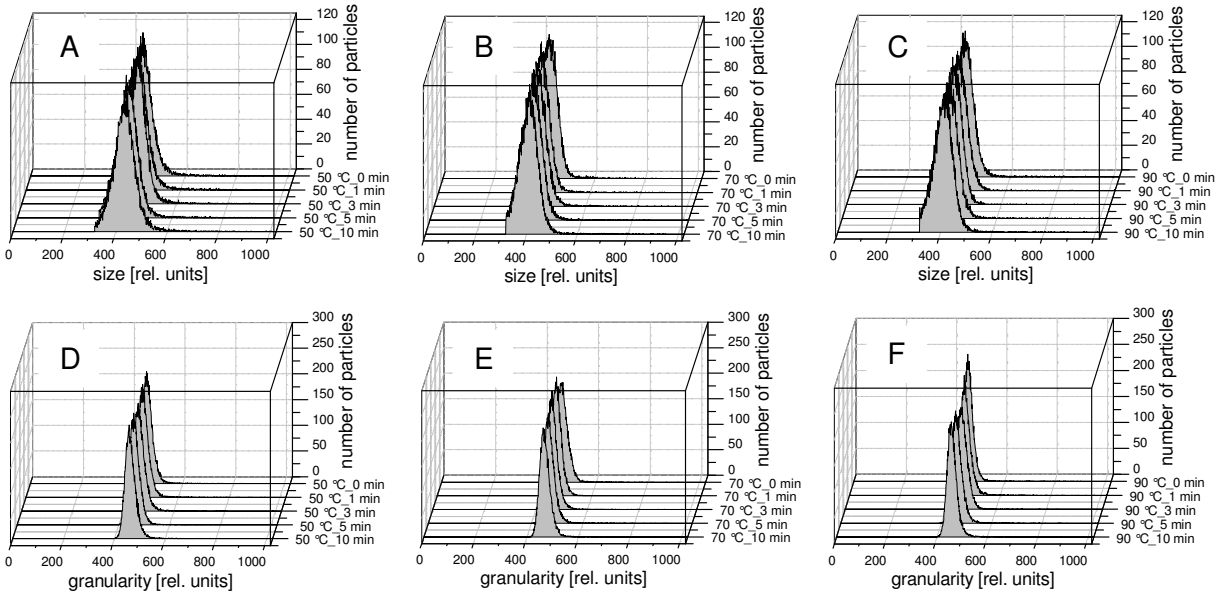

Figure 4.18: Size (A-C) and granularity (D-F) changes of *L. innocua* cells after heat treatment at temperatures of 50 °C (A,D), 70 °C (B,E), and 90 °C (C,F).

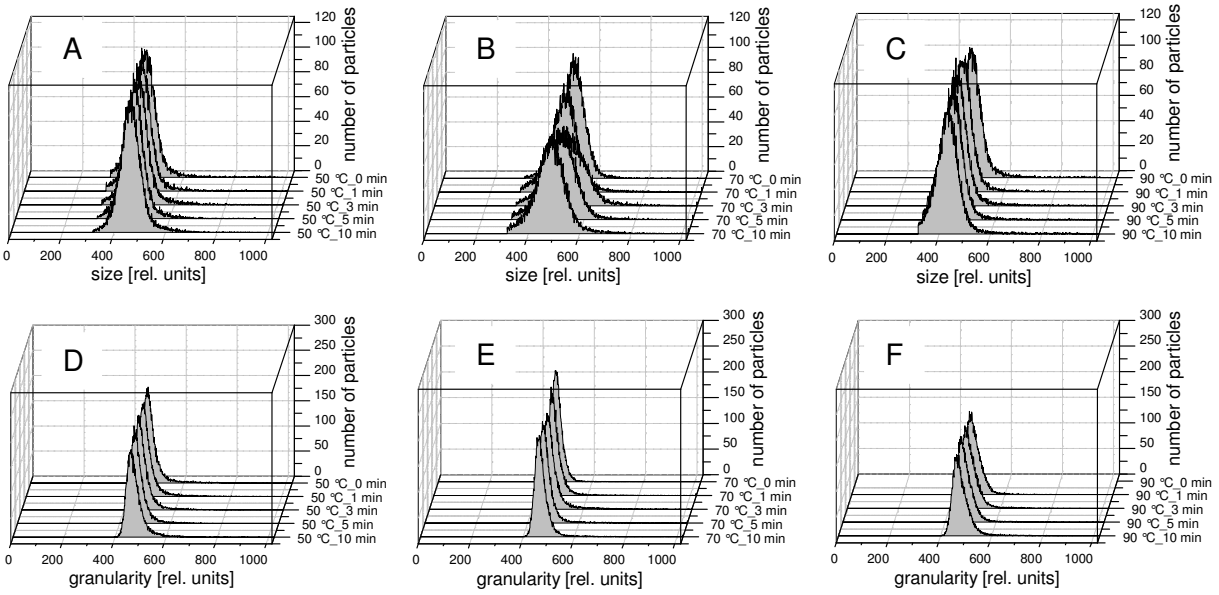

Figure 4.19: Size (A-C) and granularity (D-F) changes of *P. carotovorum* cells after heat treatment at temperatures of 50 °C (A,D), 70 °C (B,E), and 90 °C (C,F).

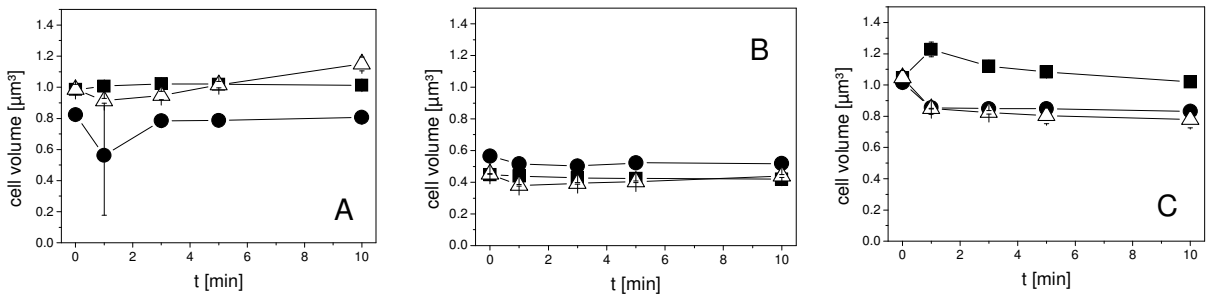

Figure 4.20: Cell volume of *E. coli* (A), *L. innocua* (B), and *P. carotovorum* (C) cells measured by Coulter Counter after heat treatment at 50 °C (squares), 70 °C (circles), and 90 °C (open triangles).

The cell volume of bacteria cells was measured by Coulter Counter before and after heat treatment (Figure 4.20). Similar to the flow cytometric measurements, a smaller cell volume of *L. innocua* in comparison to *E. coli* and *P. carotovorum* was observed. This is in agreement with the literature. According to the Bergey's Manual of Determinative Bacteriology (Holt *et al.*, 2000) the size of *L. innocua* is 0.4-0.5 µm x 0.5-2 µm, the size of *E. coli* is 1.1-1.5 µm x 2-6 µm, and the size of *P. carotovorum* is 0.5-1 µm x 1-3 µm. The cell volume of *E. coli* did not significantly change during heat treatment at 50 and 70 °C whereas at 90 °C the cell volume significantly increased. The cell volume of *L. innocua* significantly decreased during heat treatment at all tested temperatures and significant changes in cell volume were also observed for *P. carotovorum*. Thereby, the cell volume increased at 50 °C whereas a decrease was found at 70 and 90 °C. This is in contrast to the flow cytometric measurements where decreased forward scatter intensity was only observed for *E. coli* at 90 °C indicating reduced cell volume. Thus, a correlation of Coulter Counter measurements and flow cytometric measurements is not possible. Although differences in forward scatter intensities for the bacteria indicated the smaller cell volume of *L. innocua* in contrast to *E. coli* and *P. carotovorum*, the changes in cell volume detected by Coulter Counter after heat treatment could not be observed by flow cytometry. This may be explained with the dependence of the forward scatter intensity on cell size as well as on cell structure. The measured forward scatter intensity cannot be directly translated into cell size. Measurements with polystyrene beads of different sizes indicated that beads with smaller size can result in higher forward scatter intensities than beads with higher size (Shapiro, 2003). Even though the correlation of Coulter Counter measurements and flow cytometric measurements is difficult, morphological changes of bacteria after heat treatment can be observed by flow cytometry. However, the changes in forward scattered light may not be caused by changes in cell volume or refractive index (Scherer *et al.*, 1999). McGann *et al.* (1988), for example, concluded that cell volume and forward scatter intensities can vary independently.

4.4.2 Membrane integrity of heat-treated cells

Membrane integrity is an important task in cell viability. Therefore, the membrane integrity after heat treatment was tested using TO and PI in combination (Figure 4.21).

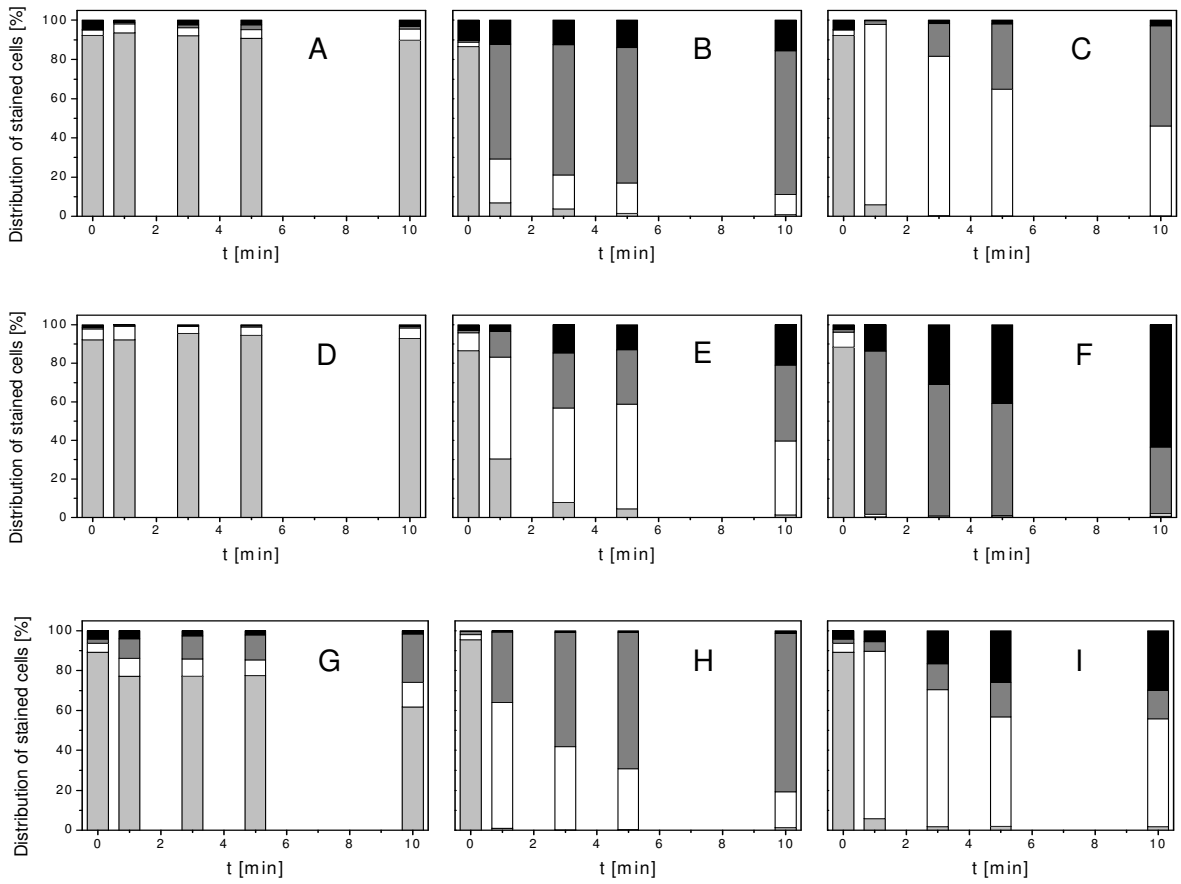

Figure 4.21: Membrane integrity of *E. coli* (A-C); *L. innocua* (D-F), and *P. carotovorum* (G-I) cells after heat treatment at 50 °C (A,D,G), 70 °C (B,E,H), and 90 °C (C,F,I). Black bars indicating cells without fluorescence, dark gray bars indicating PI-fluorescence (permeabilised cells), white bars indicating TO+PI-fluorescence (slightly permeabilised cells), light gray bars indicating TO-fluorescence (cells with membrane integrity). The standard deviation of the measurements is given in Annex 1 (Tables 1-3).

At 50 °C the percentage of TO-stained cells remained almost constant above 90 % for *E. coli* and *L. innocua* whereas the percentage of TO-stained *P. carotovorum* cells decreased by approximately 30 % during heat treatment at 50 °C for 10 min. The percentage of TO+PI-stained cells and PI-stained cells increased concurrently whereas the percentage of PI-stained cells was higher than the percentage of TO+PI-stained cells. Consequently, *E. coli* and *L. inncoua* cells remained intact during heat treatment at 50 °C while the cell membrane of certain *P. carotovorum* cells is affected by the heat treatment at 50 °C. Increasing the treatment temperature to 70 °C and 90 °C reduced the percentage of intact bacteria cells to approximately 1 % within 10 min of treatment. The distribution of TO+PI-stained and PI-

stained cells varied with different bacteria and applied treatment temperatures. At 70 °C the percentage of PI-stained *E. coli* and *P. carotovorum* cells predominated over the percentage of TO+PI-stained cells while at 90 °C the percentage of TO+PI-stained cells predominated. Additionally, the percentage of unstained *P. carotovorum* cells increased at 90 °C. In contrast, the percentage of TO+PI-stained *L. innocua* predominated at 70 °C. At 90 °C less than 2 % TO-stained and TO+PI-stained cells were detected while the percentage of unstained cells increased with increasing treatment time. This implies that the bacteria cells are affected differently by the heat. The inhomogeneous distribution of stained cells indicates that the cells were not homogeneously affected by the heat treatment. This assumption follows the probabilistic concept that not all cells behave in the same way and do not have the same probability of dying due to a lethal event (van Boekel, 2002).

The observed increase in the percentage of unstained cells may be due to a heat-induced damage of DNA and RNA. Damage of DNA and RNA has been shown in several studies (Miller & Ordal, 1972; Mackey *et al.*, 1991; Earnshaw *et al.,* 1995; Nguyen *et al.*, 2006). Both PI and TO intercalate with DNA and RNA and an unfolding of DNA and RNA or the production of subunits due to heat-induced stress may destroy target side. Therefore, an intercalation of fluorescent dye and nucleic acids is prevented. Another explanation for the high percentage of unstained cells might be a coagulation of membrane proteins at high temperatures which inhibits the uptake of TO and PI. The high percentage of TO+PI-stained *E. coli* and *P. carotovorum* cells at 90 °C indicated that the cells were only slightly permeabilised in contrast to the heat treatment at 70 °C. A third explanation may be a different production of nucleic subunits at different temperature levels. The ability of TO and PI to intercalate with subunits may vary resulting in a divers distribution of stained cells. However, it is more likely that the degree of membrane permeabilisation influences the distribution of stained cells. TO enters the cells slower than PI and Gram-negative bacteria interfere with the uptake of TO due to lipopolysaccharides (LPS) on the membrane (Alsharif & Godfrey, 2002).

At 70 °C a permeabilised cell membrane enables a fast penetration of PI while TO slowly enters the cells and therefore, PI can intercalate with the DNA or RNA before TO entered the cells. In contrast, at 90 °C the cell membrane is highly permeabilised and TO and PI can enter the cells simultaneously and intercalate with the nucleic acids resulting in double-stained cells. However, the mean TO-fluorescence intensity of *E. coli* and *P. carotovorum* at 90 °C significantly decreased in comparison to the untreated samples (Tables 4.14 to 4.16).

Table 4.14: Mean TO-fluorescence intensity of *E. coli* cells after thermal treatment at different temperature levels

Treatment time [min]	50 °C		70 °C		90 °C	
	Mean fluorescence intensity [rel. units]	SD	Mean fluorescence intensity [rel. units]	SD	Mean fluorescence intensity [rel. units]	SD
0	573.2[a]	± 48.2	527.6[a]	± 51.7	573.2[a]	± 48.2
1	299.6[b]	± 5.6	322.4[b]	± 19.5	397.3[b]	± 129.7
3	348.5[b]	± 39.5	302.9[b]	± 33.8	149.8[c]	± 14.9
5	358.2[b]	± 20.3	270.3[b,c]	± 20.3	101[c]	± 22.3
10	469[b]	± 77.5	211.7[c]	± 14.9	71.6[c]	± 4.6

SD, Standard deviation of three independent experiments
[a-c], Different letters within the columns indicate significant differences at a significance level of 0.05

The fluorescence intensity of a TO-DNA or TO-RNA complex is enhanced in comparison to unbound TO (Nygren et al., 1998). Therefore, the significantly lower mean TO-fluorescence intensity may indicate that the dye penetrated the cells but did not intercalate with the DNA or RNA. Hence, the measured TO-fluorescence can correspond to the fluorescence intensity of unbound TO adherent to the cells or cell fragments.

Table 4.15: Mean TO-fluorescence intensity of *L. innocua* cells after thermal treatment at different temperature levels

Treatment time [min]	50 °C		70 °C		90 °C	
	Mean fluorescence intensity [rel. units]	SD	Mean fluorescence intensity [rel. units]	SD	Mean fluorescence intensity [rel. units]	SD
0	166.1[a]	± 16.9	400.6[a]	± 136.8	143.3[a,c]	± 29.8
1	175.9[a,c]	± 16.9	293.1[a,b]	± 29.3	140[a,c]	± 24.6
3	276.8[b,c]	± 31.4	185.6[b]	± 0	159.6[a,b,c]	± 74
5	267[b,c]	± 20.3	159.6[b]	± 5.6	312.6[b,c]	± 19.5
10	228[c]	± 20.3	123.8[b]	± 20.3	211.7[c]	± 98.8

SD, Standard deviation of three independent experiments
[a-c], Different letters within the columns indicate significant differences at a significance level of 0.05

A significant decrease of mean TO-fluorescence intensity was also observed for *E. coli* at 50 °C (Table 4.14). This suggests that the interference of TO with LPS is enhanced at mild heat treatments and lower amounts of TO entered the cells.

Table 4.16: Mean TO-fluorescence intensity of *P. carotovorum* cells after thermal treatment at different temperature levels

Treatment time [min]	50 °C		70 °C		90 °C	
	Mean fluorescence intensity [rel. units]	SD	Mean fluorescence intensity [rel. units]	SD	Mean fluorescence intensity [rel. units]	SD
0	915.1[a]	± 53.8	830.5[a]	± 188.5	915.1[a]	± 53.8
1	1351.5[b]	± 37	267[b]	± 20.3	211.7[b]	± 148
3	1084.5[c]	± 68.4	159.8[b]	± 14.9	110.7[b]	± 5.6
5	882.6[a]	± 45.1	140[b]	± 31.4	97.7[b]	± 9.8
10	1227.8[b]	± 48.2	175.9[b]	± 58.6	94.4[b]	± 11.3

SD, Standard deviation of three independent experiments
[a-c], Different letters within the columns indicate significant differences at a significance level of 0.05

In contrast, the mean TO-fluorescence intensity of *L. innocua* (Table 4.14) and *P. carotovorum* (Table 4.16) was significantly higher with increasing time at 50 °C which may be due to the measurement of the higher fluorescent DNA-TO complex instead of a lower fluorescent TO-RNA complex. This implies that the RNA may already be affected at mild heat treatments. Similar to *E. coli* and *P. carotovorum*, higher treatment temperatures led to significantly decreased TO-fluorescence intensity of *L. innocua.* These results indicate that the membrane integrity of Gram-negative and Gram-positive bacteria is differently affected by heat treatment.

4.4.3 Esterase activity and pump activity of heat-treated bacteria

The metabolic activity reflected by esterase activity was measured using cFDA and PI in combination (Figure 4.22). At 50 °C the percentage of intact cells with esterase activity remained almost constant above 80 % for *E. coli* and *L. innocua*. The distribution of cF- and PI-stained *P. carotovorum* cells was also constant during heat treatment at 50 °C whereas high percentages of cF+PI-stained and PI-stained cells were already detected for the untreated sample. This may be attributed to the additional centrifugation steps needed for efficient staining with cF whereas *P. carotovorum* seems to be the most sensitive. In contrast to the membrane integrity measurements using TO and PI the percentage of intact cells was lower and slightly permeabilised cells could be observed. Increasing temperature to 70 °C reduced the percentage of cF-stained *E. coli* and *P. carotovorum* cells below 1 %. The percentage of cF+PI-stained and PI-stained cells increased concurrently after one treatment minute. With increasing treatment time the percentage of double-stained cells decreased again but the percentage of PI-stained cells further increased. Ultimately, the percentage of cF+PI-stained *P. carotovorum* cells was higher than the percentage of cF+PI-stained *E. coli* cells. In contrast, 26.2 % of *L. innocua* cells remained intact with esterase activity after 1 min treatment at 70 °C and fewer cells were completely permeabilised. This indicates that the

bacteria cells were not homogenously affected by the heat and some bacteria remained viable even after 1 min at 70 °C. With increased treatment time the percentage of cF-stained and cF+PI-stained cells decreased and the percentage of PI-stained cells increased. Similar results were obtained for *Lactococcus lactis* after heat treatment at 70 °C for 10 min. No esterase activity was detected after the treatment but a complete staining with PI indicating major membrane damage was detected (Bunthof *et al.*, 1999).

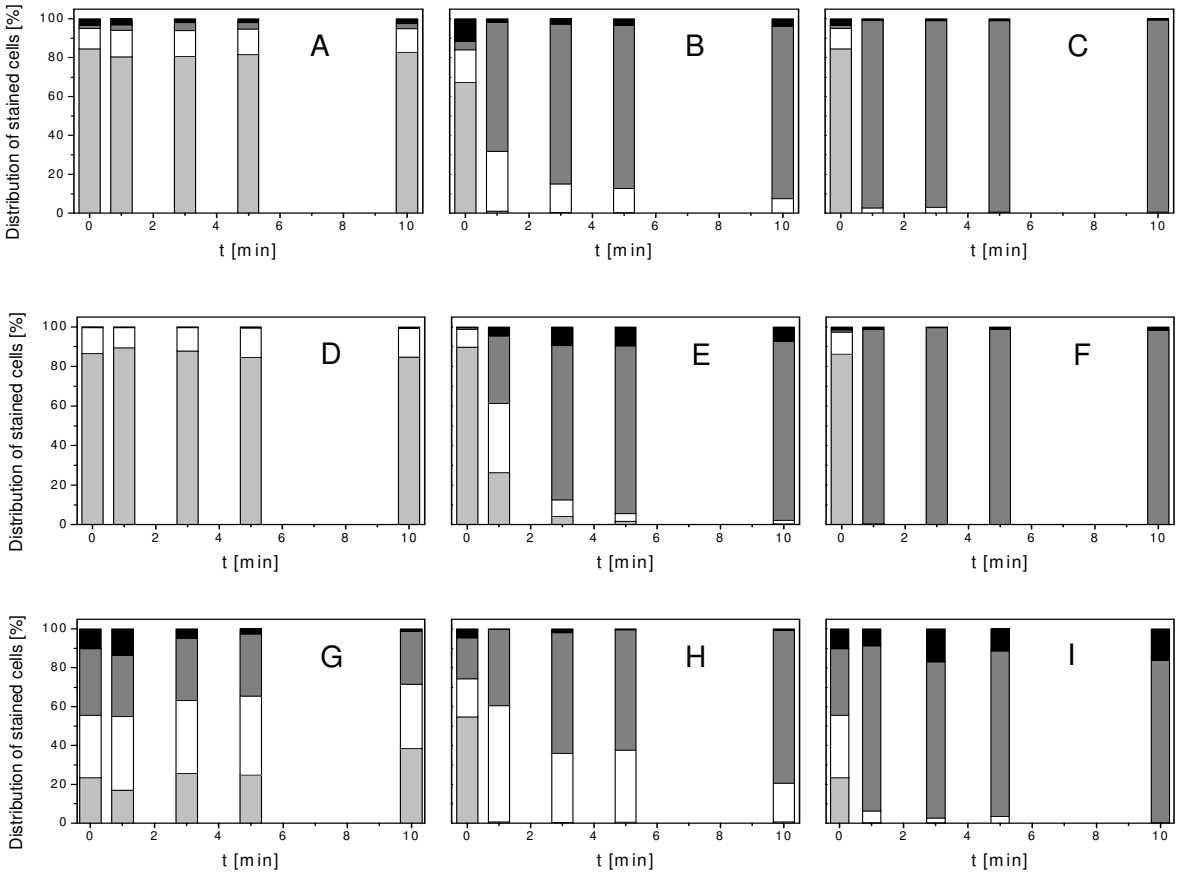

Figure 4.22: Esterase activity and membrane integrity of *E. coli* (A-C); *L. innocua* (D-F), and *P. carotovorum* (G-I) cells after heat treatment at 50 °C (A,D,G), 70 °C (B,E,H), and 90 °C (C,F,I). Black bars indicating cells without fluorescence, dark gray bars indicating PI-fluorescence (permeabilised cells), white bars indicating cF+PI-fluorescence (permeabilised cells with esterase activity), light gray bars indicating cF-fluorescence (intact cells with esterase activity). The standard deviation of the measurements is given in Annex 2 (Tables 4-6).

At 90 °C all bacteria cells were permeabilised after 1 treatment minute but residual esterase activity could be observed for *E. coli* and *P. carotovorum* cells after 3 min. The results suggest that cellular esterase can still be active after heat treatment at 70 °C even if the cell membrane is slightly permeabilised. In other studies, heat-induced cell death of *Lactobacillus planatarum, E. coli, Lactococcus lactis*, and *Lactococcus rhamnosus* was achieved in the absence of cell permeabilisation (Lievense *et al.*, 1994; Jepras *et al.*, 1995; Bunthof *et al.*,

1999; Ananta & Knorr, 2009) however, the applied temperatures were between 50 and 70 °C and the treatment procedure was different from the applied procedure in this study. *Listeria monocytogenes* showed no esterase activity after mild heat treatment at 60 °C for 20 min but the population could be divided into a fraction with major membrane damage and cells without membrane damage (Uyttendaele *et al.*, 2008).

Bunthof *et al.* (1999) suggested that the cF-labelled fraction cannot be an indicator for cell viability and reproducibility because it did not correlate with the results of plate count analyses. It was proposed that the cF-Efflux capacity of bacteria cells upon energising should be used as an additional measure of cell viability. However, the same author (Bunthof, 2002) introduced a scheme of bacterial physiological fitness (see section 2.6.3). Therein, the cells can maintain esterase activity without having reproducibility and while retaining a viable state. cF-Efflux activity of heat treated cells was investigated in this study to obtain additional information about the viability status of the test microorganism. At 50 °C the cF-fluorescence intensity of *E. coli* (Figure 4.23) and *P. carotovorum* (Figure 4.25) decreased upon energising with glucose indicating cF-Efflux capacity of the cells. But at treatment times above 3 min a subpopulation of *P. carotovorum* could be detected which was not able to exclude cF. At 90 °C the treated cells did not show esterase activity and therefore, cF-Efflux capacity was not tested. At 70 °C cF-Efflux activity was tested because a few cells showed cF-fluorescence after treatment. The energising of cF-labelled cells did not result in decreased cF-fluorescence intensity. In contrast, enhanced fluorescence intensity in comparison to non-energised cF-labelled cells was detected. The cF-Efflux ability of *L. innocua* (Figure 4.24) was different in comparison to *E. coli* and *P. carotovorum*. At 50 °C the cF-fluorescence intensity was enhanced upon energising with glucose as previously shown for heat-treated *E. coli* and *P. carotovorum* cells at 70 °C. Increasing temperature to 70 °C showed the same effect of cF-fluorescence intensity upon energising of cells as was observed at 50 °C. These results indicate that *L. innocua* did not have pump activity at either the untreated nor at the treated state. But *E. coli* and a subpopulation of *P. carotovorum* were able to exclude cF after treatment at 50 °C. Enhanced cF-Fluorescence intensity upon energising of *E. coli* and *P. carotovorum* at 70 °C and *L. innocua* at 50 and 70 °C may lead to the assumption that esterase was activated upon energising and more cFDA could be hydrolysed to cF but the accumulated cF could not be excluded. Although the excessive cFDA was removed by centrifugation before energising higher cF-fluorescence intensity was observed after incubation with glucose. A possible explanation for the phenomenon can be delayed hydrolyses of intracellular cFDA. The cFDA diffused into the cells during incubation time but was not hydrolysed by esterase. During the centrifugation step the cFDA was not removed and was retained within the cells. Upon energising and additional incubation residual

esterase may have hydrolysed the cFDA or a spontaneous hydrolyses occurred. Spontaneous hydrolyses of cFDA in aqueous suspension was previously observed by Hoefel *et al.* (2003). A quenching of cF-fluorescence at high intracellular concentrations was observed for *Saccharomyces cerivisiae* (Breeuwer *et al.*, 1995). A quenching of cF-fluorescence may also explain the lower fluorescence intensity of *L. innocua* cells at 50 °C before the addition of glucose. Due to the energising a part of the accumulated cF was excluded from the cells and the quenching effect was reduced. Thus, the cF-fluorescence intensity increased instead of the expected decrease. At temperatures above 70 °C a heat inactivation of esterase is more likely and the increased fluorescence intensity seems to be the result of spontaneous hydrolysis because the observed cF-fluorescence intensity was very low upon energising and before energising no cF-fluorescence intensity was detected.

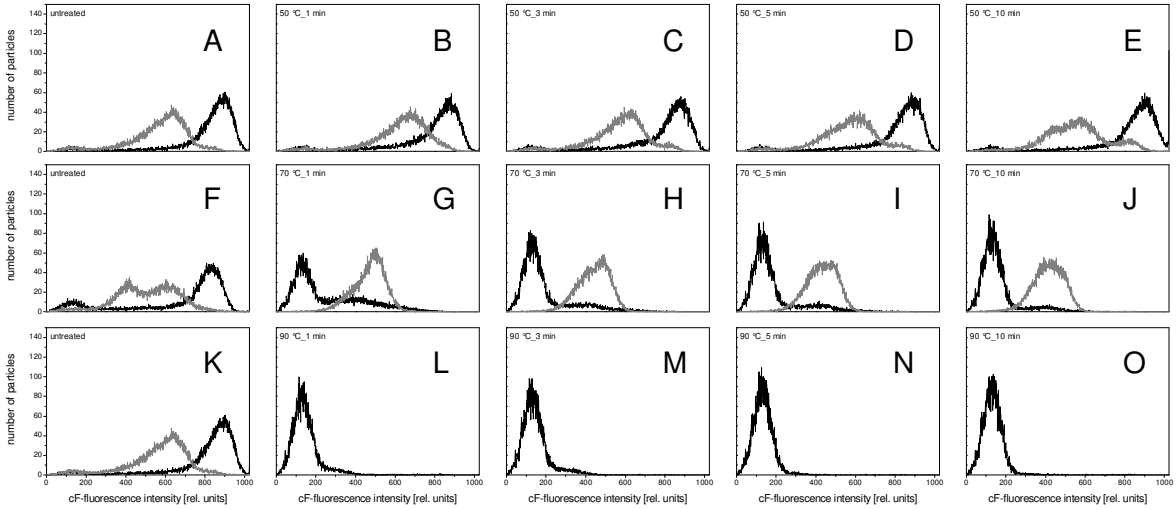

Figure 4.23: Pump activity of *E. coli* cells measured as cF-efflux capability after heat treatment at 50 °C (A-E), 70 °C (F-J), and 90 °C (K-O). Black lines represent the cF-fluorescence intensity before energising and grey lines represent cF-fluorescence intensity after energising.

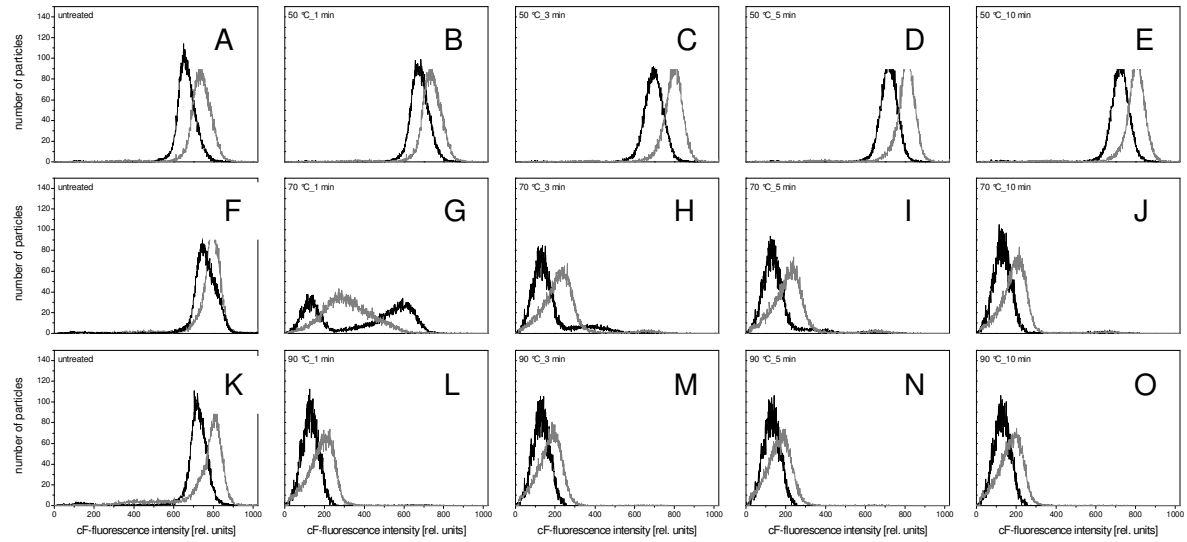

Figure 4.24: Pump activity of *L. innocua* cells measured as cF-efflux capability after heat treatment at 50 °C (A-E), 70 °C (F-J), and 90 °C (K-O). Black lines represent the cF-fluorescence intensity before energising and grey lines represent cF-fluorescence intensity after energising.

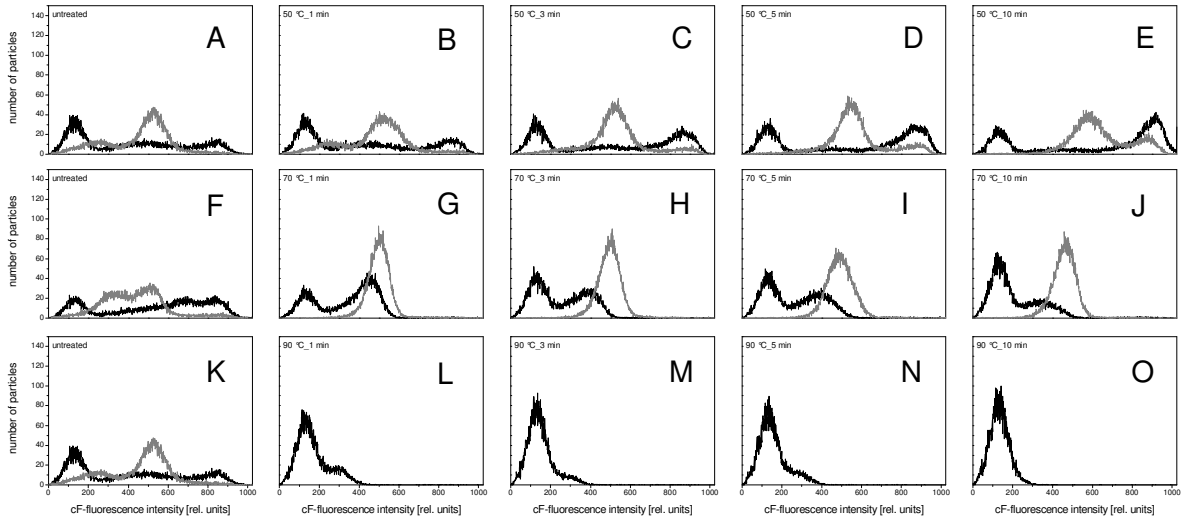

Figure 4.25: Pump activity of *P. carotovorum* cells measured as cF-efflux capability after heat treatment at 50 °C (A-E), 70 °C (F-J), and 90 °C (K-O). Black lines represent the cF-fluorescence intensity before energising and grey lines represent cF-fluorescence intensity after energising.

4.4.4 Membrane potential of heat-treated cells

The cF-Efflux is assumed to be mediated by an ATP-driven transport system (Bunthof *et al.*, 2000) and the transport of cF is driven by the membrane potential and/or pH gradient (Breeuwer *et al.*, 1994). To obtain additional information about cell viability the membrane potential of cells were measured after heat treatment using the radiometric method described by Novo *et al.* (1999), applied with some modifications. The measured ratio of red and green $DiOC_2(3)$ fluorescence was highest for *E. coli* and lowest for *L. innocua* (Figure 4.26 A,B). At

50 °C the red/green ratio remained almost constant for *E. coli,* for *L. innocua* the red/green ratio decreased after 3 min at 50 °C and a decrease of red/green ratio was observed after 1 min at 50 °C for *P. carotovorum* (Figure 4.26 C). At 70 and 90 °C all tested bacteria showed a red/green ratio ≤ 1. This indicates that the bacteria were not able to generate a membrane potential after heat treatment at 70 °C and 90 °C and it is also reduced at 50 °C and treatment times above 1 min (*P. carotovorum*) and 3 min (*L. innocua*). A loss of membrane potential at 50 to 70 °C was found for *E. coli* using the fluorescent dyes Rhodamine 123 and $DiOC_6(3)$ (Baatout *et al.*, 2005).

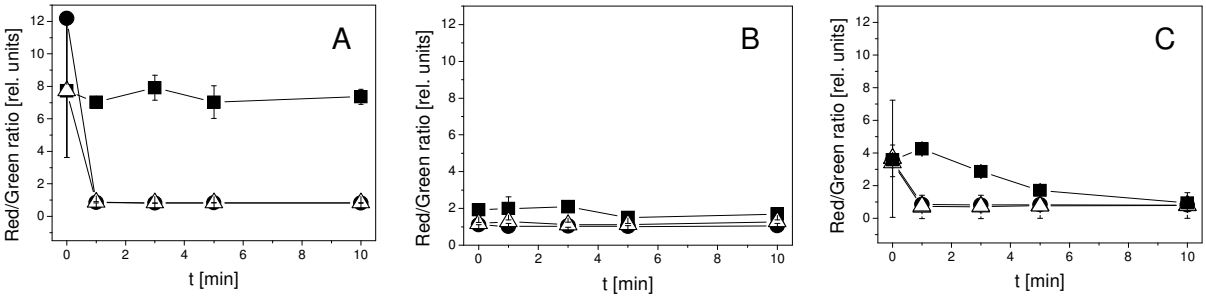

Figure 4.26: Membrane potential of *E. coli* (A), *L. innocua* (B), and *P. carotovorum* (C) cells after heat treatment at 50 °C (squares), 70 °C (circles), and 90 °C(open triangles) expressed as red/green ratio of $DiOC_2(3)$ fluorescence.

The loss of membrane potential at 70 and 90 °C corresponds with the loss of cF-Efflux ability for all tested bacteria. Accordingly, the loss of membrane potential of *P. carotovorum* cells at 50 °C and treatment times above 1 min could explain the subpopulation that was not able to exclude cF. The red/green ratio of *L. innocua* is very low even in untreated cells. This implies that the cells were either not possible to generate a membrane potential or the applied staining procedure is not suitable for these cells. However, the potential for a reliable determination of membrane potential of *L. innocua* after heat treatment with this procedure seems to be limited.

4.4.5 Impact of heat treatment on bacteria cells

It was shown that the membrane integrity, esterase activity, pump activity, and membrane potential of bacteria cells are affected by heat treatment at different temperatures. In order to evaluate critical temperatures as well as differences in inactivation effects on Gram-negative and Gram-positive bacteria the kinetics obtained were described using common mathematical models in a first approach. Kinetics with an increasing shape were modelled either with the Gompertz model or a logistic model using Origin® software. Kinetics with a

decreasing shape were modelled with the GInaFiT tool and the best fitting model was chosen according to the RMSE. An overview of the models used is given in table 4.17.

Table 4.17: Mathematical models used for the modeling of bacterial physiological parameters after thermal treatment

	Membrane permeabilisation	Membrane potential	Esterase activity
E. coli			
50 °C	log-linear regression	Gompertz	log-linear regression
70 °C	Gompertz	log –linear + tail	biphasic
90 °C	Gompertz	log –linear + tail	Log –linear + tail
L. innocua			
50 °C	log-linear regression	log-linear regression	log-linear regression
70 °C	Gompertz	log –linear + tail	biphasic
90 °C	Gompertz	log-linear regression	log –linear + tail
P. carotovorum			
50 °C	Gompertz	log-linear regression	log-linear regression
70 °C	Gompertz	log –linear + tail	log –linear + tail
90 °C	Gompertz	log –linear + tail	biphasic

The degree of complete membrane permeabilisation for all bacteria obtained by TO/PI-staining could be described with the Gompertz model with the exception of the kinetic obtained for *E. coli* and *L. innocua* at 50 °C which could be described with a log-linear regression model. Membrane permeabilisation of *Saccharomyces cerivisiae* after supercritical CO_2 pasteurisation was described with the Gompertz model by Spilimbergo *et al.* (2009). The permeabilisation rate of *L. innocua* became greater with increasing temperatures (Table 4.18). The permeabilisation rate of *E. coli* (Table 4.18) and *P. carotovorum* (Table 4.18) increased at 70 °C in comparison to 50 °C but at 90 °C the rate of permeabilisation was lower than at 70 °C. The low permeabilisation rate of *E. coli* and *P. carotovorum* at 90 °C can be explained by the increasing amount of TO+PI-stained cells. These cells are not included in the modelling and therefore an underestimation of permeabilisation rate may occur.

Table 4.18: Statistical measures and parameter values obtained from mathematical models for experimental data of thermal inactivated *E. coli*, *L. innocua*, and *P. carotovorum* (plate count and flow cytometry)

Target site	*E. coli*			*L. innocua*			*P. carotovorum*		
	50 °C	70 °C	90 °C	50 °C	70 °C	90 °C	50 °C	70 °C	90 °C
Microbial reduction [k_{max} min^{-1}]	0.00	7.21	6.91	0.01	25.44	15.83	0.01	13.70	24.84
Membrane permeabilisation [k_{max} min^{-1}]	0.00	6.13*	1.09*	0.00*	0.33*	19.94*	0.01	2.69*	1.06*
Membrane potential [k_{max} min^{-1}]	1.18*	6.16	5.19	0.02	10.34	0.00	0.15	4.47	16.30
Esterase activity [k_{max} min^{-1}]	0.00	5.03 0.29	9.76	0.00	1.4 0.28	7.77	0.06*	5.41	5.75 0.26

* indicates positive slopes of kinetics

The modelling of membrane potential of *L. innocua* was restricted due to the low values. Nevertheless, at 50 °C the decrease rate of the membrane potential obtained by the log-linear regression model was lower than the decrease rate at 70 °C obtained by the log-linear model with tailing. At 90 °C the membrane potential was constant at a low level and thus, no decrease of membrane potential could be observed using the log-linear regression model (Table 4.18). The membrane potential of *E. coli* at 50 °C could be modelled with the Gompertz model and the log-linear model with tailing was successfully applied to membrane potential kinetics at 70 °C and 90 °C. The membrane potential of *P. carotovorum* at 50 °C followed a log-linear regression and at 70 and 90 °C the membrane potential kinetics could be described with the log-linear model with tailing. According to the models applied the rate of decrease in membrane potential of *E. coli* (Table 4.18) and *P. carotovorum* (Table 4.18) increased with increasing temperatures. Thereby, the membrane potential of *L. innocua* decreased faster than the membrane potential of *P. carotovorum* and *E. coli*.

The esterase activity of *E. coli* (Table 4.18) and *L. innocua* (Table 4.18) was modelled using the log-linear regression model, a biphasic model and the log-linear model with tailing for temperatures of 50 °C, 70 °C, and 90 °C, respectively. Esterase activity of *P. carotovorum* at 50 °C was modelled using the log-linear regression model, at 70 °C the log-linear regression model with tailing was used and at 90 °C the reduction of esterase activity followed a biphasic shape (Table 4.18). The reduction rate of esterase activity was, therefore, highest for *E. coli* and lowest for *P. carotovorum* at 90 °C. At 70 °C the lowest reduction rate of esterase activity could be observed for *L. innocua*.

It is assumed that heat inactivation affects several target sites in bacteria (Earnshaw *et al.*, 1995) and the main cause of heat-induced cellular death is not clearly defined (Uyttendaele *et al.*, 2008). The comparison of heat-induced physiological changes that were measured by flow cytometry supports the assumption that there areseveral cellular target sites for heat treatment. It was shown that heat treatment at 50 °C did not lead to remarkable losses of physiological properties in all tested bacteria. The mode of action of heat treatment at 70 °C for *E. coli* in descending order is as follows: loss of culturability, loss of membrane potential, loss of membrane integrity and finally loss of esterase activity. The same order was found for *L. innocua* at 70 °C with the exception that the loss of esterase activity is faster than the loss of membrane integrity. For the *P. carotovorum* cells at 70 °C the loss of culturability is followed by the loss of esterase activity, the loss of membrane potential and the loss of membrane integrity. The inactivation pathways at 90 °C were different for all tested bacteria. *E. coli* showed a loss of esterase activity followed by a loss of culturability, loss of membrane potential and loss of membrane integrity. *L. innocua* showed a loss of membrane integrity at first followed by the loss of culturability, the loss of esterase activity and loss of membrane

potential. Finally, *P. carotovorum* losses its culturability at first followed by a loss of membrane potential, loss of esterase activity and loss of membrane integrity. In these results the permeabilised cells, slightly permeabilised cells with esterase activity and unstained cells were not taken into account. It was not possible to model the kinetics of these cells with the common mathematical models. But it could be shown that the different bacteria react differently to various temperature levels and this has to be considered in decontamination processes.

4.5 Flow cytometric analysis of PAA-treated bacteria cells

4.5.1 Morphological changes of PAA-treated cells

PAA treatment of *E. coli* at different temperature levels and different PAA concentrations led to significantly enhanced cell volume of the cells as observed by Coulter Counter measurements (Figure 4.27). The increase in cell volume seems to be independent of PAA concentrations. The cell volume of untreated *E. coli* cells before PAA treatment is smaller than the cell volume of untreated *E. coli* detected before heat treatment. This implies that the temperature has a high impact on cell volume. The cell suspension before heat treatment had a temperature of approximately 22 °C whereas the temperature of the cell suspensions before PAA treatment was between 0 and 20 °C. In the presence of sodium thiosulfate the cell volume of untreated *E. coli* cells was in the same range as PAA-treated cells. This implies that the cell volume increased due to the higher availability of nutrients. However, the low pH during PAA treatment may also influence the cell volume. Another factor influencing cell volume could be the use of potable water. The concentration of PAA was adjusted using potable water whereas the heat treatment was performed in PBS. It has been shown that cells cultivated in rich medium had larger cell sizes than cells obtained from environmental samples (Torrella & Morita, 1981).

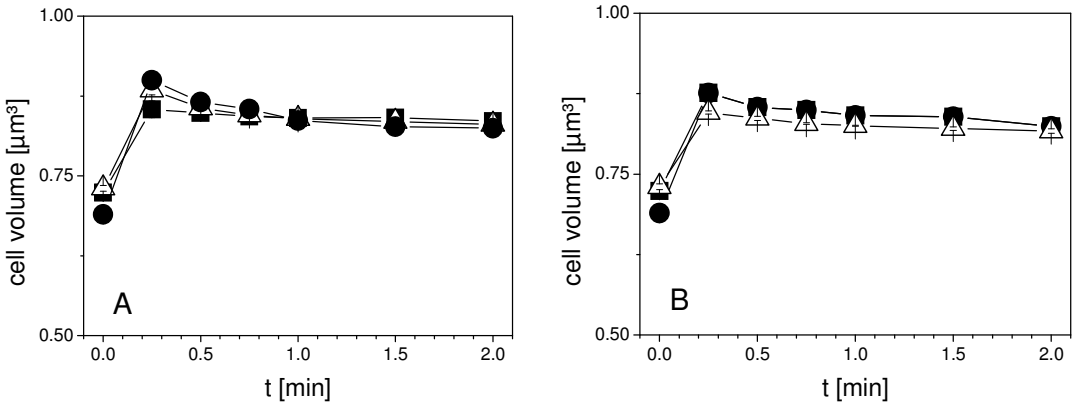

Figure 4.27: Cell volume of *E. coli* cells measured by Coulter Counter after 0.25 % (A) and 0.5 % (B) PAA treatment at 0 °C (squares), 10 °C (circles), and 20 °C (open triangles).

Baatout (2007) measured a significantly decreased level of both forward scattered light and side scattered light of *E. coli* at high and low pH values. The PAA-treated *E. coli* cells did not show this effect. But the forward scatter measurements were more homogeneous in treated samples at all test conditions than in untreated samples (Figures 4.28 & 4.29). The inhomogeneous distribution of forward scatter intensity which was not detected before heat treatment may have bewn caused by the low temperatures. The more homogeneous distribution of forward scattered light after PAA treatment indicates changes in cell size properties.

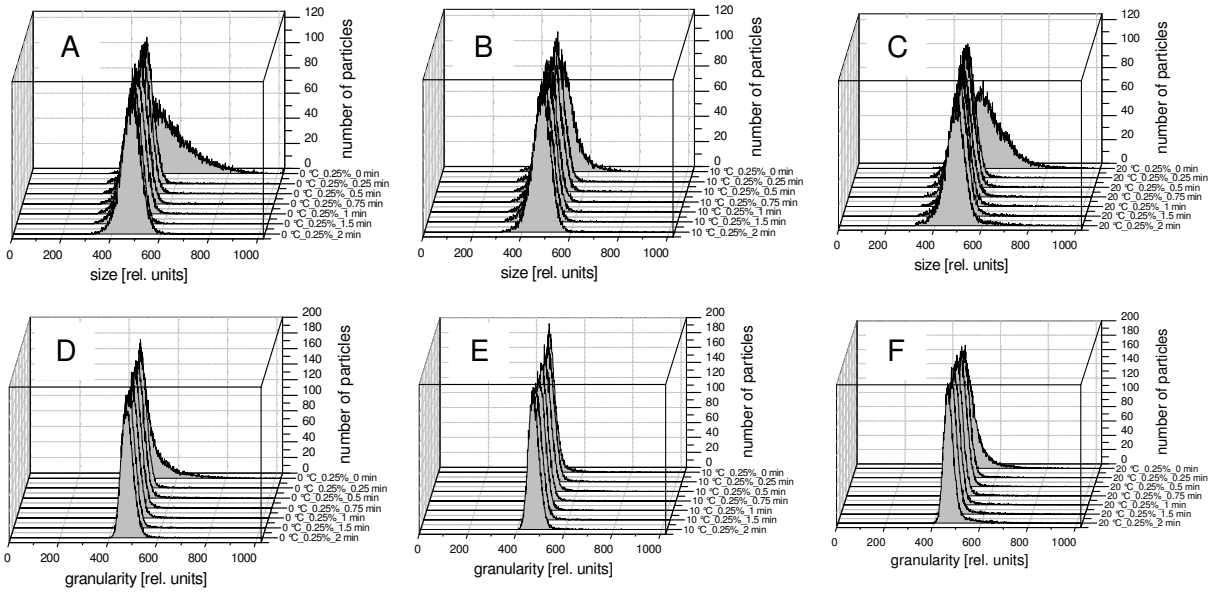

Figure 4.28: Size (A-C) and granularity (D-F) changes of *E. coli* cells after 0.25 % PAA treatment at temperatures of 0 °C (A,D), 10 °C (B,E), and 20 °C (C,F).

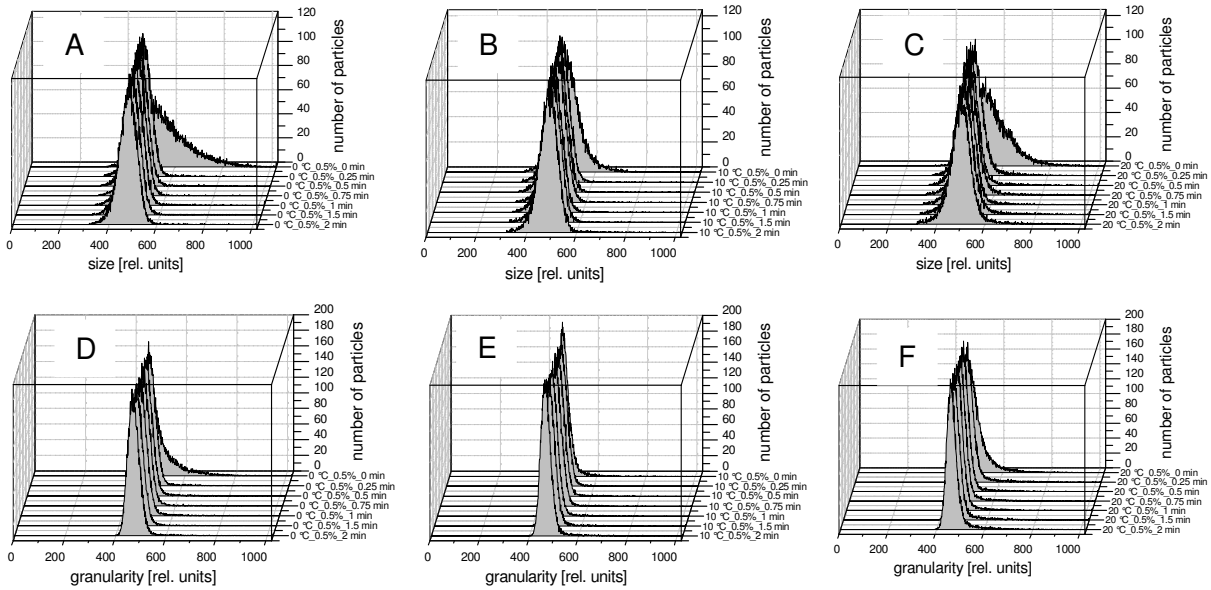

Figure 4.29: Size (A-C) and granularity (D-F) changes of *E. coli* cells after 0.5 % PAA treatment at temperatures of 0 ℃ (A,D), 10 ℃ (B,E), and 20 ℃ (C,F).

Similar to the results obtained after heat treatment, the side scatter intensities did not change after PAA treatment. This implies that the cell structure and the distribution of cell mass did not change due to PAA-treatment. As already shown for heat treated cells the forward and side scatter measurements cannot be directly translated into cell size and granularity but differences in scattered light intensities may indicate the occurrence of morphological changes due to heat or PAA treatment.

4.5.2 Membrane integrity of PAA-treated cells

The mode of action of PAA is not yet fully understood. It is assumed that the disinfectant activity is based on the release of active oxygen and the oxidation of sulfhydryl and sulphur bonds of proteins, enzymes and other metabolites. It was also demonstrated that PAA acts on DNA bases (Kitis, 2004). In order to investigate the inactivation mechanism of PAA on *E. coli* flow cytometric analyses were performed.

After 0.25 % PAA treatment the percentage of TO-stained cells remained almost constant during the first 0.5 min of treatment. With increased time, the treatment leads to a decreased percentage of TO-stained cells. The number of double-stained cells with TO and PI increased with a decreasing percentage of TO-stained cells. The percentage of PI stained cells only slightly increased. This indicates that the cell membrane of *E. coli* cells is only slightly affected during the treatment at 0 ℃. With 0.25 % PAA at 0 ℃ the shift from TO-stained cells to double-stained cells occurred earlier than at 0.5 % PAA.

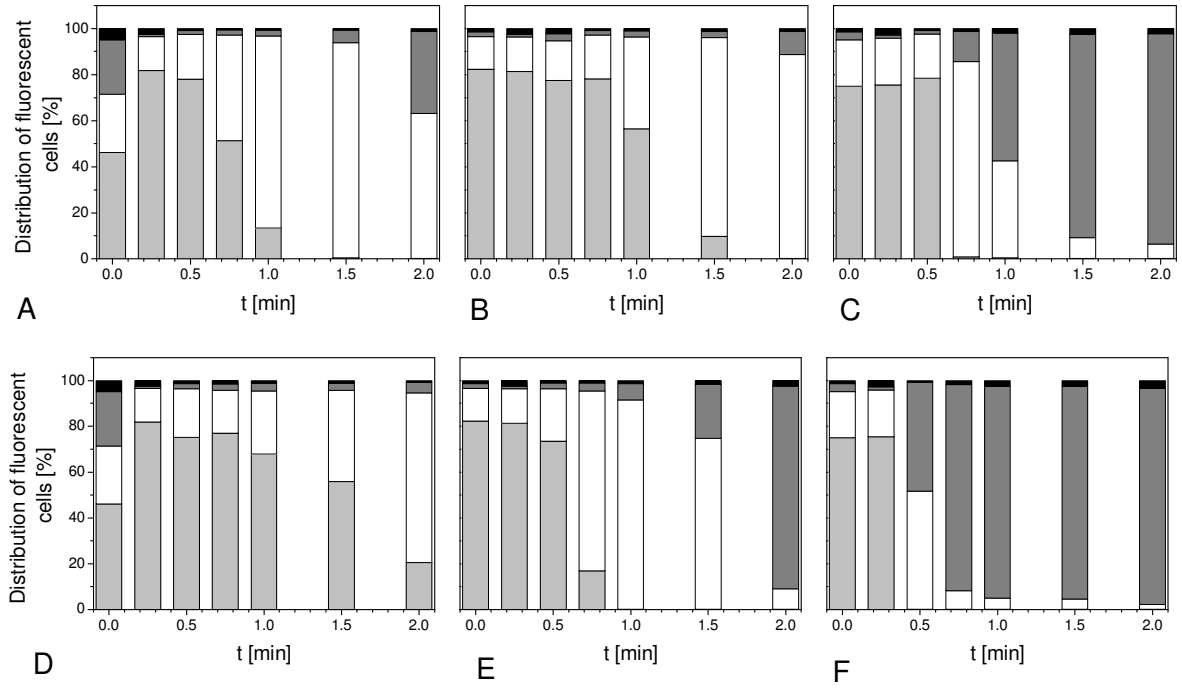

Figure 4.30: Membrane integrity of *E. coli* cells after 0.25 % (A-C) and 0.5 % (D-F) PAA treatment at 0 °C (A,D), 10 °C (B,E), and 20 °C (C,F). Black bars indicating cells without fluorescence, dark gray bars indicating PI-fluorescence (permeabilised cells), white bars indicating TO+PI-fluorescence (slightly permeabilised cells), light gray bars indicating TO-fluorescence (cells with membrane integrity). The standard deviation of the measurements is given in Annex 3 (Tables 7 & 8).

In contrast to 0.25 % PAA treatment, at 0.5 % the percentage of PI-stained cells increased after 1 min treatment time at 10 °C. With increasing treatment temperature an increase of PI-stained cells had already occurred after 0.75 min at 0.25 % PAA and after 0.25 min at 0.5 % PAA and 20 °C (Figure 4.30). This shows that at higher temperatures the cell membrane of *E. coli* is more affected by PAA than at lower temperatures. Although the flow cytometric analysis suggests that most *E. coli* cells were intact after 0.25 min PAA treatment only a small number of colony forming units were detectable by a plate count method. This implies cell permeabilisation is not the cause of the loss of culturability and other mechanisms must induce this effect. Rossi *et al.* (2007) found a constant decrease in viable heterotrophic bacteria using SYBR Green I and PI. But the percentage of intact cells was about 50 % even after 36 min PAA treatment. The percentage of damaged cells (double-stained cells with SYBR Green I+ PI) remained constant during 5 mg l^{-1} PAA treatment. Similar results were obtained for total heterotrophic bacteria during 5 mg l^{-1} PAA treatment (Antonelli *et al.*, 2006) and 15 and 25 mg l^{-1} PAA treatment (Mezzanotte *et al.*, 2003).

Table 4.19: Mean TO-fluorescence intensity of *E. coli* cells after PAA treatment at different concentrations and temperature levels

Treatment time [min]			0	0.25	0.5	0.75	1	1.5	2
0 °C	0.25 %	Mean fluorescence intensity [rel. units]	436.4^{a}	576.4^{a,d}	1113.8^{c,d}	1286.4^{c}	1178.9^{c,d}	1178.9^{c,d}	850^{d}
		SD	± 57.2	± 54.4	± 27.6	± 27.1	± 14.9	± 90.8	± 136.8
	0.5 %	Mean fluorescence intensity [rel. units]	436.4^{a}	576.4^{a,d}	1426.4^{b}	1169.1^{d}	905.4^{e}	517.8^{a}	201.9^{f}
		SD	± 57.2	± 54.4	± 96.7	± 108.1	± 83.1	± 64.1	± 5.6
10 °C	0.25 %	Mean fluorescence intensity [rel. units]	823.9^{a,d,e}	523.7^{b}	1094.2^{a,c,d}	1169.1^{c,d,e}	1003.1^{d,e}	768.6^{e}	312.6^{b}
		SD	± 108.1	± 33.4	± 27.6	± 114.1	± 20.3	± 148.3	± 42.6
	0.5 %	Mean fluorescence intensity [rel. units]	823.9^{a,d,e}	523.7^{b}	1235.9^{c}	794.6^{a}	381.0^{b}	205.2^{d}	185.6^{d}
		SD	± 108.1	± 33.4	± 34.5	± 72.0	± 9.8	± 35.2	± 16.9
20 °C	0.25 %	Mean fluorescence intensity [rel. units]	840.2^{a}	361.5^{b}	1250.6^{c}	342.0^{b}	221.5^{b}	286.6^{b}	292.8^{b}
		SD	± 153.5	± 33.8	± 55.3	± 33.8	± 14.9	± 5.6	± 10.3
	0.5 %	Mean fluorescence intensity [rel. units]	840.2^{a}	361.5^{b}	200.3^{b}	283.3^{b}	254.0^{b}	250.8^{b}	315.9^{b}
		SD	± 153.5	± 33.8	± 6.9	± 29.3	± 35.2	± 31.4	± 55.6

SD, Standard deviation of three independent experiments
$^{a-f}$, Different letters within the lines indicate significant differences at a significance level of 0.05

Increasing mean TO-fluorescence intensity of cells indicates that TO is bound to DNA and not to RNA (Nygren *et al.*, 1998). During PAA treatment the mean TO-fluorescence intensity significantly increased in the first 0.25 and 0.5 min for 0.5 and 0.25 % PAA, respectively and then significantly decreased again with increasing treatment time (Table 4.19). This implies that RNA is damaged due to PAA treatment and TO is predominantly bound to DNA. The decrease of mean TO-fluorescence intensity can be explained by the increased amount of PI in the cells that quenched the TO-fluorescence. The residual mean TO-fluorescence intensity is higher than the residual mean TO-fluorescence intensity observed after heat treatment. This implies that the observed fluorescence intensity does not correspond to the fluorescence of unbound TO as was already suggested for heat-treated cells.

4.5.3 Esterase activity and pump activity of PAA-treated bacteria

The loss of culturability after 0.25 min PAA treatment at different temperatures is evidently not related to cell death. According to Bunthof (2002) the physiological status of cells can be classified in four states with culturability as highest form of physiological fitness.

Nevertheless, the *E. coli* cells that lost culturability might be able to recover and subsequently cause disease. Existing esterase activity of *E. coli* cells after PAA treatment at a concentration of 0.25 % and 0.5 % is shown in figure 4.31.

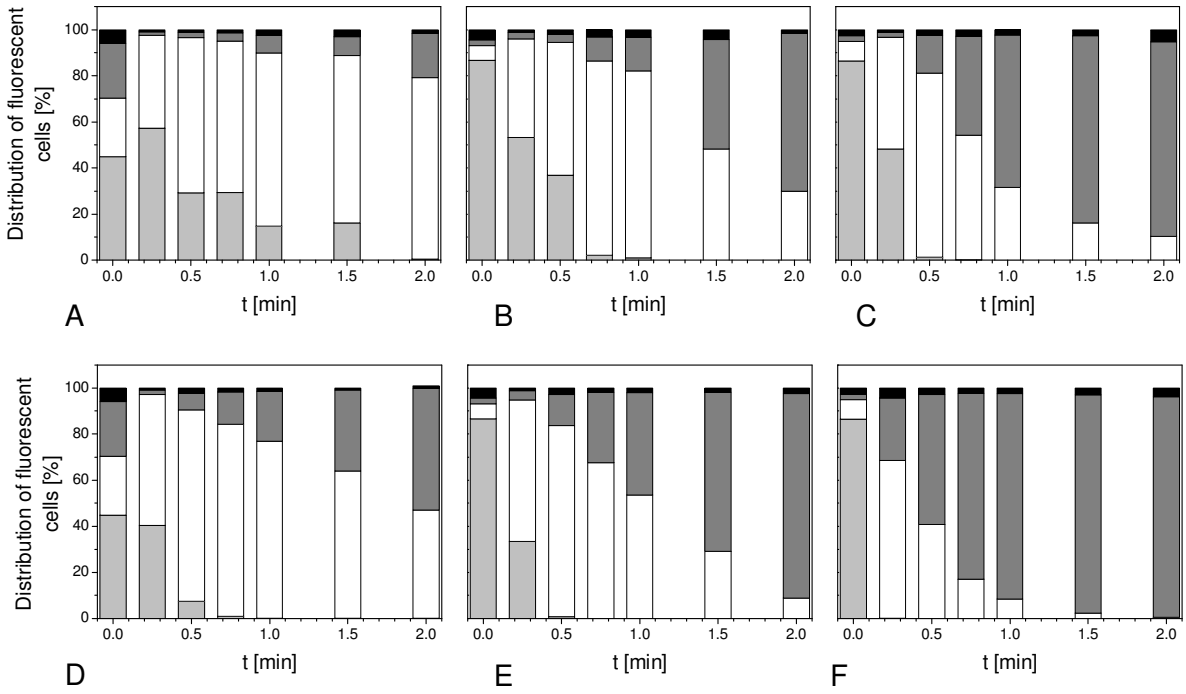

Figure 4.31: Esterase activity and membrane integrity of *E. coli* cells after 0.25 % (A-C) and 0.5 % (D-F) PAA treatment at 0 °C (A,D), 10 °C (B,E), and 20 °C (C,F). Black bars indicating cells without fluorescence, dark gray bars indicating PI-fluorescence (permeabilised cells), white bars indicating cF+PI-fluorescence (permeabilised cells with esterase activity), light gray bars indicating cF-fluorescence (intact cells with esterase activity). The standard deviation of the measurements is given in Annex 4 (Tables 9 & 10).

At 0 °C and 0.25 % PAA 80% of the cells showed cF+PI-fluorescence after 2 min and at 0.5 % PAA 40 % of the cells showed esterase activity and slightly permeabilised cells. This indicates that the cells still have metabolic activity but according to the plate count results these cells were not culturable. At 10 °C and 20 °C the percentage of cF-stained cells (intact cells with esterase activity) decreased linearly within 0.5 min treatment time. The percentage of cF+PI-stained cells simultaneously increased. The percentage of PI-stained cells increased at treatment times above 0.5 min and more than 90 % of the cells are completely permeabilised after 2 min PAA treatments at 10 and 20 °C.

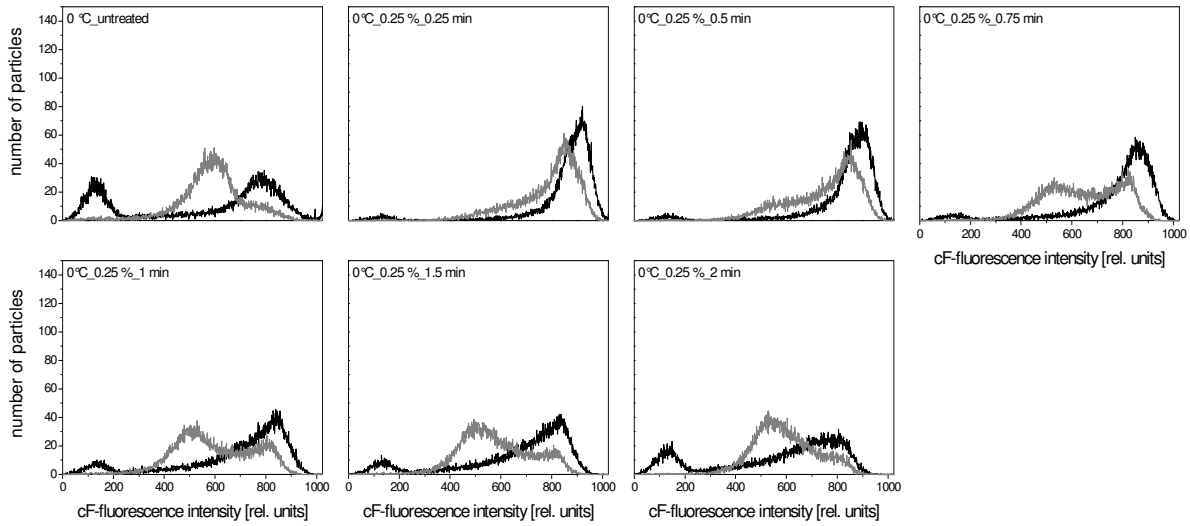

Figure 4.32: Pump activity of *E. coli* cells measured as cF-Efflux capability after 0.25 % PAA treatment at 0 °C. Black lines represent the cF-fluorescence intensity before energising and grey lines represent cF-fluorescence intensity after energising.

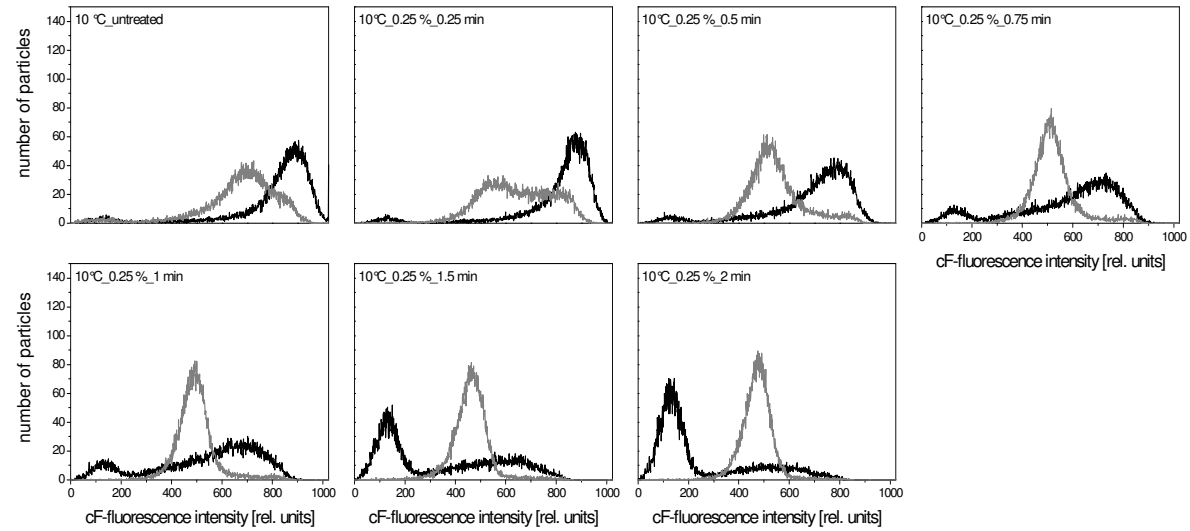

Figure 4.33: Pump activity of *E. coli* cells measured as cF-Efflux capability after heat treatment at 0.25 % PAA treatment at 10 °C. Black lines represent the cF-fluorescence intensity before energising and grey lines represent cF-fluorescence intensity after energising.

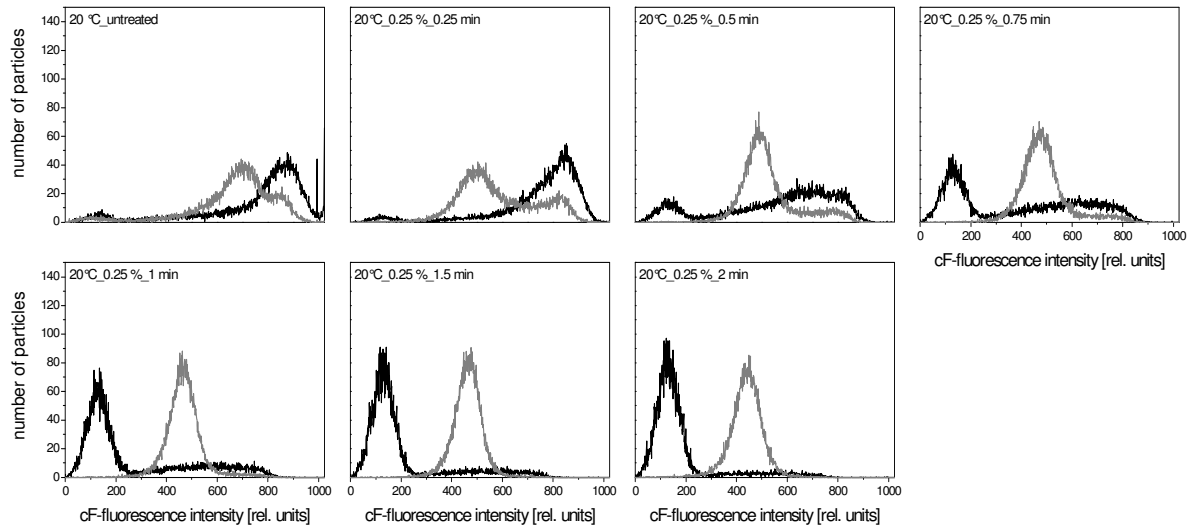

Figure 4.34: Pump activity of *E. coli* cells measured as cF-Efflux capability after heat treatment at 0.25 % PAA treatment at 20 °C. Black lines represent the cF-fluorescence intensity before energising and grey lines represent cF-fluorescence intensity after energising.

An additional indicator for bacterial viability is the pump activity measured by the cF-Efflux. Even though the cell permeabilisation increased with raised treatment time and PAA concentrations at all temperature levels, *E. coli* still showed esterase activity. However, the pump activity is reduced after PAA treatment. A homogenous decrease of cF-fluorescence intensity was observed after 0.25 % PAA treatment at 0 °C for 0.25 and 0.5 min indicating remaining pump activity (Figure 4.32). But the decrease of cF-fluorescence intensity was smaller than the decrease of cF-fluorescence intensity of untreated cells. With increasing treatment time the population of *E. coli* seems to be divided into two subpopulations. One population was able to exclude cF but the other population showed no decreased fluorescence intensity and therefore, cF was not excluded from the cells. Also, the cF-fluorescence intensity was slightly lower before being energised as observed for the cF-fluorescence intensity of the untreated control.

At 10 °C and 0.25 % PAA (Figure 4.33) *E. coli* was able to exclude cF after 0.25 min PAA treatment but in common with the longer treatment times at 0 °C the cell population seems to be divided into two subpopulations. Increasing treatment times at 10 °C showed lower cF-fluorescence intensity before energising as untreated *E. coli* cells. This indicates that a lower amount of cFDA was hydrolysed after PAA treatment which may be related to a lower amount of active esterase within the cells. This may be a result of an oxidation of enzymes by PAA (Kitis, 2004). Nevertheless, these cells also showed cF-Efflux capacity. Treatment times of 1.5 min and 2 min showed enhanced cF-fluorescence intensity upon energising. This effect was also observed for heat-treated *E. coli* cells at 70 °C. Similar results were

observed for 0.25 % PAA treatment at 20 °C whereas the enhanced cF-fluorescence intensity had already occurred after 0.75 min (Figure 4.34).

Increasing the PAA concentration to 0.5 % led to reduced cF-fluorescence intensity at treatment times ≥ 0.5 min and 0 °C (Figure 4.35). cF-efflux capacity upon energising was detected at treatment times up to 1 min. At higher treatment times the cF-fluorescence intensity increased again after energising. Similar results were obtained for 0.5 % PAA treatment at 10 °C (Figure 4.36) and 20 °C (Figure 4.37) whereas decreased cF-fluorescence intensity was already observed after 0.25 min at both temperatures. Enhanced cF-fluorescence intensity upon energising occurred after 0.75 min and 0.5 min at 10 °C and 20 °C, respectively. Thus, the results indicate that the pump activity as well as the esterase activity is affected by the PAA treatment. The effects increased with increasing treatment time and PAA concentration. The effects were also more pronounced with increasing temperatures. The disinfection with PAA was shown to be more effective with increasing temperatures (Stampi, 2001).

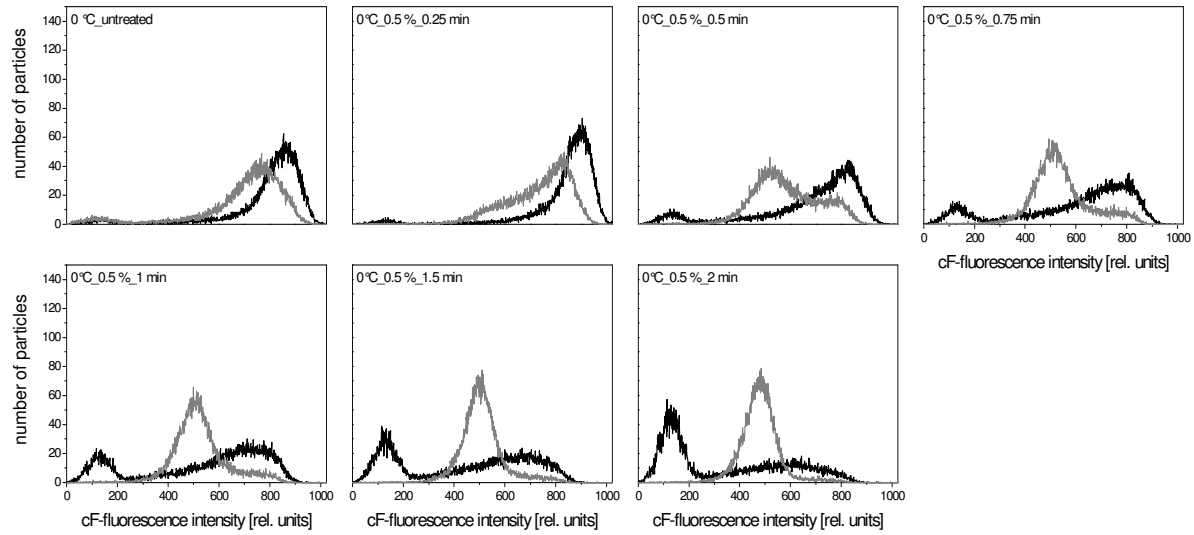

Figure 4.35: Pump activity of *E. coli* cells measured as cF-efflux capability after heat treatment at 0.5 % PAA treatment at 0 °C. Black lines represent the cF-fluorescence intensity before energising and grey lines represent cF-fluorescence intensity after energising.

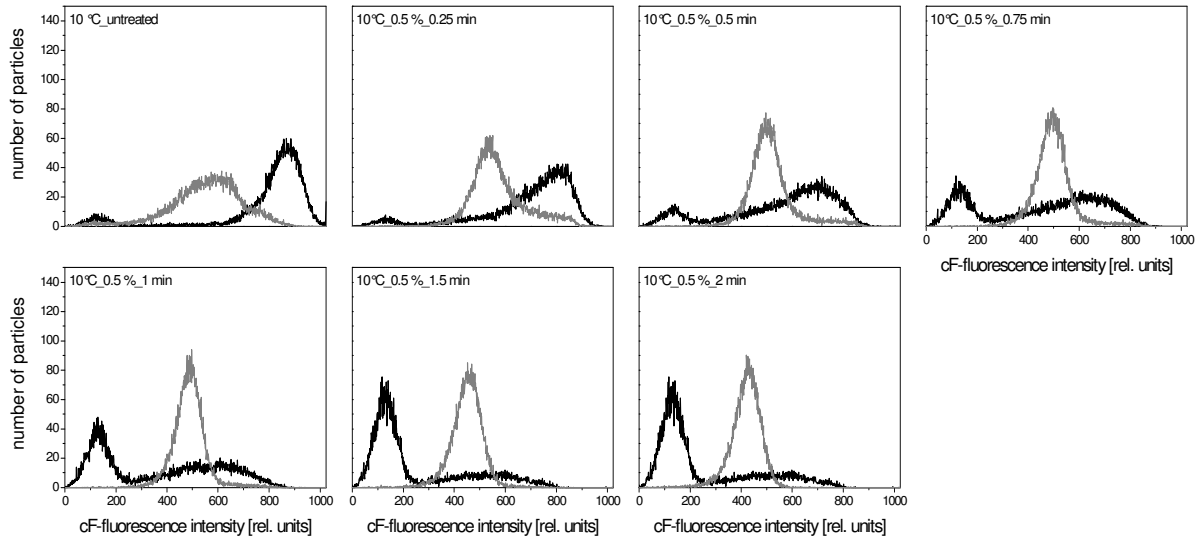

Figure 4.36: Pump activity of *E. coli* cells measured as cF-efflux capability after heat treatment at 0.5 % PAA treatment at 10 °C. Black lines represent the cF-fluorescence intensity before energising and grey lines represent cF-fluorescence intensity after energising.

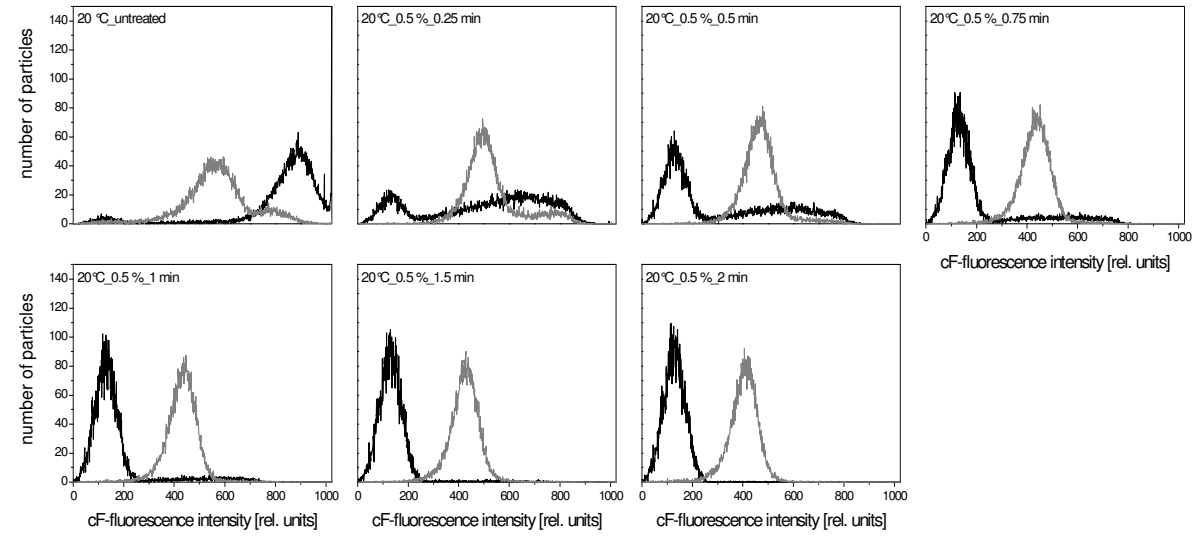

Figure 4.37: Pump activity of *E. coli* cells measured as cF-efflux capability after heat treatment at 0.5 % PAA treatment at 20 °C. Black lines represent the cF-fluorescence intensity before energising and grey lines represent cF-fluorescence intensity after energising.

4.5.4 Membrane potential of PAA-treated cells

The measurement of membrane potential using $DiOC_2(3)$ showed that the untreated cells have a red/green ratio of 4.7, 8.8, and 4.8 at 0°C, 10 °C, and 20 °C, respectively. After PAA treatment the red/green ratio was reduced to approximately 1.0 (Figure 4.38) indicating a reduced membrane potential. However, the cells are not completely depolarized because red/green ratio of completely depolarized cells is below one. The membrane potential is

involved in numerous processes of bacterial physiology and is strongly related to bacterial viability (Novo *et al.*, 1999). The measurement of a low membrane potential after PAA treatment support the assumption that the cells may still cause diseases.

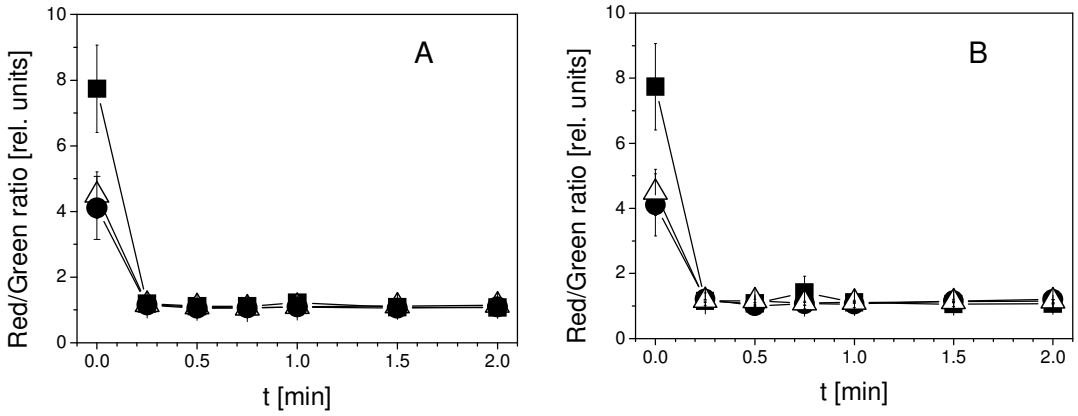

Figure 4.38: Membrane potential of *E. coli* cells after 0.25 % (A) and 0.5 % (B) PAA treatment at 0 °C (squares), 10 °C (circles), and 20 °C(triangles) expressed as red/green ratio of $DiOC_2(3)$ fluorescence.

4.5.5 Impact of PAA treatment on *E. coli* cells

It is assumed that PAA induces oxidation of proteins, enzymes, or other metabolites and acts on DNA bases (Kitis, 2004). Modelling of changes in bacterial physiological properties measured by flow cytometry after PAA treatment may help to determine the most sensitive target sites of bacteria to PAA. The membrane permeabilisation of *E. coli* cells measured by TO/PI-staining was described using the Gompertz model and the obtained permeabilisation rates are given in table 4.20. The mathematical models used are given in table 4.21. At a PAA concentration of 0.25 % the highest permeabilisation rate was observed at 20 °C and the lowest rate occurred at 10 °C. Comparably, the lowest permeabilisation rate was found at 10 °C and 0.5 % PAA but the highest rate at 0.5 % PAA was observed at 0 °C. The permeabilisation was slower at lower PAA concentrations than at higher PAA concentrations. Similar results were obtained for the membrane potential of PAA-treated cells. The lowest depolarisation rate was observed at 10 °C and the highest rate occurred at 0 °C for both concentrations (Table 4.20). The depolarisation rates were obtained from the log-linear regression model with tailing with the exception of 10 °C and 0.25 % PAA where a biphasic model showed the best fit. In contrast, the reduction rate of esterase activity increased with increasing temperature but was higher at 0.5 % PAA than at 0.25 % PAA (Table 4.20). The reduction rates of esterase activity were obtained from the log linear regression model (0 °C, 0.25 % PAA), log-linear regression model with shoulder (10 °C, 0.25 % PAA), biphasic model

with shoulder (20 °C, 0.25 % PAA), log-linear regression model with shoulder and tail (0 °C and 10 °C, 0.5 % PAA), and log-linear regression model with tailing (20 °C, 0.5 % PAA).

Table 4.20: Statistical measures and parameter values obtained from mathematical models for experimental data of PAA inactivated *E. coli* (plate count and flow cytometry)

Target site	0.25 %			0.5 %		
	0 °C	10 °C	20 °C	0 °C	10 °C	20 °C
Microbial reduction [k_{max} min^{-1}]	57.14	105.12	54.52	51.95	118.61	45.56
Membrane permeabilisation [k_{max} min^{-1}]	0.69*	0.06*	4.50*	13.01*	1.01*	11.38*
Membrane potential [k_{max} min^{-1}]	15.45	12.79	12.94	20.89	12.41	13.91
Esterase activity [k_{max} min^{-1}]	0.96	7.88	16.86 1.53	9.27	20.66	20.87

* indicates positive slopes of kinetics

Table 4.21: Mathematical models used for the modeling of bacterial physiological parameters after PAA treatment

E. coli	Membrane permeabilisation	Membrane potential	Esterase activity
0.25 % PAA			
0 °C	Gompertz	log –linear + tail	log-linear regression
10 °C	Gompertz	biphasic	log-linear +shoulder
20 °C	Gompertz	log –linear + tail	biphasic
0.5 % PAA			
0 °C	Gompertz	log –linear + tail	log-linear +shoulder + tail
10 °C	Gompertz	log –linear + tail	log-linear +shoulder + tail
20 °C	Gompertz	log –linear + tail	log –linear + tail

At 0 °C and 10 °C and a PAA concentration of 0.25 % *E. coli* initially showed a loss of culturability followed by the loss of membrane potential, loss of esterase activity and finally, the loss of membrane integrity. Both *E. coli* treated at 20 °C and 0.25 % or 0.5 % PAA and *E. coli* treated at 10 °C with 0.5 % PAA showed a loss of culturability followed by the loss of esterase activity before a depolarisation of cells occurred and the membrane integrity was lost. This implies that the mode of PAA action is the same at these tested temperatures and concentrations. At 0 °C and 0.5 % PAA the loss of culturability is followed by a loss of membrane potential, loss of membrane integrity and loss of esterase activity. The same range of physiological changes was found for *E. coli* treated cells at 70 °C. It had to be taken into account that double-stained cells on one hand represents slightly permeabilised cells, and on the other hand slightly permeabilised cells with esterase activity were not considered in the mathematical models. This may lead to an underestimation of cell permeabilisation and overestimation of the reduction of esterase activity. Nevertheless it is clear that these

temperature and PAA concentrations greatly influence the target points of PAA. These factors have to be considered during disinfection processes.

4.6 Morphological and physiological changes of bacterial properties after ozone treatment

4.6.1 Morphological changes of ozone-treated cells

It was shown that the forward scatter and side scatter intensities were not, or only slightly affected by heat and PAA treatment. This was different for the ozone treatment. The distribution of forward scatter light was more inhomogeneous after ozone treatment than before the ozone treatment (Figure 4.39).

The forward scatter intensities were slightly increased at ozone concentrations of 1.7 mg l^{-1} and 2.8 mg l^{-1} but slightly decreased at 3.8 mg l^{-1}. The side scatter intensities were also more inhomogeneous after ozone treatment and slightly enhanced for all tested concentrations. This implies that the ozone treatment strongly influences the size properties and cell mass properties of *E. coli*.

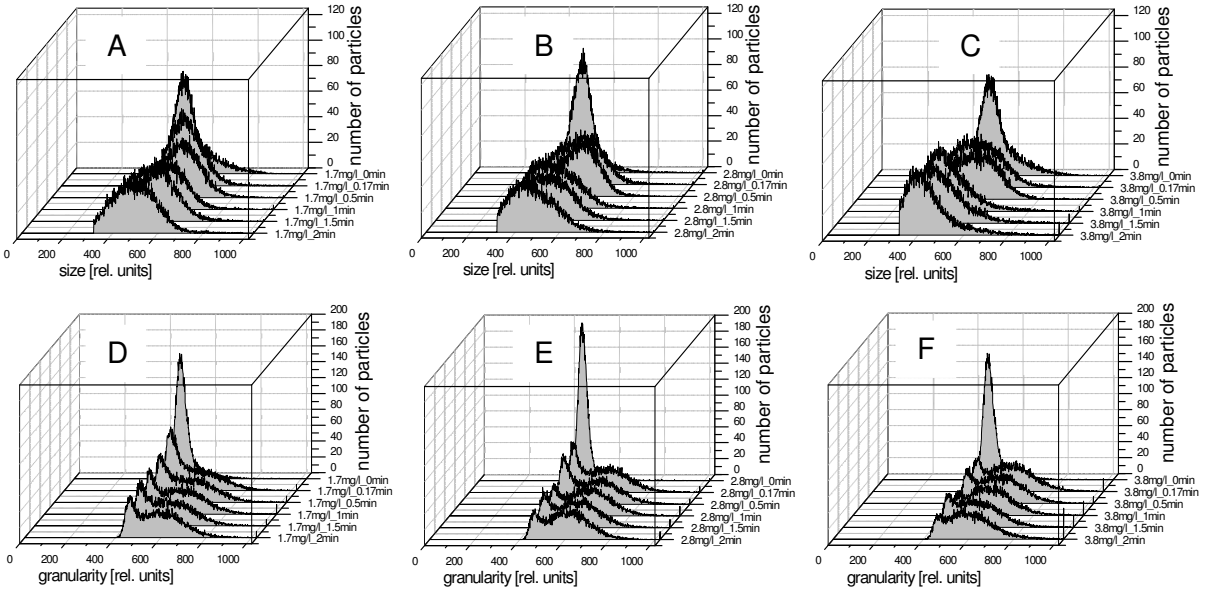

Figure 4.39: Size (A-C) and granularity (D-F) changes of *E. coli* cells after 1.7 mg l^{-1} (A,D), 2.8 mg l^{-1} (B,E), and 3.8 mg l^{-1} (C,F) ozone treatment.

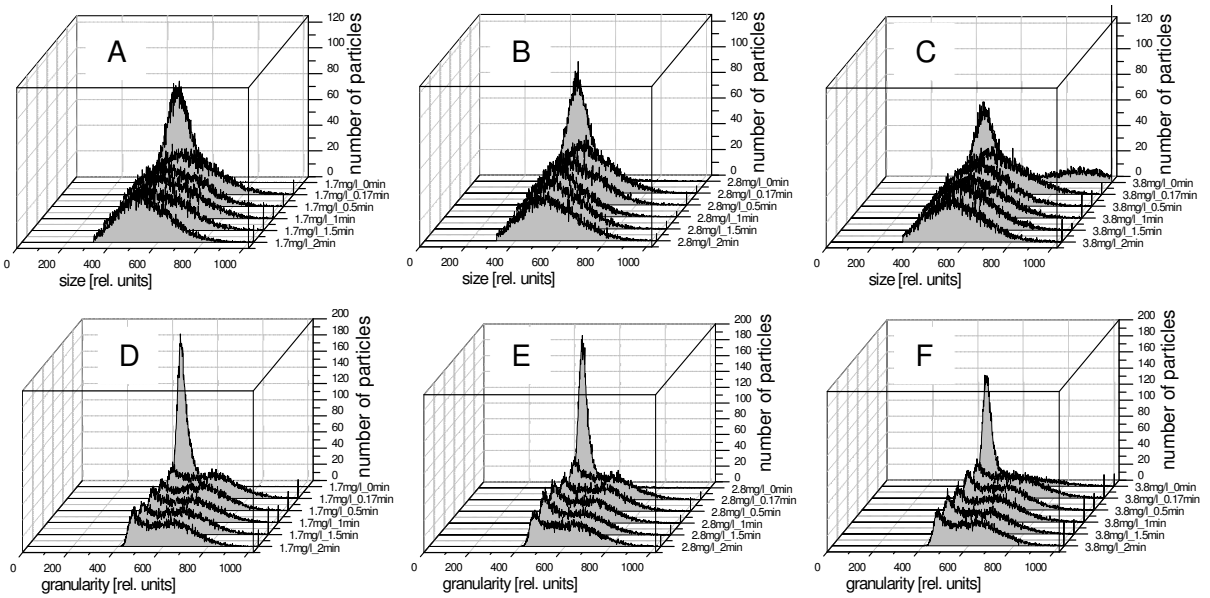

Figure 4.40: Size (A-C) and granularity (D-F) changes of *L. innocua* cells after 1.7 mg l^{-1} (A,D), 2.8 mg l^{-1} (B,E), and 3.8 mg l^{-1} (C,F) ozone treatment.

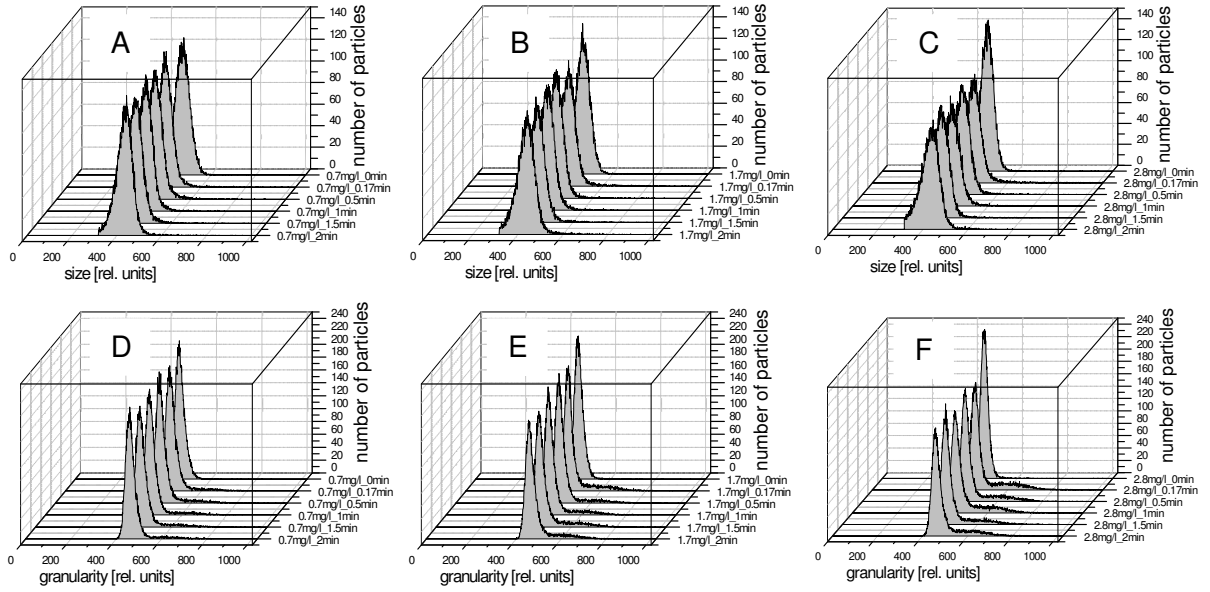

Figure 4.41: Size (A-C) and granularity (D-F) changes of *P. carotovorum* cells after 0.7 mg l^{-1} (A,D), 1.7 mg l^{-1} (B,E), and 2.8 mg l^{-1} (C,F) ozone treatment.

The forward scatter and side scatter intensities of *L. innocua* were also more inhomogeneous after ozone treatment than prior to treatment with slightly higher intensities after the ozone treatment (Figure 4.40). In contrast, the forward scatter and side scatter intensities of *P. carotovorum* cells remained homogeneous even after ozone treatment although the forward scatter intensities decreased slightly (Figure 4.41).The removal of residual ozone by

shaking was less effective than the removal of residual ozone by $Na_2S_2O_3$ as shown by plate count methods. When compared, the forward scatter intensities of the tested bacteria after ozone removal by $Na_2S_2O_3$ (Figure 4.42) were different from those obtained after removal of ozone by shaking. The forward scatter intensities of *E. coli* and *L. innocua* decreased after ozone treatment and were more homogeneous than after ozone removal by shaking. In contrast, the scatter intensities of *P. carotovorum* were more inhomogeneous.

The different scatter intensities of bacteria were also reflected in cell volume measurements (Figure 4.43) however a direct correlation of cell volume and forward scatter intensities was again not found. The cell volume of *E. coli* was reduced during ozone treatment whereas the cell volume of *L. innocua* increased after ozone treatment. The lowest ozone concentration led to an increased cell volume of *P. carotovorum* whereas increased ozone concentrations resulted in a reduction of cell volume. After stopping the ozone reaction with sodium thiosulfate, the cell volume of *E. coli* and *L. innocua* was only slightly affected in terms of a cell volume reduction but the cell volume of *P. carotovorum* showed a comparatively greater decrease.

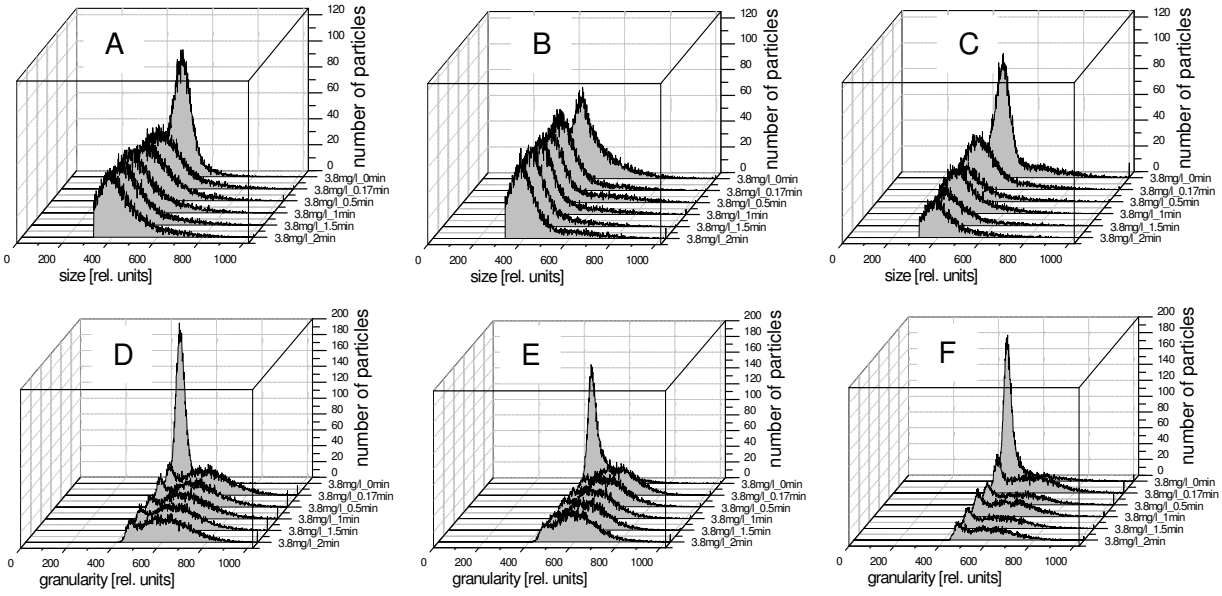

Figure 4.42: Size (A-C) and granularity (D-F) changes of *E. coli* (A,D), *L. innocua* (B,E), and *P. carotovorum* (C,F) cells after 3.8 mg l^{-1} ozone treatment; reaction stopped with sodium thiosulfate.

This indicates that the cell morphology of various bacteria is differentialy affected by ozone. (Kim, 1998) showed that Gram-negative bacteria lost their skeletal structure during ozone treatment while Gram-positive maintain their cellular structure. However, the measurements of scatter intensities and cell volume showed that the morphological changes of bacteria due

to ozone also vary between the different Gram-negative bacteria. The measured scatter intensities and cell volume of *L. innocua* are not consistent with the findings of Kim (1998) who described no structural changes in Gram-positive *L. monocytogenes* and *Leuconostoc mesenteroides*.

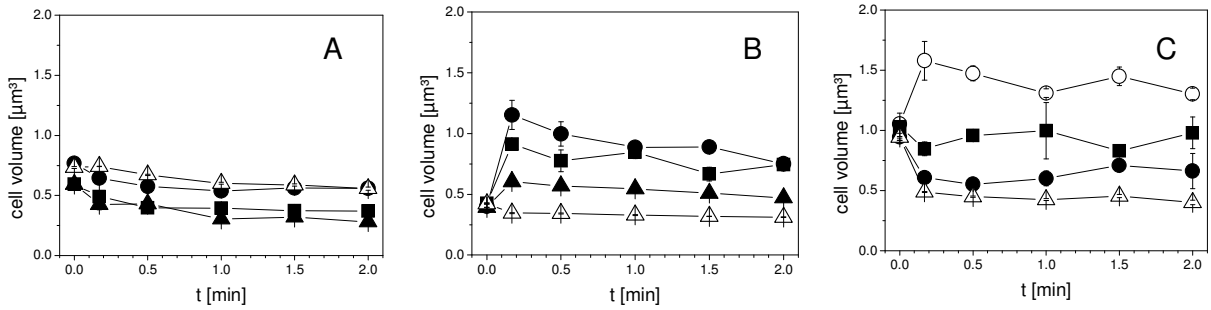

Figure 4.43: Cell volume of *E. coli* (A), *L. innocua* (B), and *P. carotovorum* (C) cells measured by Coulter Counter after 0.7 mg l^{-1} (open circles), 1.7 mg l^{-1} (squares), 2.8 mg l^{-1} (circles), and 3.8 mg l^{-1} (triangles, open triangles: with sodium thiosulfate) ozone treatment.

4.6.2 Membrane integrity of ozone-treated cells

The inactivation of bacteria by ozone is attributed to changes in cell permeability and cell lyses (Moore *et al.*, 2000) which can elicit the changes in scatter intensities. Consequently, the membrane integrity of bacteria cells after ozone treatment was investigated. At an ozone concentration of 0.7 mg l^{-1} the percentage of intact *P. carotovorum* cells was reduced to approximately 40 % after 0.17 min treatment time and remained almost constant after extended treatment times (Figure 4.44 G). Concurrently the percentages of slightly permeabilised and permeabilised cells increased, the slightly permeabilised cells being predominant. An increase of ozone concentration to 1.7 mg l^{-1} led to a further decreased percentage of intact *P. carotovorum* cells and the amount of permeabilised cells further increased (Figure 4.44 H). In contrast, no intact *E. coli* (Figure 4.44 A) and *L. innocua* (Figure 4.44 D) cells were detected at the same concentration and the fraction of slightly permeabilised cells is negligible. Overall the percentage of unstained cells increased.

The percentage of permeabilised and unstained *L. innocua* cells at ozone concentrations of 2.8 mg l^{-1} (Figure 4.44 E) and 3.8 mg l^{-1} (Figure 4.44 F) was not different from the lowest tested ozone concentration. At 2.8 mg l^{-1} ozone treatment *P. carotovorum* cells were either unstained or permeabilised after 0.17 min (Figure 4.44 I). This effect could not be detected for *E. coli* at the same ozone concentration. In contrast to ozone treatment at 1.7 mg l^{-1} almost 50 % *E. coli* cells showed a double-staining with TO and PI indicating slightly permeabilised cells (Figure 4.44 B). With increasing treatment time the percentage of

unstained cells increased. Similar results were observed with 3.8 mg l^{-1} ozone (Figure 4.44 C). The results clearly indicate that each bacterium is differently affected by ozone and the mode of action also differs within a population. The percentage of membrane permeabilised cells increased with increasing ozone concentration for *L. innocua* and *P. carotovorum* but increasing ozone concentrations did not lead to enhanced membrane permeabilisation of *E. coli* cells, instead a high percentage of double-stained and unstained cells were observed. As a result the fluorescence intensity of TO was very low (Table 4.22).

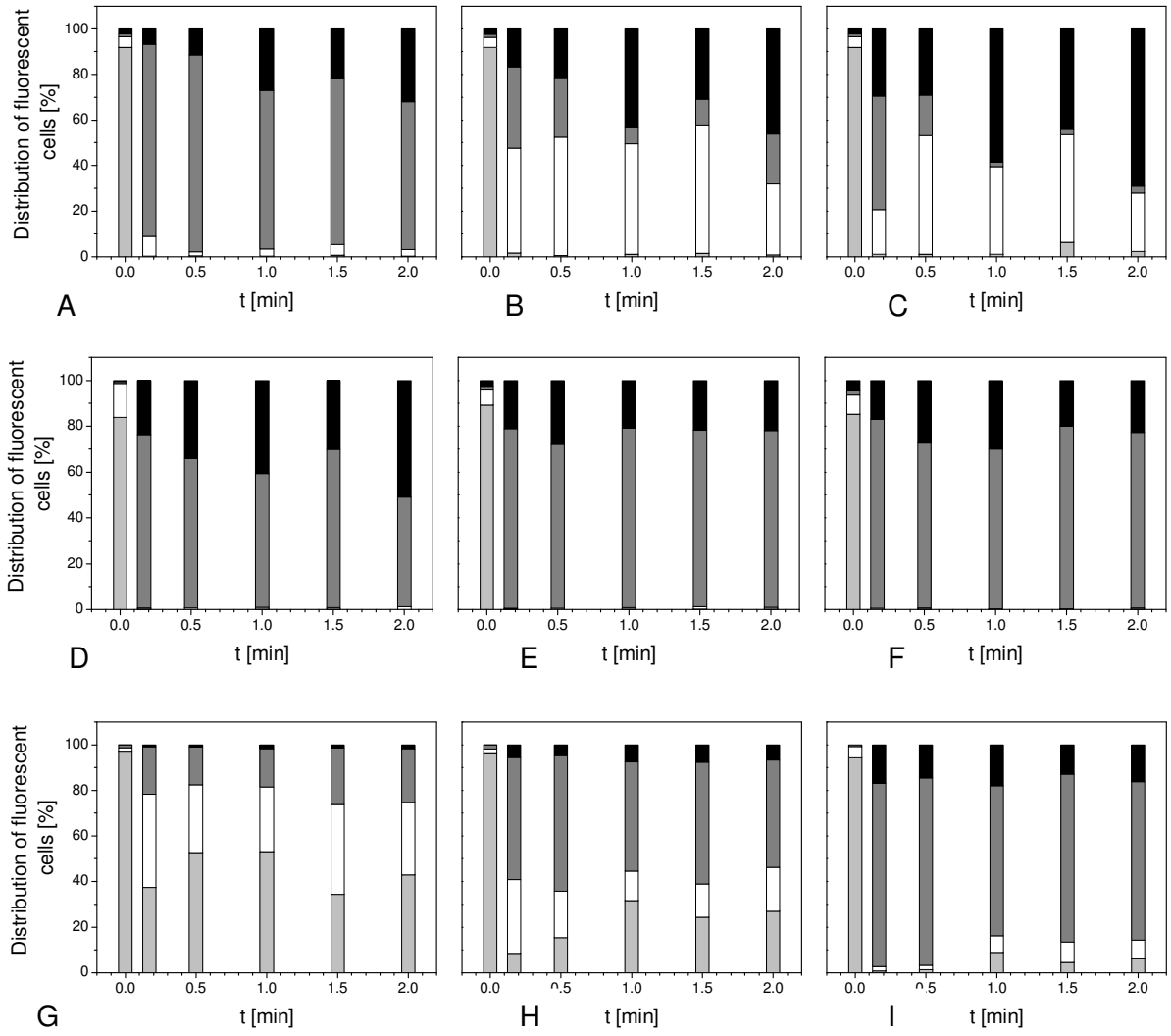

Figure 4.44: Membrane integrity of *E. coli* (A-C); *L. innocua* (D-F), and *P. carotovorum* (G-I) cells after 0.7 mg l^{-1} (G), 1.7 mg l^{-1} (A,D,H), 2.8 mg l^{-1} (B,E,I), and 3.8 mg l^{-1} (C,F) ozone treatment. Black bars indicating cells without fluorescence, dark gray bars indicating PI-fluorescence (permeabilised cells), white bars indicating TO+PI-fluorescence (slightly permeabilised cells), light gray bars indicating TO-fluorescence (cells with membrane integrity). The standard deviation of the measurements is given in Annex 5 (Tables 11-13).

Ozone leads to a rupture of cells and cell lyses with subsequent attacks on nucleic acids and enzymes (Pascual *et al.*, 2007). The low fluorescence intensity of TO can be related to unbound dye adherent to cell fragments and the occurrence of PI-fluorescence indicates that this cell population did not show cell lyses. The high percentage of double-stained cells was also observed for heat-treated cells at 90 °C. The unstained fraction indicates that the cells are highly permeabilised so that cell lyses occurred and therefore, no fluorescence could be detected. It can also be assumed that nucleic acids are affected by the ozone and therefore, an intercalating of fluorescent dyes with DNA and RNA was not possible. A complete destruction of bacteria in drinking water after ozonation was observed using SYBR Green I and propidium iodide. Along with a few detectable bacteria cells a high amount of cell debris was detected with the flow cytometer after ozonation of drinking water (Hammes *et al.*, 2008). Similar results were obtained for bacteria cells from ozonated river water after staining with SYBR Green and PI. The PI-labelled fraction was not able to form colonies on agar plates (Gregori *et al.*, 2001). The predominant fraction of *L. innocua* and *P. carotovorum* cells is permeabilised indicating that these cells were not completely destroyed by the ozone treatment. However, the unstained fraction of *L. innocua* cells was higher than the unstained fraction of *P. carotovorum* which lead to the assumption that a much greater number of the population of *L. innocua* were destroyed completely. The observed damage of Gram-negative and Gram-positive bacteria cells is consistent with the observations of Thanomsub *et al.* (2002).

E. coli (Table 4.22) showed a significant decrease of mean TO-fluorescence intensity after ozone treatment. This indicates that the measured TO-fluorescence intensity corresponds more likely to unbound TO than to a TO-DNA-complex or TO-RNA-complex. The mean TO-fluorescence intensity of *L. innocua* cells (Table 4.23) increased after ozone treatment of 0.17 min but decreased with longer treatment times.

Table 4.22: Mean TO-fluorescence intensity of *E. coli* cells after ozone treatment at different concentrations

	1.7 mg l^{-1}		2.8 mg l^{-1}		3.8 mg l^{-1}	
Treatment time [min]	**Mean fluorescence intensity [rel. units]**	**SD**	**Mean fluorescence intensity [rel. units]**	**SD**	**Mean fluorescence intensity [rel. units]**	**SD**
0	1455.7^{a}	± 35.2	853.2^{a}	± 74.6	1455.7^{a}	± 35.2
0.17	394.1^{b}	± 20.3	101.0^{b}	± 40.7	149.8^{b}	± 58.9
0.5	$280.1^{b,c}$	± 114.5	81.4^{b}	± 14.9	84.7^{b}	± 14.9
1	172.6^{c}	± 5.6	84.7^{b}	± 11.3	94.4^{b}	± 11.3
1.5	143.3^{c}	± 34.3	94.4^{b}	±24.6	127^{b}	±16.9
2	162.8^{c}	± 34.3	78.2^{b}	± 9.8	107.5^{b}	± 19.5

SD, Standard deviation of three independent experiments
$^{a-c}$, Different letters within the columns indicate significant differences at a significance level of 0.05

Table 4.23: Mean TO-fluorescence intensity of *L. innocua* cells ozone treatment at different concentrations

Treatment time [min]	1.7 mg l^{-1}		2.8 mg l^{-1}		3.8 mg l^{-1}	
	Mean fluorescence intensity [rel. units]	SD	Mean fluorescence intensity [rel. units]	SD	Mean fluorescence intensity [rel. units]	SD
0	442.9^{a,b,c,d}	± 46.2	228^{a}	± 14.9	1677.2^{a}	± 255
0.17	804.4^{a,c}	± 117.8	566.7^{a}	± 345.3	475.5^{b}	± 210.1
0.5	394.1^{b,c,d}	± 264.8	374.5^{a}	± 175.1	361.5^{b}	± 77.5
1	394.1^{b,c,d}	± 87.6	237.7^{a}	± 218.5	384.3^{b}	± 166.5
1.5	455.93^{c,d}	± 167.6	283.3^{a}	± 141.9	237.7^{b}	± 183.9
2	322.4^{d}	± 54.4	319.2^{a}	± 116.6	257.3^{b}	± 34.3

SD, Standard deviation of three independent experiments
$^{a-d}$, Different letters within the columns indicate significant differences at a significance level of 0.05

The results of the plate count methods showed the highest sensitivity of *P. carotovorum* against ozone while the highest amount of intact cells was observed by flow cytometry. Thus, the loss of culturability of *P. carotovorum* cells is not directly correlated with the loss of membrane integrity. The significant increase of mean TO-fluorescence intensity at 0.7 mg l^{-1} and 2.8 mg l^{-1} (Table 4.24) is related to the more predominant intercalating of TO with DNA than with RNA.

Table 4.24: Mean TO-fluorescence intensity of *P. carotovorum* cells after ozone treatment at different concentrations

Treatment time [min]	0.7 mg l^{-1}		1.7 mg l^{-1}		2.8 mg l^{-1}	
	Mean fluorescence intensity [rel. units]	SD	Mean fluorescence intensity [rel. units]	SD	Mean fluorescence intensity [rel. units]	SD
0	882.6^{a,c,e}	± 79	469^{a,c}	± 9.8	840.2^{a}	± 83.5
0.17	1729.3^{b,d}	± 208.9	390.8^{a}	± 260.5	706.7^{a}	± 225.6
0.5	1387.3^{b,d,e}	± 102.9	1218^{b,c,d}	± 39.5	696.9^{a}	± 395.3
1	1234.3^{c,d,e}	± 87.6	869.5^{c,d}	± 288.7	1149.6^{a}	± 55.6
1.5	1446^{d,e}	± 210.2	934.7^{d}	± 63.6	924.9^{a}	± 390.4
2	1159.4^{e}	± 120.6	1117^{d}	± 85.4	1032.4^{a}	± 305.4

SD, Standard deviation of three independent experiments
$^{a-e}$, Different letters within the columns indicate significant differences at a significance level of 0.05

Different results were obtained after ozone treatment stopped by $Na_2S_2O_3$ in comparison to the results obtained after ozone treatment stopped by shaking. For all tested bacteria a high amount of unstained cells were detected after ozone treatment. Again, *P. carotovorum* showed the highest percentage of intact cells and *L. innocua* the lowest percentage of intact cells (Figure 4.45).

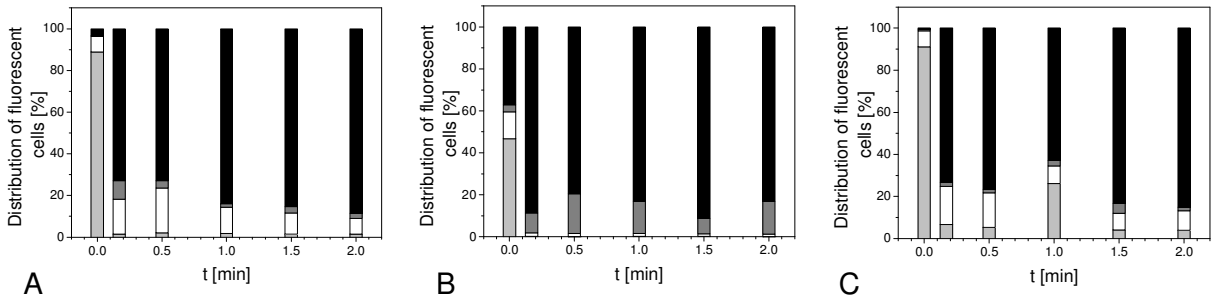

Figure 4.45: Membrane integrity of *E. coli* (A); *L. innocua* (B), and *P. carotovorum* (C) cells after 3.8 mg l^{-1} ozone treatment; reaction stopped with sodium thiosulfate. Black bars indicating cells without fluorescence, dark gray bars indicating PI-fluorescence (permeabilised cells), white bars indicating TO+PI-fluorescence (slightly permeabilised cells), light gray bars indicating TO-fluorescence (cells with membrane integrity). The standard deviation of the measurements is given in Annex 5 (Table 14).

The mean TO-fluorescence intensity of *E. coli* and *L. innocua* significantly decreased (Table 4.25) after ozone treatment indicating the measurement of unbound TO. Mean TO-fluorescence intensity of *P. carotovorum* showed no significant changes after ozone treatment. This may lead to the assumption that nucleic acids of *P. carotovorum* are less affected by ozone than nucleic acids of *E. coli* and *L. innocua*.

Table 4.25: Mean TO-fluorescence intensity of *E. coli*, *L. innocua*, and *P. carotovorum* cells after 3.8 mg l^{-1} ozone treatment with sodium thiosulfate to stop the reaction

Treatment time [min]	*E. coli*		*L. innocua*		*P. carotovorum*	
	Mean fluorescence intensity [rel. units]	SD	Mean fluorescence intensity [rel. units]	SD	Mean fluorescence intensity [rel. units]	SD
0	328.9[a]	± 24.6	436.4[a]	± 24.6	1175.7[a]	± 455.8
0.17	84.7[b]	± 11.3	211.7[b]	± 46.2	107.5[a]	± 16.9
0.5	97.7[b]	± 33.8	273.6[b]	± 59.4	94.4[a]	± 5.6
1	94.4[b]	± 5.6	214.9[b]	± 67.7	1234.3[a]	± 1977.1
1.5	91.2[b]	± 14.9	182.4[b]	± 55.6	114[a]	± 20.3
2	136.8[b]	±16.9	162.8[b]	± 46.2	110.7[a]	± 11.3

SD, Standard deviation of three independent experiments
[a-f], Different letters within the columns indicate significant differences at a significance level of 0.05

The high number of unstained cells suggests a complete destruction of bacteria cells after ozone treatment. This is inconsistent with the results obtained by plate count method because a high number of viable bacteria were detected while flow cytometric analyses of membrane integrity suggest complete destruction of cells. This implies that the unstained fraction of cells cannot necessarily be related to destroyed cells. It is possible that a flocculation of cellular proteins and an oxidation of double-bonds (Kim *et al.*, 1999) restricted the dye uptake without affecting the culturability. Alternatively, the unstained cells may have been completely destroyed cells and cell lyses occurred while the permeabilised fraction may

be able to form colonies on a medium because permeabilisation of cells is reversible. A reversible pore formation has been described for bacteria treated with pulsed electric fields (Garcia *et al.*, 2007). While the ozone improved cell permeability and enabled the uptake of PI, the availability of nutrients in terms of $Na_2S_2O_3$ can be metabolically used to support the growth of bacteria on a cultivating medium. These results clearly indicate that membrane integrity measurements cannot give reliable prediction of cell viability.

4.6.3 Esterase activity and pump activity of ozone-treated bacteria

A proposed cause of bacterial death due to ozone treatment is the oxidation of sulfhydryl groups in enzymes (Kim *et al.*, 1999). Therefore, the activity of esterase after ozone treatment was measured using cFDA. Furthermore, PI was added to measure membrane integrity simultaneously. Similar to the results obtained by TO/PI measurement, differences between all tested bacteria were obtained. No esterase activity was observed for *L. innocua* after ozone treatment for 0.17 min at all tested concentrations (Figure 4.46 D-F). The predominant fraction of *L. innocua* cells after ozone treatment is permeabilised and the residual fraction remained unstained. Thereby, the percentage of unstained cells increased with increasing ozone concentrations. After ozone treatment of *E. coli* (Figure 4.46 A-C) and *P. carotovorum* (Figure 4.46 G-H) the bacteria cells still showed residual esterase activity even if the cells were slightly permeabilised. Increasing ozone concentration enhanced the percentage of slightly permeabilised cells with esterase activity and decreased the percentage of permeabilised *E. coli* cells. In contrast, the fraction of permeabilised *P. carotovorum* cells increased with increasing ozone concentration while the percentage of slightly permeabilised cells with esterase activity decreased.

However, the cF-fluorescence intensity of both bacteria is very low after ozone treatment indicating a small amount of hydrolysed cFDA due to an inactivation of esterase. This supports the assumption that the esterase is oxidised by ozone. Alternatively, cFDA may be hydrolysed by esterase but due to the permeabilisation of cells cF cannot be retained within the cells. The centrifugation step to remove surplus cFDA may also remove the hydrolyse product cF which could lead to an underestimation of esterase activity. The fraction of unstained *E. coli* cells is lower than the fraction of unstained cells obtained by TO/PI-staining. But on the other hand the percentage of slightly permeabilised cells with esterase activity increased. This leads to the assumption that the nucleic acids are affected by the ozone before the esterase is affected. It has been shown that a short-time exposure of *E. coli* to ozone led to membrane damage while a long-time exposure affects the intracellular components (Komanapalli & Lau, 1996).

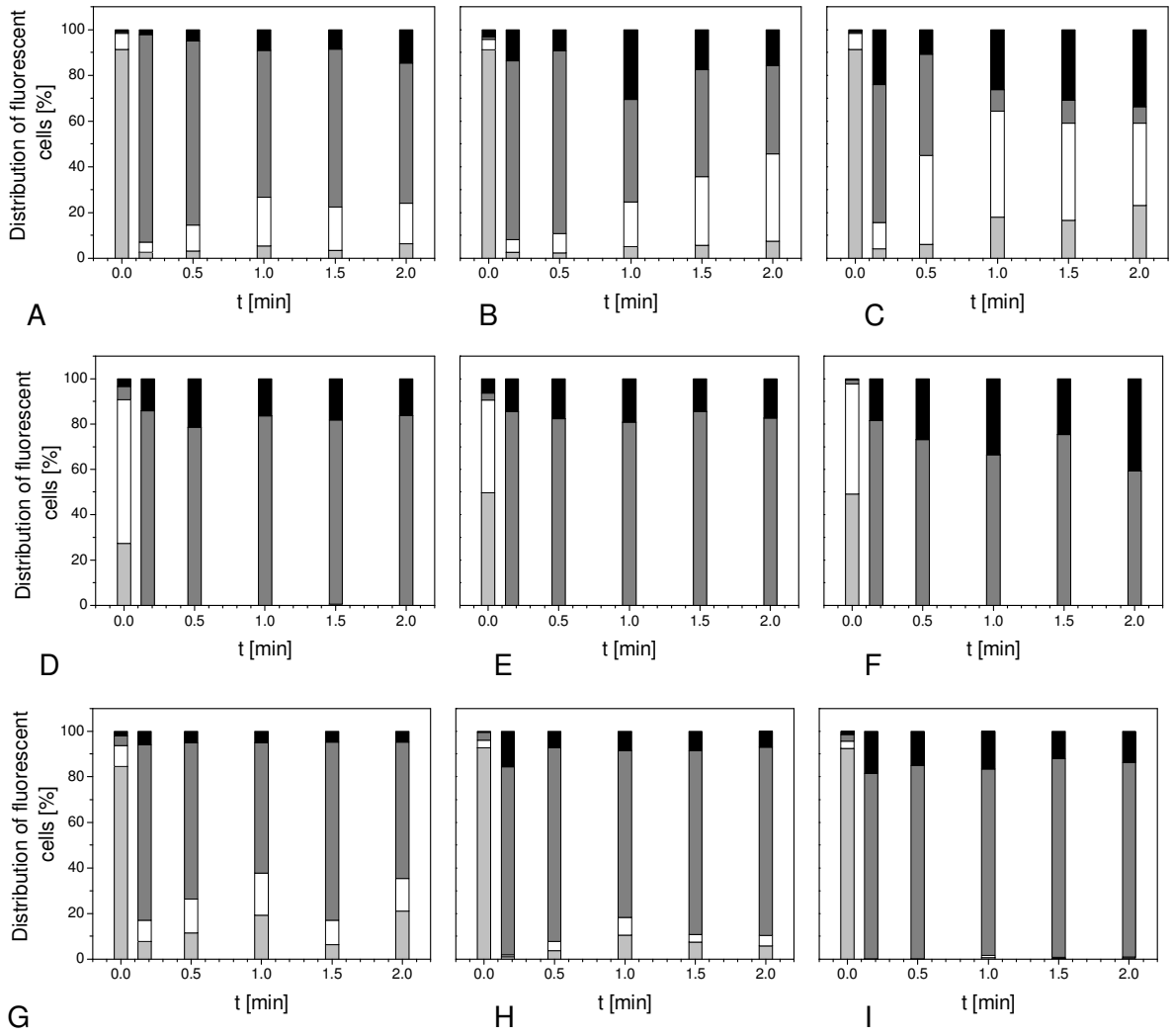

Figure 4.46: Esterase activity and membrane integrity of *E. coli* (A-C); *L. innocua* (D-F), and *P. carotovorum* (G-I) cells after 0.7 mg l^{-1} (G), 1.7 mg l^{-1} (A,D,H), 2.8 mg l^{-1} (B,E,I), and 3.8 mg l^{-1} (C,F) ozone treatment. Black bars indicating cells without fluorescence, dark gray bars indicating PI-fluorescence (permeabilised cells), white bars indicating cF+PI-fluorescence (permeabilised cells with esterase activity), light gray bars indicating cF-fluorescence (intact cells with esterase activity). The standard deviation of the measurements is given in Annex 6 (Tables 15-17).

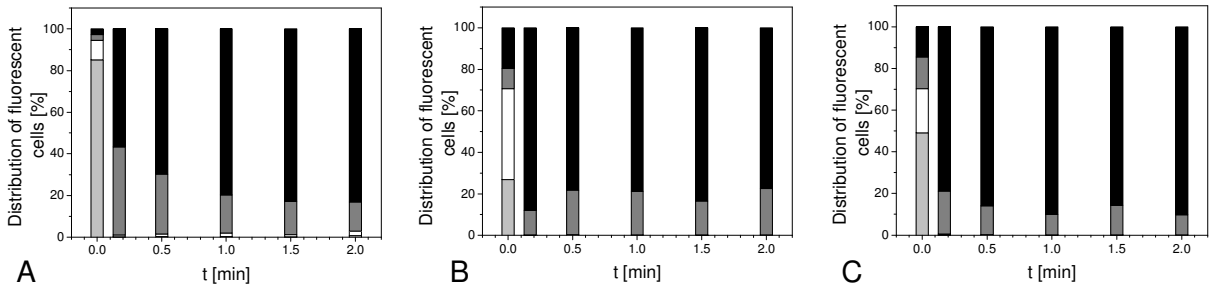

Figure 4.47: Esterase activity of *E. coli* (A); *L. innocua* (B), and *P. carotovorum* (C) cells after 3.8 mg l^{-1} ozone treatment; reaction stopped with sodium thiosulfate. Black bars indicating cells without fluorescence, dark gray bars indicating PI-fluorescence (permeabilised cells), white bars indicating cF+PI-fluorescence (permeabilised cells with esterase activity), light gray bars indicating cF-fluorescence (intact cells with esterase activity). The standard deviation of the measurements is given in Annex 6 (Table 18).

Esterase activity of bacteria was also tested after ozone treatment and quenching of ozone by $Na_2S_2O_3$. No esterase activity was observed after 0.17 min ozone treatment for all tested bacteria (Figure 4.47). Similar to the results obtained by the measurement of membrane integrity, the predominant fraction of cells remained unstained. This supports the assumption that the unstained fraction represents completely ruptured cells and that cell lyses occurred. This also implies that cell permeabilisation measured by PI uptake is reversible and cells were able to form colonies on agar medium in the presence of nutrient. The oxidation of phospholipids and proteins in cell membranes is shown to alter the regulation of cell permeability without affecting cell permeability (Cronan & Vagelos, 1972). Thus, the uptake of dyes may be prevented resulting in a high percentage of unstained cells.

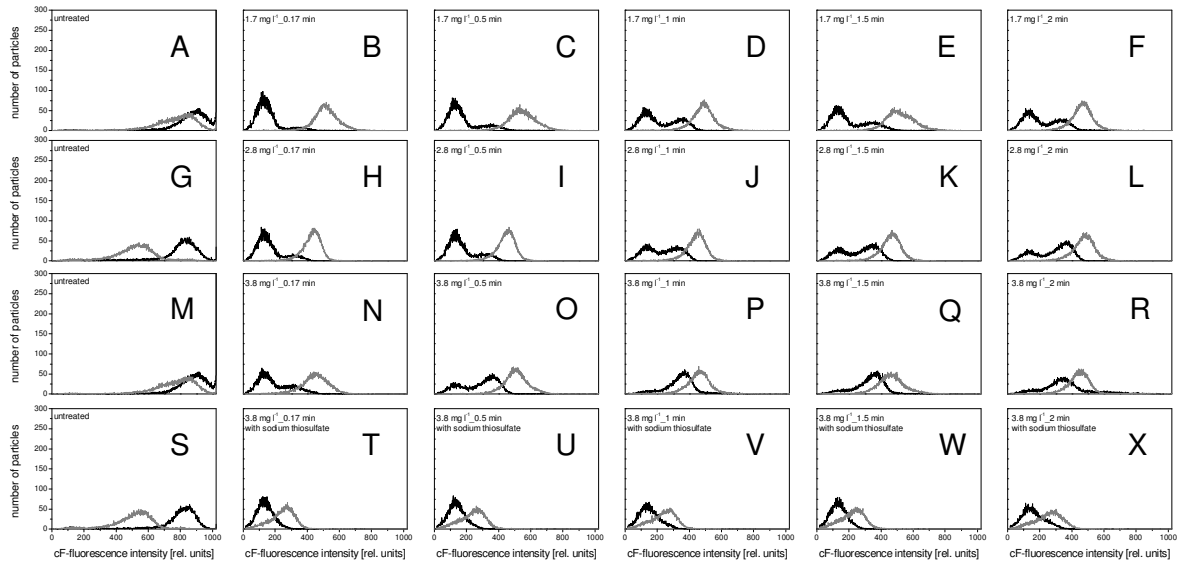

Figure 4.48: Pump activity of *E. coli* cells measured as cF-efflux capability after at concentrations of 1.7 mg l^{-1} (A-F), 2.8 mg l^{-1} (G-L), 3.8 mg l^{-1} without (M-R) or with (S-X) sodium thiosulfate. Black lines represent the cF-fluorescence intensity before energising and grey lines represent cF-fluorescence intensity after energising.

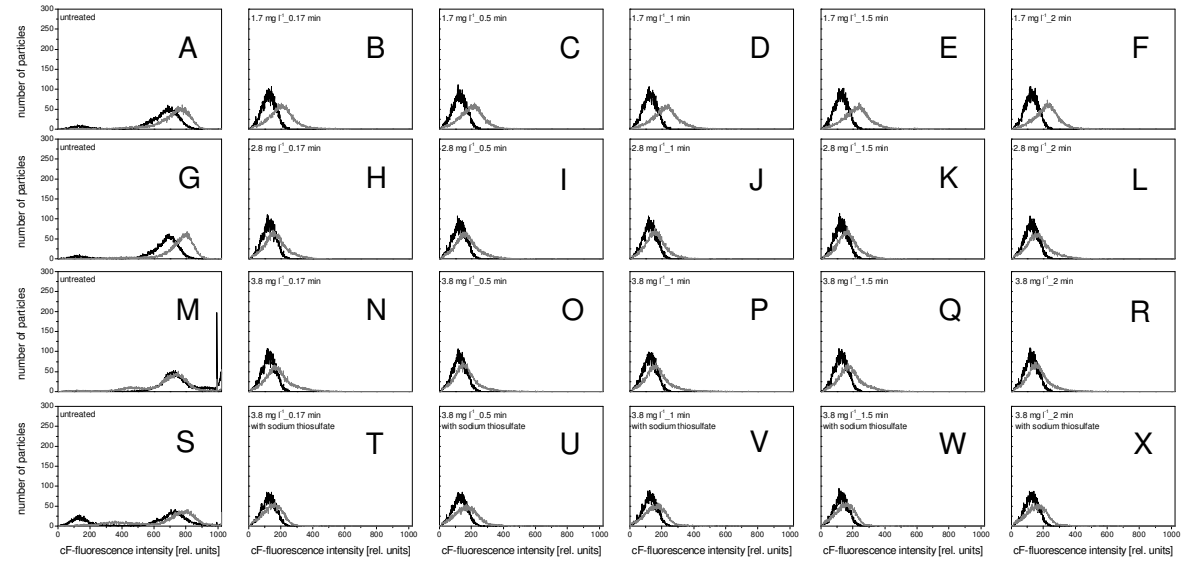

Figure 4.49: Pump activity of *L. innocua* cells measured as cF-efflux capability after ozone treatment at concentrations of 1.7 mg l^{-1} (A-F), 2.8 mg l^{-1} (G-L), 3.8 mg l^{-1} without (M-R) or with (S-X) sodium thiosulfate. Black lines represent the cF-fluorescence intensity before energising and grey lines represent cF-fluorescence intensity after energising.

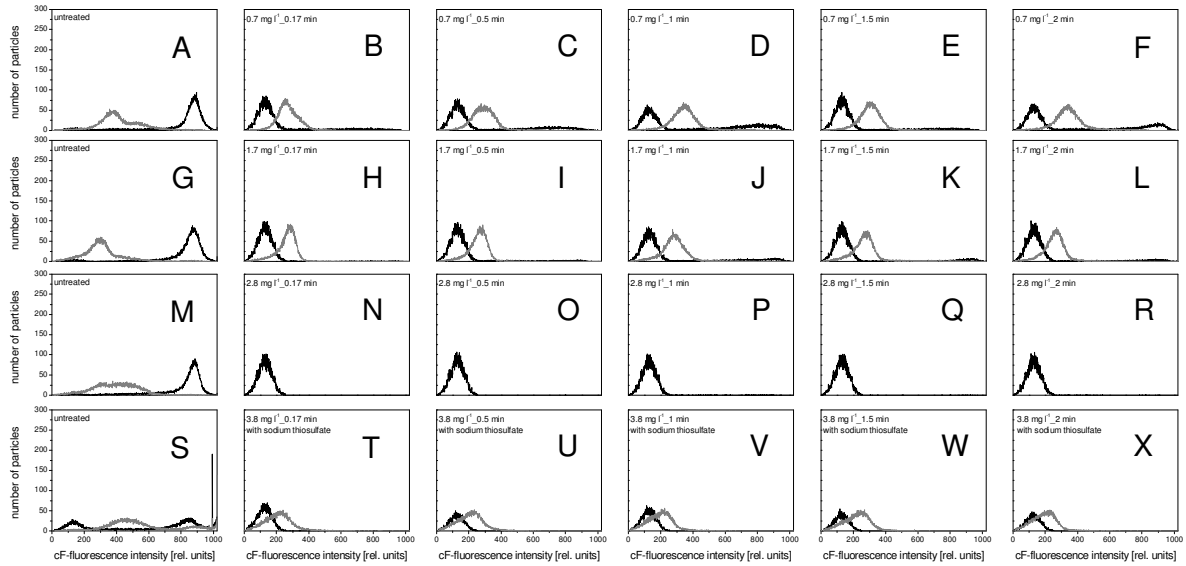

Figure 4.50: Pump activity of *P. carotovorum* cells measured as cF-efflux capability after ozone treatment at concentrations of 0.7 mg l^{-1} (A-F), 1.7 mg l^{-1} (G-L), 2.8 mg l^{-1} (M-R), and 3.8 mg l^{-1} with sodium thiosulfate (S-X). Black lines represent the cF-fluorescence intensity before energising and grey lines represent cF-fluorescence intensity after energising.

Although no or minimal esterase activity of ozone-treated cells was detected the elimination of cF due to intact pump activity was observed. All bacteria showed slightly enhanced cF-fluorescence intensity on energising after ozone treatment at different concentrations (Figures 4.48 to 4.50). The slightly enhanced cF-fluorescence intensity after energising was also detected in heat-treated and PAA-treated cells. It is assumed that cFDA diffused into

cells but was not hydrolysed. The cFDA is not removed by the centrifugation step but is hydrolysed upon energising by spontaneous hydrolysis or by remaining esterases. The amount of accumulated cF is very low so that a spontaneous hydrolysis is more likely than hydrolysis by residual esterases. It is therefore not clear whether the cFDA diffused into the permeabilised cells or into the unstained cells.

4.6.4 Membrane potential of ozone-treated cells

The generation of a membrane potential seems to be dependent on the surrounding medium. The red/green ratio of untreated bacteria was higher before heat treatment than the ratio before ozone treatment. The treatment medium for heat treatment was PBS and the ozone was dissolved into potable water. The generation of membrane potential by tested bacteria was restricted after ozone treatment at different concentrations but the red/green ratio was > 1 indicating that the cells were not completely depolarised after ozone treatment (Figure 4.51).

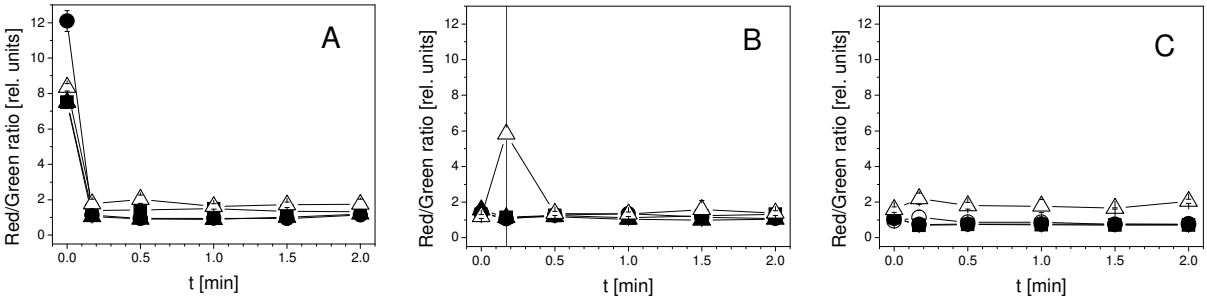

Figure 4.51: Membrane potential of *E. coli* (A), *L. innocua* (B), and *P. carotovorum* (C) cells after ozone treatment at concentrations of 0.7 mg l^{-1} (open circles), 1.7 mg l^{-1} (squares), 2.8 mg l^{-1} (circles), and 3.8 mg l^{-1} without (triangles) and with (open triangles) sodium thiosulfate to stop the reaction; expressed as red/green ratio of $DiOC_2(3)$ fluorescence.

The depolarisation of the cells increased with increasing ozone concentration. However, the highest membrane potential was observed for bacteria cells after ozone treatment (3.8 mg l^{-1}) stopped by the addition of sodium thiosulfate. This implies that the cells are still able to generate membrane potential after ozone treatment although the application of TO/PI and cFDA/PI did not clearly indicate cell viability. It is not possible to distinguish which cells were able to generate membrane potential after ozone treatment because the measurement represents the average of membrane potential of a population and not the membrane potential of single cells.

4.6.5 Impact of ozone treatment on bacteria cells

After ozone treatment the application of fluorescent dyes did not clearly differentiate between viable, sublethally damaged and lethally damaged cells. A high fraction of unstained cells restricted the interpretation of physiological properties. Nevertheless, the obtained data were modelled in order to compare the different inactivation treatments and to describe the mode of action of ozone. According to Davidson & Branden (1981) the mode of microbial inactivation of ozone is categorised into three groups: i) cell membrane is permeabilised and loss of cellular compounds occurs; ii) inactivation of essential enzymes; and iii) destruction or functional inactivation of genetic material.

The used mathematical models for the modelling of flow cytometric data are given in table 4.26.

Table 4.26: Mathematical models used for the modeling of bacterial physiological parameters after ozone treatment

	Membrane permeabilisation	Membrane potential	Esterase activity
E. coli			
1.7 mg l^{-1}	Gompertz	biphasic	log –linear + tail
2.8 mg l^{-1}	Gompertz	log –linear + tail	log –linear + tail
3.8 mg l^{-1}	Gompertz	log –linear + tail	log –linear + tail
3.8 mg l^{-1} + $Na_2S_20_3$	logistic	biphasic	Log –linear + tail
L. innocua			
1.7 mg l^{-1}	Gompertz	log-linear regression	log –linear + tail
2.8 mg l^{-1}	Gompertz	log –linear regression	log –linear + tail
3.8 mg l^{-1}	logistic	biphasic	log –linear + tail
3.8 mg l^{-1} + $Na_2S_20_3$	Gompertz	log-linear regression	log –linear + tail
P. carotovorum			
0.7 mg l^{-1}	Gompertz	log-linear regression	log –linear + tail
1.7 mg l^{-1}	Gompertz	log –linear + tail	log –linear + tail
2.8 mg l^{-1}	/	log –linear + tail	log –linear + tail
3.8 mg l^{-1} + $Na_2S_20_3$	Gompertz	log –linear regression	log –linear + tail

The membrane permeabilisation of *E. coli* was modelled with the Gompertz model (1.7 mg l^{-1}, 2.8 mg l^{-1}, 3.8 mg l^{-1}) and a logistic model (3.8 mg l^{-1} + $Na_2S_2O_3$) using the Origin® software. The loss of membrane potential followed a biphasic kinetic (1.7 mg l^{-1}, 3.8 mg l^{-1} + $Na_2S_2O_3$) and a log-linear regression with tailing (2.8 mg l^{-1}, 3.8 mg l^{-1}). A log linear regression was observed for the inactivation of esterase activity at an ozone concentration of 3.8 mg l^{-1} + $Na_2S_2O_3$ and a log-linear shape with tailing was found for ozone concentrations of 1.7 mg l^{-1}, 2.8 mgl^{-1}, 3.8 mg l^{-1}. The Gompertz model (1.7 mg l^{-1}, 2.8 mg l^{-1}, 3.8 mg l^{-1} + $Na_2S_2O_3$) and the logistic model (3.8 mg l^{-1}) were also used to model the

membrane permeabilisation *of L. inncoua.* The models used to describe the depolarisation rate of *L. innocua* were the log-linear model (1.7 mg l^{-1}, 2.8 mg l^{-1}, and 3.8 mg l^{-1} + $Na_2S_2O_3$) and a biphasic model (3.8 mg l^{-1}). The inactivation of esterase activity was modelled using the log-linear regression with tailing for all ozone concentrations tested. The cell permeabilisation of *P. carotovorum* at an ozone concentration of 2.8 mg l^{-1} could not be described with the applied models but the Gompertz model could be used to model cell permeabilisation at ozone concentrations of 0.7 mg l^{-1} and 1.7 mg l^{-1} and the logistic model described cell permeabilisation at 3.8 mg l^{-1} + $Na_2S_2O_3$. The inactivation of esterase activity followed the log-linear regression with tailing at all ozone concentrations tested. The obtained rates of cell permeabilisation, inactivation of esterase activity and depolarisation are given in table 4.27.

Table 4.27: Statistical measures and parameter values obtained from mathematical models for experimental data of ozone inactivated *E. coli*, *L. innocua*, and *P. carotovorum* (plate count and flow cytometry)

Target site	*E. coli* Ozone concentration [mg l^{-1}]				*L. innocua* Ozone concentration [mg l^{-1}]				*P. carotovorum* Ozone concentration [mg l^{-1}]			
	1.7	**2.8**	**3.8**	**3.8^{+}**	**1.7**	**2.8**	**3.8**	**3.8^{+}**	**0.7**	**1.7**	**2.8**	**3.8^{+}**
Microbial reduction [k_{max} min^{-1}]	75.0	87.1	97.9	60.4 1.3	163.0	172.3	182.2	48.1 0.6	0.0	168.8	151.3	42.9
Membrane permeabilisation [k_{max} min^{-1}]	2261.4*	1.5*	8.7*	9.2*	0.4*	126.1*	9.2*	11.4*	115.7*	18.3*	#	0.8*
Membrane potential [k_{max} min^{-1}]	62.6 0.1	25.9	28.7	59.7 0.1	0.1*	0.1	46.2 0.1	0.1	0.2	72.9	58.9	0.1*
Esterase activity [k_{max} min^{-1}]	111.8	104.4	0.1*	136.7	118.3	92.1	97.2	46.6	97.6	104.7	128.5	40.2

$^{+}$ ozone reaction stopped by sodium thiosulfate
* indicates positive slopes of kinetics
# none of the applied models fitted the obtained curve

The target sites of ozone seem to be different at various ozone concentrations and for the different bacteria. At an ozone concentration of 1.7 mg l^{-1} *E. coli* initially lost membrane integrity, followed by the loss of esterase activity, loss of culturability and finally the loss of membrane potential. At 3.8 mg l^{-1} the loss of culturability is followed by the depolarisation of cells, loss of membrane integrity and loss of esterase activity. The same mode of action was found for ozone concentrations of 2.8 mg l^{-1} and 3.8 mg l^{-1} with addition of $Na_2S_2O_3$. At these ozone concentrations *E. coli* cells initially lost their esterase activity and subsequently their culturability, membrane potential and membrane integrity. The same mode of action was found for heat-treated *E. coli* cells at 90 °C. In contrast, the first target site of ozone on *L. innocua* cells was the culturability at all tested ozone concentrations and with exception of ozone concentration of 2.8 mg l^{-1} the next target site was the esterase activity. At 2.8 mg l^{-1} the membrane integrity was affected directly after loss of culturability followed by loss of

esterase activity and finally the loss of membrane potential. At 3.8 mg l^{-1} the third target point of ozone was the membrane potential and finally the membrane integrity. The same mode of action of ozone was obtained at ozone concentrations of 1.7 mg l^{-1} and 3.8 mg l^{-1} + $Na_2S_2O_3$. In these cases, the third target site was the membrane integrity before depolarisation of cells occurred. Initially, *P. carotovorum* cells lost their membrane integrity at 0.7 mg l^{-1} followed by the loss of esterase activity, loss of membrane potential and finally, culturability. Increasing ozone concentrations led to a different mode of microbial inactivation. Firstly, the culturability is lost, followed by the loss of esterase activity, the loss of membrane potential is the next target site of ozone at concentrations of 1.7 mg l^{-1} and 2.8 mg l^{-1} followed by the loss of membrane integrity whereas the rate of membrane permeabilisation could not be determined for 2.8 mg l^{-1} due to the lack of an applicable model. After stopping the ozone reaction with $Na_2S_2O_3$ the membrane integrity was lost before the loss of membrane potential. This was similar for all tested bacteria. Due to the high percentage of unstained cells and double-stained cells which were not included in the modelling an overestimation or underestimation of the rates of physiological changes may occur. It could not be verified if the unstained fraction after ozone treatment corresponds to complete ruptured cells or to cells that still have intact physiological properties which were not detected with the applied fluorescent dyes due to restricted dye uptake.

4.7 Flow cytometric analysis of plasma-treated bacteria

4.7.1 Morphological changes of plasma-treated cells

The settings for morphological measurements by flow cytometer after plasma treatment were different from measurements after heat, PAA, and ozone treatment. The flow cytometer settings were adapted to the tested inactivation treatments and optimised for the inactivation processes to obtain reliable results. Therefore, the scatter intensities obtained from the plasma experiments were originally lower than the measured scatter intensities obtained from the other experiments. This restricts the direct comparison of scatter intensities after different inactivation techniques.

The scatter properties after plasma treatment at different operating powers and between the three tested bacteria were, however, comparable. The forward scatter intensities and side scatter intensities of *E. coli* did not change after plasma treatment (Figure 4.52). This implies that the size and cellular mass was not affected by the plasma treatment. But as shown for heat, PAA and ozone treatment the forward scatter and side scatter intensities cannot directly be related to structural changes. It was already shown by McGann *et al.* (1988) that

cell volume and scatter properties can vary independently. Similar results were obtained for *L. innocua* (Figure 4.53) and *P. carotovorum* (Figure 4.54). Independent on plasma operating power and treatment time the side scatter intensities and forward scatter intensities remained at the same level.

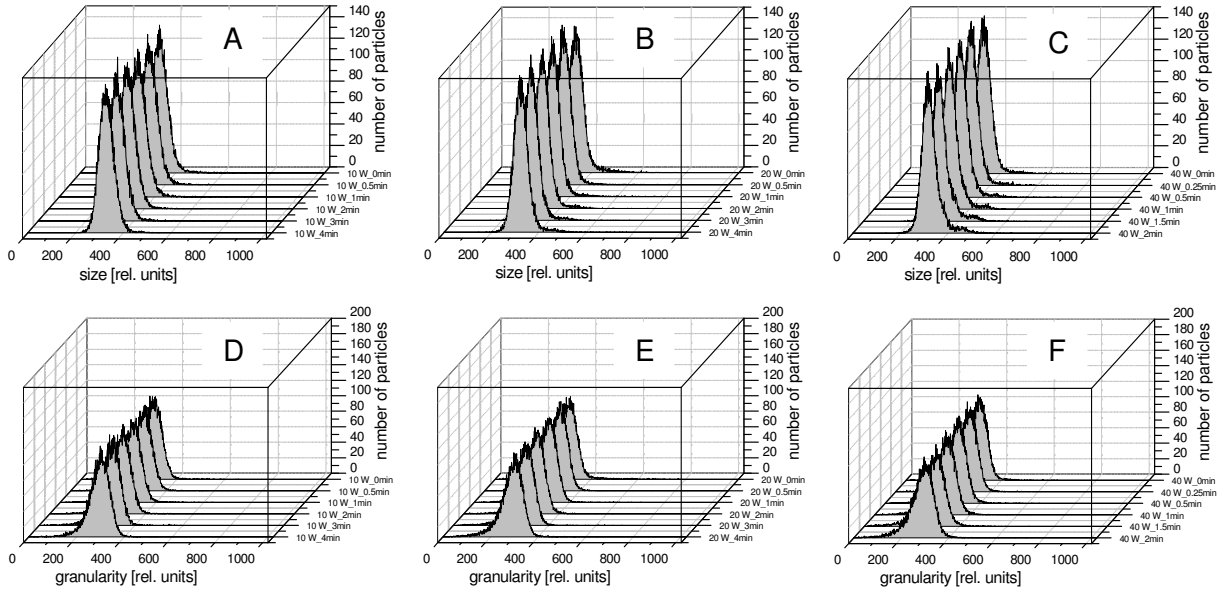

Figure 4.52: Size (A-C) and granularity (D-F) changes of *E. coli* cells after 10 W (A,D), 20 W (B,E), and 40 W (C,F) plasma treatment.

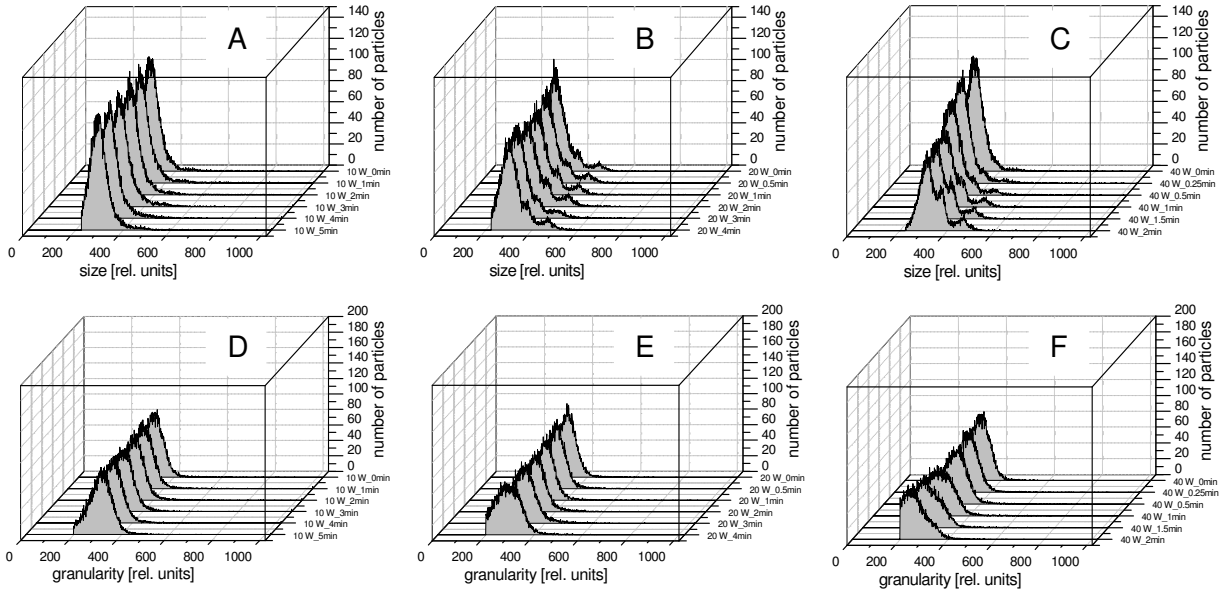

Figure 4.53: Size (A-C) and granularity (D-F) changes of *L. innocua* cells after 10 W (A,D), 20 W (B,E), and 40 W (C,F) plasma treatment.

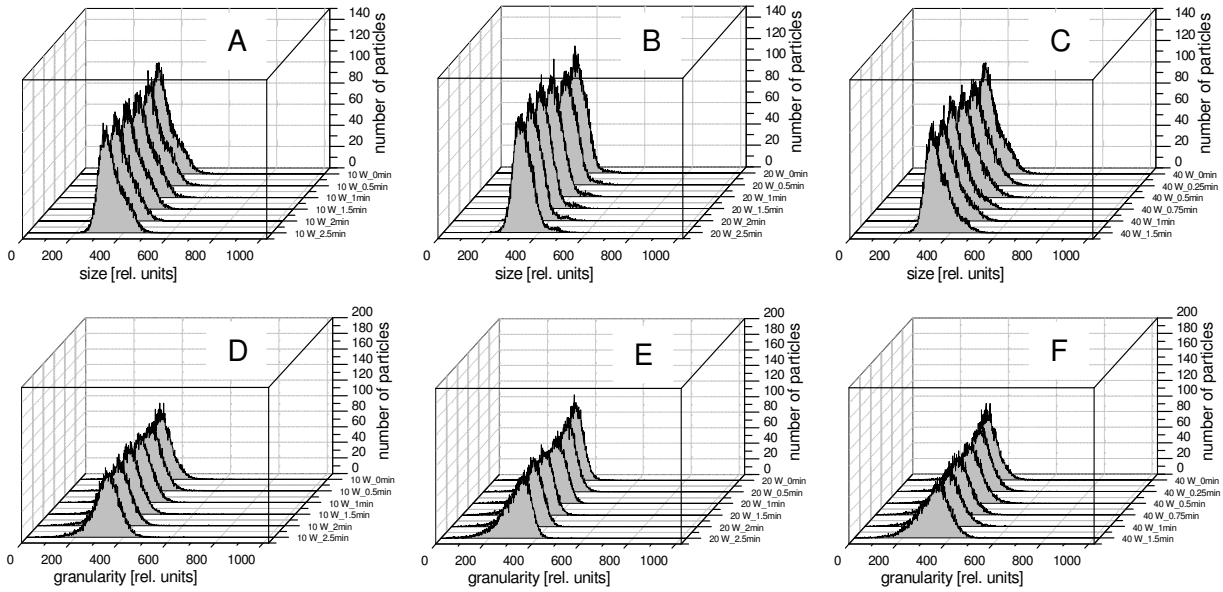

Figure 4.54: Size (A-C) and granularity (D-F) changes of *P. carotovorum* cells after 10 W (A,D), 20 W (B,E), and 40 W (C,F) plasma treatment.

No significant changes in cell volume were observed by Coulter Counter measurements after plasma treatment of *E. coli* at operating powers of 10 W and 40 W (Figure 4.55 A). At an operating power of 20 W a significant increase of cell volume was observed. A significant increase of cell volume was also observed for *L. innocua* at all tested plasma operating powers (Figure 4.55 B). The cell volume of *P. carotovorum* significantly increased during plasma treatment at 10 W and at higher operating powers the cell volume significantly decreased (Figure 4.55 C). A possible explanation for the decrease in cell count could be the disruption of the cells by the plasma treatment resulting in a measurement of cell debris by the Coulter Counter. Another explanation for the decrease of cell size might be the mistaken measurement of gel pieces. During plasma treatment the gel surface can be modified which may result in a greater amount of gel pieces during re-suspension. These gel pieces are also measured by Coulter Counter and may lead to a misinterpretation of cell size.

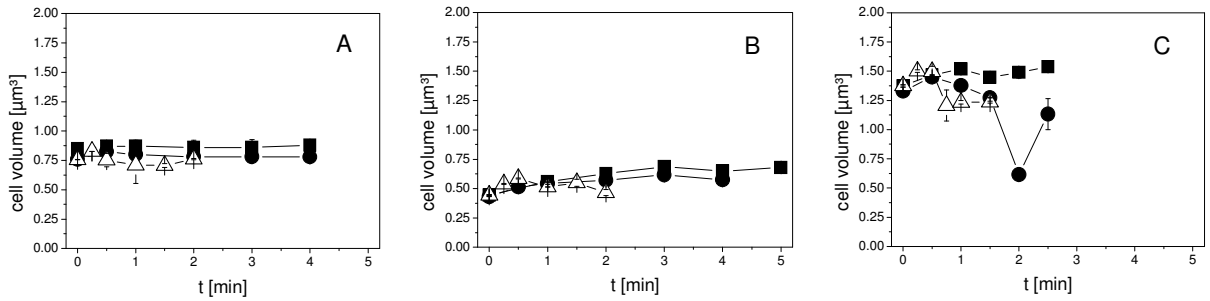

Figure 4.55: Cell volume of *E. coli* (A), *L. innocua* (B), and *P. carotovorum* (C) cells measured by Coulter Counter after plasma treatment at 10 W (squares), 20 W (circles), and 40 W (open triangles).

These measurements indicate the different mode of plasma action on the different bacteria. But the measurements once again show that the forward scatter measurements cannot directly be translated into cell volume.

4.7.2 Membrane integrity of plasma-treated cells

To investigate the inactivation mechanism of APPJ on *E. coli*, *L. innocua,* and *P. carotovorum* inoculated on a polysaccharide gel flow cytometric analyses were performed after treatment. The use of TO and PI in combination showed that the cell membranes of *E. coli*, *L. innocua, and P. carotovorum* were just slightly affected at an operating power of 10 W in comparison to the untreated control. At 20 W differences between the Gram-positive *L. innocua* and the Gram-negative *E. coli* and *P. carotovorum* were observed. The percentage of complete permeabilised *E. coli* and *P. carotovorum* cells increased with increasing treatment time to approximately 55 % while the percentage of slightly permeabilised cells remained almost constant. In contrast, the percentage of complete permeabilised *L. innocua* cells only slightly increased but the percentage of slightly permeabilised cells increased to 42 % after 4 min. Furthermore the percentage of unstained cells increased with increasing treatment time while the percentage of unstained *E. coli* and *P. carotovorum* remained almost constant at 20 W. Increasing operating power to 40 W showed that the percentage of permeabilised *L. innocua* cell membrane increased up to 30 %. Simultaneously, the percentage of unstained cells increased to 55 %. The distribution of stained *E. coli* cells at 40 W is similar to the distribution of stained *E. coli* cells at 20 W but a slight increase of unstained cells could be observed. The percentage of complete permeabilised *P. carotovorum* cells increased at 40 W to 70 % within 2.5 min and the percentage of unstained cells remained almost constant (Figure 4.56).

At 10 W the percentage of intact bacteria cells slightly changed as a result of microbial heterogeneity. The changes are not significant. At 20 W the percentage of intact *L. innocua* cells decreased but the percentage of PI stained cells did not increase proportionally. The large amount of unstained cells may indicate a complete rupture of the cell membrane and associated cell lyses. In contrast, the percentage of unstained Gram-negative bacteria remained almost constant after plasma treatment at different operating powers.

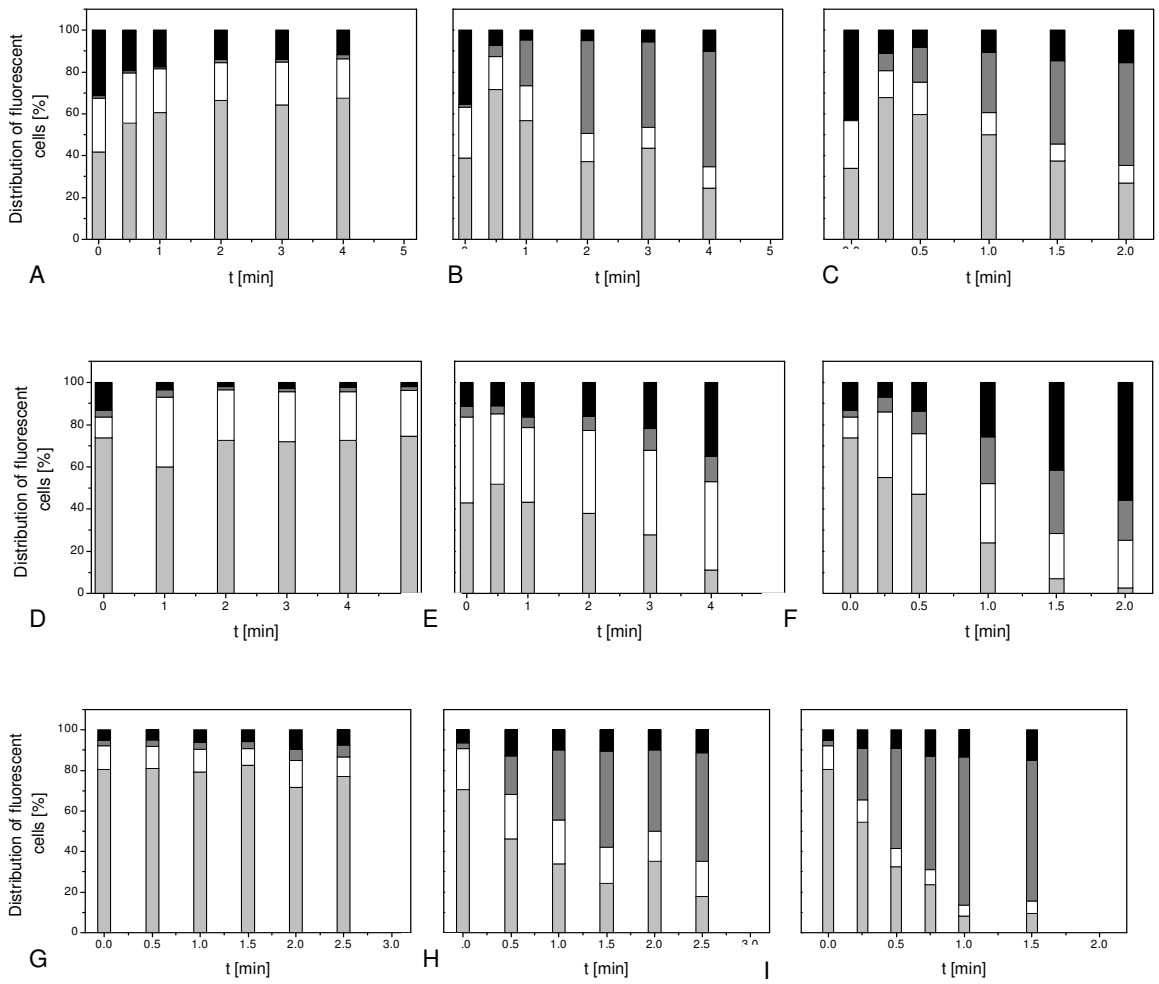

Figure 4.56: Membrane integrity of *E. coli* (A-C), *L. innocua* (D-F), and *P. carotovorum* (G-I) cells after plasma treatment at 10 W (A,D,G), 20 W (B,E,H), and 40 W (C,F,I). Black bars indicating cells without fluorescence, dark gray bars indicating PI-fluorescence (permeabilised cells), white bars indicating TO+PI-fluorescence (slightly permeabilised cells), light gray bars indicating TO-fluorescence (cells with membrane integrity). The standard deviation of the measurements is given in Annex 7 (Tables 19-21).

Scanning electron microscopy (SEM) images of Gram-positive *B. subtilis* and Gram-negative *E. coli* on filters after resistive barrier discharge plasma treatment showed that Gram-positive bacteria do not undergo morphological changes (Laroussi, 2002). Similar results were obtained for *E. coli* and *S. aureus* treated with One Atmosphere Uniform Glow Discharge and analysed with Transmission Electron Microscopy (TEM). Additionally, measurements of *E. coli* and *S. aureus* with a spectrophotometer were performed to evaluate changes in absorbency at 260 nm reflecting leakage of ultraviolet absorbing proteins, RNA, and DNA from the cytoplasm into extracellular fluid. Large concentrations of these macromolecules were detected after 10 s plasma treatment of *E. coli*, whereas the leakage of components of *S. aureus* was delayed indicating a tougher cell wall. This supported the evidence from measurements of TEM indicating membrane damage of *E. coli* after plasma treatment (Gadri *et al.*, 2000). A possible explanation for the membrane rupture of Gram-negative cells is

given by Mendis *et al.* (2000). They proposed that the charge accumulation on the outer surface of the membrane of Gram-negative bacteria overcomes the tensile strength of the membrane resulting in its rupture. In contrast to Gram-negative bacteria, Gram-positive bacteria have a smoother surface and a thicker murein layer and therefore, a higher strength and rigidity. The inactivation of Gram-positive bacteria by plasma treatment might possibly be explained by the diffusion of reactive species through the cell membrane into the cell where they directly react with intracellular compounds (Laroussi *et al.*, 2003). Therefore, the high percentage of unstained cells after APPJ treatment suggests that the RNA and DNA were affected by the treatment and cell lyses only occurred after higher operating powers and longer treatment times. This assumption is supported by the significant increase in mean TO fluorescence intensity during plasma treatment (Table 4.28).

Table 4.28: Mean fluorescence intensity of TO-stained *E. coli* cells after non-thermal plasma treatment determined by flow cytometry

	10 W		20 W		40 W	
treatment time [min]	**Mean TO-fluorescence intensity [rel. units]**	**SD**	**Mean TO-fluorescence intensity [rel. units]**	**SD**	**Mean TO-fluorescence intensity [rel. units]**	**SD**
0	109.3[a]	± 5.3	136.8[a]	± 36.7	92.3[a]	± 6.9
0.25	n.a.	n.a.	n.a.	n.a.	316.5[b]	± 11.1
0.5	198.3[b]	± 27.3	365.7[b]	± 79.8	342.6[b]	± 4.1
1	217.2[b,c]	± 22.9	371.3[b]	± 69.3	325.7[b]	± 17.2
1.5	n.a.	n.a.	n.a.	n.a.	333.8[b]	± 12.2
2	256[b,c]	± 17.7	367.4[b]	± 49.5	337[b]	± 19.1
3	258.9[c]	± 27.2	375.2[b]	± 52.6	n.a.	n.a.
4	268.3[c]	± 21.4	331.2[b]	± 33.9	n.a.	n.a.

SD, Standard deviation of three independent experiments
n.a., not analysed
[a-c], Different letters within the columns indicate significant differences at a significance level of 0.05

A significant increase of mean TO-fluorescence intensity was observed for all tested bacteria and all tested plasma operating powers (Tables 4.29 & 4.30). This indicates that even at low plasma operating power damage to RNA occurred. In contrast to *E. coli* and *P. carotovorum* the mean TO-fluorescence intensity of *L. innocua* decreased again with increasing treatment time at all tested operating powers whereas the decrease at 10 W was not significantly. It is not clear whether the RNA and DNA damage is caused by UV radiation or due to oxidation by oxygen radicals as both of these have been suggested as possible inactivation mechanisms for high pressure plasma. Previous experiments showed that the UV irradiation generated by a similar plasma jet had minor influence on the bacteria (Brandenburg *et al.*, 2007). However, argon supported the UV transmission and UV can support the inactivation.

Table 4.29: Mean fluorescence intensity of TO-stained *L. innocua* cells after non-thermal plasma treatment determined by flow cytometry

	10 W		20 W		40 W	
treatment time [min]	**Mean TO-fluorescence intensity [rel. units]**	**SD**	**Mean TO-fluorescence intensity [rel. units]**	**SD**	**Mean TO-fluorescence intensity [rel. units]**	**SD**
0	201.9[a]	± 5.6	205.2[a]	± 9.8	201.9[a,b]	± 5.6
0.25	n.a.	n.a.	n.a.	n.a.	299.6[a]	± 109.8
0.5	n.a.	n.a.	270.3[a]	± 45.1	342.0[a]	± 78.2
1	296.4[b]	± 24.6	390.8[b]	± 64.1	276.8[a,b]	± 56.4
1.5	n.a.	n.a.	n.a.	n.a.	263.8[a,b]	± 67.7
2	364.88[b,c]	± 24.6	442.9[b]	± 39.5	107.5[b]	± 33.8
3	413.6[c]	± 14.9	433.1[b]	± 49.2	n.a.	n.a.
4	394.1[c]	± 31.4	52.1[c]	± 5.6	n.a.	n.a.
5	390.8[c]	± 44.8	n.a.	n.a.	n.a.	n.a.

SD, Standard deviation of three independent experiments
n.a., not analysed
[a-c], Different letters within the columns indicate significant differences at a significance level of 0.05

The decrease of TO-intensity with increasing treatment time may be the result of enhanced membrane permeabilisation resulting in competitive intercalating of PI and TO with DNA and quenching of TO-fluorescence by the PI-fluorescence.

Table 4.30: Mean fluorescence intensity of TO-stained *P. carotovorum* cells after non-thermal plasma treatment determined by flow cytometry

	10 W		20 W		40 W	
treatment time [min]	**Mean TO-fluorescence intensity [rel. units]**	**SD**	**Mean TO-fluorescence intensity [rel. units]**	**SD**	**Mean TO-fluorescence intensity [rel. units]**	**SD**
0	282.7[a,b,c]	± 31.2	138.4[a]	± 3.1	282.7[a]	± 31.2
0.25	n.a.	n.a.	n.a.	n.a.	503.5[b,d]	± 51.7
0.5	255[a]	± 11.8.	237.4[b]	± 4.9	491.1[b,d]	± 6.9
0.75	n.a.	n.a.	n.a.	n.a.	717.4[c,d]	± 94.2
1	261.5[a,b]	± 24.5	265.4[b]	± 23.6	599.2[d]	± 17.8
1.5	298[a,b,c]	± 27.4	489.5[c]	± 45.4	582.9[d]	± 582.9
2	325[b,c]	± 32.7	601.8[d]	± 41.9	n.a.	n.a.
2.5	325[c]	± 10.3	608.3[d]	± 49.9	n.a.	n.a.

SD, Standard deviation of three independent experiments
n.a., not analysed
[a-d], Different letters within the columns indicate significant differences at a significance level of 0.05

4.7.3 Esterase activity of plasma-treated bacteria

The impact of atmospheric pressure plasma on intracellular compounds was investigated by measuring esterase activity of bacteria cells after treatment using cFDA and PI in combination. The different modes of plasma action against Gram-positive bacteria and Gram-negative bacteria detected by membrane integrity measurements were confirmed by measuring esterase activity.

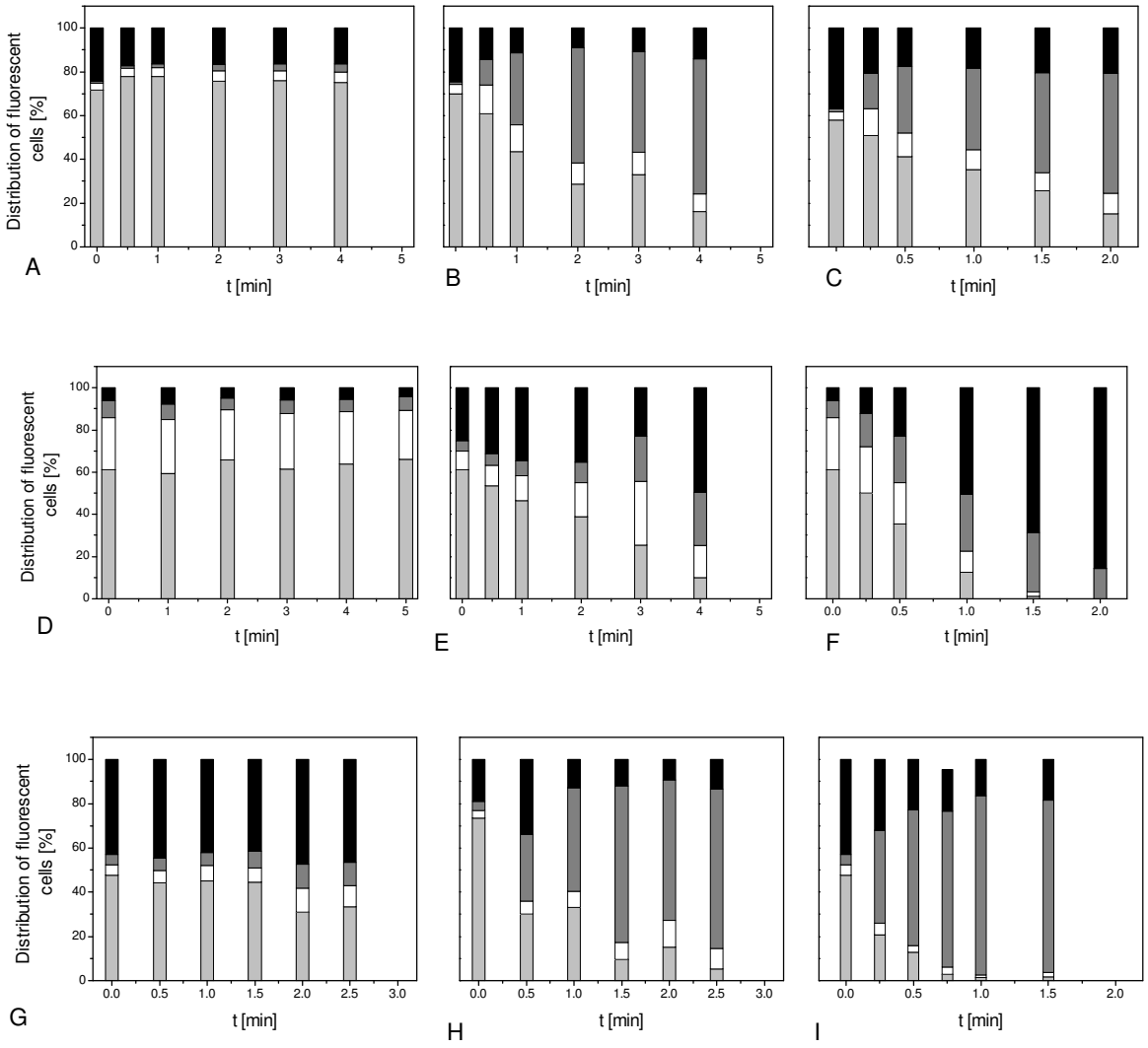

Figure 4.57: Esterase activity and membrane integrity of *E. coli* (A-C), *L. innocua* (D-F), and *P. carotovorum* (G-I) cells after plasma treatment at 10 W (A,D,G), 20 W (B,E,H), and 40 W (C,F,I). Black bars indicating cells without fluorescence, dark gray bars indicating PI-fluorescence (permeabilised cells), white bars indicating cF+PI-fluorescence (permeabilised cells with esterase activity), light gray bars indicating cF-fluorescence (intact cells with esterase activity). The standard deviation of the measurements is given in Annex 8 (Tables 22-24).

At 10 W operating power minor effects of plasma on esterase activity of tested bacteria were detected. The amount of unstained *E. coli* and *P. carotovorum* cells at 10 W was higher than the amount of unstained cells obtained by TO/PI-staining but was similar for plasma-treated and untreated cells. This suggests that the bacteria were already stressed due to the inoculation of the polysaccharide gel. The lack of PI uptake indicates that the cells were not permeabilised. The lack of cF-fluorescence may indicate the reduction of metabolic activity to improve survival under stress conditions. A nearly linear reduction of esterase activity to 10 % within 4 min was obtained for *L. innocua* at 20 W. The highest inactivation of esterase was found at 40 W with a reduction to 0.1 % after 1.5 min of treatment. For the treatment parameters 10, 20, and 40 W the percentage of cells with cF and PI staining representing

cells with esterase activity and slightly permeabilised cell membrane remained nearly constant. Increasing the operating power to 20 and 40 W increased the percentage of permeabilised cells to 25 % and 14 %, respectively. The percentage of unstained cells including cell debris and gel particles remained nearly constant at 10 W and increased at 20 W and 40 W to 50 % and 86 % within the last treatment minute (Figure 4.57). In contrast, the percentage of unstained *E. coli* and *P. carotovorum* remained almost constant at 20 W and 40 W but the percentage of permeabilised cells without esterase activity increased with increasing treatment time. Thereby, the distribution of stained *E. coli* at 20 W is similar to the distribution of stained *E. coli* cells at 40 W as was previously observed by TO/PI-staining.

Similar to the results obtained by TO/PI-staining the percentage of complete permeabilised *P. carotovorum* cells increased with increasing treatment time and increasing operating powers. This indicates that the permeabilised cells also lost their esterase activity. The reduction of esterase activity and the lack of proportional increasing PI-stained cells indicating permeabilised cell membranes suggest that the cell membrane of *L. innocua* remained intact during plasma treatment and that the plasma compounds react with cellular components whereas the cell membrane and cellular components of *E. coli* and *P. carotovorum* were affected by the plasma. Gallagher *et al.* (2007) performed flow cytometric analyses of *E. coli* bioaerosol using SYBR Green I and PI after Dielectric Barrier Grating Discharge treatment. They found that the intensity of PI fluorescence was negligible after treatment and suggested that the outer membrane of *E. coli* was not ruptured while 97 % of *E. coli* was reduced after 0.73 ms direct plasma exposure and subsequent 3.5 log reduction in the following two minutes of remote exposure. They suggested that the reduction in culturability of *E. coli* was due to chemically active components present in the plasma. The lack of fluorescence intensity may have been due to an oxidation of cellular proteins and lipids (as assumed for ozone inactivation) which restricted or prevented the uptake, binding and conversion of fluorescence dyes.

The influence of temperature can be disregarded because the temperature of the gel surface remained below 50 °C for the highest power level and below 30 °C for the other power levels applied. The heat may have caused damage to free RNA and DNA if cells had been ruptured but esterase activity was shown to be heat resistant by the accumulation of cF detected after heat treatment at 60 °C (Breeuwer *et al.*, 1994).

4.7.4 Impact of plasma treatment on bacteria cells

Modelling of plasma inactivation kinetics obtained by plate count methods showed that the time needed for the first decimal reduction was highest for *L. innocua* at all tested plasma

operating powers. The time for the first decimal reduction of *P. carotovorum* at 10 and 20 W was lower than the time needed to reduce *E. coli* and at 40 W *E. coli* showed the lowest time for first decimal reduction. This is in contrast to the heat and ozone treatments where *L. inncoua* seems to be more sensitive than *E. coli* and *P. carotovorum*. The mathematical models used for description of bacterial physiological properties after plasma treatment are given in table 4.31. The Gompertz model was used to described the cell permeabilisation kinetics of *E. coli* (10, 20, 40 W), *L. innocua* and *P. carotovorum* (20, 40 W) and the log-linear regression model was applied to cell permeabilisation kinetics of *P. carotovorum* (10 W). The cell permeabilisation kinetic of *L. innocua* at 10 W followed the log-linear regression with shoulder and tailing. The logistic model was applied to esterase inactivation kinetics of *E. coli* at 10 W and at 20 W the esterase inactivation followed the log-linear regression. An additional shoulder formation was found for esterase inactivation of *E. coli* at 40 W. A shoulder formation with log-linear regression was also observed for esterase inactivation of *L. innocua* at 20 and 40 W. At 10 W the Gompertz model was applied to describe the esterase inactivation kinetic. The inactivation of *P. carotovorum* esterase was described with the log-linear regression model with shoulder formation and tailing, the log-linear regression model, and the log-linear regression model with tailing for plasma operating powers of 10, 20, and 40 W, respectively. The rates of physiological property changes obtained are given in table 4.32.

Table 4.31: Mathematical models used for the modeling of bacterial physiological parameters after plasma treatment

	Membrane permeabilisation	Esterase activity
E. coli		
10 W	Gompertz	logisitc
20 W	Gompertz	log –linear regression
40 W	Gompertz	log –linear + tail
L. innocua		
10 W	log –linear + tail	Gompertz
20 W	Gompertz	log –linear shoulder
40 W	Gompertz	log –linear shoulder
P. carotovorum		
10 W	logistic	log –linear + shoulder + tail
20 W	Gompertz	log –linear regression
40 W	Gompertz	log –linear + tail

Table 4.32: Statistical measures and parameter values obtained from mathematical models for experimental data of plasma inactivated *E. coli*, *L. innocua*, and *P. carotovorum* (plate count and flow cytometry)

Target site	*E. coli*			*L. innocua*			*P. carotovorum*		
	10 W	20 W	40 W	10 W	20 W	40 W	10 W	20 W	40 W
First decimal reduction δ [min]	2.88	1.4	1.06	7.29	2.11	3.11	1.54	1.20	1.38
Membrane permeabilisation [k_{max} min^{-1}]	3.45*	2.16*	0.55*	14.14	0.02*	2.80*	0.34*	2.89*	4.78*
Esterase activity [k_{max} min^{-1}]	0.00	0.35	1.19	2.06	1.25	6.51	0.70	0.96	3.06

* indicates positive slopes of kinetics

The rate of membrane permeabilisation decreased with increasing plasma operating powers for *E. coli* and increased with increasing operating powers for *L. innocua* and *P. carotovorum*. The loss of esterase activity in *L. inncoua* occurred earlier than membrane permeabilisation. Same results were observed for *P. carotovorum* at an operating power of 10 W and for *E. coli* at an operating power of 40 W. In contrast, at operating powers of 10 W and 20 W cell membrane permeabilisation of *E. coli* occurred before the esterase was inactivated. This was also found for *P. carotovorum* treated with plasma at operating powers of 20 and 40 W. These results imply that the cellular components of Gram-positive bacteria were affected by APPJ before cell membrane permeabilisation was induced and that cell rupture of Gram-negative bacteria occurred before cellular components were affected. This is in agreement with the literature, where the different modes of action are described (Mendis *et al.*, 2000; Gadri *et al.*, 2000; Laroussi, 2002; Laroussi *et al.*, 2003). The dependence of treatment time on cellular effects was shown by Pompl *et al.* (2009). They found cell rupture in Gram-positive bacteria using atomic force microscopy after elongated plasma exposure. However, the high percentage of unstained cells may lead to an overestimation or underestimation of physiological properties. Nevertheless, differences between the applied plasma operating powers as well as differences between the bacteria species could be detected with the chosen fluorescent dyes.

5. Conclusion and perspective

The reduction of microbial load on fresh produce is necessary to minimize the risk of foodborne diseases and postharvest losses. This requirement for appropriate preservation methods is limited by the potential affects of preservation treatments on product quality. The heat-sensitivity of fresh produce limits the application of thermal treatments and the use of chemical disinfectants may lead to the formation of potential hazardous by-products. Therefore, there is an increasing demand for alternative non-thermal treatment techniques. These non-thermal techniques include both chemical and physical treatment methods.

Detailed knowledge of inactivation effects is required for successful implementation of inactivation treatments in the production chain. Furthermore, the success of the inactivation process has to be verified online to ensure product safety. Due to the short shelf-life of fresh produce the results need to be obtained within a limited time period to enable contamination-related process control. Conventional microbiological techniques such as plate count methods are very time consuming and an absence of culturability cannot be directly related to cellular death. Therefore, the implementation of these methods in the processing chain is limited. In response to these limitations minimal duration methods to monitor inactivation treatments are required. Flow cytometry is a promising tool in food microbiology as it enables measurements on a single cell level and the detection of physiological property changes of bacteria after certain treatment processes.

This work combines the investigation of inactivation efficiency of innovative technologies such as heat, PAA, ozone, and atmospheric pressure plasma against different bacteria using conventional plate count methods and the investigation of the potential of flow cytometric measurements to monitor these treatment processes. Thereby, important insights into the mode of microbial inactivation of the different treatments were obtained by flow cytometric measurements using the fluorescent dyes TO, PI, cFDA and $DiOC_2(3)$ to evaluate membrane integrity, esterase activity, pump activity and membrane potential of bacteria cells, respectively. The application of these dyes showed the potential of flow cytometric measurements to monitor the inactivation of bacteria. The results obtained from plate count methods and flow cytometric measurements were modelled with common mathematical models to allow a comparison between the investigated inactivation processes. Different modes of microbial inactivation of *E. coli, P. carotovorum,* and *L. innocua* were determined and related to the selected treatment methods as well as differences between the inactivation methods and treatment conditions.

The application of fluorescent dyes to evaluate physiological properties can be restricted by the cell structure of bacteria. It was shown that the uptake of macromolecules by Gram-negative bacteria is inhibited by the additional cell membrane and therefore, the measurement of esterase activity using cFDA is limited. To overcome this limitation an appropriate method for cFDA staining of Gram-negative bacteria was developed within this study using *P. carotovorum* as a test organism. The application of chelating reagents did not lead to enhanced cFDA uptake and hydrolyses but instead increased membrane permeabilisation of bacteria was detected. The higher amount of permeabilised cells after addition of chelating reagents was even detected at low concentrations of the applied reagents indicating irreversible membrane damage. Thus, the application of chelating reagents to improve dye uptake is not suitable, particularly with regard to reliable detection of inactivation efficiencies. However, enhanced uptake of cFDA by *P. carotovorum* was achieved using high dye concentrations and elongated incubation times. Additionally, a successful transfer of the developed cFDA-staining method to Gram-negative bacteria such as *E. coli* was achieved. Reliable and reproducible measurements of esterase activity of untreated and inactivated pure Gram-negative bacteria cultures were possible. Hence, cFDA could be used to measure esterase activity of bacteria after certain treatments.

The inactivation efficiency of heat treatment obtained by plate count methods increased with increasing temperature for all tested bacteria. But all tested bacteria showed a tailing due to heat resistance of bacteria subpopulations or heterogeneity of the treatments. An inactivation of *L. innocua* and *P. carotovorum* below the detection limit was only achieved at 90 °C but *E. coli* was not completely reduced by the applied temperatures. Furthermore, the heat inactivation of bacteria is dependent of the initial bacteria concentration. Whereas the inactivation rate of *L. innocua* decreased with decreasing initial concentration, the inactivation rate of *E. coli* and *P. carotovorum* was higher at lower initial concentrations at 70 °C. At high initial bacteria counts *L. innocua* was more heat sensitive than *P. carotovorum* and *E. coli* while controversial results were obtained at lower initial bacteria counts with *L. innocua* being the most heat resistant bacteria. The negative impact of temperatures above 45 °C on fresh produce and the negligible inactivation of bacteria at 50 °C (with exception of *P. carotovorum*) already in pure suspensions leads to the conclusion that heat treatment is not applicable to the postharvest production chain of fresh produce. Additionally, the application of flow cytometry using diverse fluorescent dyes indicates different modes of microbial inactivation for different bacteria species within the tested temperature levels. It was shown that the cells were affected at different target sites and cellular death is the result of the loss of culturability, loss of membrane potential, metabolic activity and membrane integrity. Thereby, the range of target sites is variable depending on tested temperature

levels and the bacteria selected. Thus, the selection of appropriate temperature levels for the treatment of products is limited and requires detailed knowledge of the amount and diversity of microbial load.

In contrast to the heat treatment, a reduction of *E. coli* to the detection limit was achieved at a concentration of 0.25 % PAA. Independently of treatment temperature and PAA concentration a five log reduction of *E. coli* was detected after 0.25 min. However, metabolic activity in terms of esterase activity and pump activity was demonstrated by flow cytometric measurements after PAA treatment. This clearly indicates that the cells lost their culturability but were not completely inactivated and can still cause product damage or human disease. Similar to the heat treatment cellular death of *E. coli* induced by PAA is the result of the impact on different target sites. However, the mode of microbial inactivation of *E. coli* by PAA appears to be similar for all tested PAA concentrations and treatment temperatures. This enables a more reliable prediction of microbial inactivation.

The application of ozone to inactivate *E. coli, L. innocua,* and *P. carotovorum* also induced a loss of culturability after a short treatment time (0.17 min). But the inactivation rates of *E. coli* after ozone treatment were lower than the highest inactivation rate obtained by PAA treatment. However, a five log reduction of all tested bacteria was found after 0.17 min and ozone concentrations above 1.7 mg l^{-1}. *E. coli* was the most resistant against the ozone treatment and *L. innocua* the most sensitive bacteria against the ozone treatment. Similarly to the heat treatment, the initial bacteria concentration also influences the inactivation efficiency of ozone. The inactivation rate of *E. coli* obtained after ozone treatment was higher at lower initial bacteria counts which reflected the result for the heat treatment. But the inactivation rate of *L. innocua* and *P. carotovorum* decreased with decreasing initial count. The application of flow cytometric measurements using different fluorescent dyes was restricted due to the enormous structural changes of bacteria cells. These ozone-induced structural changes detected in size and granularity changes were measured by flow cytometry. In contrast, these morphological changes were not observed after heat and PAA treatment. It can be assumed that the cells were rupture by the ozone treatment and cell lyses occurred. This would result in a high amount of unstained cells and also in indefinable fluorescence with increasing ozone concentrations and treatment time. Nevertheless, the flow cytometric measurements indicate that the ozone affects the bacteria cells at different target points. Thereby, the mode of microbial inactivation is different for all tested bacteria and ozone concentrations and also the results may be influenced by the high amount of unstained cells. The comparison of ozone reactions stopped by degassing of residual ozone and ozone reactions stopped by quenching of residual ozone by $Na_2S_2O_3$ showed that the degassing method does not efficiently remove the ozone. A reduced inactivation of all

bacteria was found after stopping the reaction with $Na_2S_2O_3$. This indicates that the ozone still reacts after removal by degassing. In comparison to the ozone reaction stopped by degassing, *E. coli* was the most sensitive bacteria against ozone treatment stopped by $Na_2S_2O_3$ and *P. carotovorum* the most resistant bacteria. The measurement of physiological properties by flow cytometric techniques after stopping the ozone reaction with $Na_2S_2O_3$ led to an increased amount of unstained cells but the changes of size and granularity were not as distinctive as after ozone removal by degassing. At one hand, it can be assumed that the uptake of fluorescent dyes is limited by an ozone-induced oxidation of membrane components resulting in the high amount of unstained cells; at the other hand it is possible that the membrane permeabilisation is a reversible state and theses cells are still able to form colonies. A reliable assertion on the physiological state of this population is not possible. However, these results also indicate that a reliable dosage of ozone is restricted and successive reactions can occur which may also influence the product quality.

Atmospheric pressure plasma is of growing interest for food surface decontamination but the mechanism of action and the disinfectant potential has not been fully understood until now. The inactivation efficiency of an atmospheric pressure plasma jet was evaluated using an inoculated polysaccharide gel to simulate bacteria adherent on food surfaces. A reduction of *E. coli, L. innocua*, and *P. carotovorum* to the detection limit was achieved at a plasma operating power of 40 W after 2 min, 1.5 min, and 0.75 min, respectively, but temperature measurements of the gel surface exceeded the critical temperature of fresh produce. Thus, the product quality may be affected at this plasma operating power. This study did reveal that at an operating power of 10 W only minor inactivation effects on potential humanpathogenic bacteria could be observed. Therefore, the most promising plasma operating power for food surface decontamination seems to be 20 W with a reduction to the detection limit after 4 min (*E. coli* and *L. innocua*) and 2.5 min (*P. carotovorum*). This operating power led to surface temperatures below 30 °C and thus, the product quality may not be affected by heat. In contrast to the other applied disinfectant methods, *L. innocua* is the most resistant bacteria against APPJ followed by *E. coli* and *P. carotovorum*. The mode of microbial inactivation of APPJ seems to be distinctly different for Gram-negative and Gram-positive bacteria. While the cell membrane of Gram-negative *E. coli* and *P. carotovorum* is affected before the esterase activity is reduced, the esterase activity of Gram-positive *L. innocua* is reduced before cell permeabilisation occurred. Consequently, the inactivation of Gram-negative bacteria seems to be predominantly caused by cell permeabilisation while the predominant inactivation of Gram-positive bacteria is caused by the inactivation of cellular components. This assumption is supported by the high amount of unstained Gram-positive bacteria after APPJ treatment indicating intact cell membranes but a lack of metabolic activity. It is unlikely

that the unstained cells correspond to ruptured cells as assumed for ozone-treated cells, because the morphological changes observed after ozone treatment could not be detected after APPJ treatment. However, the physiological state of unstained cells is not verified and requires further investigations.

Although, the time needed to achieve a reduction to the detection limit is longer for APPJ treatment than for PAA and ozone treatment, APPJ seems to be the most promising process for food surface decontamination. Although it should be noted that the comparison of PAA, ozone, and APPJ treatment was restricted, bacteria cells were treated with PAA and ozone in suspension whereas bacteria cells treated with APPJ were adherent on a surface (because of the formation of different bacteria layers on the surface of the gel, the superficial bacteria layer may have protective effects against the lowest bacteria layer resulting in reduced inactivation). However, the APPJ treatment procedure is more related to food surface decontamination than the other tested treatment procedures.

Generally, the application of common mathematical models to describe inactivation kinetics obtained by plate count methods after heat, PAA, ozone and APPJ treatment is possible but may be restricted in some cases. In particular, in the cases of instantaneously inactivation (ozone) or inactivation within a very short time (PAA) the modelling may lead to misinterpretation of the shape of survivor curves due to the limited number of data points. A decrease in length of treatment time to evaluate more data points is not practical for ozone treatment due to ozone reaction even after removal of ozone after defined treatment times. A successful quenching of ozone reduced the bacteria just by approximately 4 log units with tailing, the APPJ treatment reduced bacteria by 4 log units and modelling of the survivor curves indicates additional inactivation with increasing treatment time. The presence of organic matter will further reduce the antimicrobial effects of ozone. The interference of organic matter on effectiveness of APPJ is unknown until now and should be object of further investigations. Furthermore, the use of additional fluorescent dyes to evaluate other physiological changes of bacteria after APPJ treatment is necessary for a better characterisation of the mode of microbial inactivation by APPJ.

The use of flow cytometric measurements to characterise different inactivation treatments enables the examination of inactivation effects at a single cell level within a short time. With the applied fluorescent dyes it was possible to evaluate the membrane integrity, esterase activity, pump activity, and membrane potential of Gram-negative and Gram-positive bacteria after the different inactivation treatments used in this study. It was shown that the bacteria were not homogeneously inactivated by the treatments tested because different cell populations were detected by flow cytometry. It appears that the different inactivation

processes result in different distributions of subpopulations. The reliability of measurements is dependent on the inactivation processes applied. In case of complete membrane rupture and cell lyses the application of fluorescent dyes seems to be restricted because a high amount of undefined fluorescence is detected. Furthermore, as a result of the damage of intracellular components the applied fluorescent dyes could not intercalate or could not be metabolized. This also leads to a high amount of unstained cells which may result in an overestimation or underestimation of inactivation effects. Nevertheless, it was shown that flow cytometric measurements provide important information of bacteria cell status after different inactivation treatments within a short time. The modelling of physiological property changes obtained by flow cytometric measurements can help to predict inactivation kinetics. The detailed knowledge of inactivation effects is absolutely necessary for the implementation of inactivation processes in the production chain. In a first approach, the membrane integrity was modelled with the Gompertz model or a logistic and esterase activity and membrane potential were modelled with the GInaFIT tool. Thus, the determination of permeabilisation, depolarisation, and the esterase inactivation rates was possible and facilitates the comparison of different inactivation processes as well as the prediction of inactivation effects. However, the kinetics of unstained cells and double-stained cells are not considered in the modelling. Thus, important information regarding the inactivation mechanisms could have been lost. It was not possible to model the obtained curves for unstained cells and double-stained cells with common available mathematical models due to the irregular shape of the curves. This may lead to a misinterpretation of inactivation mechanisms.

This work clearly indicates the potential of flow cytometric measurements for monitoring of inactivation processes. Conceivably, a miniaturised flow cytometry could be implemented after the inactivation process in the production line to verify the inactivation success. This could provide the facility to improve and guarantee product safety. In order to achieve a reliable online-enabled flow cytometric measurement the staining procedure of bacteria should be optimized in future investigations to reduce the amount of undefined cells as well as to reduce the number of preparation steps. Additionally, the analysis and interpretation of flow cytometric data should be improved to obtain reliable prediction models for physiological changes of bacteria after certain inactivation treatments.

References

Abadias M, Usall J, Anguera M, Solsona C, & Viñas I (2008) Microbiological quality of fresh, minimally-processed fruit and vegetables, and sprouts from retail establishments. International Journal of Food Microbiology, 123(1-2), 121-129.

Abou-Ghazala A, Katsuki S, Schoenbach KH, Dobbs FC, & Moreira KR (2002) Bacterial decontamination of water by means of pulsed-corona discharges. IEEE Transactions on Plasma Science, 30(4), 1449-1453.

Aguayo E, Escalona VH, & Artés F (2006) Effect of cyclic exposure to ozone gas on physicochemical, sensorial and microbial quality of whole and sliced tomatoes. Postharvest Biology and Technology, 39(2), 169-177.

Aguirre JS, Pin C, Rodriguez MR, & de Fernando GDG (2009) Analysis of the variability in the number of viable bacteria after mild heat treatment of food. Applied and Environmental Microbiology, 75(22), 6992-6997.

Akbas MY & Ölmez H (2007) Effectiveness of organic acid, ozonated water and chlorine dippings on microbial reduction and storage quality of fresh-cut iceberg lettuce. Journal of the Science of Food and Agriculture, 87(14), 2609-2616.

Akbas MY & Ozdemir M (2008) Application of gaseous ozone to control populations of *Escherichia coli, Bacillus cereus* and *Bacillus cereus* spores in dried figs. Food Microbiology, 25(2), 386-391.

Alsharif R & Godfrey W (2002) Bacterial detection and live/dead discrimination by flow cytometry. Application Note, 1-6.

Alvarez-Barrientos A, Arroyo J, Canton R, Nombela C, & Sanchez-Perez M (2000) Applications of flow cytometry to clinical microbiology. Clinical Microbiology Reviews, 13(2), 167-+.

Alvaro JE, Moreno S, Dianez F, Santos M, Carrasco G, & Urrestarazu M (2009) Effects of peracetic acid disinfectant on the postharvest of some fresh vegetables. Journal of Food Engineering, 95(1), 11-15.

Amann RI, Binder BJ, Olson RJ, Chisholm SW, Devereux R, & Stahl DA (1990) Combination of 16s ribosomal-RNA-targeted oligonucleotide probes with flow-cytometry for analyzing mixed microbial-populations. Applied and Environmental Microbiology, 56(6), 1919-1925.

An J, Zhang M, & Lu Q (2007) Changes in some quality indexes in fresh-cut green asparagus pretreated with aqueous ozone and subsequent modified atmosphere packaging. Journal of Food Engineering, 78(1), 340-344.

Ananta E, Voigt D, Zenker M, Heinz V, & Knorr D (2005) Cellular injuries upon exposure of *Escherichia coli* and *Lactobacillus rhamnosus* to high-intensity ultrasound. Journal of Applied Microbiology, 99, 271-278.

Ananta E, Heinz V, & Knorr D (2004) Assessment of high pressure induced damage on *Lactobacillus rhamnosus* GG by flow cytometry. Food Microbiology, 21(5), 567-577.

Ananta E & Knorr D (2009) Comparison of inactivation pathways of thermal or high pressure inactivated *Lactobacillus rhamnosus* ATCC 53103 by flow cytometry analysis. Food Microbiology, 26(5), 542-546.

Ananata E (2005) Impact of environmental factors on viability and stability and high pressure pretreatment on stress tolerance of *Lactobacillus rhamnosus* GG (ATCC 53103) during spray drying. PhD Thesis. TU Berlin.

Anderson WA, Hedges ND, Jones MV, & Cole MB (1991) Thermal inactivation of *Listeria monocytogenes* studied by differential scanning calorimetry. Journal of General Microbiology, 137(6), 1419-1424.

Antonelli M, Rossi S, Mezzanotte V, & Nurizzo C (2006) Secondary effluent disinfection: PAA long term efficiency. Environmental Science & Technology, 40(15), 4771-4775.

Aronsson K, Ronner U, & Borch E (2005) Inactivation of *Escherichia coli, Listeria innocua* and *Saccharomyces cerevisiae* in relation to membrane permeabilization and subsequent leakage of intracellular compounds due to pulsed electric field processing. International Journal of Food Microbiology, 99(1), 19-32.

Baatout S, De Boever P, & Mergeay M (2005) Temperature-induced changes in bacterial physiology as determined by flow cytometry. Annals of Microbiology, 55(1), 73-80.

Baatout S, Leys N, Hendrickx L, Dams A, & Mergeay M (2007) Physiological changes induced in bacteria following pH stress as a model for space research. Acta Astronautica, 60(4-7), 451-459.

Babic I, Roy S, Watada AE, & Wergin WP (1996) Changes in microbial populations on fresh cut spinach. International Journal of Food Microbiology, 31(1-3), 107-119.

Baert L, Uyttendaele M, Van Coillie E, & Debevere J (2008) The reduction of murine norovirus 1, *B. fragilis* HSP40 infecting phage B40-8 and *E. coli* after a mild thermal pasteurization process of raspberry puree. Food Microbiology, 25(7), 871-874.

Baldry MGC, French MS, & Slater D (1991) The activity of peracetic-acid on sewage indicator bacteria and viruses. Water Science and Technology, 24(2), 353-357.

Baranyi J & Roberts TA (1994) A dynamic approach to predicting bacterial growth in food. International Journal of Food Microbiology, 23(3-4), 277-294.

Barras F, van Gijsegem F, & Chatterjee AK (1994) Extracellular enzymes and pathogenesis of soft-rot *Erwinia*. Annual Review of Phytopathology, 32(1), 201-234.

Basaran P, Basaran-Akgul N, & Oksuz L (2008) Elimination of *Aspergillus parasiticus* from nut surface with low pressure cold plasma (LPCP) treatment. Food Microbiology, 25(4), 626-632.

Baur S, Klaiber R, Hammes WP, & Carle R (2004) Sensory and microbiological quality of shredded, packaged iceberg lettuce as affected by pre-washing procedures with chlorinated and ozonated water. Innovative Food Science & Emerging Technologies, 5(1), 45-55.

Beirne T & Hutcheon JM (1957) A photoelectric particle counter for use in the sieve range. Journal of Scientific Instruments, 34(5), 196-200.

Ben- Amor K, Breeuwer P, Verbaarschot P, Rombouts FM, Akkermans ADL, De Vos WM, & Abee T (2002) Multiparametric flow cytometry and cell sorting for the assessment of viable, injured, and dead *Bifidobacterium* cells during bile salt stress. Applied and Environmental Microbiology, 68(11), 5209-5216.

Ben-Amor K (2004) Microbial eco- physiology of the human intestinal tract: a flow cytometry approach. PhD Thesis. Wageningen University.

Benito A, Ventoura G, Casadei M, Robinson T, & Mackey B (1999) Variation in resistance of natural isolates of *Escherichia coli* O157 to high hydrostatic pressure, mild heat, and other stresses. Applied and Environmental Microbiology, 65(4), 1564-1569.

Berdalet E & Dortch Q (1991) New double-staining technique for RNA and DNA measurement in marine-phytoplankton. Marine Ecology-Progress Series, 73(2-3), 295-305.

Berkman RM & Wyatt PJ (1970) Differential light scattering measurements of heat-treated bacteria. Applied and Environmental Microbiology, 20(3), 510-512.

Berney M, Weilenmann HU, & Egli T (2006) Flow-cytometric study of vital cellular functions in *Escherichia coli* during solar disinfection (SODIS). Microbiology, 152(6), 1719-1729.

Berney M, Hammes F, Bosshard F, Weilenmann HU, & Egli T (2007) Assessment and interpretation of bacterial viability by using the LIVE/DEAD BacLight™ Kit in combination with flow cytometry. Applied and Environmental Microbiology, 73(10), 3283-3290.

Beuchat LR (1998) Surface decontamination of fruits and vegetables eaten raw: a review. WHO/FSF/FOS/98.2.

Beuchat LR, Adler BB, & Lang MM (2004) Efficacy of chlorine and a peroxyacetic acid sanitizer in killing *Listeria monocytogenes* on iceberg and romaine lettuce using simulated commercial processing conditions. Journal of Food Protection, 67, 1238-1242.

Beuchat LR (1996) Pathogenic microorganisms associated with fresh produce. Journal of Food Protection, 59, 204-216.

Bezirtzoglou E, Cretoiu SM, Moldoveanu M, Alexopoulos A, Lazar V, & Nakou M (2008) A quantitative approach to the effectiveness of ozone against microbiota organisms colonizing toothbrushes. Journal of Dentistry, 36(8), 600-605.

Bialka KL & Demirci A (2007) Efficacy of aqueous ozone for the decontamination of *Escherichia coli* O157:H7 and *Salmonella* on raspberries and strawberries. Journal of Food Protection, 70, 1088-1092.

Bore SL (2005) Characterization of micro-organisms isolated from dairy industry after cleaning and fogging disinfection with alkyl amine and peracetic acid. Journal of Applied Microbiology, 98(1), 96-105.

Boudam MK, Moisan M, Saoudi B, Popovici C, Gherardi N, & Massines F (2006) Bacterial spore inactivation by atmospheric-pressure plasmas in the presence or absence of UV photons as obtained with the same gas mixture. Journal of Physics D-Applied Physics, 39(16), 3494-3507.

Brandenburg R, Ehlbeck J, Stieber M, von Woedtke T, Zeymer J, Schlüter O, & Weltmann KD (2007) Antimicrobial treatment of heat sensitive materials by means of atmospheric pressure rf-driven plasma jet. Contributions to Plasma Physics, 47(1-2), 72-79.

Breeuwer P, Drocourt JL, Rombouts FM, & Abee T (1994) Energy-dependent, carrier-mediated extrusion of carboxyfluorescein from *Saccharomyces cerevisiae* allows rapid assessment of cell viability by flow cytometry. Applied and Environmental Microbiology, 60(5), 1467-1472.

Breeuwer P, Drocourt J, Rombouts FM, & Abee T (1996) A novel method for continuous determination of the intracellular pH in bacteria with the internally conjugated fluorescent probe 5 (and 6-)-carboxyfluorescein succinimidyl ester. Applied and Environmental Microbiology, 62(1), 178-183.

Breeuwer P, Drocourt J-L, Bunschoten N, Zwietering MH, Rombouts FM, & Abee T (1995) Characterization of uptake and hydrolysis of fluorescein diacetate and carboxyfluorescein diacetate by intracellular esterases in *Saccharomyces cerevisiae*, which result in accumulation of fluorescent product. Applied and Environmental Microbiology, 61(4), 1614-1619.

Breidt JR F (2006) Safety of minimally processed, acidified, and fermented vegetable products. *In* Microbiology of fruits and vegetables, pp. 313-335: Taylor and Francis Group, CRC Press.

Briñez WJ, Roig-Saguès AX, Hernández Herrero MM, López-Pedemonte T, & Guamis B (2006) Bactericidal efficacy of peracetic acid in combination with hydrogen peroxide against pathogenic and non pathogenic strains of *Staphylococcus* spp., *Listeria* spp. and *Escherichia coli*. Food Control, 17(7), 516-521.

Broadwater W, Hoehn R, & King P (1973) Sensitivity of three selected bacterial species to ozone. Applied microbiology, 26(3), 391-393.

Brul S, Rommens AJM, & Verrips CT (2000) Mechanistic studies on the inactivation of *Saccharomyces cerevisiae* by high pressure. Innovative Food Science & Emerging Technologies, 1(2), 99-108.

Budde BB & Rasch M (2001) A comparative study on the use of flow cytometry and colony forming units for assessment of the antibacterial effect of bacteriocins. International Journal of Food Microbiology, 63(1-2), 65-72.

Bunthof CJ & Abee T (2002) Development of a flow cytometric method to analyze subpopulations of bacteria in probiotic products and dairy starters. Applied and Environmental Microbiology, 68(6), 2934-2942.

Bunthof CJ, van den Braak S, Breeuwer P, Rombouts FM, & Abee T (1999) Rapid fluorescence assessment of the viability of stressed *Lactococcus lactis*. Applied and Environmental Microbiology, 65(8), 3681-3689.

Bunthof CJ, van den Braak S, Breeuwer P, Rombouts FM, & Abee T (2000) Fluorescence assessment of *Lactococcus lactis* viability. International Journal of Food Microbiology, 55(1-3), 291-294.

Bunthof CJ, Bloemen K, Breeuwer P, Rombouts FM, & Abee T (2001) Flow cytometric assessment of viability of lactic acid bacteria. Applied and Environmental Microbiology, 67(5), 2326-2335.

Bunthof CJ (2002) Flow cytometry, fluorescent probes, and flashing bacteria. PhD Thesis. Wageningen University.

Carlin F, Nguyenthe C, & Dasilva AA (1995) Factors affecting the growth of *Listeria-Monocytogenes* on minimally processed fresh endive. Journal of Applied Bacteriology, 78(6), 636-646.

Carlin F, Nguyenthe C, & Morris CE (1996) Influence of background microflora on *Listeria monocytogenes* on minimally processed fresh broad-leaved endive (*Cichorium endivia* var *latifolia*). Journal of Food Protection, 59(7), 698-703.

CAST-Council for Agricultural Science and Technology (2009) Food safety and fresh produce: an update. CAST Commentary QTA2009-1.

Castillo A, McKenzie KS, Lucia LM, & Acuff GR (2003) Ozone treatment for reduction of *Escherichia coli* O157:H7 and *Salmonella* serotype *typhimurium* on beef carcass surfaces. Journal of Food Protection, 66, 775-779.

Cerf O (1977) Tailing of survival curves of bacterial-spores. Journal of Applied Bacteriology, 42(1), 1-19.

Chitarra LG, Breeuwer P, Abee T, & Bulk R (2006) The use of fluorescent probes to assess viability of the plant pathogenic bacterium *Clavibacter michiganensis* subsp. *michiganensis* by flow cytometry. Fitopatologia Brasileira, 32(4), 349-356.

Codex Alimentarius Commitee on Food Hygiene (2003) Code of hygienic practice for fresh fruits and vegetables.

Condon S, Garcia ML, Otero A, & Sala FJ (1992) Effect of culture age, preincubation at low-temperature and pH on the thermal-resistance of *Aeromonas-Hydrophila*. Journal of Applied Bacteriology, 72(4), 322-326.

Cornwall JB & Davison RM (1960) Rapid counter for small particles in suspension. Journal of Scientific Instruments, 37(11), 414-417.

Coulter, WH (1956). High speed automatic blood cell counter and cell size analyzer. Proceedings of the National Electronics Conference Volume *12*, pp. 1034-1040. National Electronics Conference, Chigago.

Couvert O, Gaillard S, Savy N, Mafart P, & Leguérinel I (2005) Survival curves of heated bacterial spores: effect of environmental factors on Weibull parameters. International Journal of Food Microbiology, 101(1), 73-81.

Critzer FJ, Kelly-Wintenberg K, South SL, & Golden DA (2007) Atmospheric plasma inactivation of foodborne pathogens on fresh produce surfaces. Journal of Food Protection, 70(10), 2290-2296.

Cronan J & Vagelos PR (1972) Metabolism and function of the membrane phospholipids of *Escherichia coli*. Biochimica et Biophysica Acta (BBA) - Reviews on Biomembranes, 265(1), 25-60.

Crossland-Taylor PJ (1953) A device for counting small particles suspended in a fluid through a tube. Nature, 171(4340), 37-38.

Cullen PJ, Tiwari BK, O'Donnell CP, & Muthukumarappan K (2009) Modelling approaches to ozone processing of liquid foods. Trends in Food Science & Technology, 20(3-4), 125-136.

Da Silveira MG, San Romao MV, Loureiro-Dias MC, Rombouts FM, & Abee T (2002) Flow cytometric assessment of membrane integrity of ethanol-stressed *Oenococcus oeni* cells. Applied and Environmental Microbiology, 68(12), 68.

Da Silveira MG & Abee T (2009) Activity of ethanol-stressed *Oenococcus oeni* cells: a flow cytometric approach. Journal of Applied Microbiology, 106(5), 1690-1696.

Das E, Gürakan GC, & BayIndIrll A (2006) Effect of controlled atmosphere storage, modified atmosphere packaging and gaseous ozone treatment on the survival of *Salmonella Enteritidis* on cherry tomatoes. Food Microbiology, 23(5), 430-438.

Davey HM, Weichart DH, Kell DB, & Kaprelyants AS (1999) Estimation of microbial viability using flow cytometry. In Current Protocols in Cytometry, p. 11.3.1-11.3.20.

Davey HM (2002) Flow cytometric techniques for the detection of microorganisms. Methods in Cell Science, 24, 91-97.

Davey HM & Kell DB (1996) Flow cytometry and cell sorting of heterogeneous microbial populations: the importance of single-cell analyses. Microbiological Reviews, 60(4), 641-696.

Davidson PM & Branden AL (1981) Anti-microbial activity of non-halogenated phenolic-compounds. Journal of Food Protection, 44(8), 623-&.

De Roever C (1998) Microbiological safety evaluations and recommendations on fresh produce. Food Control, 9(6), 321-347.

Dell'Erba A, Falsanisi D, Liberti L, Notarnicola M, & Santoro D (2007) Disinfection by-products formation during wastewater disinfection with peracetic acid. Desalination, 215, 177-186.

Deng SB, Ruan R, Mok CK, Huang GW, Lin XY, & Chen P (2007) Inactivation of *Escherichia coli* on almonds using nonthermal plasma. Journal of Food Science, 72(2), M62-M66.

Deng SX, Cheng C, Ni GH, Meng YD, & Chen H (2008) Bacterial inactivation by atmospheric pressure dielectric barrier discharge plasma jet. Japanese Journal of Applied Physics, 47(8), 7009-7012.

Deng XT, Shi JJ, Shama G, & Kong MG (2005) Effects of microbial loading and sporulation temperature on atmospheric plasma inactivation of *Bacillus subtilis* spores. Applied Physics Letters, 87(15), 153901-153903.

Deng XT, Shi JJ, Chen HL, & Kong MG (2007) Protein destruction by atmospheric pressure glow discharges. Applied Physics Letters, 90(1).

Diaper JP & Edwards C (1994) The use of fluorogenic esters to detect viable bacteria by flow cytometry. Journal of Applied Bacteriology, 77, 221-228.

Dickey RS (1979) *Erwinia-Chrysanthemi* - comparative-study of phenotypic properties of strains from several hosts and other *Erwinia* species. Phytopathology, 69(4), 324-329.

Dietrich JP, Loge FJ, Ginn TR, & Basagˆaogˆlu (2007) Inactivation of particle-associated microorganisms in wastewater disinfection: modeling of ozone and chlorine reactive diffusive transport in polydispersed suspensions. Water Research, 41(10), 2189-2201.

Doyle MP & Erickson MC (2008) Summer meeting 2007 - the problems with fresh produce: an overview. Journal of Applied Microbiology, 105, 317-330.

Drake JF & Tsuchiya HM (1973) Differential counting in mixed cultures with Coulter Counters. Applied Microbiology, 26(1), 9-13.

Earnshaw RG, Appleyard J, & Hurst RM (1995) Understanding physical inactivation processes: combined preservation opportunities using heat, ultrasound and pressure. International Journal of Food Microbiology, 28(2), 197-219.

Ehlbeck J, Brandenburg R, von Woedtke T, Krohmann U, Stieber M, & Weltmann KD (2008) PLASMOSE - antimicrobial effects of modular atmospheric plasma sources. GMS Krankenhaushygiene interdisziplinär, 3(1).

El Shafie A, Fouda MMG, & Hashem M (2009) One-step process for bio-scouring and peracetic acid bleaching of cotton fabric. Carbohydrate Polymers, 78(2), 302-308.

Estrela C, Estrela CRA, Decurcio DA, Hollanda ACB, & Silva JA (2007) Antimicrobial efficacy of ozonated water, gaseous ozone, sodium hypochlorite and chlorhexidine in infected human root canals. International Endodontic Journal, 40(2), 85-93.

European Commission (2004) Commission Regulation (EC) No. 852/2004 of the European Parliament and of the Council of 29 April 2004 on the hygiene of foodstuffs.

European Commission (2007) Commission Regulation (EC) No. 1441/2007 of 5 December 2007 amending (EC) No. 2073/2005 on microbiological criteria for foodstuffs.

European Commission (2008) Commission Regulation (EC) No. 1333/2008 of the European Parliament and of the Council of 16 December 2008 on food additives.

Everis L (2004) Risks of pathogens in ready-to-eat fruits, vegetables, and salads through the production process. Review, Campden & Chorleywood Food Research Association: No.44, vii + 94pp., (44).

Fassihiani A & Nedaeinia R (2008) Characterization of Iranian *Pectobacterium carotovorum* strains from sugar beet by phenotypic tests and whole-cell proteins profile. Journal of Phytopathology, 156(5), 281-286.

FDA U.S.Food and Drug Administration (2008) Guidance for industry: guide to minimize microbial food safety hazards of fresh-cut fruits and vegetables.

Fedio WM & Jackson H (1989) Effect of tempering on the heat resistance of *Listeria monocytogenes*. Letters in Applied Microbiology, 9(5), 157-160.

Fielding LM, Hall A, & Peters AC (2007) An evaluation of ozonated water as an alternative to chemical cleaning and sanitisation of beer lines. Journal of Foodservice, 18(2), 59-68.

Fitzgerald MS (2004) Mode of antimicrobial action of vanillin against *Escherichia coli, Lactobacillus plantarum* and *Listeria innocua*. Journal of Applied Microbiology, 97(1), 104-113.

Fouchet P, Jayat C, Héchard Y, Ratinaud MH, & Frelat G (1993) Recent advances of flow cytometry in fundamental and applied microbiology. Biology of the Cell, 78, 95-109.

Francis GA, Thomas C, & O'beirne D (1999) The microbiological safety of minimally processed vegetables. International Journal of Food Science 38; Technology, 34, 1-22.

Fridman A, Chirokov A, & Gutsol A (2005) Non-thermal atmospheric pressure discharges. Journal of Physics D-Applied Physics, 38(2), R1-R24.

Fridman G, Brooks AD, Balasubramanian M, Fridman A, Gutsol A, Vasilets VN, Ayan H, & Friedman G (2007) Comparison of direct and indirect effects of non-thermal atmospheric-pressure plasma on bacteria. Plasma Processes and Polymers, 4(4), 370-375.

Frommer PL (1962) An automatic counter for blood cells. Annals of the New York Academy of Sciences, 99(2), 233-&.

Fulwyler MJ (1965) Electronic separation of biological cells by volume. Science, 150(3698), 910-&.

Gadri RB, Roth RJ, Montie TC, Kelly-Wintenberg K, Tsai PPY, Helfritch DJ, Feldman P, Sherman DM, Karakaya F, Chen Z, & UTK Plasma Sterilization Team (2000) Sterilization and plasma processing of room temperature surfaces with a one atmosphere uniform glow discharge plasma (OAUGDP). Surface and Coatings Technology, 131(1-3), 528-541.

Gallagher MJ, Vaze N, Gangoli S, Vasilets VN, Gutsol AF, Milovanova TN, Anandan S, Murasko DM, & Fridman AA (2007) Rapid inactivation of airborne bacteria using atmospheric pressure dielectric barrier grating discharge. IEEE Transactions on Plasma Science, 35(5), 1501-1510.

Garcia D, Gomez N, Manas P, Raso J, & Pagan R (2007) Pulsed electric fields cause bacterial envelopes permeabilization depending on the treatment intensity, the treatment medium pH and the microorganism investigated. International Journal of Food Microbiology, 113(2), 219-227.

Gaunt LF, Beggs CB, & Georghiou GE (2006) Bactericidal action of the reactive species produced by gas-discharge nonthermal plasma at atmospheric pressure: a review. IEEE Transactions on Plasma Science, 34(4), 1257-1269.

Geeraerd AH, Herremans CH, & Van Impe JF (2000) Structural model requirements to describe microbial inactivation during a mild heat treatment. International Journal of Food Microbiology, 59(3), 185-209.

Geeraerd AH, Valdramidis VP, & Van Impe JF (2005) GInaFiT, a freeware tool to assess non-log-linear microbial survivor curves. International Journal of Food Microbiology, 102(1), 95-105.

Gehr R, Wagner M, Veerasubramanian P, & Payment P (2003) Disinfection efficiency of peracetic acid, UV and ozone after enhanced primary treatment of municipal wastewater. Water Research, 37(19), 4573-4586.

Gil MI, Selma MV, López-Gálvez F, & Allende A (2009) Fresh-cut product sanitation and wash water disinfection: problems and solutions. International Journal of Food Microbiology, 134(1-2), 37-45.

Gill CO & Badoni M (2004) Effects of peroxyacetic acid, acidified sodium chlorite or lactic acid solutions on the microflora of chilled beef carcasses. International Journal of Food Microbiology, 91(1), 43-50.

Goncalves AA (2009) Ozone: an emerging technology for the seafood industry. Brazilian Archives of Biology and Technology, 52, 1527-1539.

Gonzalez RJ, Luo YG, Ruiz-Cruz S, & Mcevoy JL (2004) Efficacy of sanitizers to inactivate *Escherichia coli* O157:H7 on fresh-cut carrot shreds under simulated process water conditions. Journal of Food Protection, 67(11), 2375-2380.

Gorny J (2006) Microbial contamination of fresh fruits and vegetables. In Microbiology of fruits and vegetables, pp. 3-32: Taylor and Francis Group, CRC Press.

Graham D (1997) Use of ozone for food processing. Food Technology, 51(6), 72-76.

Gram L, Bagge-Ravn D, Ng YY, Gymoese P, & Vogel BF (2007) Influence of food soiling matrix on cleaning and disinfection efficiency on surface attached *Listeria monocytogenes*. Food Control, 18(10), 1165-1171.

Greene A, Few BK, & Serafini JC (1993) A comparison of ozonation and chlorination for the disinfection of stainless steel surfaces. Journal of Diary Science, 76, 3617-3620.

Gregori G, Citterio S, Ghiani A, Labra M, Sgorbati S, Brown S, & Denis M (2001) Resolution of viable and membrane-compromised bacteria in freshwater and marine waters based on analytical flow cytometry and nucleic acid double staining. Applied and Environmental Microbiology, 67(10), 4662-4670.

Grzegorzewski F, Rohn S, Kroh LW, Geyer M, & Schlüter O (2010) Surface morphology and chemical composition of lamb's lettuce (*Valerianella locusta*) after exposure to a low-pressure oxygen plasma. Food Chemistry, 122(4).

Guan D & Hoover DG (2006) Novel nonthermal treatments. In Microbiology of fruits and vegetables , pp. 497-522: Taylor and Francis Group, CRC Press.

Gucker FT, Okonski CT, Pickard HB, & Pitts JN (1947) A photoelectronic counter for colloidal particles. Journal of the American Chemical Society, 69(10), 2422-2431.

Guzel-Seydim Z, Greene A, & Seydim A (2004) Use of ozone in the food industry. Food Science and Technology, 37(4), 453-460.

Hammes F, Berney M, Wang YY, Vital M, Koster O, & Egli T (2008) Flow-cytometric total bacterial cell counts as a descriptive microbiological parameter for drinking water treatment processes. Water Research, 42(1-2), 269-277.

Hassenberg K, Fröhling A, Geyer M, Schlüter O, & Herppich WB (2008) Ozonated wash water for inhibition of *Pectobacterium carotovorum* on carrots and the effect on the physiological behaviour of produce. European Journal of Horticultural Science, 73(1), 37-42.

Haugland RP (1994) Chapter 37: Spectra of fluorescent dyes used in flow cytometry. *In* Methods in Cell Biology Flow Cytometry, pp. 641-663: Academic Press.

Heise, M., Franken, O., Neff, W., Wunderlich, J., & Muranyi, P. (2004). Decontamination of polymer foils with a combined UV-plasma source at atmospheric pressure.

Herrero M, Quiros C, Garcia LA, & Diaz M (2006) Use of flow cytometry to follow the physiological states of microorganisms in cider fermentation processes. Applied and Environmental Microbiology, 72(10), 6725-6733.

Herrmann HW, Henins I, Park J, & Selwyn GS (1999) Decontamination of chemical and biological warfare, (CBW) agents using an atmospheric pressure plasma jet (APPJ). Physics of Plasmas, 6(5), 2284-2289.

Hewitt CJ & Nebe-von-Caron G (2004) The application of multi-parameter flow cytometry to monitor individual microbial cell physiological status. Advances in Biochemical Engineering / Biotechnology, 89, 197-223.

Hilgren J, Swanson KMJ, Diez-Gonzalez F, & Cords B (2007) Inactivation of *Bacillus anthracis* spores by liquid biocides in the presence of food residue. Applied and Environmental Microbiology, 73(20), 6370-6377.

Hilgren JAS (2000) Antimicrobial efficacy of a peroxyacetic/octanoic acid mixture in fresh-cut-vegetable process waters. Journal of Food Science, 65(8), 1376-1379.

Hoefel D, Monis P, Grooby W, Andrews S, & Saint C (2005) Profiling bacterial survival through a water treatment process and subsequent distribution system. Journal of Applied Microbiology, 99, 175-186.

Hoefel D, Grooby WL, Monis PT, Andrews S, & Saint CP (2003) A comparative study of carboxyfluorescein diacetate and carboxyfluorescein diacetate succinimidyl ester as indicators of bacterial activity. Journal of Microbiological Methods, 52(3), 379-388.

Holt JG, Krieg NR, Sneath PHA, Saley JT, & Williams ST (2000) Bergey`s Manual® of determinative bacteriology. Lippincott Williams & Wilkins,

Iannelli D, D'Apice L, Fenizia D, Serpe L, Cottone C, Viscardi M, & Capparelli R (1998) Simultaneous identification of antibodies to *Brucella abortus* and *Staphylococcus aureus* in milk samples by flow cytometry. Journal of Clinical Microbiology, 36(3), 802-806.

Inan F, Pala M, & Doymaz I (2007) Use of ozone in detoxification of aflatoxin B1 in red pepper. Journal of Stored Products Research, 43(4), 425-429.

Janex ML, Savoye P, Roustan M, Do-Quang Z, La+«n+® JM, & Lazarova V (2000) Wastewater disinfection by ozone: Influence of water quality and kinetics modeling. Ozone: Science & Engineering: The Journal of the International Ozone Association, 22(2), 113-121.

Jepras RI, Carter J, Pearson SC, Paul FE, & Wilkinson MJ (1995) Development of a robust flow cytometric assay for determining numbers of viable bacteria. Applied and Environmental Microbiology, 61(7), 2696-2701.

Joux F & Lebaron P (2000) Use of fluorescent probes to assess physiological functions of bacteria at single-cell level. Microbes and Infection, 2(12), 1523-1535.

Julia O, Comas J, & Vives-Rego J (2000) Second-order functions are the simplest correlations between flow cytometric light scatter and bacterial diameter. Journal of Microbiological Methods, 40(1), 57-61.

Kamat AS & Nair PM (1996) Identification of *Listeria innocua* as a biological indicator for inactivation of *L. monocytogenes* by some meat processing treatments. Lebensmittel-Wissenschaft und-Technologie, 29, 714-720.

Kamentsky LA, Melamed MR, & Derman H (1965) Spectrophotometer - New instrument for ultrarapid cell analysis. Science, 150(3696), 630-&.

Kamgang-Youbi G, Herry JM, Bellon-Fontaine MN, Brisset JL, Doubla A, & Naitali M (2007) Evidence of temporal postdischarge decontamination of bacteria by gliding electric discharges: Application to *Hafnia alvei*. Applied and Environmental Microbiology, 73(15), 4791-4796.

Kamgang-Youbi G, Herry JM, Meylheuc T, Brisset JL, Bellon-Fontaine MN, Doubla A, & Naitali M (2009) Microbial inactivation using plasma-activated water obtained by gliding electric discharges. Letters in Applied Microbiology, 48(1), 13-18.

Kamgang RB (2007) Destruction of planktonic, adherent and biofilm cells of *Staphylococcus epidermidis* using a gliding discharge in humid air. Journal of Applied Microbiology, 103(3), 621-628.

Karabulut O, Arslan U, & Kuruoglu G (2004) Control of postharvest diseases of organically grown strawberry with preharvest applications of some food additives and postharvest hot water dips. Journal of Phytopathology, 152(4), 224-228.

Karabulut O, Arslan U, Kuruoglu G, & Ozgenc T (2004) Control of postharvest diseases of sweet cherry with ethanol and hot water. Journal of Phytopathology, 152(5), 298-303.

Karaca H & Velioglu YS (2007) Ozone applications in fruit and vegetable processing. Food Reviews International, 23, 91-106.

Kayes MM, Critzer FJ, Kelly-Wintenberg K, Roth JR, Montie TC, & Golden DA (2007) Inactivation of foodborne pathogens using a one atmosphere uniform glow discharge plasma. Foodborne Pathogens and Disease, 4(1), 50-59.

Keener KM (2008) Atmospheric non-equilibrium plasma. Encyclopedia of Agricultural, Food, and Biological Engineering, 1(1), 1-5.

Kelly-Wintenberg K, Montie TC, Brickman C, Roth JR, Carr AK, Sorge K, Wadsworth LC, & Tsai PPY (1998) Room temperature sterilization of surfaces and fabrics with a one atmosphere uniform glow discharge plasma. Journal of Industrial Microbiology and Biotechnology, 20(1), 69-74.

Kelly-Wintenberg K, Hodge A, Montie TC, Deleanu L, Sherman D, Roth JR, Tsai P, & Wadsworth L (1999). Use of a one atmosphere uniform glow discharge plasma to kill a broad spectrum of microorganisms. Papers from the 45th National Symposium of the American Vacuum Society. Volume 17 (4), pp. 1539-1544. Baltimore, Maryland (USA): AVS.

Kemp GK & Schneider KR (2000) Validation of thiosulfate for neutralization of acidified sodium chlorite in microbiological testing. Poultry Science, 79(12), 1857-1860.

Ketteringham L, Gausseres R, James SJ, & James C (2006) Application of aqueous ozone for treating pre-cut green peppers (*Capsicum annuum L.*). Journal of Food Engineering, 76(1), 104-111.

Khadre M, Yousef A, & Kim J-G (2001) Microbiological aspects of ozone applications in food: a review. Journal of Food Science, 66(9), 1242-1252.

Kielland J (1945) Method and apparatus for counting blood corpuscles. (Patent No. 2369577).

Kim H, Ryu JH, & Beuchat LR (2006) Survival of *Enterobacter sakazakii* on fresh produce as affected by temperature, and effectiveness of sanitizers for its elimination. International Journal of Food Microbiology, 111(2), 134-143.

Kim J-G, Yousef A, & Dave S (1999) Application of ozone for enhancing the microbiological safety and quality of foods: a review. Journal of Food Protection, 62(9), 1071-1087.

Kim J-G, Yousef A, & Chism G (1999) Use of ozone to inactivate microorganisms on lettuce. Journal of Food Safety, 19, 17-34.

Kim J-G & Yousef A (2000) Inactivation kinetics of foodborne spoilage and pathogenic bacteria by ozone. Journal of Food Science, 65, 521-528.

Kim J-G, Yousef A, & Khadre M (2003) Ozone and its current and future application in the food industry. Advances in food and nutrition research, 45, 167-218.

Kim J-G (1998) Ozone as an antimicrobial agent in minimally processed foods. PhD Thesis. The Ohio State University, Columbus, OH.

Kim SJ, Chung TH, Bae SH, & Leem SH (2009) Bacterial inactivation using atmospheric pressure single pin electrode microplasma jet with a ground ring. Applied Physics Letters, 94(14).

Kitis M (2004) Disinfection of wastewater with peracetic acid: a review. Environment International, 30(1), 47-55.

Klockow P.A & Keener KM (2008). Quality and safety assessment of packaged spinach treated with a novel atmospheric, non-equilibrium plasma system. ASABE Annual Meeting 2008. June 29 – July 2, 2008, Providence, Rhode Islands, USA. Paper Number: 084396.

Klockow PA & Keener KM (2009) Safety and quality assessment of packaged spinach treated with a novel ozone-generation system. LWT - Food Science and Technology, 42(6), 1047-1053.

Koch AL, Robertson BR, & Button DK (1996) Deduction of the cell volume and mass from forward scatter intensity of bacteria analyzed by flow cytometry. Journal of Microbiological Methods, 27(1), 49-61.

Koivunen J & Heinonen-Tanski H (2005a) Inactivation of enteric microorganisms with chemical disinfectants, UV irradiation and combined chemical/UV treatments. Water Research, 39(8), 1519-1526.

Koivunen J & Heinonen-Tanski H (2005b) Peracetic acid (PAA) disinfection of primary, secondary and tertiary treated municipal wastewaters. Water Research, 39(18), 4445-4453.

Kolb JF, Mohamed AAH, Price RO, Swanson RJ, Bowman A, Chiavarini RL, Stacey M, & Schoenbach KH (2008) Cold atmospheric pressure air plasma jet for medical applications. Applied Physics Letters, 92(24).

Komanapalli IR & Lau BHS (1996) Ozone-induced damage of *Escherichia coli* K-12. Applied Microbiology and Biotechnology, 46(5), 610-614.

Koseki S, Yoshida K, Isobe S, & Itoh K (2001) Decontamination of lettuce using acidic electrolyzed water. Journal of Food Protection, 64(5), 652-658.

Koseki S, Yoshida K, Isobe S, & Itoh K (2004) Efficacy of acidic electrolyzed water for microbial decontamination of cucumbers and strawberries. Journal of Food Protection, 67(6), 1247-1251.

Krämer J (1997) Lebensmittelmikrobiologie. Verlag Eugen Ulmer Stuttgart,

KRÍHA, V. (2007). Corona discharge bactericidal effect on *Escherichia coli* protected by gel layer. 28th ICPIG, July 15-20, Prague, Czech Republic. Topic number: 16, pp. 1439-1441.

Kunigk L & Almeida MCB (2001) Action of peracetic acid on *Escherichia coli* and *Staphylococcus aureus* in suspension and on stainless steel surfaces. Brazilian Journal of Microbiology, 32(1), 38-41.

Kunigk L, Gomes DR, Forte F, Vidal KP, Gomes LF, & Sousa PF (2001) The influence of temperature on the decomposition kinetics of peracetic acid in solutions. Brazilian Journal of Chemical Engineering, 18(2), 217-220.

Kusunoki H, Kobayashi K, Kita T, Tajima T, Sugii S, & Uemura T (1998) Analysis of enterohemorrhagic *Escherichia coli* serotype O157:H7 by flow cytometry using monoclonal antibodies. The Journal of Veterinary Medical Science, 60(12), 1315-1319.

Lambert MDJ (1999) A kinetic study of the effect of hydrogen peroxide and peracetic acid against *Staphylococcus aureus* and *Pseudomonas aeruginosa* using the bioscreen disinfection method. Journal of Applied Microbiology, 87(5), 782-786.

Laroussi M (2002) Nonthermal decontamination of biological media by atmospheric-pressure plasmas: review, analysis and prospects. IEEE Transactions on Plasma Science, 30(4), 1409-1415.

Laroussi M, Mendis DA, & Rosenberg M (2003) Plasma interaction with microbes. New Journal of Physics, 5, 41.1-41.10.

Laroussi M (2005) Low temperature plasma-based sterilization: Overview and state-of-the-art. Plasma Processes and Polymers, 2(5), 391-400.

Laroussi M, Tendero C, Lu X, Alla S, & Hynes WL (2006) Inactivation of bacteria by the plasma pencil. Plasma Processes and Polymers, 3(6-7), 470-473.

Lassen KS, Nordby B, & Grun R (2005) The dependence of the sporicidal effects on the power and pressure of RF-generated plasma processes. Journal of Biomedical Materials Research Part B-Applied Biomaterials, 74B(1), 553-559.

Lavilla M, Marzo I, Luis Rd, Perez MD, Calvo M, & Sánchez L (2010) Detection of *Clostridium tyrobutyricum* spores using polyclonal antibodies and flow cytometry. Journal of Applied Microbiology, 108(2), 488-498.

Leaper S (1984) Synergistic killing of spores of *Bacillus subtilis* by peracetic acid and alcohol. International Journal of Food Science and Technology, 19(3), 355-360.

Lee J & Kaletunc G (2002) Evaluation of the heat inactivation of *Escherichia coli* and *Lactobacillus plantarum* by differential scanning calorimetry. Applied and Environmental Microbiology, 68(11), 5379-5386.

Lee LG, Chen CH, & Chiu LA (1986) Thiazole orange - A new dye for reticulocyte analysis. Cytometry, 7(6), 508-517.

Lerouge S, Wertheimer MR, Marchand R, Tabrizian M, & Yahia L'H (2000) Effect of gas composition on spore mortality and etching during low-pressure plasma sterilization. Journal of Biomedical Materials Research, 51(1), 128-135.

Lerouge S, Fozza AC, Wertheimer MR, Marchand R, & Yahia L'H (2000) Sterilization by low-pressure plasma: the role of vacuum-ultraviolet radiation. Plasmas and Polymers, 5(1), 31-46.

Lerouge S, Wertheimer MR, & Yahia L'H (2001) Plasma sterilization: a review of parameters, mechanisms, and limitaions. Plasmas and Polymers, 6(3), 175-188.

Li C-S & Wang Y-C (2003) Surface germicidal effects of ozone for microorganisms. AIHA Journal, 64(4), 533-537.

Liao C-H & Fett WF (2001) Analysis of native microflora and selection of strains antagonistic to human pathogens on fresh produce. Journal of Food Protection, 64, 1110-1115.

Liao C-H (2006) Bacterial soft rot. In Microbiology of fruits and vegetables, pp. 117-133: Taylor and Francis Group, CRC Press.

Liao CH & Sapers GM (1999) Influence of soft rot bacteria on growth of *Listeria monocytogenes* on potato tuber slices. Journal of Food Protection, 62, 343-348.

Liberti AL & Notarnicola M (1999) Disinfection with peracetic acid for domestic sewage re-use in agriculture. Water and Environment Journal, 13(4), 262-269.

Lievense LC, Verbreek MAM, Noomen A, & van't Riet K (1994) Mechanism of dehydration inactivation of *Lactobacillus plantarum*. Applied Microbiology and Biotechnology, 41(1), 90-94.

Liew CL & Prange RK (1994) Effect of ozone and storage-temperature on postharvest diseases and physiology of carrots (*Daucus-Carota L*). Journal of the American Society for Horticultural Science, 119(3), 563-567.

Little CL & Gillespie IA (2008) Prepared salads and public health. Journal of Applied Microbiology, 105(6), 1729-1743.

Luscher C, Balasa A, Fröhling A, Ananta E, & Knorr D (2004) Effect of high-pressure-induced ice I-to-ice III phase transitions on inactivation of *Listeria innocua* in frozen suspension. Applied and Environmental Microbiology, 70(7), 4021-4029.

Macauley JJ, Qiang Z, Adams CD, Surampalli R, & Mormile MR (2006) Disinfection of swine wastewater using chlorine, ultraviolet light and ozone. Water Research, 40(10), 2017-2026.

Mackey BM & Derrick CM (1986) Elevation of the heat resistance of *Salmonella typhimurium* by sublethal heat shock. Journal of Applied Bacteriology, 61(5), 389-393.

Mackey BM & Derrick CM (1987) The effect of prior heat shock on the thermoresistance of *Salmonella thompson* in foods. Letters in Applied Microbiology, 5(6), 115-118.

Mackey BM, Miles CA, Parsons SE, & Seymour DA (1991) Thermal denaturation of whole cells and cell components of *Escherichia coli* examined by differential scanning calorimetry. Journal of General Microbiology, 137(10), 2361-2374.

Mahapatra A, Muthukumarappan K, & Julson J (2005) Applications of ozone, bacteriocins and irradiation in food processing: a review. Critical Reviews in Food Science and Nutrition, 45, 447-461.

Malik MA, Ghaffar A, & Malik SA (2001) Water purification by electrical discharges. Plasma Sources Science & Technology, 10(1), 82-91.

Manas P & Mackey BM (2004) Morphological and physiological changes induced by high hydrostatic pressure in exponential- and stationary-phase cells of *Escherichia coli*: relationship with cell death. Applied and Environmental Microbiology, 70(3), 1545-1554.

Manousaridis G, Nerantzaki A, Paleologos EK, Tsiotsias A, Savvaidis IN, & Kontominas MG (2005) Effect of ozone on microbial, chemical and sensory attributes of shucked mussels. Food Microbiology, 22(1), 1-9.

Mari M, Gregori R, & Donati I (2004) Postharvest control of *Monilinia laxa* and *Rhizopus stolonifer* in stone fruit by peracetic acid. Postharvest Biology and Technology, 33, 319-325.

Marks BP (2008) Status of microbial modeling in food process models. Comprehensive Reviews in Food Science and Food Safety, 7(1), 137-143.

Marques SC, Rezende JDOS, Alves LAD, Silva BC, Alves E, de Abreu LR, & Piccoli RH (2007) Formation of biofilms by *Staphylococcus aureus* on stainless steel and glass surfaces and its resistance to some selected chemical sanitizers. Brazilian Journal of Microbiology, 38(3), 538-543.

Mathys A, Chapman B, Bull M, Heinz V, & Knorr D (2007) Flow cytometric assessment of *Bacillus* spore response to high pressure and heat. Innovative Food Science & Emerging Technologies, 8(4), 519-527.

Mcgann LE, Walterson ML, & Hogg LM (1988) Light-scattering and cell volumes in osmotically stressed and frozen-thawed cells. Cytometry, 9(1), 33-38.

Mendis DA, Rosenberg M, & Azam F (2000) A note on the possible electrostatic disruption of bacteria. IEEE Transactions on Plasma Science, 28(4), 1304-1306.

Messerer P, Halfmann H, Czichy M, Schulze M, & Awakowicz P (2005). Plasma sterilisation and surface modification of thermolabile materials.

Meylheuc T, Renault M, & Bellon-Fontaine MN (2006) Adsorption of a biosurfactant on surfaces to enhance the disinfection of surfaces contaminated with *Listeria monocytogenes*. International Journal of Food Microbiology, 109(1-2), 71-78.

Mezzanotte V, Antonelli M, Azzellino A, Citterio S, & Nurizzo C (2003) Secondary effluent disinfection by peracetic acid (PAA): microrganism inactivation and regrowth, preliminary results. Water Science and Technology, 3(4), 269-275.

Mezzanotte V, Antonelli M, Citterio S, & Nurizzo C (2007) Wastewater disinfection alternatives: chlorine, ozone, peracetic acid, and UV light. Water Environment Research, 79(12), 2373-2379.

Miller LL & Ordal ZJ (1972) Thermal injury and recovery of *Bacillus subtilis*. Applied microbiology, 24(6), 878-884.

Miyanaga K, Takano S, Morono Y, Hori K, Unno H, & Tanji Y (2007) Optimization of distinction between viable and dead cells by fluorescent staining method and its application to bacterial consortia. Biochemical Engineering Journal, 37(1), 56-61.

Moats WA (1971) Kinetics of thermal death of bacteria. Journal of Bacteriology, 105(1), 165-171.

Model I (1997) Lohnt sich eine Melkzeugzwischendesinfektion? Milchpraxis, 3 (35. Jg), 126-130.

Moeller TM, Alexander ML, Engelhard MH, Gaspar DJ, Luna ML, & Irving PM (2002) Surface decontamination of simulated chemical warfare agents using a nonequilibrium plasma with off-gas monitoring. IEEE Transactions on Plasma Science, 30(4), 1454-1459.

Moisan M, Barbeau J, Moreau S, Pelletier J, Tabrizian M, & Yahia LH (2001) Low-temperature sterilization using gas plasmas: a review of the experiments and an analysis of the inactivation mechanisms. International Journal of Pharmaceutics, 226(1-2), 1-21.

Moisan M, Barbeau J, Crevier M-C, Pelletier J, Philip N, & Saoudi B (2002) Plasma sterilization. Methods and mechanisms. Pure and Applied Chemistry, 74(3), 349-358.

Moldavan A (1934) Photo-electric technique for the counting of microscopical cells. Science, 80(2069), 188-189.

Montenegro RR (2002) Inactivation of *E. coli* O157:H7 using a pulsed nonthermal plasma system. Journal of Food Science, 67(2), 646-648.

Montie TC, Kelly-Wintenberg K, & Roth JR (2000) An overview of research using the one atmosphere uniform glowdischarge plasma (OAUGDP) for sterilization of surfaces and materials. IEEE Transactions on Plasma Science, 28(1), 41-50.

Moore G, Griffith C, & Peters A (2000) Bactericidal properties of ozone and its potential application as a terminal disinfectant. Journal of Food Protection, 63(8), 1100-1106.

Moreau M, Orange N, & Feuilloley MGJ (2008) Non-thermal plasma technologies: new tools for bio-decontamination. Biotechnology Advances, 26(6), 610-617.

Moreau S, Moisan M, Tabrizian M, Barbeau J, Pelletier J, Ricard A, & Yahia L (2000) Using the flowing afterglow of a plasma to inactivate *Bacillus subtilis* spores: Influence of the operating conditions. Journal of Applied Physics, 88(2), 1166-1174.

Morono Y, Takano S, Miyanaga K, Tanji Y, Unno H, & Hori K (2004) Application of glutaraldehyde for the staining of esterase-active cells with carboxyfluorescein diacetate. Biotechnology Letters, 26, 379-383.

Morris JG (1993) Bacterial shock responses. Endeavour, 17(1), 2-6.

Morris R (1993) Reduction of microbial levels in sewage effluents using chlorine and peracetic-acid disinfectants. Water Science and Technology, 27(3-4), 387-393.

Muranyi P, Wunderlich J, & Heise M (2008) Influence of relative gas humidity on the inactivation efficiency of a low temperature gas plasma. Journal of Applied Microbiology, 104(6), 1659-1666.

Murphy RY, Marks BP, Johnson ER, & Johnson MG (2000) Thermal inactivation kinetics of *Salmonella* and *Listeria* in ground chicken breast meat and liquid medium. Journal of Food Science, 65(4), 706-710.

Nadas A, Olmo M, & Garcia J (2003) Growth of *Botrytis cinerea* and strawberry quality in ozone-enriched atmospheres. Journal of Food Science, 68(5), 1798-1802.

Nagatsu M, Terashita F, Nonaka H, Xu L, Nagata T, & Koide Y (2005) Effects of oxygen radicals in low-pressure surface-wave plasma on sterilization. Applied Physics Letters, 86(21).

Nagayoshi M, Fukuizumi T, Kitamura C, Yano J, Terashita M, & Nishihara T (2004) Efficacy of ozone on survival and permeability of oral microorganisms. Oral Microbiology Immunology, 19, 240-246.

Nagayoshi M, Kitamura C, Fukuizumi T, Nishihara T, & Terashita M (2004) Antimicrobial effect of ozonated water on bacteria invading dentinal tubules. Journal of Endodontics, 30(11), 778-781.

Naitou S & Takahara H (2008) Recent developments in food and agricultural uses of ozone as an antimicrobial agent-food packaging film sterilizing machine using ozone. Ozone-Science & Engineering, 30(1), 81-87.

Najafi MBH & Khodaparast MHH (2009) Efficacy of ozone to reduce microbial populations in date fruits. Food Control, 20(1), 27-30.

Nebe-von-Caron G & Badley RA (1995) Viability assessment of bacteria in mixed populations using flow cytometry. Journal of Microscopy, 179(1), 55-66.

Nebe-von-Caron G, Stephens PJ, Hewitt CJ, Powell JR, & Badley RA (2000) Analysis of bacterial function by multi-colour fluorescence flow cytometry and single cell sorting. Journal of Microbiological Methods, 42(1), 97-114.

Nebe-von Caron G, Stephens P, & Badley RA (1998) Assessment of bacterial viability status by flow cytometry and single cell sorting. Journal of Applied Microbiology, 84, 988-998.

Nguyen HTT, Corry JEL, & Miles CA (2006) Heat resistance and mechanism of heat inactivation in thermophilic *Campylobacters*. Applied and Environmental Microbiology, 72(1), 908-913.

Nguyenthe C & Carlin F (1994) The microbiology of minimally processed fresh fruits and vegetables. Critical Reviews in Food Science and Nutrition, 34(4), 371-401.

Niemira BA & Sites J (2008) Cold plasma inactivates *Salmonella stanley* and *Escherichia coli* O157:H7 inoculated on Golden Delicious apples. Journal of Food Protection, 71(7), 1357-1365.

Novo D, Perlmutter NG, Hunt RH, & Shapiro HM (1999) Accurate flow cytometric membrane potential measurement in bacteria using diethyloxacarbocyanine and a ratiometric technique. Cytometry, 35(1), 55-63.

Novo DJ, Perlmutter NG, Hunt RH, & Shapiro HM (2000) Multiparameter flow cytometric analysis of antibiotic effects on membrane potential, membrane permeability, and bacterial counts of *Staphylococcus aureus* and *Micrococcus luteus*. Antimicrobial Agents and Chemotherapy, 44(4), 827-834.

Nygren J, Svanvik N, & Kubista M (1998) The interactions between the fluorescent dye thiazole orange and DNA. Biopolymers, 46(1), 39-51.

Oh SW, Gray PM, Dougherty RH, & Kang DH (2005) Aerosolization as novel sanitizer delivery system to reduce food-borne pathogens. Letters in Applied Microbiology, 41(1), 56-60.

Oliver JD (2005) The viable but nonculturable state in bacteria. The Journal of Microbiology, 43(S), 93-100.

Orsat V, Gariepy Y, Raghavan GSV, & Lyew D (2001) Radio-frequency treatment for ready-to-eat fresh carrots. Food Research International, 34(6), 527-536.

Orth R (1998) The importance of disinfection for the hygiene in the dairy and beverage production. International Biodeterioration & Biodegradation, 41(3-4), 201-208.

Ölmez H & Kretzschmar U (2009) Potential alternative disinfection methods for organic fresh-cut industry for minimizing water consumption and environmental impact. LWT - Food Science and Technology, 42(3), 686-693.

Ölmez H & Akbas MY (2009) Optimization of ozone treatment of fresh-cut green leaf lettuce. Journal of Food Engineering, 90(4), 487-494.

Pagan R & Mackey B (2000) Relationship between membrane damage and cell death in pressure-treated *Escherichia coli* cells: Differences between exponential- and stationary-phase cells and variation among strains. Applied and Environmental Microbiology, 66(7), 2829-2834.

Pascual A, Llorca I, & Canut A (2007) Use of ozone in food industries for reducing the environmental impact of cleaning and disinfection activities. Trends in Food Science & Technology, 18 (Supplement 1), S29-S35.

Patil S, Bourke P, Frias JM, Tiwari BK, & Cullen PJ (2009) Inactivation of *Escherichia coli* in orange juice using ozone. Innovative Food Science & Emerging Technologies, in press, Corrected Proof.

Peleg M (2000) Microbial survival curves-- the reality of flat "shoulders" and absolute thermal death times. Food Research International, 33(7), 531-538.

Perez A, Sanz C, Rios J, Olias R, & Olias J (1999) Effects of ozone treatment on postharvest strawberry quality. Journal of Agricultural and Food Chemistry, 47(4), 1652-1656.

Perni S, Deng XTT, Shama G, & Kong MG (2006) Modeling the inactivation kinetics of *Bacillus subtilis* spores by nonthermal plasmas. IEEE Transactions on Plasma Science, 34(4), 1297-1303.

Perni S, Shama G, & Kong MG (2008) Cold atmospheric plasma disinfection of cut fruit surfaces contaminated with migrating microorganisms. Journal of Food Protection, 71(8), 1619-1625.

Perni S, Liu DW, Shama G, & Kong MG (2008) Cold atmospheric plasma decontamination of the pericarps of fruit. Journal of Food Protection, 71(2), 302-308.

Petit J-M, Denis-Gay M, & Ratinaud M-H (1993) Assessment of fluorochromes for cellular structure and function studies by flow cytometry. Biology of the Cell, 78, 1-13.

Pine L, Weaver RE, Carlone GM, Pienta PA, Rocourt J, Goebel W, Kathariou S, Bibb WF, & Malcolm GB (1987) *Listeria-monocytogenes* ATCC-35152 and NCTC-7973 contain a nonhemolytic, nonvirulent variant. Journal of Clinical Microbiology, 25(11), 2247-2251.

Pompl R, Jamitzky F, Shimizu T, Steffes B, Bunk W, Schmidt HU, Georgi M, Ramrath K, Stolz W, Stark RW, Urayama T, Fujii S, & Morfill GE (2009) The effect of low-temperature plasma on bacteria as observed by repeated AFM imaging. New Journal of Physics, 11. 1-11.

Privalov PL & Khechinashvili NN (1974) A thermodynamic approach to the problem of stabilization of globular protein structure: a calorimetric study. Journal of Molecular Biology, 86(3), 665-684.

Propokov T & Tanchev S (2007) Methods of food preservation. In Food Safety: A practical and case study approach, pp. 3-25: Springer Science+Business Media.

Purevdorj D, Igura N, Hayakawa I, & Ariyada O (2002) Inactivation of *Escherichia coli* by microwave induced low temperature argon plasma treatments. Journal of Food Engineering, 53(4), 341-346.

Rajkovic A, Smigic N, & Devlieghere F (2009) Contemporary strategies in combating microbial contamination in food chain. International Journal of Food Microbiology, In Press, Corrected Proof.

Ramaswamy HS & Singh RP (1997) Sterilization process engineering. In Handbook of food engineering practise, pp. 37-70: CRC Press.

Ratkowsky DA (2004) Model fitting and uncertainty. *In:* Modeling microbial responses in food, pp. 151-196: CRC Press.

Rediers H, Claes M, Peeters L, & Willems KA (2009) Evaluation of the cold chain of fresh-cut endive from farmer to plate. Postharvest Biology and Technology, 51(2), 257-262.

Restaino L, Frampton EW, Hemphill JB, & Palnikar P (1995) Efficacy of ozonated water against various food-related microorganisms. Applied and Environmental Microbiology, 61(9), 3471-3475.

Rico D, Martin-Diana AB, Barat JM, & Barry-Ryan C (2007) Extending and measuring the quality of fresh-cut fruit and vegetables: a review. Trends in Food Science & Technology, 18(7), 373-386.

Ritz M, Tholozan JL, Federighi M, & Pilet MF (2001) Morphological and physiological characterization of *Listeria monocytogenes* subjected to high hydrostatic pressure. Applied and Environmental Microbiology, 67(5), 2240-2247.

Ritz M, Tholozan JL, Federighi M, & Pilet MF (2002) Physiological damages of *Listeria monocytogenes* treated by high hydrostatic pressure. International Journal of Food Microbiology, 79(1-2), 47-53.

Robinson JP (2004) Flow cytometry. *In:* Encyclopedia of Biomaterials and Biomedical Engineering pp. 630-640.

Rodriguez SB & Thornton RJ (2008) Use of flow cytometry with fluorescent antibodies in real-time monitoring of simultaneously inoculated alcoholic-malolactic fermentation of Chardonnay. Letters in Applied Microbiology, 46(1), 38-42.

Rossi F, Kylián O, & Hasiwa M (2006) Decontamination of surfaces by low pressure plasma discharges. Plasma Processes and Polymers, 3(6-7), 431-442.

Rossi S, Antonelli M, Mezzanotte V, & Nurizzo C (2007) Peracetic acid disinfection: a feasible alternative to wastewater chlorination. Water Environment Research, 79(4), 341-350.

Rossoni EMM & Gaylarde CC (2000) Comparison of sodium hypochlorite and peracetic acid as sanitising agents for stainless steel food processing surfaces using epifluorescence microscopy. International Journal of Food Microbiology, 61(1), 81-85.

Ruiz-Cruz S, Acedo-Felix E, Diaz-Cinco M, Islas-Osuna MA, & Gonzalez-Aguilar GA (2007) Efficacy of sanitizers in reducing *Escherichia coli* O157:H7, *Salmonella* spp. and *Listeria monocytogenes* populations on fresh-cut carrots. Food Control, 18(11), 1383-1390.

Salustiano VC, De Andrade NJ, Brandao SCC, Junior WM, & Nacife GP (2004) An assessment of chemical sanitizers on the microbiological profile of air in a milk processing plant. Journal of Food Safety, 24(3), 159-167.

Santoro MM, Liu Y, Khan SMA, Hou LX, & Bolen DW (1992) Increased thermal stability of proteins in the presence of naturally occurring osmolytes. Biochemistry, 31(23), 5278-5283.

Sapers GM (2001) Efficacy of washing and sanitizing methods for disinfection of fresh fruit and vegetable products. Food Techology and Biotechnology, 39(4), 305-311.

Scherer JM, Stillwell W, & Jenski LJ (1999) Anomalous changes in forward scatter of lymphocytes with loosely packed membranes. Cytometry, 37(3), 184-190.

Schlesinger MJ (1990) Heat shock proteins. Journal of Biological Chemistry, 265(21), 12111-12114.

Schlüter O, Foerster J, Geyer M, Knorr D, & Herppich W (2009) Characterization of high-hydrostatic-pressure effects on fresh produce using chlorophyll fluorescence image analysis. Food and Bioprocess Technology, 2(3), 291-299.

Schmidt M (2010) Plasma sources. *In:* Non-thermal Plasma Chemistry and Physics, pp. 52-70.

Schumann R, Schiewer U, Karsten U, & Rieling T (2003) Viability of bacteria from different aquatic habitats. II. Cellular fluorescent markers for membrane integrity and metabolic activity. Aquatic Microbial Ecology, 32(2), 137-150.

Schütze A, Jeong JY, .Babayan SE, Jaeyoung Park, Selwyn GS, & Hicks RF (1998) The atmospheric-pressure plasma jet: a review and comparison to other plasma sources. IEEE Transactions on Plasma Science, 26(6), 1685-1694.

Schwabedissen A, Lacinski P, Chen X, & Engemann J (2007) *PlasmaLabel* - a new method to disinfect goods inside a closed package using dielectric barrier discharges. Contributions to Plasma Physics, 47(7), 551-558.

SCF- Scientific Committee on Food (2002) Risk profile on the microbiological contamination of fruits and vegetables eaten raw.

Selcuk M, Oksuz L, & Basaran P (2008) Decontamination of grains and legumes infected with *Aspergillus* spp. and *Penicillum* spp. by cold plasma treatment. Bioresource Technology, 99(11), 5104-5109.

Selma MV, Beltran D, Allende A, Chacon-Vera E, & Gil MI (2007) Elimination by ozone of *Shigella sonnei* in shredded lettuce and water. Food Microbiology, 24(5), 492-499.

Selma MV, Ibñez AM, Allende A, Cantwell M, & Suslow T (2008) Effect of gaseous ozone and hot water on microbial and sensory quality of cantaloupe and potential transference of *Escherichia coli* O157:H7 during cutting. Food Microbiology, 25(1), 162-168.

Selma MV, Ibáñez AM, Cantwell M, & Suslow T (2008) Reduction by gaseous ozone of Salmonella and microbial flora associated with fresh-cut cantaloupe. Food Microbiology, 25(4), 558-565.

Shapiro HM (2003) Practical flow cytometry. John Wiley & Sons, Inc.,

Shapiro HM (1994) Chapter 8: Cell membrane potential analysis. *In:* Methods in Cell Biology - Flow Cytometry Second Edition, Part A, pp. 121-133: Academic Press.

Shapiro HM (2000) Membrane potential estimation by flow cytometry. Methods, 21(3), 271-279.

Shen T, Bos AP, & Brul S (2009) Assessing freeze-thaw and high pressure low temperature induced damage to *Bacillus subtilis* cells with flow cytometry. Innovative Food Science & Emerging Technologies, 10(1), 9-15.

Shi XM, Zhang GJ, Yuan YK, Ma Y, Xu GM, & Yang Y (2008) Research on the inactivation effect of low-temperature plasma on *Candida albicans*. IEEE Transactions on Plasma Science, 36(2), 498-503.

Sigmond RS, Kurdelova B, & Kurdel M (1999) Action of corona discharges on bacteria and spores. Czechoslovak Journal of Physics, 49(3), 405-420.

Skog L & Chu C (2001) Effect of ozone on qualities of fruit and vegetables in cold storage. Canadian Journal of Plant Science, 81, 773-778.

Sladek REJ, Filoche SK, Sissons CH, & Stoffels E (2007) Treatment of *Streptococcus mutans* biofilms with a nonthermal atmospheric plasma. Letters in Applied Microbiology, 45(3), 318-323.

Smilanick J, Margosan D, & Gabler F (2002) Impact of ozonated water on the quality and shelf-life of fresh citrus fruit, stone fruit and table grapes. Ozone-Science & Engineering, 24(5), 343-356.

Smith DeWaal C, Hicks G, Barlow K, Alderton L, & Vegosen L (2006) Food associated with food-borne illness outbreaks from 1990 through 2003. Food Protection Trends, 26(7), 466-473.

Smith Dewaal C & Bhuiya F (2007) Outbreaks by the numbers: fruits and vegetables 1990–2005.

Smither R (1975) Use of a coulter counter to detect discrete changes in cell numbers and volume during growth of *Escherichia coli*. Journal of Applied Microbiology, 39(2), 157-165.

Song HP, Kim B, Choe JH, Jung S, Moon SY, Choe W, & Jo C (2009) Evaluation of atmospheric pressure plasma to improve the safety of sliced cheese and ham inoculated by 3-strain cocktail *Listeria monocytogenes*. Food Microbiology, 26(4), 432-436.

Spilimbergo S, Mantoan D, Quaranta A, & Della Mea G (2009) Real-time monitoring of cell membrane modification during supercritical CO2 pasteurization. Journal of Supercritical Fluids, 48(1), 93-97.

Stampi S (2001) Evaluation of the efficiency of peracetic acid in the disinfection of sewage effluents. Journal of Applied Microbiology, 91(5), 833-838.

Steen HB (2000) Flow cytometry of bacteria: glimpses from the past with a view to the future. Journal of Microbiological Methods, 42, 65-74.

Steenstrup JDF (2002) Statistical modeling of D- and z-value of *E. coli* O157:H7 and pH in apple cider containing preservatives. Journal of Food Science, 67(2), 793-796.

Steinkamp JA (1984) Review article - flow cytometry. Review of Scientific Instruments, 55(9), 1375-1400.

Stephens PJ & Jones MV (1993) Reduced ribosomal thermal-denaturation in *Listeria-monocytogenes* following osmotic and heat shocks. FEMS Microbiology Letters, 106(2), 177-182.

Suller MTE & Lloyd D (1999) Fluorescence monitoring of antibiotic-induced bacterial damage using flow cytometry. Cytometry, 35, 235-241.

Sun YZ, Qiu YC, Nie AL, & Wang XD (2007) Experimental research on inactivation of bacteria by using dielectric barrier discharge. IEEE Transactions on Plasma Science, 35(5), 1496-1500.

Swanton EM, Curby WA, & Lind HE (1962) Experiences with the coulter counter in bacteriology. Applied Microbiology, 10(5), 480-485.

Swern D (1949) Organic peracids. Chemical Reviews, 45(1), 1-68.

Taneja S & Ahmad F (1994) Increased thermal stability of proteins in the presence of amino acids. Biochemical Journal, 303(1), 147-153.

Tang YZ, Gin KYH, & Lim TH (2005) High-temperature fluorescent in situ hybridization for detecting *Escherichia coli* in seawater samples, using rRNA-targeted oligonucleotide probes and flow cytometry. Applied and Environmental Microbiology, 71(12), 8157-8164.

Tanino M, Xilu W, Takashima K, Katsura S, & Mizuno A (2007) Sterilization using dielectric barrier discharge at atmospheric pressure. International Journal of Plasma Environmental Science & Technology, 1(1), 102-107.

Te Giffel MC, Beumer RR, Van Dam WF, Slaghuis BA, & Rombouts FM (2010) Sporicidal effect of disinfectants on *Bacillus cereus* isolated from the milk processing environment. International Biodeterioration & Biodegradation, 36(3-4), 421-430.

Thanomsub B, Anupunpisit V, Chanphetch S, Watcharachaipong T, Poonkhum R, & Srisukonth C (2002) Effects of ozone treatment on cell growth and ultrastructural changes in bacteria. Journal of Genetics and Applied Microbiology, 48(4), 193-199.

The Codex Alimentarius Commission (1997) Recommended international code of practice: general principles of food hygiene. 1-1969, Rev.3.

Thomas J-C, Desrosiers, Marcel, St-Pierre Y, Lirette P, Bisaillon J-G, Beaudet R, & Villemur R (1997) Quantitative flow cytometric detection of specific microorganisms in soil samples using rRNA targeted fluorescent probes and ethidium bromide. Cytometry, 27(3), 224-232.

Tiwari BK, Muthukumarappan K, O'Donnell CP, Chenchaiah M, & Cullen PJ (2008) Effect of ozonation on the rheological and colour characteristics of hydrocolloid dispersions. Food Research International, 41(10), 1035-1043.

Tiwari BK, O'Donnell CP, Patras A, Brunton N, & Cullen PJ (2009) Effect of ozone processing on anthocyanins and ascorbic acid degradation of strawberry juice. Food Chemistry, 113(4), 1119-1126.

Tiwari BK, Muthukumarappan K, Donnell CP, & Cullen PJ (2008) Kinetics of freshly squeezed orange juice quality changes during ozone processing. Journal of Agricultural and Food Chemistry, 56(15), 6416-6422.

Torrella F & Morita RY (1981) Microcultural study of bacterial size changes and microcolony and ultramicrocolony formation by heterotrophic bacteria in seawater. Applied and Environmental Microbiology, 41(2), 518-527.

Trambarulo R, Ghosh SN, Burrus J, & Gordy W (1953) The molecular structure, dipole moment, and g factor of ozone from its microwave spectrum. The Journal of Chemical Physics, 21(5), 851-855.

Tscheuschner H-D (2000) Grundzüge der Lebensmitteltechnik. Behr`s Verlag GmbH & Co. KG Hamburg,

Ueckert J, Breeuwer P, Abee T, Stephens P, Nebe von Caron G, & ter Steeg PF (1995) Flow cytometry applications in physiological study and detection of foodborne microorganisms. International Journal of Food Microbiology, 28(2), 317-326.

Uhm HS, Lim JP, & Li SZ (2007) Sterilization of bacterial endospores by an atmospheric-pressure argon plasma jet. Applied Physics Letters, 90(26).

Uyttendaele M, Rajkovic A, Van Houteghem N, Boon N, Thas O, Debevere J, & Devlieghere F (2008) Multi-method approach indicates no presence of sub-lethally injured *Listeria monocytogenes* cells after mild heat treatment. International Journal of Food Microbiology, 123(3), 262-268.

Vachon JF, Kheadr EE, Giasson J, Paquin P, & Fliss I (2002) Inactivation of foodborne pathogens in milk using dynamic high pressure. Journal of Food Protection, 65(2), 345-352.

Vallejo CG & Serrano R (1989) Physiology of mutants with reduced expression of plasma membrane H+-ATPase. Yeast (Chichester, England), 5(4), 307-319.

van Boekel MAJS (2002) On the use of the Weibull model to describe thermal inactivation of microbial vegetative cells. International Journal of Food Microbiology, 74(1-2), 139-159.

Van Dilla MA, Mullaney PF, & Coulter JR (1967) Los Alamos scientific laboratory report. LA-3848-MS, 100 pp.

Vandekinderen I, Devlieghere F, De Meulenaer B, Ragaert P, & Van Camp J (2009) Optimization and evaluation of a decontamination step with peroxyacetic acid for fresh-cut produce. Food Microbiology, 26(8), 882-888.

Veal DA, Deere D, Ferrari B, Piper J, & Attfield PV (2000) Fluorescence staining and flow cytometry for monitoring microbial cells. Journal of Immunological Methods, 243(1-2), 191-210.

Veschetti E, Cutilli D, Bonadonna L, Briancesco R, Martini C, Cecchini G, Anastasi P, & Ottaviani M (2003) Pilot-plant comparative study of peracetic acid and sodium hypochlorite wastewater disinfection. Water Research, 37(1), 78-94.

Vesey G, Narai J, Ashbolt N, Williams K, & Veal D (1994) Chapter 29: Detection of specific microorganisms in environmental samples using flow cytometry. *In* Methods in Cell Biology - Flow Cytometry, pp. 489-522: Academic Press.

Virto R, Sanz D, Alvarez I, Condon S, & Raso J (2006) Application of the Weibull model to describe inactivation of *Listeria monocytogenes* and *Escherichia coli* by citric and lactic acid at different temperatures. Journal of the Science of Food and Agriculture, 86(6), 865-870.

Vives-Rego J, Lebaron P, & Nebe-von Caron G (2000) Current and future applications of flow cytometry in aquatic microbiology. FEMS Microbiology Reviews, 24(4), 429-448.

Vleugels M, Shama G, Deng XT, Greenacre E, Brocklehurst T, & Kong MG (2005) Atmospheric plasma inactivation of biofilm-forming bacteria for food safety control. IEEE Transactions on Plasma Science, 33(2), 824-828.

Waggoner AS (1979) Dye indicators of membrane potential. Annual Review of Biophysics and Bioengineering, 8(1), 47-68.

Wagner M, Brumelis D, & Gehr R (2002) Disinfection of wastewater by hydrogen peroxide or peracetic acid: development of procedures for measurement of residual disinfectant and application to a physicochemically treated municipal effluent. Water Environment Research, 74, 33-50.

Wallner G, Amann R, & Beisker W (1993) Optimizing fluorescent *in situ* hybridization with ribosomal-RNA-targeted oligonucleotide probes for flow cytometric identification of microorganisms. Cytometry, 14(2), 136-143.

Wan J, Coventry J, Swiergon P, Sanguansri P, & Versteeg C (2009) Advances in innovative processing technologies for microbial inactivation and enhancement of food safety - pulsed electric field and low-temperature plasma. Trends in Food Science & Technology, 20(9), 414-424.

Wang C (2000) Effect of moist hot air treatment on some postharvest quality attributes of strawberries. Journal of Food Quality, 23(1), 51-59.

Wang H, Feng H, & Luo Y (2004) Microbial reduction and storage quality of fresh-cut cilantro washed with acidic electrolyzed water and aqueous ozone. Food Research International, 37(10), 949-956.

Wang H, Feng H, & Lao Y (2006) Dual-phasic inactivation of Escherichia coli O157:H7 with peroxyacetic acid, acidic electrolyzed water and chlorine on cantaloupes and fresh-cut apples. Journal of Food Safety, 26(4), 335-347.

Weitzel G, Pilatus U, & Rensing L (1987) The cytoplasmic pH, ATP content and total protein synthesis rate during heat-shock protein inducing treatments in yeast. Experimental Cell Research, 170(1), 64-79.

Wells JM & Butterfield JE (1999) Incidence of *Salmonella* on fresh fruits and vegetables affected by fungal rots or physical injury. Plant Disease, 83(8), 722-726.

Weltmann KD, Brandenburg R, von Woedtke T, Ehlbeck J, Foest R, Stieber M, & Kindel E (2008) Antimicrobial treatment of heat sensitive products by miniaturized atmospheric pressure plasma jets (APPJs). Journal of Physics D: Applied Physics, 41(19).

Williams RC, Sumner SS, & Golden DA (2005) Inactivation of *Escherichia coli* O157:H7 and *Salmonella* in apple cider and orange juice treated with combinations of ozone, dimethyl dicarbonate, and hydrogen peroxide. Journal of Food Science, 70(4), M197-M201.

Wilson CL & Wisniewski ME (1989) Biological control of postharvest diseases of fruits and vegetables: an emerging technology. Annual Review of Phytopathology, 27(1), 425-441.

Winson MK & Davey HM (2000) Flow cytometric analysis of microorganisms. Methods: A Companion to Methods in Enzymology, 21, 231-240.

Wouters PC, Bos AP, & Ueckert J (2001) Membrane permeabilization in relation to inactivation kinetics of *Lactobacillus* species due to pulsed electric fields. Applied and Environmental Microbiology, 67(7), 3092-3101.

Xu GM, Zhang GJ, Shi XM, Ma Y, Wang N, & Li Y (2009) Bacteria inactivation using DBD plasma jet in atmospheric pressure argon. Plasma Science & Technology, 11(1), 83-88.

Xu L (1999) Use of ozone to improve the safety of fresh fruits and vegetables. Food Technology, 53(10), 58-62.

Yaqub S, Anderson JG, MacGregor SJ, & Rowan NJ (2004) Use of a fluorescent viability stain to assess lethal and sublethal injury in food-borne bacteria exposed to high-intensity pulsed electric fields. Letters in Applied Microbiology, 39(3), 246-251.

Yu CH (2007) Bacterial inactivation using a low-temperature atmospheric plasma brush sustained with argon gas. Journal of Biomedical Materials Research Part B: Applied Biomaterials, 80B(1), 211-219.

Yu H, Perni S, Shi JJ, Wang DZ, Kong MG, & Shama G (2006) Effects of cell surface loading and phase of growth in cold atmospheric gas plasma inactivation of *Escherichia coli* K12. Journal of Applied Microbiology, 101(6), 1323-1330.

Yuan Z, Ni Y, & VanHeiningen ARP (1997) Kinetics of peracetic acid decomposition. 1. Spontaneous decomposition at typical pulp bleaching conditions. Canadian Journal of Chemical Engineering, 75(1), 37-41.

Yuan Z, Ni Y, & Van Heiningen ARP (1997) Kinetics of the peracetic acid decomposition. 2. pH effect and alkaline hydrolysis. Canadian Journal of Chemical Engineering, 75(1), 42-47.

Yuk HG, Bartz JA, & Schneider KR (2006) The effectiveness of sanitizer treatments in inactivation of *Salmonella* spp. from bell pepper, cucumber, and strawberry. Journal of Food Science, 71(3), M95-M99.

Zhang L, Lu Z, Yu Z, & Gao X (2005) Preservation of fresh-cut celery by treatment of ozonated water. Food Control, 16(3), 279-283.

Zhao J & Cranston P (1995) Microbial decontamination of black pepper by ozone and the effect of the treatment on volatile oil constituents of the spice. Journal of the Science of Food and Agriculture, 68, 11-18.

Zheleva I & Kamburova V (2009) Modeling of heating during food processing. *In:* Predictive modeling and risk assessment, pp. 79-100. New York: Springer Science+Business Media.

List of publications

Publications

Fröhling A, Wienke M, Rose-Meierhöfer S, Schlüter O (2010) Mastitis detection and prevention during milking process. Food and Bioprocess Technology 3,892-900.

Knorr D, Fröhling A, Jäger H, Reineke K, Schlüter O, Schössler K (*accepted*): Emerging technologies in food processing. Annual Review of Food Science and Technology.

Hausdorf L, Fröhling A, Schlüter O, Klocke M *(submitted)* Analysis of the bacterial community within a carrot washing facility. Canadian Journal of Microbiology.

Fröhling A, Klocke S, Hausdorf L, Klocke M, Schlüter O (*in preparation*) A method for viability testing of *Pectobacterium carotovorum* in postharvest processing by means of flow cytometry. Food and Bioprocess Technology.

Fröhling A, Baier M, Baranyai L, Ehlbeck J, Knorr D, Schlüter O (*in preparation*) Comparison of kinetic models for non-thermal plasma inactivation of *Listeria innocua*. Journal of Food Engineering.

Fröhling A, Baier M, Ehlbeck J, Knorr D, Geyer M, Schlüter O (*in preparation*) A flow cytometric approach to analyze non-thermal plasma effects on *Listeria innocua*. Food Microbiology.

Herppich WB, Hassenberg K, Fröhling A, Geyer M (*in preparation*) Effects of ozonated wash water on the physiological behaviour of carrots. Journal of Applied Botany and Food Quality

Hausdorf L, Fröhling A, Schlüter O, Klocke M, Adamzig H, Walter AD (2008) Hygieneüberwachung per Chip: Prozessbegleitende Detektion von human- und phytopathogenen Mikroorganismen bei der Aufbereitung von Frischeprodukten. (Hygiene monitoring per chip: detecting human- and phytopathogens during postharvest vegetable processing. URL: http://www.landtechnik-net.com). Landtechnik 63 (4): 224-225.

Hassenberg K, Fröhling A, Geyer M, Schlüter O, Herppich WB (2008) Ozonated Wash Water for Inhibition of *Pectobacterium carotovorum* on Carrots and the Effect on the Physiological Behaviour of Produce. European Journal of Horticultural Science, 73 (1): 37-42.

Hassenberg K, Herppich WB, Idler C, Fröhling A, Popelar P, Geyer M, Schlüter O (2005) Ozontes Wasser zur Qualitätssicherung bei Waschmöhren. Landtechnik 60 (6): 350-351.

Luscher C, Balasa A, Fröhling A, Ananta E, Knorr D (2004): Effect of High-Pressure-Induced Ice I-to-Ice III Phase Transitions on Inactivation of *Listeria innocua* in Frozen Suspension. Applied and Environmental Microbiology, July 2004, p. 4021–4029.

Proceedings

Fröhling A, Schlüter O (2010) Fast mastitis detection during milking process for milk quality monitoring. International Workshop „The future of the quarter individual milking“, September 14th -15th 2010, Potsdam, Germany. Bornimer Agrartechnische Berichte Heft 76, 2010, p. 99-105 *(oral presentation)*.

Fröhling A, Wienke M, Rose-Meierhöfer S, Lochotzke HM, Schlüter O (2010) Fast mastitis detection during milking process for milk quality monitoring. Proceedings of the 5th IDF International Mastitis Conference March 21st – 24th, 2010, Christchurch, New Zealand *(oral presentation)*.

Fröhling A, Wienke M, Rose-Meierhöfer S, Lochotzke HM, Schlüter O (2009) Mastitis detection and prevention during milking process. Proceedings of CIGR – 5th International Postharvest Symposium, 31 Aug - 2 Sept, Potsdam, Germany (ISBN 978-3-00-028811-1), p1353-62 *(poster presentation).*

Fröhling A, Wienke M, Rose-Meierhöfer S, Lochotzke HM, Schlüter O (2008) A new approach to fast mastitis detection - a tool for monitoring milk quality. Proceedings of the ASABE Annual International Meeting, June 29th – July 2nd, Providence, Rhode Island, USA; Paper Number: 084265 *(poster presentation).*

Schlüter O, Foerster J, Fröhling A, Herppich WB, Geyer M, Knorr D (2008) Stress response of physiological active food products on high hydrostatic pressures up to 250 MPa. Proceedings of the ASABE Annual International Meeting, June 29th – July 2nd, Providence, Rhode Island, USA *(oral presentation).*

Schlüter O, Foerster J, Fröhling A, Geyer M, Herppich WB, Brandenburg R, Ehlbeck J, Knorr D (2008) Comprehensive evaluation of innovative physical treatments for preservation of fresh produce. 4th International Symposium on Machinery and Mechatronics for Agricultural and Biosystems Engineering (ISMAB), May 27th -29th, Taichung, Taiwan *(oral presentation).*

Hausdorf L, Fröhling A, Nettmann E, Schlüter O, Klocke M (2008) Detection of Arcobacter during processing of vegetables. Conference proceedings CD: 1176926. International Conference on Agricultural Engineering (AgEng), June 23rd – 25th, Crete, Greece *(poster presentation)*.

Hassenberg K, Geyer M, Popelar P, Fröhling A, Schlüter O, Herppich WB, Idler C (2006) Ozontes Wasser zur Qualitätssicherung bei Waschmöhren, 43. Gartenbauwissenschaftliche Tagung, Potsdam, BHGL Schriftenreihe 24, 141.

Luscher C, Fröhling A, Balasa A, Knorr D (2004) Inactivation of *Listeria innocua* and *E. coli* at high pressure and subzero temperature with consideration of the phase transitions of water. Proceedings on CD-Rom paper #776. ICEF 9 – International Congress on Engineering and Food (Montpellier, France).

Oral and poster presentations

Fröhling A, Baier M, Klocke S, Ehlbeck J, Knorr D, Schlüter O (2010) Modelling of bacterial physiological property changes measured by flow cytometry. 2010 EFFoST ANNUAL MEETING Food and Health, November 10th -12th, 2010, Dublin, Ireland *(poster presentation).*

Jäger H, Fröhling A, Voigt E, Schulz A, Gruber A, Schlüter O, Knorr D (2010) Microbial inactivation by electrochemically activated water – mechanisms of action on a cellular level. European PHD Conference in Food Science and Technology (BerlinFood2010), September 8th -10th, 2010, Berlin, Germany *(poster presentation).*

Fröhling A, Baier M, Klocke S, Ehlbeck J, Knorr D, Schlüter O (2010) Evaluation of physico-chemical impact on bacteria by means of flow cytometry. European PHD Conference in Food Science and Technology (BerlinFood2010), September 8th -10th, 2010, Berlin, Germany *(poster presentation).*

Fröhling A, Baier M, Ehlbeck J, Knorr D, Schlüter O (2010) Modeling non-thermal plasma inactivation of pathogens. IFT Annual Meeting, July 17th -July 20th, 2010, Chicago, IL, USA *(poster presentation).*

Fröhling A, Baier M, Klocke S, Schlüter O (2010) Flow cytometric comparison of gentle treatment techniques. IAFP European Symposium on Food Safety, June 9th -11th, 2010, Dublin, Ireland *(poster presentation).*

Baier M, Fröhling A, Klocke S, Meda V, Ehlbeck J, Knorr D, Schlüter O (2010) Antimicrobial treatment of food surfaces using non-thermal atmospheric pressure plasma. ISP PhD Congress 2010, February 17th–18th, 2010, Karlsruhe, Germany *(poster presentation).*

Fröhling A, Baier M, Baranyai L, Geyer M, Ehlbeck J, Knorr D, Schlüter O (2009) Plasmabehandlung einer Lebensmittelmatrix – Inaktivierungskinetiken und durchflusszytometrische Analysen von vegetativen Bakterien. GDL-Kongress Lebensmitteltechnologie 2009, Oktober 22nd – 24th, Lemgo, Germany *(oral presentation).*

Fröhling A, Baier M, Ehlbeck J, Knorr D, Schlüter O (2009) Food surface decontamination using non-thermal plasma. IAFP European Symposium on Food Safety, October 7th - 9th, 2009, Berlin, Germany *(poster presentation).*

McIntyre L, Prematane A, Hudson A, Billington C, Fröhling A, Schlüter O (2009) ISEKI_Mundus 2 – contributing to international exchange of expertise in food safety research. 5th International Postharvest Symposium, 31 Aug - 2 Sept, Potsdam, Germany (ISBN 978-3-00-028811-1), p1524 *(poster presentation).*

Fröhling A, Baier M, Ehlbeck J, Knorr D, Schlüter O (2009) Non-thermal plasma decontamination of food surfaces: flow cytometric analyses of bacteria and inactivation mechanisms. IFT Annual Meeting, June 6th June 9th, 2009, Anaheim, CA, USA *(poster presentation).*

Schlüter O, Fröhling A, Loffhagen D, Ehlbeck J (2009) Modeling an atmospheric cool plasma jet and its performance in food surface decontamination. IFT Annual Meeting, June 6 – 9, Anaheim, CA, USA *(invited lecture).*

Fröhling A, Baier M, Foerster J, Ehlbeck J, Knorr D, Schlüter O (2009) Anwendung von Atmosphärendruckplasma zur Produkt schonenden Inaktivierung von humanpathogenen Bakterien. Jahrestreffen des ProcessNet-Fachausschusses „Lebensmittelverfahrenstechnik“, March 23rd -25th, 2009, Lausanne, Switzerland *(oral presentation)*

Fröhling A, Baier, M, Ehlbeck J, Geyer M, Schlüter O (2009) Durchflusszytometrische Untersuchungen zur Inaktivierung von phytopathogenen Bakterien mittels Niedertemperaturplasma. 45. Gartenbauwissenschaftliche Tagung, February 25th -28th, 2009, Berlin, Germany *(oral presentation).*

Schlüter O, Fröhling A, McIntyre L, Hudson A, Billington C (2008) ISEKI_Mundus – a base to foster international exchange of expertise in food safety research. NZMS Conference 2008 - “Germs and Genomes in the Garden City”, November 18th - 21st, Christchurch, New Zealand *(poster presentation)*

Schlüter O, Baier M, Fröhling A, Knorr D, Ehlbeck J (2008) Cold plasma treatment of bacterial pathogens: Inactivation kinetics and flow cytometric analysis. First European Food Congress, November 4th – 9th Ljubljana, Slovenia *(oral presentation).*

Fröhling A, Adamzig H, Walter A, Hausdorf L, Klocke M, Schlüter O, (2008) Biosensors for the detection of pathogenic microorganisms – Concepts for determination of pathogens in fruits and vegetable processing using PCR-techniques and flow cytometry. ProSenso.net2 Workshop at the Postharvest unlimited, Nov. 4th – 7th, Potsdam, Germany *(oral presentation).*

Fröhling A, Hausdorf L, Klocke M, Schlüter O (2008) Determination of pathogen viability in fruit and vegetable processing by means of flow cytometry. Postharvest unlimited, Nov. 4th – 7th, Potsdam, Germany *(oral presentation)*.

Schlüter O, Fröhling A, Herppich WB, Brandenburg R, Ehlbeck J, Knorr D (2008) Impact of cold plasma treatment on bacterial pathogens and plant-related foods. IFT Annual Meeting, June 28th – July 1st, New Orleans, USA *(oral presentation).*

Schlüter O, Adamzig H, Walter AD, Fröhling A, Hausdorf L, Klocke M (2008) Microtechnology for in-situ detection of pathogens during postharvest processing of vegetables. 10th International Congress of Engineering and Food, April 20th – 24th, Viña del Mar, Chile *(oral presentation).*

Fröhling A, Geyer M, Knorr D, Ramminger N, Schlüter O (2008) Einsatzpotenzial der Durchflusszytometrie zur Chargen gerechten Prozessführung bei der Herstellung von leichtverderblichen pflanzlichen Lebensmitteln, Sitzung des ProcessNet-Fachausschusses „Lebensmittelverfahrenstechnik“, March 10th – 14th, 2008, Weihenstephan/Freising, München, Germany *(oral presentation*).

Walter AD, Mertsch O, Adamzig H, Fröhling A, Hausdorf L, Klocke S, Klocke M, Schlüter O, Schondelmaier D, Loechel B (2007) Contamination Control of Agricultural Products by On-Chip PCR and Flow Cytometry, 12th International Commercialization of Micro and Nano Systems Conference, 2nd - 6th September, Melbourne, Australia *(oral presentation*).

Awards

Poster Presentation Award 3rd place – Paper Title: Evaluation of physico-chemical impact on bacteria by means of flow cytometry. BerlinFood2010, September 8th – 10th, 2010, Berlin, Germany. Funded by the Commission of the European Communities, Framework 6, Priority 5 'Food Quality and Safety', Integrated Project NovelQ FP6-CT-2006 015710.

Student Poster Award – Paper Title: Food surface decontamination using non-thermal plasma. IAFP`s Fifth European Symposium on Food Safety, October 7th – 9th 2009, Berlin, Germany.

GNT Poster Award for Young Scientists – Second Best Presentation in the Field of Food Processing, Monitoring Technology in Bioprocesses and Food Quality Management with an Original Paper Entitled: Mastitis detection and prevention during milking process. 5th CIGR Section VI, International Technical Symposium 2009, 31st August-2nd September, Potsdam, Germany.

Annex

Annex 1: Standard deviation of membrane integrity measurements after thermal treatment

Table 1: Standard deviation (±) of membrane integrity measurements of thermal treated *E. coli* cells

Treatment time [min]	50 °C				70 °C				90 °C			
	PI	TO+ PI	TO	unstained	PI	TO+ PI	TO	unstained	PI	TO+ PI	TO	unstained
0	0.06	1.13	1.26	2.31	0.23	0.55	0.61	0.36	0.06	1.13	1.26	2.31
1	0.20	0.29	0.31	0.15	1.91	2.16	1.45	1.78	1.76	5.92	7.31	0.12
3	0.15	0.65	1.55	0.75	0.31	1.08	0.45	1.78	3.75	3.36	0.06	0.80
5	2.32	0.68	3.66	1.07	2.27	0.46	0.31	2.38	11.29	11.70	0.15	0.76
10	1.21	0.85	3.27	1.58	3.20	0.32	0.15	3.43	6.54	6.32	0.15	0.20

Table 2: Standard deviation (±) of membrane integrity measurements of thermal treated *L. innocua* cells

Treatment time [min]	50 °C				70 °C				90 °C			
	PI	TO+ PI	TO	unstained	PI	TO+ PI	TO	unstained	PI	TO +PI	TO	unstained
0	0.06	1.80	1.29	0.72	0.31	3.90	7.32	3.33	0.29	2.77	2.97	0.64
1	0.25	0.53	0.47	0.15	0.17	3.55	3.30	0.90	0.74	0.66	0.06	0.86
3	0.32	0.35	0.10	0.12	3.42	2.17	1.89	0.68	5.62	0.15	0.12	5.52
5	0.12	0.45	0.20	0.29	0.67	5.21	0.80	4.13	26.29	0.35	0.15	25.81
10	0.40	0.23	0.80	0.25	1.60	7.79	0.32	7.21	7.61	0.40	0.15	7.37

Table 3: Standard deviation (±) of membrane integrity measurements of thermal treated *P. carotovorum* cells

Treatment time [min]	50 °C				70 °C				90 °C			
	PI	TO+ PI	TO	unstained	PI	TO+ PI	TO	unstained	PI	TO+ PI	TO	unstained
0	1.46	1.35	4.11	2.51	1.00	0.50	0.70	0.15	1.46	1.35	4.11	2.51
1	0.61	0.62	0.81	0.31	3.51	3.85	0.26	0.20	6.63	7.27	7.62	1.03
3	1.42	0.60	2.54	0.55	5.55	5.90	0.15	0.35	3.55	11.81	0.31	8.04
5	1.07	0.76	1.79	0.30	7.01	6.86	0.12	0.12	7.38	1.93	0.56	6.39
10	0.68	1.78	1.37	0.49	8.64	8.74	0.98	0.40	6.30	9.65	0.36	4.50

Annex 2: Standard deviation of esterase activity measurements after thermal treatment

Table 4: Standard deviation (±) of esterase activity measurements of thermal treated *E. coli* cells

Treatment time [min]	50 °C				70 °C				90 °C			
	PI	cF+ PI	cF	unstained	PI	cF+ PI	cF	unstained	PI	cF+ PI	cF	unstained
0	0.45	7.01	7.12	0.38	1.48	3.23	2.92	1.80	0.45	7.01	7.12	0.38
1	0.92	2.65	2.32	0.67	3.07	2.72	0.35	0.06	1.00	1.22	0.06	0.29
3	1.59	1.23	2.61	0.47	0.55	0.89	0.15	0.53	4.16	3.81	0.00	0.36
5	0.98	1.02	1.87	0.38	1.63	1.21	0.06	0.47	0.17	0.15	0.00	0.21
10	1.77	3.55	6.22	1.07	1.08	0.96	0.06	1.06	0.45	0.25	0.06	0.17

Table 5: Standard deviation (±) of esterase activity measurements of thermal treated *L. innocua* cells

Treatment time [min]	50 °C				70 °C				90 °C			
	PI	cF+ PI	cF	unstained	PI	cF+ PI	cF	unstained	PI	cF+ PI	cF	unstained
0	0.00	3.93	3.93	0.06	0.57	4.50	5.29	0.25	0.23	3.55	3.74	0.38
1	0.06	1.88	1.82	0.06	1.76	1.47	1.73	0.45	0.78	0.15	0.06	0.62
3	0.06	1.59	1.48	0.06	8.98	4.15	2.14	2.72	0.06	0.06	0.00	0.06
5	0.06	2.07	1.96	0.15	3.02	1.70	0.35	1.55	0.70	0.06	0.00	0.67
10	0.06	0.98	0.95	0.10	3.11	1.14	0.20	1.79	0.45	0.00	0.00	0.45

Table 6: Standard deviation (±) of esterase activity measurements of thermal treated *P. carotovorum* cells

Treatment time [min]	50 °C				70 °C				90 °C			
	PI	cF+ PI	cF	unstained	PI	cF+ PI	cF	unstained	PI	cF+ PI	cF	unstained
0	7.76	4.03	8.96	5.16	8.21	3.14	13.47	2.20	7.76	4.03	8.96	5.16
1	1.75	3.80	1.10	1.50	15.29	15.33	0.12	0.15	3.16	3.75	0.10	2.07
3	3.93	4.01	1.82	1.88	8.36	8.37	0.26	1.14	8.28	2.17	0.10	9.96
5	1.34	1.89	0.06	0.52	21.94	21.97	0.23	0.20	1.28	2.70	0.06	2.69
10	9.00	2.75	11.95	0.51	13.40	14.17	0.38	0.40	0.15	0.06	0.00	0.15

Annex 3: Standard deviation of membrane integrity measurements after PAA treatment

Table 7: Standard deviation (±) of membrane integrity measurements of PAA treated (0.25 % PAA) *E. coli* cells

Treatment time [min]	0 °C				10 °C				20 °C			
	PI	TO+ PI	TO	unstained	PI	TO+ PI	TO	unstained	PI	TO+ PI	TO	unstained
0	22.66	3.64	19.81	2.45	0.85	2.25	3.59	0.53	1.89	6.25	8.23	0.31
0.25	0.26	1.27	1.94	0.61	0.25	2.25	3.31	1.04	0.12	2.85	3.58	0.62
0.5	0.14	0.35	0.14	0.35	0.57	4.24	5.44	0.64	0.64	2.90	3.75	0.21
0.75	0.87	6.37	6.41	0.44	0.23	1.00	1.37	0.15	2.89	3.53	0.40	0.50
1	0.26	6.86	7.15	0.10	0.35	6.75	6.46	0.31	23.09	22.50	0.49	0.15
1.5	1.82	2.01	0.12	0.32	0.70	11.68	12.26	0.17	0.51	0.60	0.06	0.75
2	4.78	4.68	0.06	0.32	3.36	3.82	0.00	0.51	0.96	0.75	0.00	0.35

Table 8: Standard deviation (±) of membrane integrity measurements of PAA treated (0.5 % PAA) *E. coli* cells

Treatment time [min]	0 °C				10 °C				20 °C			
	PI	TO+PI	TO	unstained	PI	TO+ PI	TO	unstained	PI	TO+ PI	TO	unstained
0	22.66	3.64	19.81	2.45	0.85	2.25	3.59	0.53	1.89	6.25	8.23	0.31
0.25	0.26	1.27	1.94	0.61	0.25	2.25	3.31	1.04	0.12	2.85	3.58	0.62
0.5	0.21	1.06	0.92	0.07	0.49	3.75	4.10	0.14	8.13	7.78	0.07	0.28
0.75	2.65	6.30	10.37	1.44	0.44	5.86	6.15	0.10	1.88	1.56	0.10	1.04
1	0.25	4.88	4.76	0.42	0.62	0.90	0.06	0.25	0.90	0.38	0.06	1.17
1.5	0.49	7.88	8.09	0.40	7.35	7.50	0.06	0.21	0.95	0.97	0.06	0.21
2	1.23	11.12	12.46	0.17	0.85	0.26	0.06	0.53	1.84	0.90	0.15	1.45

Annex 4: Standard deviation of esterase activity measurements after PAA treatment

Table 9: Standard deviation (±) of esterase activity measurements of PAA treated (0.25 % PAA) *E. coli* cells

Treatment time [min]	0 °C				10 °C				20 °C			
	PI	cF+ PI	cF	unstained	PI	cF+ PI	cF	unstained	PI	cF+ PI	cF	unstained
0	20.64	2.75	23.20	1.37	1.19	3.20	6.35	2.19	1.40	1.04	2.66	0.31
0.25	0.14	27.08	27.08	0.14	0.28	21.85	21.14	0.42	0.35	2.62	3.25	0.28
0.5	1.71	30.37	28.18	0.60	1.04	7.92	8.29	0.79	3.03	2.86	0.49	0.32
0.75	0.93	25.41	25.90	0.32	1.82	1.37	1.48	1.02	7.85	7.85	0.32	0.45
1	3.04	6.76	9.39	0.81	2.08	2.70	0.92	1.39	5.13	4.90	0.06	0.35
1.5	3.20	9.84	13.50	1.01	10.25	13.07	0.00	2.84	2.06	1.65	0.06	0.52
2	1.06	0.87	0.06	0.36	4.93	5.01	0.00	0.15	2.27	4.69	0.00	3.22

Table 10: Standard deviation (±) of esterase activity measurements of PAA treated (0.5 % PAA) *E. coli* cells

Treatment time [min]	0 °C				10 °C				20 °C			
	PI	cF+ PI	cF	unstained	PI	cF+ PI	cF	unstained	PI	cF+ PI	cF	unstained
0	20.64	2.75	23.20	1.37	1.19	3.20	6.35	2.19	1.40	1.04	2.66	0.31
0.25	0.14	11.60	11.53	0.21	1.06	19.73	21.07	0.28	9.19	8.34	0.07	0.78
0.5	1.67	3.28	5.10	0.32	3.44	3.21	1.16	0.81	5.87	6.16	0.00	0.40
0.75	3.02	2.63	0.61	0.32	3.01	3.07	0.12	0.61	6.13	6.22	0.06	0.29
1	2.38	1.67	0.10	1.04	7.17	7.70	0.12	0.64	0.76	1.14	0.00	0.53
1.5	9.09	9.36	0.00	0.45	2.59	2.21	0.00	0.38	1.58	0.78	0.06	0.96
2	9.96	9.37	0.00	0.38	0.50	0.25	0.00	0.25	1.79	0.12	0.00	1.71

Annex 5: Standard deviation of membrane integrity measurements after ozone treatment

Table 11: Standard deviation (±) of membrane integrity measurements of ozone treated *E. coli* cells

Treatment time [min]	1.7 mg l^{-1}				2.8 mg l^{-1}				3.8 mg l^{-1}			
	PI	TO+ PI	TO	unstained	PI	TO+ PI	TO	unstained	PI	TO+ PI	TO	unstained
0	0.56	1.32	2.57	0.74	0.59	0.76	1.59	1.31	0.56	1.32	2.57	0.74
0.17	9.75	13.25	0.06	3.53	31.35	31.17	1.89	3.68	36.51	25.55	0.78	13.21
0.5	4.14	1.12	0.35	3.16	26.25	30.75	0.31	4.78	19.50	18.24	1.00	1.63
1	3.49	1.32	0.12	2.10	4.84	9.26	0.65	12.70	0.55	5.35	0.84	4.91
1.5	1.37	3.90	0.87	5.57	8.64	13.29	1.21	7.27	1.59	16.04	3.82	19.50
2	9.14	1.06	0.00	8.08	10.75	2.80	0.61	7.55	2.14	11.67	2.32	11.42

Table 12: Standard deviation (±) of membrane integrity measurements of ozone treated *L. innocua* cells

Treatment time [min]	1.7 mg l^{-1}				2.8 mg l^{-1}				3.8 mg l^{-1}			
	PI	TO+ PI	TO	unstained	PI	TO+ PI	TO	unstained	PI	TO+ PI	TO	unstained
0	0.95	1.60	3.51	2.10	0.59	0.31	3.29	2.47	0.15	6.45	6.39	0.20
0.17	2.13	0.12	0.00	2.04	3.70	0.12	0.06	3.72	1.60	0.06	0.06	1.50
0.5	1.45	0.10	0.06	1.55	4.38	0.17	0.00	4.21	3.55	0.12	0.06	3.62
1	1.59	0.31	0.00	1.30	5.57	0.12	0.06	5.48	7.95	0.15	0.00	7.82
1.5	2.76	0.21	0.06	2.91	2.18	0.00	0.06	2.14	2.21	0.06	0.00	2.20
2	1.99	0.15	0.00	2.11	1.62	0.25	0.00	1.82	4.63	0.52	0.06	4.80

Table 13: Standard deviation (±) of membrane integrity measurements of ozone treated *P. carotovorum* cells

Treatment time [min]	0.7 mg l^{-1}				1.7 mg l^{-1}				2.8 mg l^{-1}			
	PI	TO+ PI	TO	unstained	PI	TO+ PI	TO	unstained	PI	TO+ PI	TO	unstained
0	0.31	0.31	0.45	0.06	0.20	0.26	0.38	0.06	0.32	0.96	0.85	0.00
0.17	2.63	6.58	8.93	0.30	38.93	41.14	0.53	2.23	1.73	0.40	0.23	1.53
0.5	3.32	2.75	5.81	0.35	4.57	2.42	3.96	1.88	2.73	1.93	1.56	0.82
1	5.55	3.92	9.41	0.10	32.77	9.53	24.49	1.22	4.31	2.59	3.43	2.79
1.5	7.59	5.06	12.99	0.44	7.11	1.76	6.01	1.39	7.22	3.26	3.82	2.73
2	8.42	5.15	13.30	0.17	15.35	4.85	15.80	2.41	8.89	7.35	6.69	5.39

Table 14: Standard deviation (±) of membrane integrity measurements of ozone treated (3.8 mg l^{-1} ozone, reaction stopped with $Na_2S_2O_3$) bacteria *cells*

Treatment time [min]	*E. coli*				*L. innocua*				*P. carotovorum*			
	PI	TO+PI	TO	unstained	PI	TO+ PI	TO	unstained	PI	TO+ PI	TO	unstained
0	0.15	0.42	0.46	0.21	0.67	1.70	3.84	1.63	0.25	2.09	2.40	0.15
0.17	6.70	5.31	0.32	10.00	1.26	0.10	0.06	1.15	0.59	2.43	0.81	3.42
0.5	0.86	12.37	0.15	12.75	5.63	0.67	0.06	4.91	0.75	2.60	0.66	1.44
1	0.50	1.60	0.31	1.76	4.58	0.10	0.06	4.44	2.55	7.00	36.78	27.74
1.5	0.06	2.21	0.10	2.36	1.35	0.32	0.06	1.45	1.76	1.35	0.57	2.44
2	0.59	0.44	0.23	0.98	2.25	0.06	0.00	2.19	0.44	0.40	0.44	1.12

Annex 6: Standard deviation of esterase activity measurements after ozone treatment

Table 45: Standard deviation (±) of esterase activity measurements of ozone treated *E. coli* cells

Treatment time [min]	1.7 mg l^{-1}				2.8 mg l^{-1}				3.8 mg l^{-1}			
	PI	cF+ PI	cF	unstained	PI	cF+ PI	cF	unstained	PI	cF+ PI	cF	unstained
0	0.35	1.16	1.57	0.25	0.25	0.76	0.46	0.52	0.35	1.16	1.57	0.25
0.17	4.50	2.07	1.50	1.91	5.60	4.20	1.55	5.95	10.60	8.96	0.91	20.12
0.5	7.09	1.15	2.30	6.09	3.01	3.41	0.35	2.70	3.86	4.51	0.49	3.01
1	0.40	2.07	0.93	0.75	10.22	15.66	3.04	9.43	2.41	3.52	2.41	2.51
1.5	12.15	16.82	1.76	5.93	8.96	11.61	1.21	6.40	5.56	14.14	1.87	14.53
2	4.08	1.00	1.68	2.75	9.29	5.49	1.00	4.68	3.35	16.67	14.23	27.63

Table 16: Standard deviation (±) of esterase activity measurements of ozone treated *L. innocua* cells

Treatment time [min]	1.7 mg l^{-1}				2.8 mg l^{-1}				3.8 mg l^{-1}			
	PI	cF+ PI	cF	unstained	PI	cF+ PI	cF	unstained	PI	cF+ PI	cF	unstained
0	3.04	6.90	10.38	1.00	1.73	27.99	24.57	5.50	1.27	14.24	14.82	0.17
0.17	0.56	0.00	0.00	0.56	1.77	0.06	0.00	1.74	0.45	0.06	0.00	0.40
0.5	3.36	0.00	0.00	3.36	7.60	0.06	0.00	7.65	2.15	0.00	0.00	2.15
1	1.13	0.00	0.00	1.13	2.04	0.00	0.00	2.04	5.57	0.00	0.00	5.57
1.5	1.42	0.23	0.06	1.67	0.66	0.00	0.00	0.66	1.84	0.00	0.00	1.84
2	2.42	0.12	0.00	2.32	1.76	0.06	0.00	1.80	4.44	0.00	0.00	4.44

Table 17: Standard deviation (±) of esterase activity measurements of ozone treated *P. carotovorum* cells

Treatment time [min]	0.7 mg l^{-1}				1.7 mg l^{-1}				2.8 mg l^{-1}			
	PI	cF+ PI	cF	unstained	PI	cF+ PI	cF	unstained	PI	cF+ PI	cF	unstained
0	0.20	0.90	1.36	0.45	0.66	0.32	0.97	0.10	0.10	0.23	0.10	0.35
0.17	15.12	5.51	7.70	2.18	3.35	0.40	1.30	2.36	0.44	0.06	0.06	0.40
0.5	4.68	1.21	3.14	0.64	6.68	1.33	5.23	0.61	1.93	0.10	0.06	2.06
1	13.03	3.59	9.90	1.07	11.16	6.81	9.95	4.76	2.95	0.44	0.10	3.30
1.5	11.25	5.78	6.12	1.15	1.90	0.84	2.36	1.16	2.35	0.35	0.53	1.85
2	14.73	3.21	11.42	0.36	11.28	4.91	7.76	2.22	4.66	0.35	0.35	4.94

Table 18: Standard deviation (±) of esterase activity measurements of ozone treated (3.8 mg l^{-1} ozone, reaction stopped with $Na_2S_2O_3$) bacteria *cells*

Treatment time [min]	*E. coli*				*L. innocua*				*P. carotovorum*			
	PI	cF+ PI	cF	unstained	PI	cF+ PI	cF	unstained	PI	cF+ PI	cF	unstained
0	0.72	0.76	1.56	0.23	2.08	3.02	9.56	6.17	1.84	7.39	8.54	3.50
0.17	3.16	0.15	0.10	3.41	0.95	0.00	0.06	1.01	1.35	0.23	0.15	1.10
0.5	8.76	0.31	0.23	8.43	4.09	0.26	0.00	3.86	3.35	0.06	0.00	3.30
1	1.06	1.01	0.40	2.36	1.04	0.00	0.00	1.04	1.15	0.06	0.06	1.19
1.5	1.65	0.17	0.00	1.56	2.95	0.06	0.06	2.91	4.27	0.06	0.06	4.27
2	1.91	1.57	1.01	4.49	3.14	0.12	0.00	3.25	1.21	0.06	0.00	1.15

Annex 7: Standard deviation of membrane integrity measurements after plasma treatment

Table 59: Standard deviation (±) of membrane integrity measurements of plasma treated *E. coli* cells

Treatment time [min]	10 W				20 W				40 W			
	PI	TO+ PI	TO	unstained	PI	TO+ PI	TO	unstained	PI	TO+ PI	TO	unstained
0	1.04	2.38	5.06	5.01	0.49	2.76	1.80	2.13	0.44	3.32	9.27	12.84
0.25	n.a.	n.a.	n.a.	n.a.	n.a.	n.a.	n.a.	n.a.	2.07	0.78	2.55	0.78
0.5	0.23	0.90	4.96	5.90	2.83	0.52	1.98	1.44	1.86	0.89	2.50	0.40
1	0.15	0.42	3.58	3.23	2.67	0.71	2.84	0.67	7.94	0.81	6.81	1.48
1.5	n.a.	n.a.	n.a.	n.a.	n.a.	n.a.	n.a.	n.a.	1.67	1.17	2.55	2.17
2	0.25	2.48	5.56	3.30	8.51	1.39	8.49	0.64	3.40	1.01	2.83	0.31
3	0.06	1.59	3.42	1.87	6.47	0.31	6.27	1.06	n.a.	n.a.	n.a.	n.a.
4	0.65	0.79	2.63	3.31	6.16	2.02	8.45	3.48	n.a.	n.a.	n.a.	n.a.

n.a., not analysed

Table 20: Standard deviation (±) of membrane integrity measurements of plasma treated *L. innocua* cells

Treatment time [min]	10 W				20 W				40 W			
	PI	TO+ PI	TO	unstained	PI	TO+ PI	TO	unstained	PI	TO+ PI	TO	unstained
0	0.74	0.74	0.03	2.52	0.74	0.74	0.02	4.31	0.74	0.74	0.03	2.52
0.25	n.a.	n.a.	n.a.	n.a.	n.a.	n.a.	n.a.	n.a.	2.25	2.25	0.15	12.19
0.5	2.56	2.56	0.07	9.93	0.87	0.87	0.02	4.58	2.04	2.04	0.09	6.40
1	0.35	0.35	0.06	2.61	0.12	0.12	0.01	0.76	8.61	8.61	0.04	6.59
1.5	n.a.	n.a.	n.a.	n.a.	n.a.	n.a.	n.a.	n.a.	3.58	3.58	0.01	3.25
2	0.06	0.06	0.06	2.96	0.95	0.95	0.03	6.79	2.57	2.57	0.01	0.55
3	0.23	0.23	0.06	3.79	2.70	2.70	0.02	2.55	n.a.	n.a.	n.a.	n.a.
4	0.12	0.12	0.04	2.04	0.36	0.36	0.00	4.24	n.a.	n.a.	n.a.	n.a.

n.a., not analysed

Table 21: Standard deviation (±) of membrane integrity measurements of plasma treated *P. carotovorum* cells

Treatment time [min]	10 W				20 W				40 W			
	PI	TO+ PI	TO	unstained	PI	TO+ PI	TO	unstained	PI	TO+ PI	TO	unstained
0	0.68	3.75	6.72	3.47	0.89	0.56	0.46	0.36	0.68	3.75	6.72	3.47
0.25	n.a.	n.a.	n.a.	n.a.	n.a.	n.a.	n.a.	n.a.	8.47	2.20	6.30	1.20
0.5	1.03	1.89	3.06	0.49	2.69	0.26	2.36	0.35	4.44	1.16	5.88	2.36
0.75	n.a.	n.a.	n.a.	n.a.	n.a.	n.a.	n.a.	n.a.	1.97	0.42	4.06	4.16
1	0.17	1.26	1.08	1.19	2.46	0.50	1.99	0.21	3.22	0.65	4.83	2.64
1.5	0.00	0.10	0.61	0.59	5.76	1.53	3.84	1.45	8.36	0.91	9.22	3.40
2	1.35	0.95	5.17	3.70	5.83	0.81	6.52	0.50	n.a.	n.a.	n.a.	n.a.
2.5	0.55	2.22	4.85	2.23	8.13	2.86	5.80	0.78	n.a.	n.a.	n.a.	n.a.

n.a., not analysed

Annex 8: Standard deviation of esterase activity measurements after plasma treatment

Table 22: Standard deviation (±) of esterase activity measurements of plasma treated *E. coli* cells

Treatment time [min]	10 W				20 W				40 W			
	PI	cF+ PI	cF	unstained	PI	cF+ PI	cF	unstained	PI	cF+ PI	cF	unstained
0	0.21	0.30	2.48	2.02	0.23	0.12	4.01	3.82	0.42	0.85	5.87	6.86
0.25	n.a.	n.a.	n.a.	n.a.	n.a.	n.a.	n.a.	n.a.	2.50	0.45	2.94	0.98
0.5	0.26	0.25	2.32	1.90	2.60	0.15	1.59	1.04	4.08	0.40	4.02	0.96
1	0.25	0.06	2.35	2.29	3.08	1.20	1.39	3.25	8.00	0.65	6.53	0.97
1.5	n.a.	n.a.	n.a.	n.a.	n.a.	n.a.	n.a.	n.a.	2.53	0.38	2.42	1.75
2	0.46	0.15	2.07	2.31	8.80	1.80	6.86	2.19	1.20	1.33	2.29	1.23
3	0.45	0.50	1.08	0.31	5.91	0.32	3.49	2.58	n.a.	n.a.	n.a.	n.a.
4	0.78	0.64	1.44	1.07	7.63	1.05	6.85	1.81	n.a.	n.a.	n.a.	n.a.

n.a., not analysed

Table 23: Standard deviation (±) of esterase activity measurements of plasma treated *L. innocua* cells

Treatment time [min]	10 W				20 W				40 W			
	PI	cF+ PI	cF	unstained	PI	cF+ PI	cF	unstained	PI	cF+ PI	cF	unstained
0	0.55	0.80	0.15	0.26	0.15	1.64	0.98	2.70	0.55	0.80	0.15	0.26
0.25	n.a.	n.a.	n.a.	n.a.	n.a.	n.a.	n.a.	n.a.	1.68	0.81	4.13	2.22
0.5	2.95	1.15	7.69	3.59	1.01	0.89	1.92	1.72	2.30	1.55	3.08	3.39
1	0.06	1.74	1.92	2.00	1.46	2.55	3.03	2.31	4.88	2.34	5.23	2.96
1.5	n.a.	n.a.	n.a.	n.a.	n.a.	n.a.	n.a.	n.a.	4.98	1.80	1.47	7.39
2	0.10	2.64	3.41	0.76	1.05	0.46	5.43	3.99	2.89	0.00	0.06	2.85
3	0.85	4.11	6.96	3.44	6.73	3.59	2.75	5.75	n.a.	n.a.	n.a.	n.a.
4	0.62	5.83	7.22	0.78	4.53	7.33	5.14	10.38	n.a.	n.a.	n.a.	n.a.

n.a., not analysed

Table 24: Standard deviation (±) of esterase activity measurements of plasma treated *P. carotovorum* cells

Treatment time [min]	10 W				20 W				40 W			
	PI	cF+ PI	cF	unstained	PI	cF+ PI	cF	unstained	PI	cF+ PI	cF	unstained
0	1.82	1.34	2.00	5.11	0.38	0.25	0.67	1.12	1.82	1.34	2.00	5.11
0.25	n.a.	n.a.	n.a.	n.a.	n.a.	n.a.	n.a.	n.a.	13.24	0.65	0.95	12.16
0.5	1.70	0.98	1.04	3.43	4.03	0.71	3.48	0.85	2.27	0.35	0.32	2.56
0.75	n.a.	n.a.	n.a.	n.a.	n.a.	n.a.	n.a.	n.a.	3.30	0.72	0.72	2.18
1	0.55	0.62	5.78	5.90	4.79	0.52	6.11	1.03	2.25	0.87	1.57	2.18
1.5	0.40	0.70	2.45	2.92	5.28	0.72	4.26	1.29	4.35	1.57	2.23	5.56
2	2.58	0.32	12.65	10.14	4.23	1.31	4.15	1.27	n.a.	n.a.	n.a.	n.a.
2.5	2.25	0.81	9.00	6.49	1.45	2.33	1.91	5.29	n.a.	n.a.	n.a.	n.a.

n.a., not analysed